PHD

A theoretical analysis of the flow in regenerative pumps.

Mohammad, Ahmed Ibrahim Elhag

Award date:
1979

Awarding institution:
University of Bath

A THEORETICAL ANALYSIS OF THE FLOW IN REGENERATIVE PUMPS

Submitted by
Ahmed Ibrahim Elhag Mohammad
for the degree of Ph.D. of the
University of Bath
1979

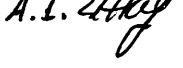

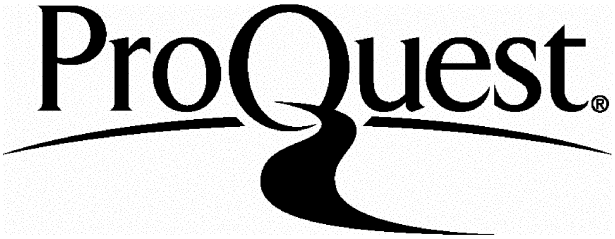

ACKNOWLEDGEMENTS

I would like to acknowledge the help and advice I have received from many people during the course of this work, and I am grateful to them all. In particular, I have drawn extensively on the time and experience of my supervisor, M. J. C. Swainston, who has been a continual source of inspiration, guidance and help.

I also wish to express my gratitude to Professor F. J. Wallace, Head of the School of Engineering, for his most valuable advice and encouragement throughout.

I would also acknowledge the help offered by the many staff of the University of Bath, in particular the staff of the Computer Unit, during the preparation of the computer programs.

This thesis was typed by Patricia Sherrin to whom many thanks are due for the appearance and accuracy of the final result. Any mistakes are my own.

Thanks are also due to the University of Khartoum for giving me the chance to undertake the work reported herein; the Sudan Government for sponsoring my scholarship and finally to my family for their support and encouragement.

SUMMARY

This thesis describes work concerned with the theory and development of a method of analysis of the flow in regenerative machines and its use to calculate the flow details and predict the overall performance of specified pumps.

A flow model is assumed based on the view that these machines operate as genuine rotodynamic devices. The equations derived reveal that

a) the familiar Euler's equation has to be supplemented by an extra term accounting for the tangential pressure gradient so that it can apply to rotors of regenerative machines, and

b) to compute the head rise, the tangential displacements of flow in the rotor have to be determined.

The meridional velocity field is represented by a streamfunction given by an empirical expression which is determined iteratively by solving the flow along streamlines and applying the condition that the net head rise per flow cycle should exactly match the product of the circumferential displacement and pressure gradient. An attempt is made to write both the momentum and energy equations such that the effect of friction is incorporated with reasonable consistency. Conventional models are used to estimate skin friction losses in the blade passages and in the channel, losses at entry to impeller blading and the effect of slip. However, towards compeltion of the work it was realised that the tangential pressure gradient should enhance the slip and discussion is presented of this aspect. In modelling the flow in the port and stripper regions, leakage and carry-over losses are included. However, a convincing model of the ports losses which accounts for their design remains to be established.

Computer programs written to implement the method on a digital computer are described and samples of the results of their use to investigate the flow in pumps of various configurations are discussed . It is found that the method is generally stable and convergent and it seems to enable the magnitude and interdependence of various flow parameters to be quantified. The computed overall performance characteristics led to the realisation that the slip effect is a function of the

tangential pressure gradient. They can also be interpreted as suggesting that the length of the effective pumping passage varies with the pressure gradient. Suggestions are made for the improvement of the accuracy of prediction and refinement of the procedure.

This work provides some novel findings regarding both the theory of regenerative machines and the procedures for the solution of their internal flows.

40-word summary suitable for retention in an automatic data processing system:

'Regenerative (side-channel) machine theory is investigated. Euler's equation requires an extra term, computable only from the flow tangential displacements in the rotor. The circumferential pressure gradient increases the relative eddy (slip). Overall performance predictions made employ detailed internal flow calculations'.

CONTENTS

NOTATION

A	area	m^2
	coefficient of streamfunction	m^3/s rad
a	area	m^2
	index of streamfunction	
B	blockage factor	
b	index of streamfunction	
C	clearance	m
	depth of peripheral channel	m
	constant	
c	centre of circulation	
	index of streamfunction	
D	impeller outer diameter	m
	diameter	m
d	index of streamfunction	
e	specific energy	J/kg
F	blade force per unit mass of fluid	N/kg
	function	
f	friction factor	
	function	
	specific friction force	N/kg
g	acceleration due to gravity	m/s^2
H	total enthalpy (Appendix A)	J/kg
	total head per unit weight (text)	m
h	head loss per unit weight	m
	specific enthalpy (Appendix A)	J/kg
k	constant	
	loss coefficient	
	counter	
L	length	m
ℓ	length	m
M	torque	N-m
m	meridional co-ordinate	
N	impeller rotational speed	rev/min
n	normal co-ordinate	
Ns	specific speed	$N\sqrt{Q}/H^{\frac{3}{4}}$
P	power	J/s
p	pressure	N/m^2

Q	volume flow rate	m^3/s
R	radius	m
r	radial co-ordinate	
Re	Reynolds number	
S	surface	
s	specific entropy (Appendix A)	J/kg
T	temperature	^oK
t	blade thickness	m
	time	s
U	blade circumferential speed	m/s
V	velocity	m/s
v	volume	m^3
W	relative velocity	m/s
X	axial width	m
	non-dimensionalising length	m
Y	non-dimensionalising length	m
Z	number of impeller blades	
z	axial co-ordinate	
α	absolute angle of flow with meridional	deg
β	relative angle of flow with meridional	deg
	blade angle	deg
Δ	finite change	
δ	angle (see Chapter 4)	deg
ε	eddy viscosity	m^2/s
η	efficiency	
θ	angle	deg
	tangential co-ordinate	
λ	streamsurface meridional angle	deg
μ	coefficient of viscosity	N s/m^2
ν	kinematic viscosity	m^2/s
ρ	density	kg/m^3
Σ	sum	
σ	slip factor	
ϕ	non-dimensional flow rate $(Q/(wD^3))$	
Ψ	streamfunction	m^3/s-rad
ψ	non-dimensional head $(gH/(\omega^2D^2))$	
ω	angular velocity	rad/s
$\bar{\nabla}$	gradient (vector operator)	

SUBSCRIPTS

av	average quantity
b	blade
c	calculated specific head
	channel
	circulatory
co	carry-over
e	effective
f	fluid
h	hydraulic
i	incidence
	impeller
	inner
in	ineffective entry angle
ℓ	leakage
	linear section of pump
m	for matching coefficient of streamfunction
	for radius of centre of circulation
	meridional
n	net
o	outer
p	port
	pumping passage
pc	peripheral channel
R	ratio of matching coefficients
	relative
r	radial
re	recovery
s	stagnation
	stripper
t	tangential
tc	tangential in the channel
u	in the circumferential direction
z	axial
θ	specific head rise from computed θ and assumed $\frac{\partial P}{\partial \theta}$
123'3	flow cycle
1,3	just inside impeller
2	exit from impeller
3'	last point of cycle in channel

SUPERSCRIPTS

'	Euler head
"	head due to tangential pressure gradient
′	non-dimensional quantity
-	vector quantity
^	unit vector

1. INTRODUCTION

The work presented in this thesis is concerned with the development of a theoretical analysis of regenerative pumps. In this chapter regenerative pumps are introduced as a group of self-priming pumps which have attracted more attention and interest than any of the rest. Descriptions are given of typical regenerative pumps and their mode of self-priming. Their fieldsof use, advantages and disadvantages are reviewed.

Some published theoretical and experimental works on these pumps are reported in brief. However, full coverage of these works may be found in the original papers which are here referred to and listed at the end of the text.

1.1 Aims of Work

Although considerable qualitative information is available regarding the behaviour of regenerative pumps, there are no published quantitative data with respect to the flow phenomena inside these machines. Different methods have been reported in the literature, developed on the basis of overall effects, for the prediction of the performance of some of these pumps. All these approaches, however, needed empirical factors to be determined from experimental tests which must be carried out on the pumps themselves. Moreover, these experimentally determined factors have not been proved to be universal for a particular pump geometry and they may be expected to depend on the absolute dimensions of the pump, fluid viscosity, etc., in unknown ways. Solutions of the flow fields in these pumps, comparable, for example, with solutions of flows in other rotodynamic machines, have not been published.

The information in the literature, therefore, has been, up to now, largely descriptive in nature. The theory of the pumping mechanism of these pumps does not seem to have been completely clarified yet; and hence the way in which they can best be designed has not so far been published. Hence there appears to be an infinite number of geometrical shapes and arrangements that may be used to construct regenerative pumps. As the pump is small and easily constructed, the trend being followed is that a suitable design is obtained by trial, utilizing the characteristics of previous designs and practical

experience. However, all the accumulated experience has not so far been able to raise the peak pump efficiency to above about 50%.

What is needed therefore is a theoretical analysis on basis of which a reasonable amount of knowledge of the flow phenomena and the mechanism of energy transfer could be obtained. Such an analysis should provide for two things:

1) A procedure to predict the performance of a pump of a specified design with reasonable accuracy.

2) A sound basis for design improvements.

It has been reported in the literature, however, that attempts to solve the flows in these pumps in detail and to predict the characteristics without the need for experimentally determined empirical factors were not successful because of the complexity of the flows. Yet in this work an attempt is made to solve the flows and predict the characteristics theoretically.

The work presented in this thesis has been aimed at evolving a computer aided theoretical analysis of regenerative pumps to meet the two requirements stated above.

1.2 Regenerative Pumps

These are a group of rotodynamic pumps which have two useful characteristics:

1) They are completely self-priming.

2) They operate on a range of specific speeds lower than that of any other group of rotodynamic pumps, i.e. they develop high-heads at low-flow rates.

Where needed, these two important characteristics give these pumps many advantages over other pumps; and indeed they are needed in many applications. The disadvantage of regenerative pumps is that they have low efficiencies.

1.2.1 The need for self-priming pumps

Ordinary impeller pumps have one general drawback which makes them more difficult to operate, namely: when they are working against a

suction head, they and their suction piping must be filled with the pumped liquid and carefully vented. In addition they are also sensitive to the presence of air and other gases in the liquid entering the pump. This can be caused either by a leak in the suction piping, or the liquid level falling below the strainder, or by the evolution of gases from volatile liquids, such as petrol, ether, etc. Under such circumstances the pump might lose its prime and stop pumping. The reason is that the pressure difference generated across these ordinary pumps impellers is proportional to the density of the fluid filling them. With fluids of low density like air, gases or vapours, the pressure gradient could be too small to maintian a flow taking into account the losses in the impeller.

Although positive-displacement pumps are self-priming, they are generally open to the following objections:

1) The small clearances between their parts make them relatively costly to manufacture, have relatively rapid wear, and unsuited to handling fluids which may contain solid particles or having poor lubricating properties.

2) They are more bulky than rotodynamic pumps for a given duty of flow rate and the flow from most is unsteady and often requires smoothing.

Self-priming pumps are needed for many applications, some of which are:

1) When a pump is required to be arranged to operate completely automatically without the need of attention and priming each time it is started.

2) When a pump is required to be mounted such that it has a high suction lift.

3) When the medium pumped is a mixture of liquids and gases.

4) When the pumped liquids are at or near their vapour pressures such as hot condensate, highly volatile liquids, liquid gases, etc.

5) When a pump is needed to prime other pumps or to maintain a vacuum in a system.

In the search for self-priming pumps, which were to be free of the disadvantages of positive-displacement pumps, liquid-ring pumps came into being.

1.2.2 Liquid-ring pumps

The common characteristic of these pumps is that inside them a ring of liquid is formed, at least in the priming stage of their operation. They are self-priming, i.e. they have the ability to remove a low density medium from the suction piping and fill it with liquid. However, they may be divided into three different kinds:

1) Pumps with eccentric impellers.

2) Pumps with eccentric screw impellers.

3) Pumps with concentric impeller.

This work is concerned with the last group only. However, it may be useful to touch upon the first two groups in brief.

1) Pumps with eccentric impellers

A typical eccentric impeller water-ring pump is shown in Fig. (1-1a). The casing is partly filled with the liquid which is entrained by the rotation of the impeller and due to the centrifugal forces a water-ring is formed moving concentrically to the casing. The water-ring touches the hub of the impeller at one point, if sufficient liquid is admitted, and a crescent-shaped free space is formed between the hub and the free surface of the ring as shown in the figure. As the impeller rotates the volume of each cell increases and then decreases: the cells are closed axially by the side discs. Air is thus drawn in, due to the increase of volume of the cells, then compressed and expelled due to the reduction in volume, through the inlet and outlet ducts respectively. Fig. (1-1b) shows an idealised diagram for calculating the flow rate and Fig. (1-1c) shows typical characteristics of such pumps.

The main application areas are those which require vacuum to be maintained. However, they have low efficiencies and have no particular attraction as liquid pumps. Hence they are not used as independent liquid pump.

2) Pumps with eccentric screw impellers

Fig. (1-2) shows a pump of this type. A mixture of gases and liquids may enter the pump axially. Centrifugal forces throw the liquid outwards so that it forms a cylindrical body rotating with the

impeller. The gases remain trapped between the liquid-ring and the impeller hub and thus they are carried by the screw from the inlet end of the pump to the exit end.

These machines are still in a stage of development. The mechanism of fluid flow is still largely unclear; and there is little data to allow an appraisal of their advantages and disadvantages.

3) Pumps with concentric impellers

This category is the subject of the rest of this work. There are many different designs of self-priming pumps with concentric impellers and there is considerable difference of opinion among engineers as to the precise mechanism by which these pumps produce their pumping effect. Hence different names are used by different writers for the same type of pump, depending on what opinion the writer has about its mode of operation. Names like periphery, side-channel, vortex, turbulence, friction, traction, turbine, tangential and regenerative are all used to refer to pumps essentially of the same type. In this work the name 'regenerative pumps' is used to refer to pumps of this category for reasons which become clear in section (1·4).

1.2.3 Description of regenerative pumps

Fig. (1-3) shows an exploded view of a typical regenerative pump and Fig. (1-4) shows two different designs reproduced from ref. (23). Essentially, however, they all have the following common features:

The impeller (1) is a disc with blades, which are in general radial, machined into it on one or both sides. The impeller is mounted on a shaft (2) concentrically within the casing (3). A side channel (4) is cut into one or both side-plates (5) which are situated close on each side of the impeller. There may also be a peripheral channel (6) cut in the cylindrical part of the casing, such that with the side-channel they form one channel whose meridional cross-section has an inverted L-shape. An inlet port (7) and a discharge port (8) are cut through the side-plates with the channel communicating between them from the inlet, going in the direction of the impeller rotation, to the outlet. The two ports are separated by 15% of the circumference. Between them, the walls of both side-plates and the wall of the cylindrical part of the casing are as close to the

impeller as possible, so that there is a barrier or stripper (9) between the two ports. The stripper closes the channel and thus blocks the fluid in the discharge side from communicating with that in the inlet port region such that only the fluid trapped within the blade passages can pass through the stripper. Of course there is also the leakage through the clearances between the stripper and the impeller due to the pressure difference across the stripper. In the sector of the stripper there must be at least one blade at any one time so that a seal is formed all the time. The more the blades there are in it at any one time the better is the sealing effect.

1.2.4 Mode of operation

As with all rotodynamic machines pumping liquid, before a regenerative pump is started for the first time, it must be filled with liquid; subsequently, this is not necessary since the inlet and discharge brances are both directed upwards so that a residual charge of liquid remains in the pump. The operation can be described in two stages: priming stage and normal running.

1) The priming stage:

The suction piping is full of air or any other gas for that matter. As the impeller rotates, the liquid is thrown outwards by the centrifugal forces to form a ring in the outer part of the blades and the channel. A pressure gradient is created between the free space, which is formed between the liquid ring and the hub, and the suction pipe. Air is thus drawn in through the inlet port. As each successive blade cell approaches the discharge port, it starts filling with the liquid in the channel because the latter progressively tapers and closes in towards the stripper. The contents of the inner part of the cell is thus compressed and expelled when the cell comes abreast of the discharge port. The latter is situated radially rather closer to the axis than the impeller outer diameter. The channel is completely blocked by the stripper immediately after the discharge port.

When a blade cell passes the stripper and thus reappears opposite the suction port, the liquid filling it is again thrown radially outwards under centrifugal forces to reform the ring at the outer part of the impeller and channel. A free space is recreated between the hub and the liquid ring and more gas and liquid enter the pump under the

resulting pressure gradient. This cycle continues until the gas has been evacuated from the suction pipe. The pump then draws liquid only and the priming stage is completed. The liquid ring is no longer a mechanism in the pump operation. Other patterns of flow develop.

2) Normal running

There is considerable difference of opinion about the flow patterns and the mechanism of energy transfer after the priming stage is completed. Two main schools of thought will be considered in detail in section (1.3). In this work, however, it is considered that the fluid, in the working section of the pump, follows streamlines which are roughly helical in shape. These are formed because the flow repeats a circulatory motion in the meridional plane while it travels in the tangential direction towards the exit. The motion is broadly radial and outwards in the impeller under its centrifugal effect. Fluid in the channel moves into the lower part of the impeller to replace it. The fluid leaving at the outer part of the impeller enters the channel at is outer part. It then moves mainly radially inwards in the channel. The fluid thus circulates between the impeller and the channel while it moves also in the tangential direction. This impeller re-entering is repeated several times before the fluid reaches the discharge port. Each time it enters the impeller more energy is transferred to it.

The flow pattern has much in common with that found in fluid couplings and torque convertors.

1.2.5 Performance characteristics

There are three main features in the performance characteristics of regenerative pumps:

1) They develop high heads at low flow rates and relatively low shaft speeds i.e. they are applied for low specific speeds.

2) They are completely self-priming.

3) They have relatively low efficiencies.

Features (1) and (3) are reflected in the general diagram of the maximum efficiency plotted against specific speed, see Fig. (1-5), which shows approximately the ranges of application of different types of pumps.

Fig. (1-6) shows the dimensionless performance characteristics of a typical relatively low-head regenerative pump compared with those of a typical high-head design shown in Fig. (1-7).

Although regenerative pump applications cover the lowest range of the specific speed and those of the propeller pumps cover the highest range, the trends of their performance curves are very similar. The curve $H = f(Q)$ is stable and falls steeply. The power input attains a maximum at zero flow.

1) Low specific speed applications

Regarding the high-head characteristics, comparison with centrifugal pumps is more revealing because both groups operate on the low side of the specific speed range.

From published data it appears that the head generated by a regenerative pump may vary from 2.5 to 10 times the head generated by an ordinary centrifugal pump with comparable impeller diameter and speed. Table (1-1) shows a general comparison between regenerative and centrifugal pumps.

Single-stage pump	Range of (Ns) $(N\sqrt{Q}/H^{3/4})$	Range of $(\dot{Q}/(\omega D^3))$	Range of $(gH/(\omega^2 D^2))$
Centrifugal pump	10 - 100	0.01 - 0.02	0.2 - 1.0
Regenerative pump	1 - 10	0.005 - 0.01	1.0 - 2.0

Table (1-1): Comparison of Centrifugal and Regenerative Pumps

Due to their low specific speeds regenerative pumps are replacing multi-stage centrifugal pumps in some applications: their size and weight are smaller and they are easier and cheaper to build. For the same reason they also replace single-stage centrifugal pumps in the range of specific speeds where their efficiencies are comparable: the size and weight are a deciding factor in many applications. They have been found particularly attractive for lubrication, control, filtering and boosting systems as in boiler feed, spraying, fire fighting, high pressure washing, etc.

As an example Table (1-2) gives a comparison between candidate pumps for use in screen wash units in automobiles. Some of the requirements are: self-priming, high-pressure, low discharge, small in size and light in weight.

Pump	Pressure head (atms)	Flow rate ($m^3/s \times 10^{-6}$)	Speed (rpm)	Effective Diameter (mm)	Efficiency (%)
Eccentric rotor positive displacement	1.02	15.0	930	7.925	21.0
Radial centrifugal	0.816	11.0	1400	19.4	7.5
Regenerative	1.02	15.0	940	12.323	45.0

Table (1-2): Comparitive Pump Performance Data (reproduced from ref. (19))

2) Self-priming

The suction lift of many regenerative pumps is reported to be as high as 90% of the atmospheric pressure. They exhaust air and vapour from the suction spaces rapidly. In normal operating conditions lifts of about 7 metres are common practice. Regenerative pumps are therefore used for the applications listed in section (1.2.1)

3) Low efficiency

Overall efficiencies achieved in regenerative pumps range from 20% to 45% in most cases while the maximum peak efficiency claimed, up to now, is not more than 50%. However, the pumps are usually utilised for handling small flow rates and hence the absolute extra consumption of

power could be small and, in many applications, outweighed by their combined advantages.

Low efficiencies are due to energy losses caused mainly by the following factors:

1) The circulation of the fluid between the impeller and the channel: this involves shock losses at entrance to the blades, losses in the blade passages and losses in the channel.

2) Shocks experienced as the fluid leaving the inlet port enters the working passage of the pump.

3) Shocks experienced as the fluid is forced to leave the impeller and enter the discharge port: the flow direction there is opposite to that of the centrifugal force because the port is opposite the hub rather than the tip of the impeller.

4) Losses in the ports themselves: the shape, size and orientation of these ports are usually dictated by the need to ensure self-priming.

5) The leakage through the clearances between the stripper and the impeller from the high pressure discharge port region to the inlet region.

Losses mentioned in (3) may be eliminated if the liquid is taken off through a port, cut mainly radially in the casing opposite the tip of the impeller, such that the flow into it is in the same direction as the flow under the effect of the impeller centrifugal forces. This is not done, however, because the pump would then lose its capacity as a self-priming pump.

One of the objectives of this work is to minimise the losses mentioned in (1) by providing an understanding of the flow pattern within the machine.

1.3 Historical Survey

A number of works devoted to the theoretical and experimental study of the operation of regenerative pumps have been published. With the aid of experimentally determined empirical performance factors some theoretical methods were developed to predict the performance characteristics of particular designs. However, the results so far obtained are not sufficiently conclusive to allow any definite recommendations to be made in regard to the design of a pump for any specified operating conditions. The design of these pumps is believed to be based chiefly on experimental data obtained from tests on existing pumps.

In the following the two main schools of thought regarding the flow patterns in these pumps and some other important works are outlined.

1.3.1 The two main theories

All theoretical methods developed up to now to investigate regenerative pumps may be associated to one or the other of two main theories as to the way in which, after priming has been accomplished, the energy is transferred from the impeller to the fluid. The two main theories are:

1) The re-entrant centrifugal-pumping theory:

This theory considers that the energy transfer is accomplished through repeated circulation of the fluid from the impeller to the channel and back under the centrifugal effect of the impeller. The fluid follows approximately helical paths because while it circulates between the impeller and the channel it also moves in the tangential direction towards the discharge port. The pump is considered, in essence, as a centrifugal device and the energy transfer is considered to be through dynamic action.

The fluid in the impeller flows outwards mainly radially and on leaving the impeller at its outer parts it returns to the channel from which the fluid flows back into the impeller at its lower part. In the channel the circulatory flow is largely radially inwards. As this motion takes place the fluid also moves tangentially in the direction of the impeller rotation. The circulatory motion is repeated several times while the fluid traverses from the inlet to

the outlet: each time it enters the impeller more energy is added to it by the impeller.

This pattern of the fluid motion is shown schematically in Fig. (1-8), such theory is supported by: Willson, Santole and Oelrich (7), Pfleiderer (8), Bartels (9), Wright (10) and others. The theory is best represented by the analysis given by Willson, Santole and Oelrich in Ref. (7). In the model analysed in that reference the entire pump flow was assumed to be represented by a mean streamline. All the circulatory flow was assumed to leave the impeller at the tip of the blades. The mean streamline was assumed to be of the form shown in Fig. (1-9) so that in each of the four segments of the streamline the tangential velocity (V_θ) in the channel could be expressed as a function of one variable only: either (r) or (z).

Expressions were derived for the prediction of the performance characteristics of the model in terms of three empirical parameters. These three parameters were determined by forcing agreement, at three points, between the theoretical and the actual characteristics.

2) The turbulent-drag theory

This theory considers turbulent friction between the impeller (moving as a rough surface) and the fluid in the channel to be the primary force causing the pumping action. The circulatory motion induced by the centrifugal forces and which is the backbone of the previous theory is not recognised. The impeller is considered, in effect, as a rough surface moving in a channel full of fluid. The fluid is dragged along by the shearing effect of the impeller and, with suitable restraints in the channel, the fluid head is increased in the direction of the flow. Such pattern of flow is shown schematically in Fig. (1-10).

This theory is supported by Senoo (1), Wilson (2), (20), Miyadzu (3), Iversen (4) and others. Iversen (4) has given the simplest and most straightforward application of the turbulent-drag theory. He has analysed the performance of a pump in terms of shear stresses from consideration of a linear system as shown in Fig. (1-11). He did not include any detailed specification of the fluid motion within the pump but merely specified a pumping shear between the impeller and the fluid in the channel and a retarding shear between the fluid in the channel and the channel walls. Expressions were derived for the

prediction of the performance of the pump. The expressions involved three empirical factors: two shear coefficients and an effective impeller velocity. The end points of the experimental head curve $H = H(Q)$ and the end point of that of the power curve $P = P(Q)$ at zero flow rate were used to obtain three equations to evaluate the three factors. The theoretical relations were therefore forced to match with the experimentally determined end-points.

1.3.2. Comments on the two analyses:

Each of the two types of analysis reported above needed three empirical factors to be determined experimentally from tests on the pump being analysed. The distinction between the two idealisations is, however, more fundamental: in the first analysis the pump is treated, in essence, as a centrifugal device and the impeller as a mainly radial flow runner; in the second analysis the centrifugal effects are entirely neglected and the impeller is treated as a super-rough surface.

Regarding the scope of the two analyses, the following may be pointed out:

1) Since the internal flow mechanism is not specified in detail, there are no conclusive results as to the way in which the impeller and channel can be designed.

2) Independent prediction of the magnitude of the three empirical factors is not reported to be possible and when determined experimentally for a particular pump design, their applicability to geometrically similar pumps is yet to be verified.

3) Since the fluid viscosity has been ignored in these analyses, its influence on the limits of application of the derived relations remains to be investigated.

The compatibility of each of the two theories with observed flow trends can be examined in the light of the experimental work reported in the next section.

1.3.3 Experimental studies

In the literature several investigators have reported experimental tests carried out on regenerative pumps in order to obtain an understanding of their internal flow.

Bartles (49) tested three rotors in the same pump casing. The first rotor was a smooth disc, having no grooves or vanes; the second was grooved out to leave the radial vanes of conventional design; and the third had conventional radial vanes plus additional vanes normal to them. If the first rotor pumped, it would have to be due to the viscous drag of a smooth metal disc. If the second rotor pumped, it might be due either to the shearing stresses of viscous and turbulent drag or to the mechanism in which the fluid circulates into and out of the impeller along helical paths under the centrifugal forces. If the third rotor produced pumping it would prove that the shearing stresses are the primary force causing the pumping because any possible radial flow was largely prevented by the cross blades; if it did not pump, or largely rendered ineffective, then the pumping would be proved mainly due to centrifugal action because the shearing capacity of the radial blades could hardly be affected by the cross-blades. He found that the pump would work only when the impeller design permitted circulatory motion and centrifugal pumping.

Crewdson (13) also examined the role of the circulatory flow, or the centrifugal pumping, in the process of energy transfer in a regenerative pump. A thin brass strip was soldered along the middle of the side channel so that the side channel is divided into two parts, see Fig. (1-12a). Thus any circulatory flow, which is mainly radially inwards in the channel, would be greatly affected and it might have been split into two: one in the lower part of the channel and one in the upper part - as shown in the figure. The effect of this arrangement on the fluid motion inside the impeller could not be easily judged. However, the suggestion is that although greatly hindered, the circulatory flow was not eliminated completely because there were still the centrifugal forces and the channel, although the latter was plit into two. Performance curves of such a pump, with and without the brass strip, are reproduced in Fig. (1-12b). The lowering of the head curve, $H = H(Q)$, makes clear that the reduction in the circulatory flow greatly reduces the pumping effectiveness.

Lazo and Hopkins (5) and Lutz (6) conducted experiments with a small thread probe to determine the direction of the velocity at different points in a section of the annular flow passage of the pump. They were able to corroborate an expectation that the fluid follows helical streamlines as shown in Fig. (1-8).

1.3.4 Experiments to investigate design parameters

Experimental studies were also conducted by different investigators with the aim of establishing the effects of the various design parameters on regenerative pumps performance. Such researches were intended to furnish for comprehensive design and performance-prediction schemes which take into account the effects of impeller shape and dimensions, channel shape and dimensions, clearances, suction and discharge ports design, etc.

Senoo (1) experimentally investigated the influences of the suction port location on the characteristics of a regenerative pump. He established that when the inlet port is very close to the barrier, the fluid enters the pumping passage too far upstream where the impeller effect is not fully realised. A pressure difference is thus needed between the inlet port and the entry region to maintain the in-coming flow. Such a pressure drop constitutes a considerable energy loss when the discharge flow rate is high because the necessary acceleration is high. He reported that the pump performance could be considerably improved if the inlet port is appropriately located downstream from the barrier such that fluid entered the pump passage in a region where the impeller effect was reasonably established. He gave the figure of 65 degrees for the angle between the barrier and the inlet port as the optimum angle for the design he considered.

However, such a parameter has not been correlated with other design parameters. Similar experimental investigations are, therefore, necessary for each other design.

Shimosoka and Yamazak (17) investigated the effects of varying the dimensions of the channel, impeller and the clearances. Fixing some of the dimensions they established the effects of varying the others on the performance of the pump. They found that, due to the numerous

variables involved, it was not possible to establish a comprehensive scheme for the performance prediction. They concluded that the dimensions of a high efficiency pump can be obtained by systematic experimentation.

1.4 Outline of Present Work

The experimental studies reported in section (1.3,3) indicate that the turbulent-drag theory is not compatible with the direct observations of the pump flow mechanisms. These studies support the theory that the fluid follows helical streamlines and that the circulatory flow is an important factor in the process of energy transfer to the fluid. The work reported in this thesis is founded on basis of this theory.

The repeated re-entering of the fluid into the impeller and the corresponding repeated energy addition to it could be described as internal multi-stage flow pattern or regenerative. It is therefore appropriate to use the name 'regenerative' to refer to these pumps.

In this work a theoretical analysis of regenerative pumps is developed. A typical pump for which the analysis is applicable is shown schematically in Fig. (1-13).

In this analysis, a section of the pump circumference is defined in which the tangential pressure gradient is essentially constant. In this section the flow is modelled such that, when the principles of fluid mechanics are applied to it, the resulting flow equations are solvable by numerical methods with the aid of a digital computer. The velocity and pressure fields are thus estimated in the linear section and its performance is evaluated. The performance of the remaining section of the pump, here referred to as the non-linear section, is estimated by modelling the performance of the stripper and the ports on overall effect basis. Thus the performance of the pump as a whole is predicted at any desired operating condition. The latter is represented by a pressure gradient in the linear working section.

The analysis does not involve empirical factors which need to be determined experimentally from tests on the pump considered. However,

well established loss empirical parameters, such as the friction loss factors of flows in closed condiuts, are used to estimate losses where appropriate in the system.

The basic assumption made is that the flow field is steady and incompressible. Hence only the velocity and the pressure are to be computed using the flow equations.

The analysis predicts the performance of a given pump. The information needed to carry out the analysis include the shape and dimensions of the impeller, the dimensions of the channel, the number of blades, the stripper angle and clearances.

The solutions of this direct method are carried out by assuming a stream function relationship to represent the meridional velocity everywhere in the linear section under a specified pressure gradient. A procedure is developed to establish the appropriate relationship under given conditions. The remaining parameters, the tangential velocity and the pressure, are obtained by solving the equations of motion and the energy equation (the equation of continuity being already used to set up the stream function relationship). The flow field is thus approximately solved.

The analysis is used to predict the performance of a number of pumps whose experimental performance characteristics are available and results are compared.

This approach differs from those published up to now in many ways. The simplified flow equations of the system are solved along any desired streamline. Useful light is therefore shed upon the details of the internal flow of the pump. The behaviour of the flow in the blade passages, in the channel, across the incidence transition from the channel into the impeller, and in the stripper region is detailed and the corresponding losses are explicitly estimated separately. Thus in effect the method can be used as a first approximation design method because the effects of the various design parameters can be investigated without the need to actually build the pump.

1.5 Summary

Regenerative pumps are self-priming, high-head low-discharge pumps which are suited for operation in the low range of specific speeds. Their main drawback lies in their low efficiency which is, up to now, below 50%. However, even so they may be more efficient than centrifugal pumps operating in the same low range of specific speeds. In some applications they may be chosen for their ligh weight, compactness and self-priming characteristics and because their low efficiency usually results in insignificant extra consumption of power since the pumps handle small flow rates.

Although the pattern of their internal flows has been sufficiently clarified by experimental tests performed by several investigators, the prediction of their performance characteristics by purely theoretical methods has not up to now been published. The objective of this work is to develop a theoretical analysis which should enable their internal flows to be quantitatively solved and their performance to be predicted. Of the two well-known, but fundamentally different schools of thought regarding their mechanism of pumping, the circulatory impeller-channel re-entrant motion, which is maintained by the centrifugal forces, is considered in this work to be the mechanism through which the pumping is effected.

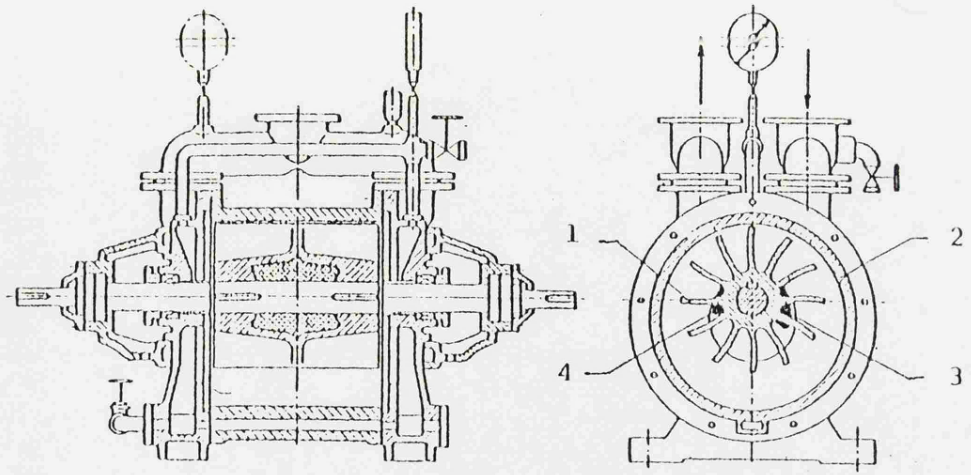

(a) Eccentric impeller water-ring pump

1 - Impeller, 2 - Casing, 3 - Inlet port,
4 - Outlet Port, 5 - Side plate.

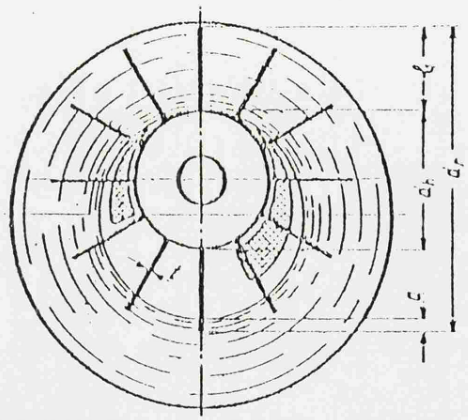

(b) Diagram for calculating the theoretical discharge flow rate (Q_i)

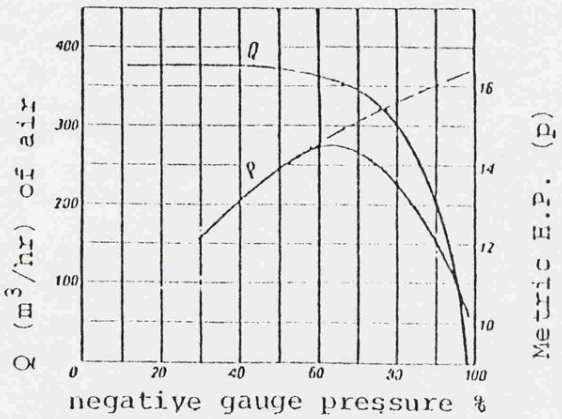

(c) Characteristics of pump shown above

$$Q_i = \frac{W_b N}{60} \frac{\pi}{4} (d_r - a - d_h^2) - Z(\ell_1 - a)t$$

where:

W_b = axial width of impeller

Z = number of blades

Fig. (1.1): Typical eccentric impeller water-ring pump reproduced from ref (23)

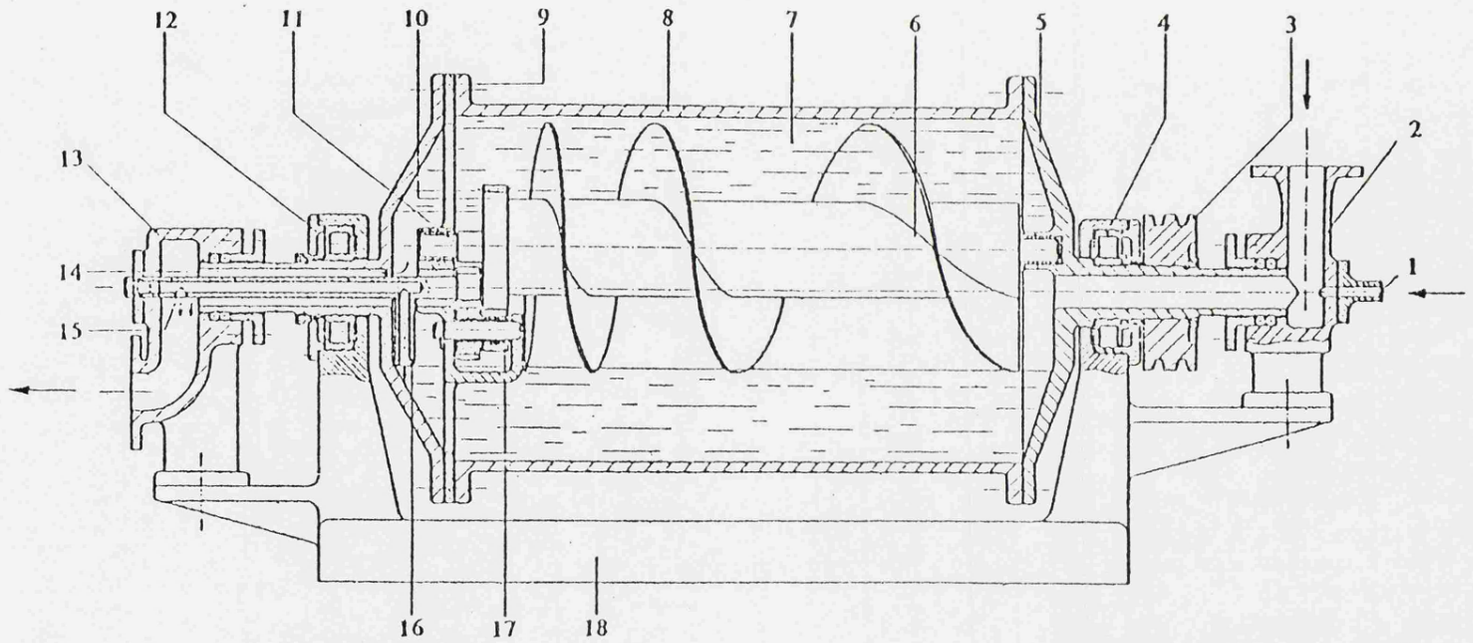

1. Ring liquid inlet
2. Intake branch mounting
3. Drive pulley
4. Guide bearing
5. Revolving casing cover
6. Screw impeller
7. Liquid ring
8. Revolving casing
9. Bearing disc
10. Impeller pinion
11. Bearing pins
12. Expansion bearing
13. Discharge branch mounting
14. Gas outlet duct
15. Ring liquid outlet
16. Level control
17. Gearing
18. Main bearing pedasta

Fig. (1.2): Longitudinal section of liquid-ring pump with eccentric screw impeller (reproduced from ref. (18))

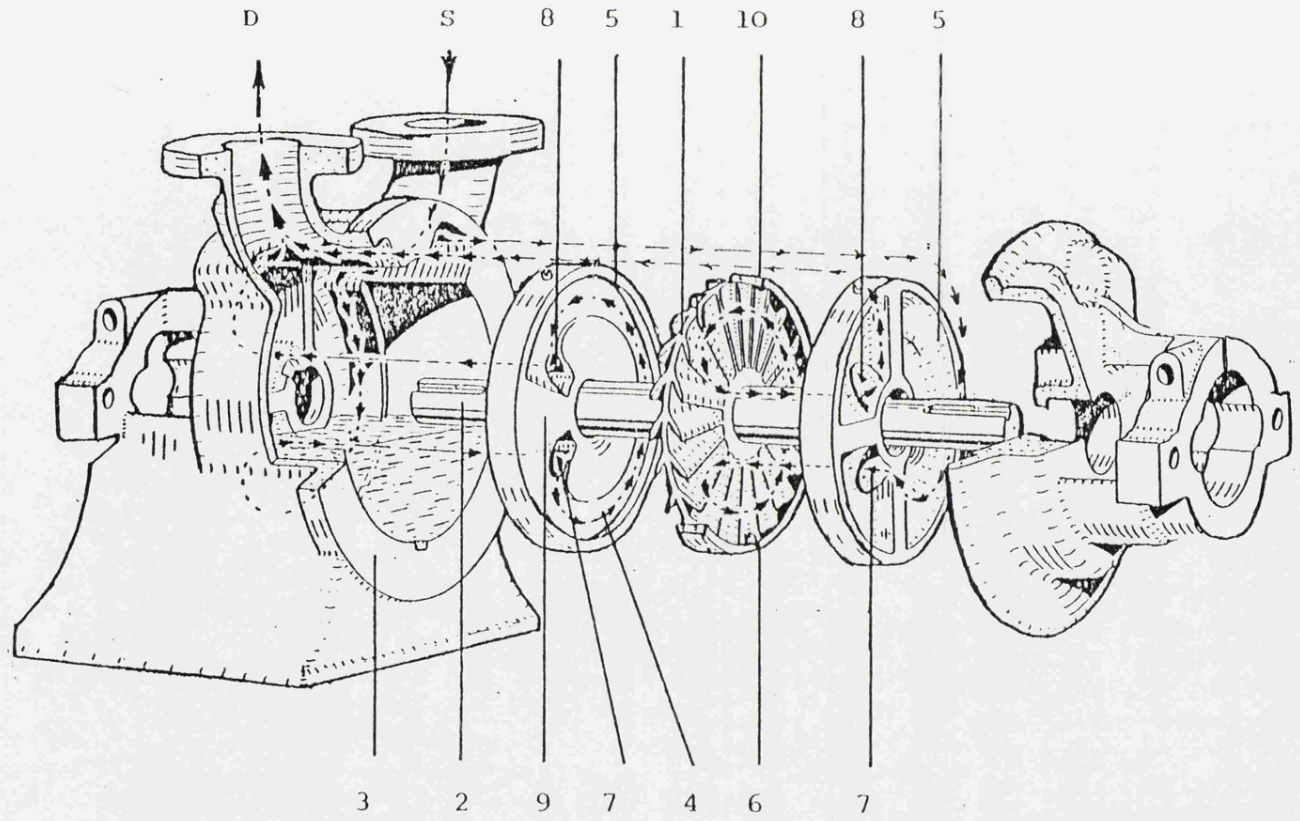

1. Impeller
2. Casing
3. Shaft
4. Side channel
5. Side plates
6. Peripheral channel
7. Inlet port
8. Discharge port
9. Stripper
10. Cylindrical ring
S: Suction branch
D: Delivery branch

Fig. (1.3): An exploded view of a typical regenerative pump (adopted from a GGG Publication)

Fig. (1.3)

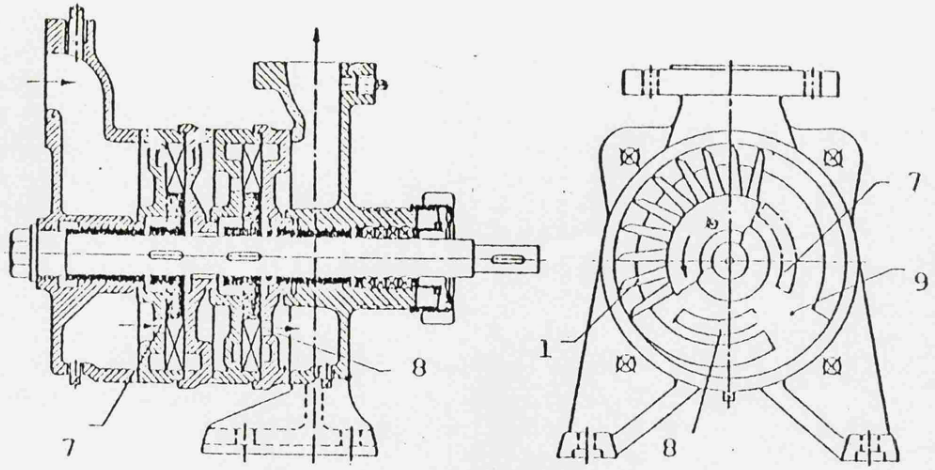

(a) A design normally known as the side-channel pump and its characteristics

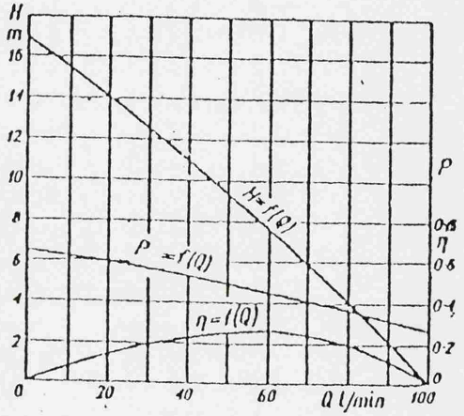

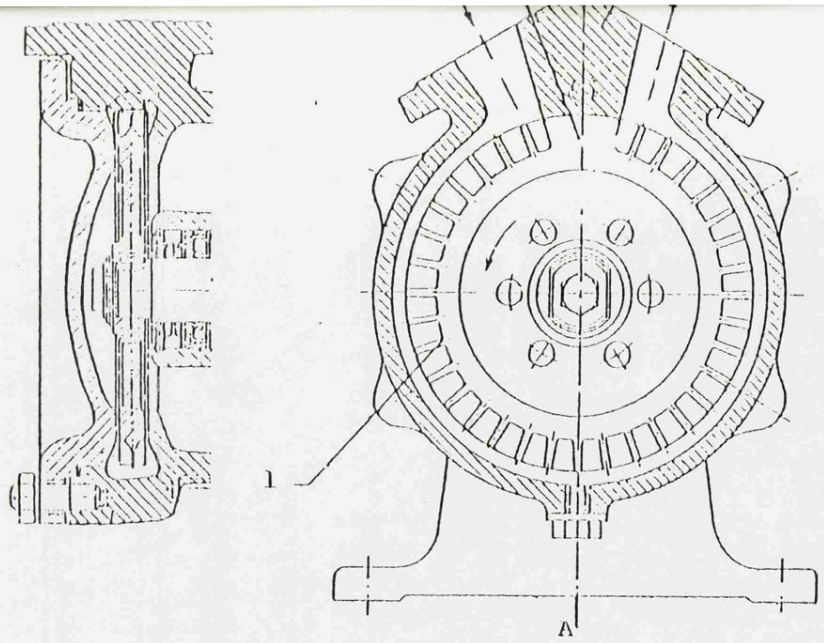

(b) A design usually known as the peripheral pump and a sample of its characteristics

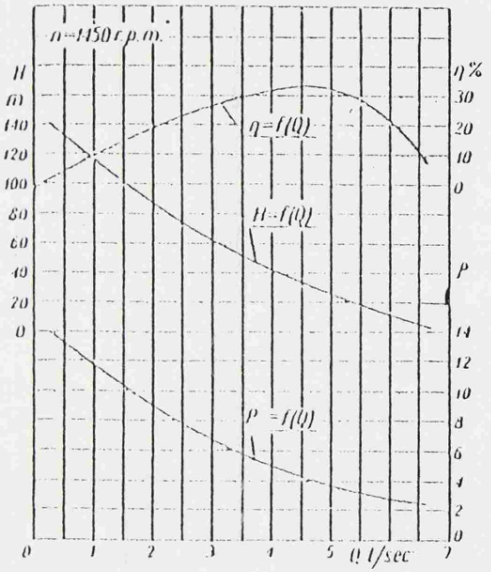

Fig. (1.4): Two different designs of regenerative pumps

Fig. (1.4)

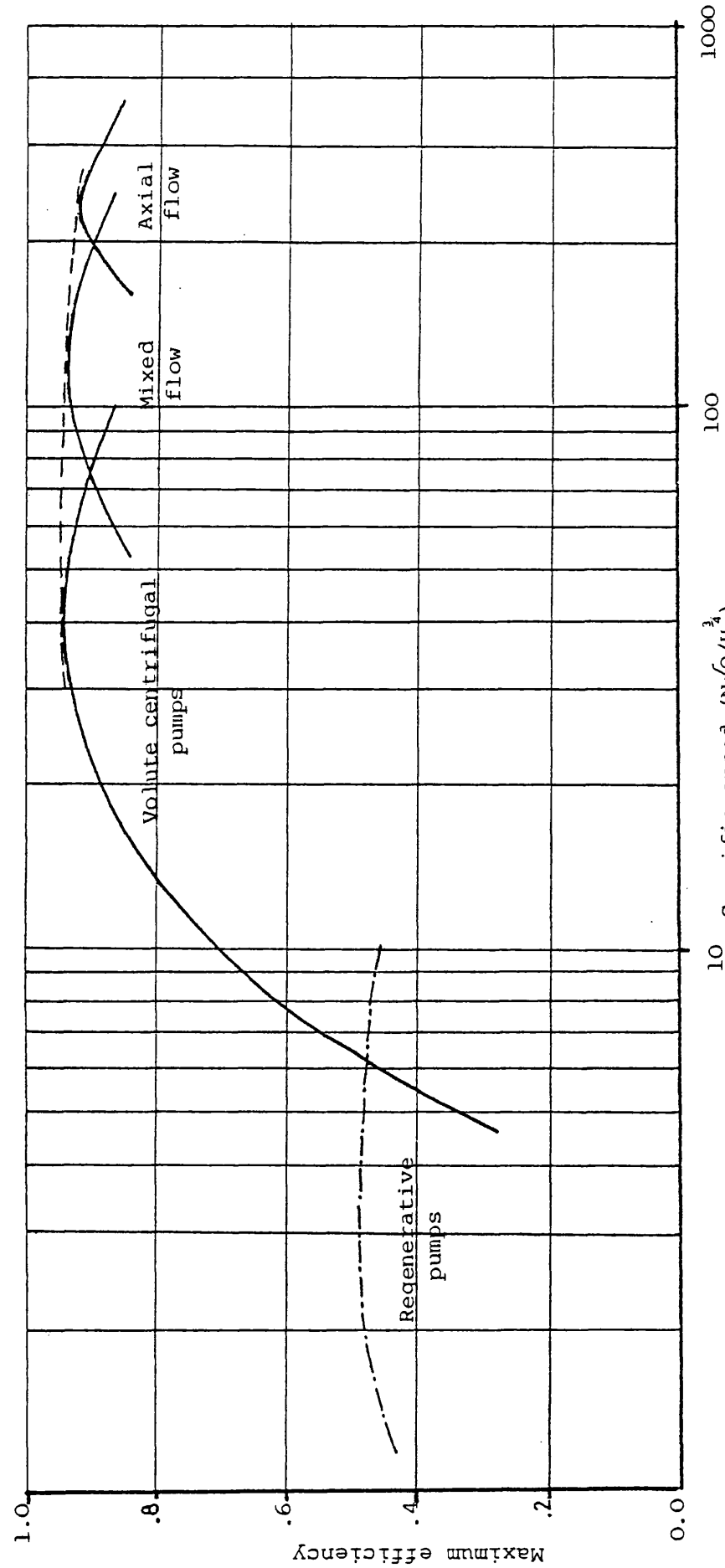

Fig. (1.5): Maximum efficiency vis specific speed for different categories of pumps

Fig. (1.6)

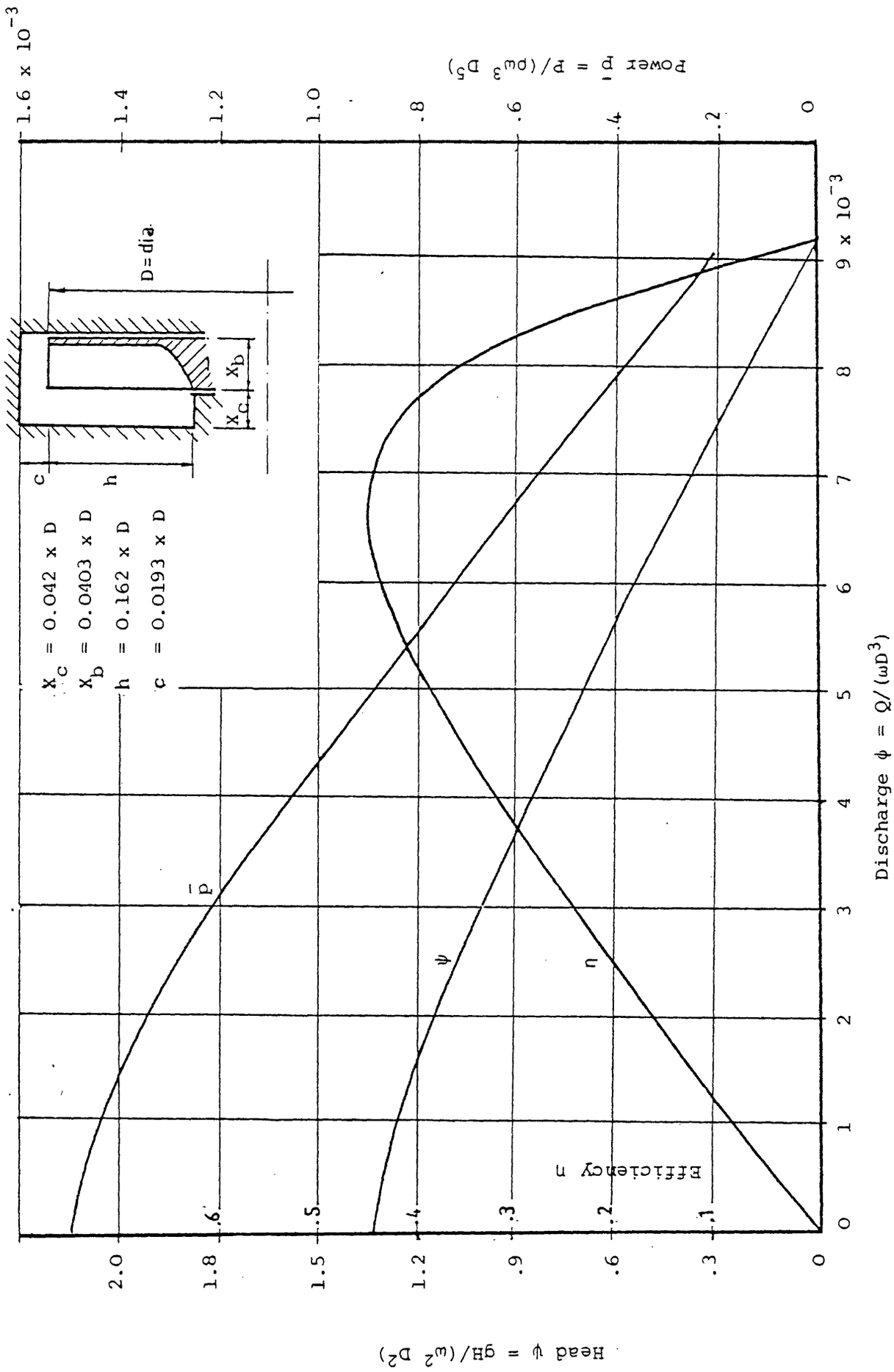

Fig. (1.6): Performance characteristics of STA-RITE TH-7 pump

Fig. (1.7)

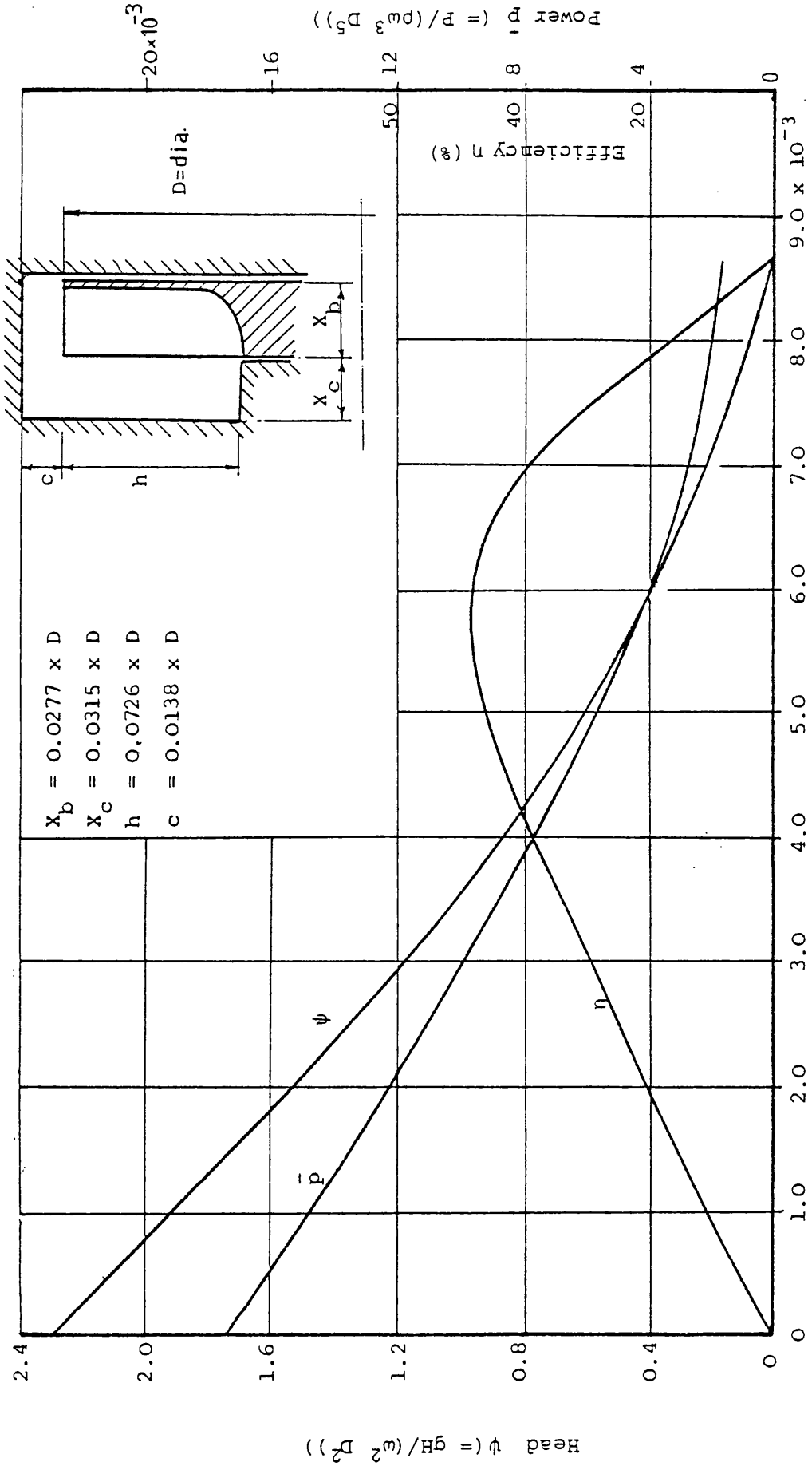

Fig. (1.7) : Performance characteristics of a typical high-head regenerative pump

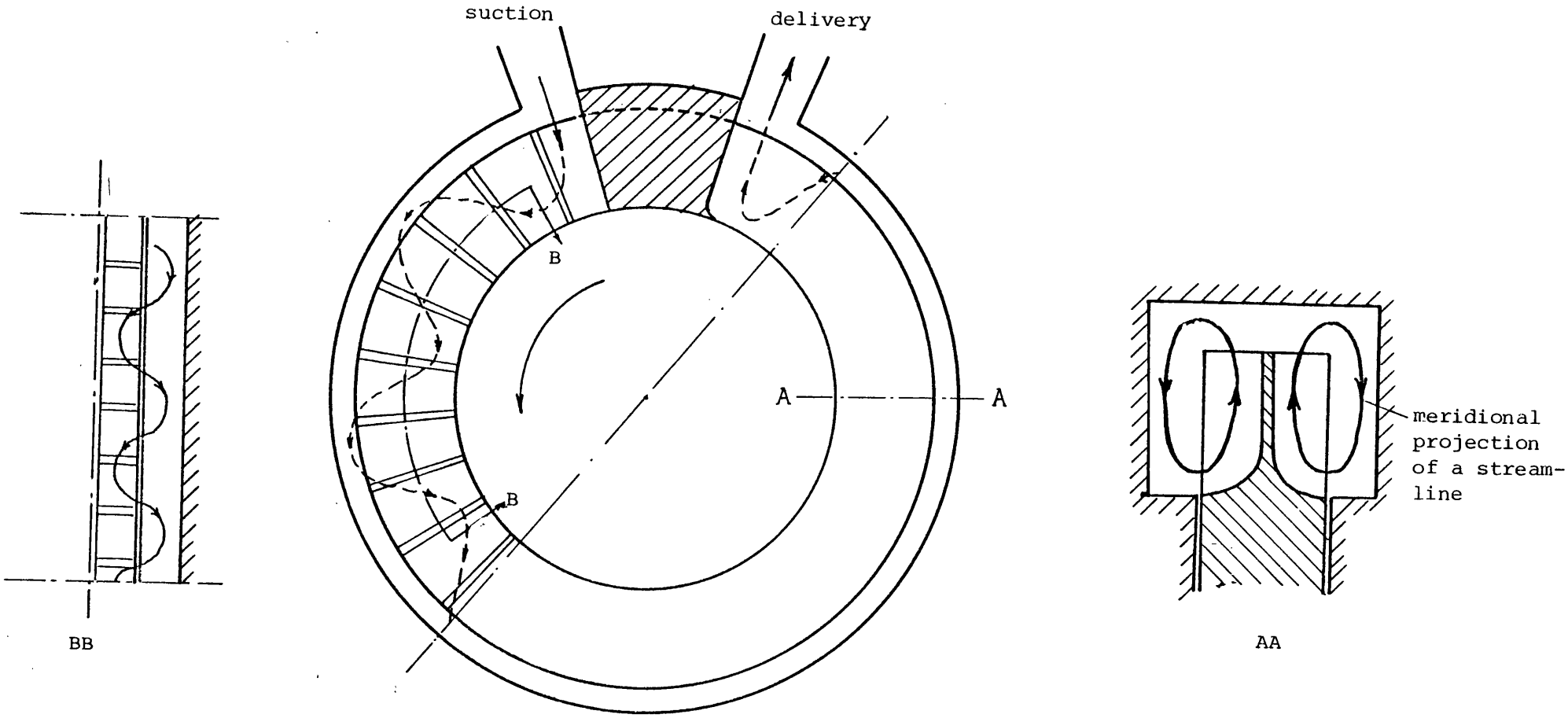

Fig. (1.8): Schematic diagram showing the pattern of the re-entral circulatory flow

Fig. (1.8)

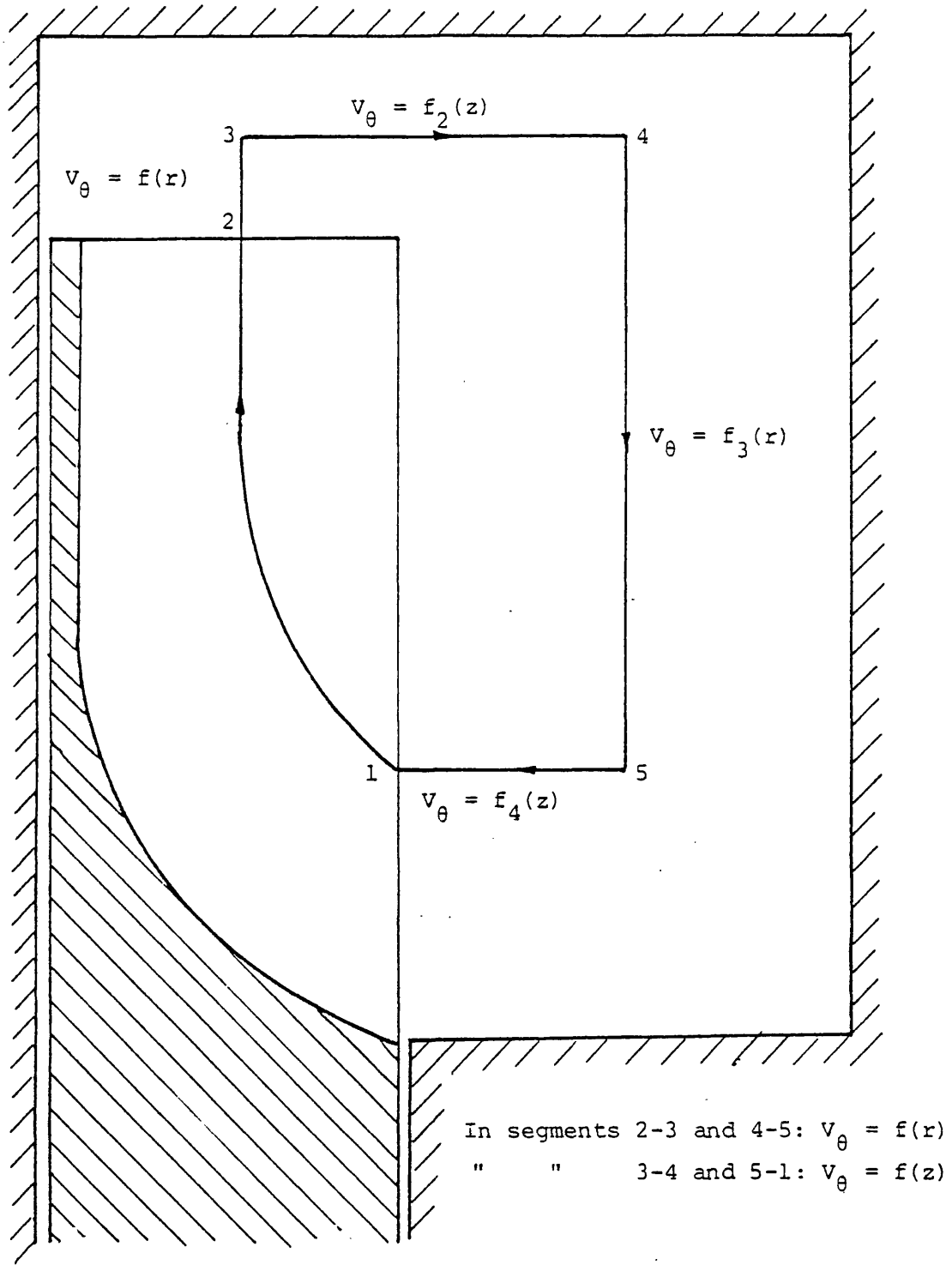

Fig. (1.9): Idealised mean streamline used by Wilson (7) to represent the entire flow

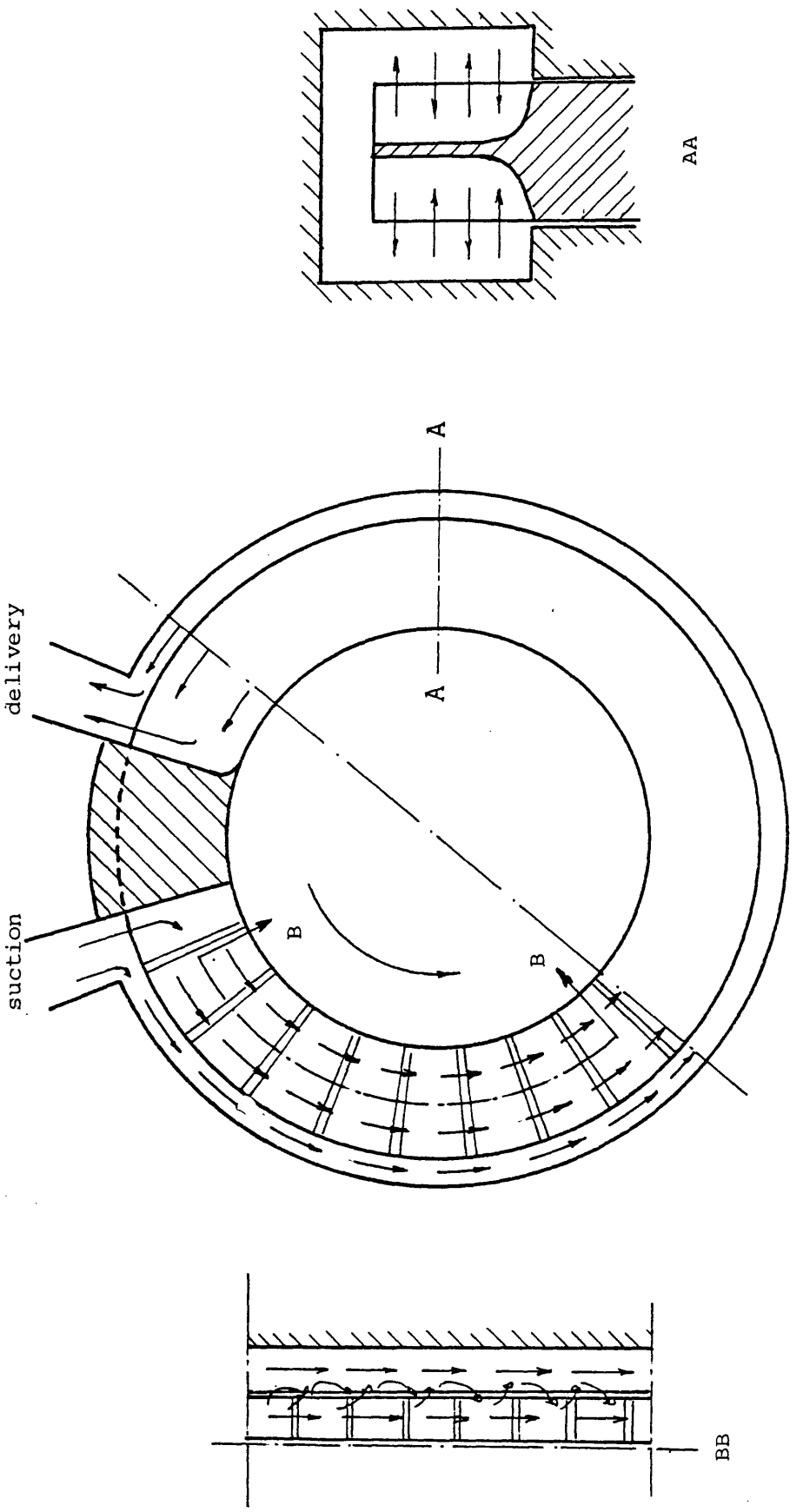

Fig. (1.10): Schematic diagram depicting the flow pattern according to the drag-theory

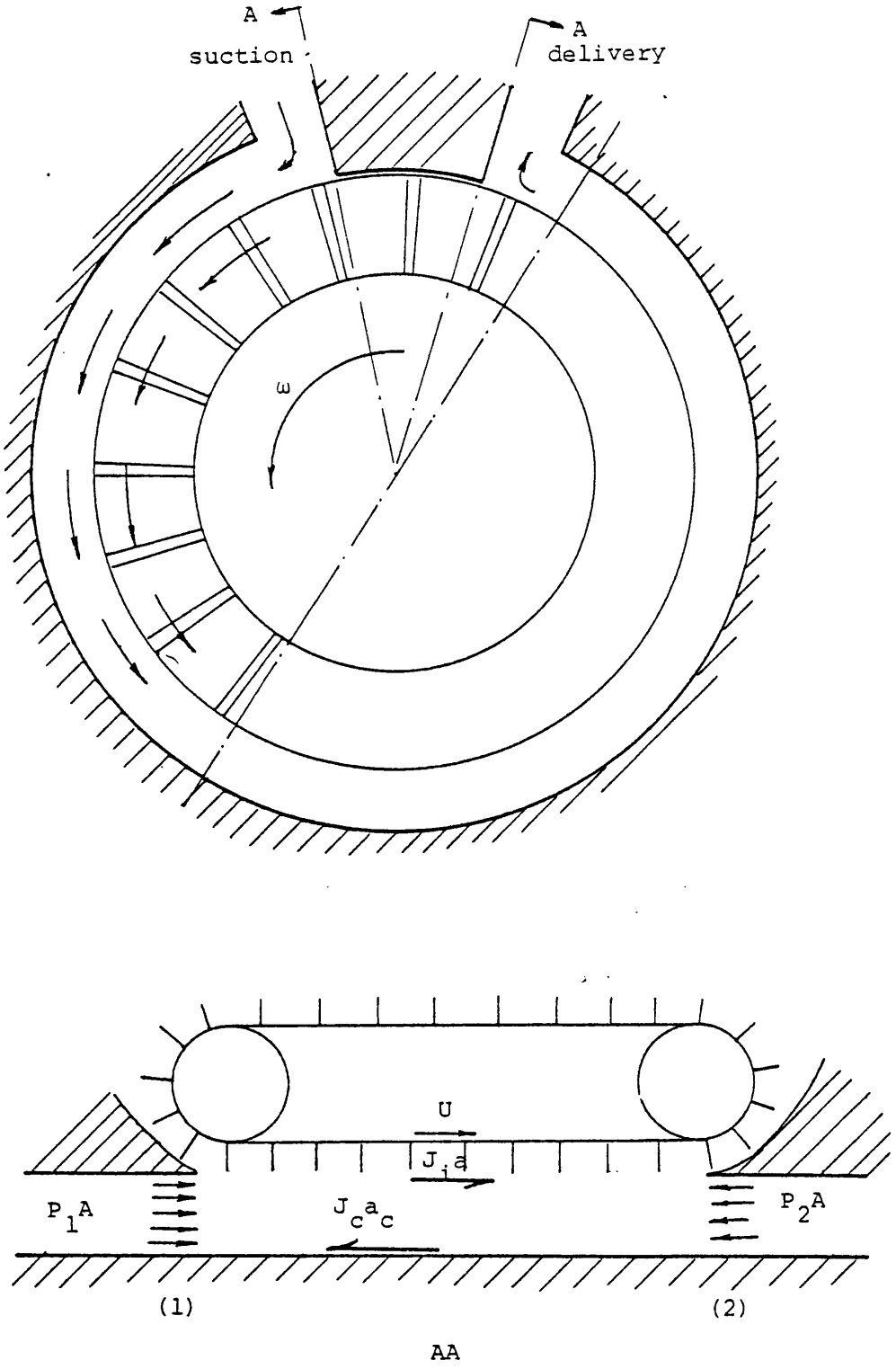

Fig. (1.11): Iversen representation of the pumping action by a linear motion of a rough surface

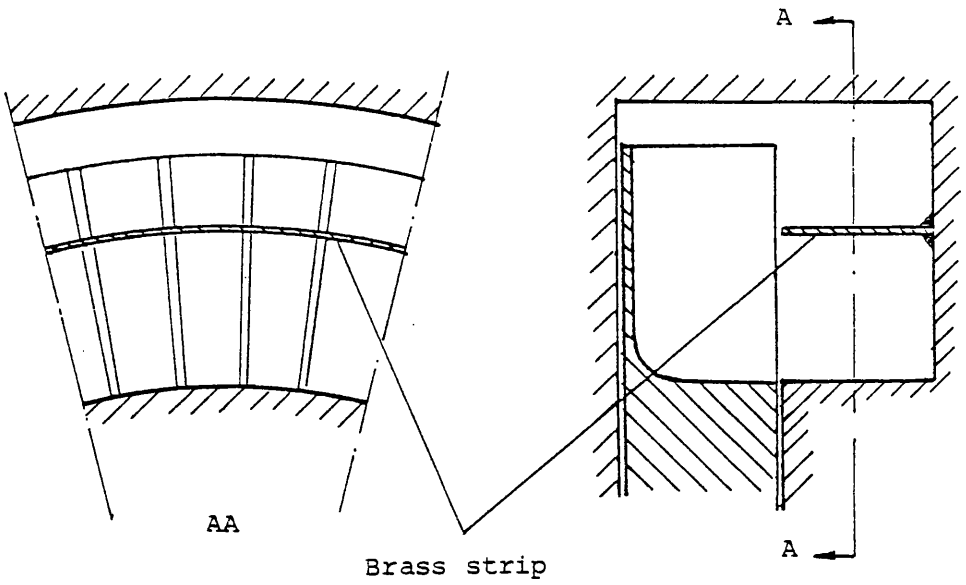

(a) Brass strip soldered in channel

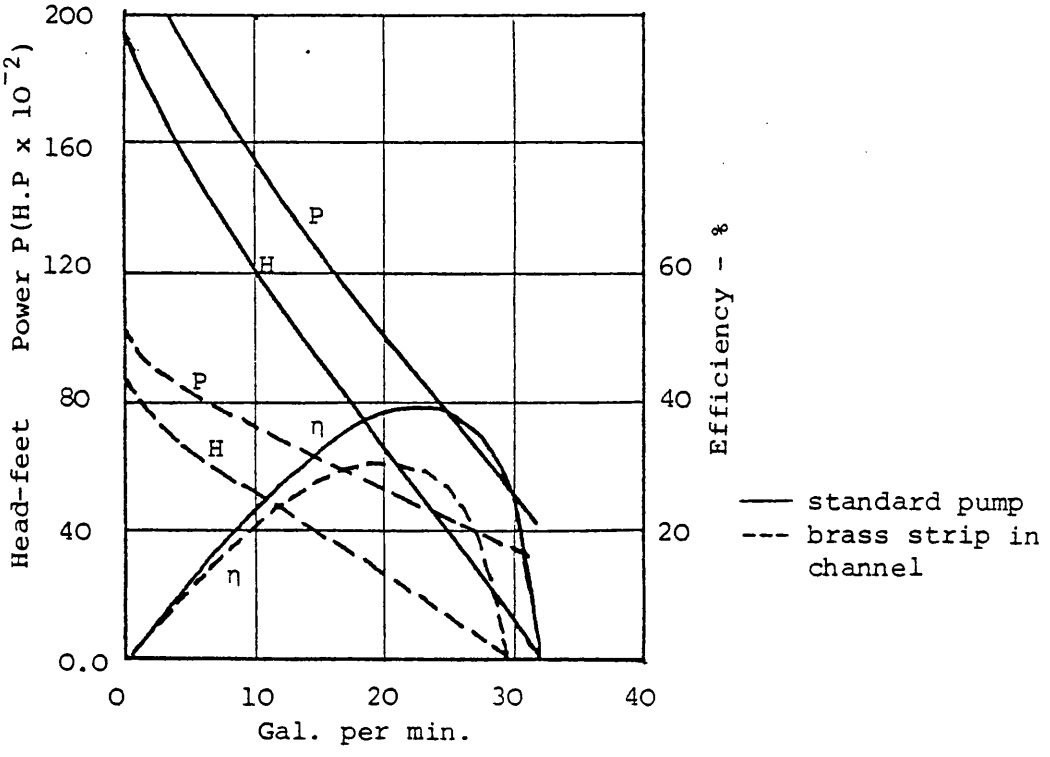

(b) Performance of a standard pump at 950 rev/min: reproduced from ref. (13)

Fig. (1.12): Effect of reducing the circulatory flow

Fig. (1.13)

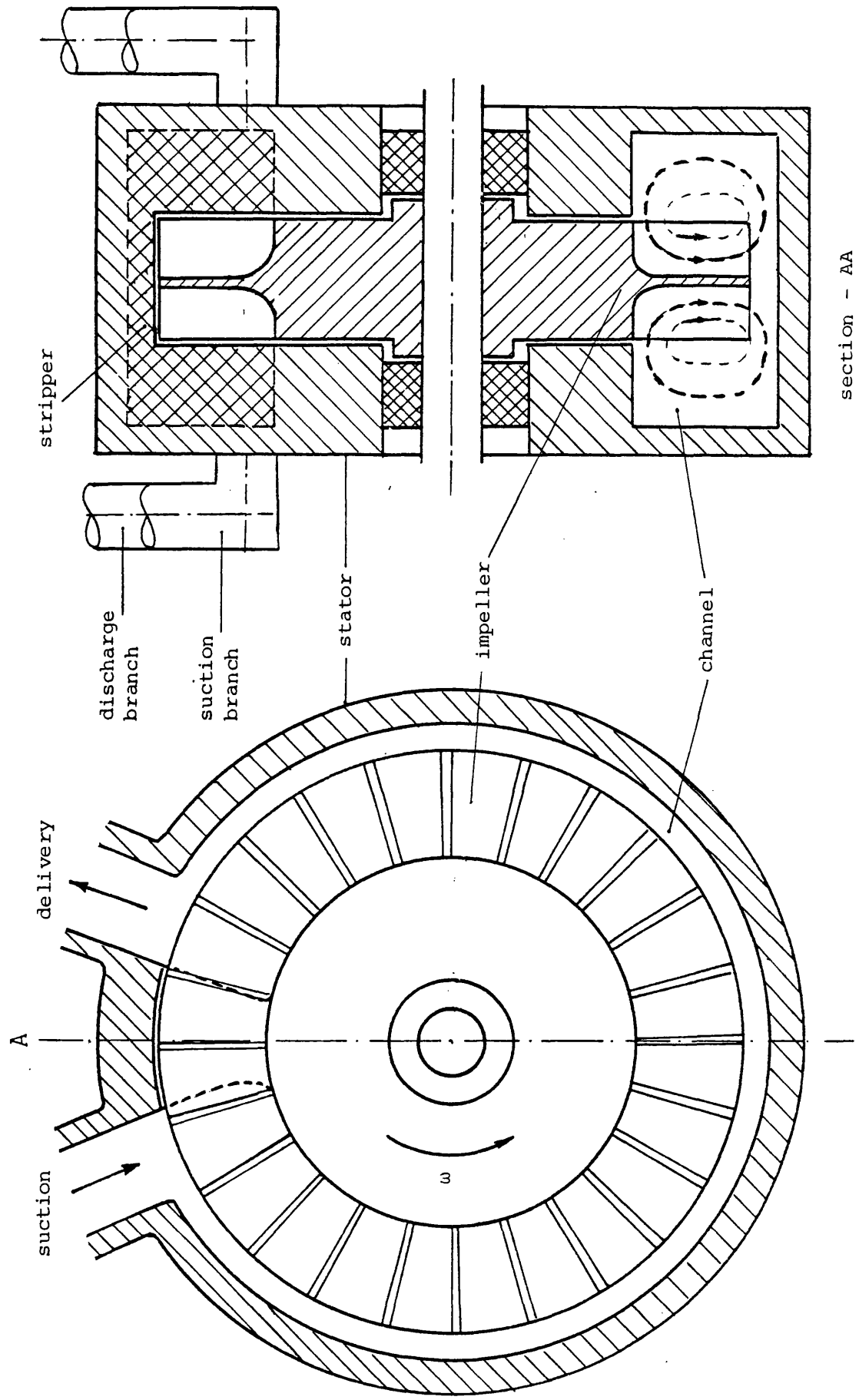

Fig. (1.13): Schematic diagram of a regenerative pump of a two-sided impeller

2. ANALYSIS OF THE LINEAR SECTION

In theory the velocity and the pressure fields in any incompressible flow can be related mathematically to the forces acting on the flow. However, the resulting mathematical equations are usually too complex to solve. Instead, the actual flow situations are approximated by model representations for which solvable equations can be derived.

As a basis of a theoretical analysis of regenerative pumps a hypothesis of operation of these pumps is assumed in light of the experimental evidence reported in section (1.3.3). A complex fluid flow pattern is thus replaced by a simplified hypothetical flow model.

In this chapter the flow field in the linear section is modelled. The general features of the actual flow are used and justifiable simplifying assumptions are made to develop the flow model. The principles of fluid mechanics are applied to write its flow equations.

Fluid frictional losses are discussed and empirical loss factors are used to estimate them.

2.1 Basic Flow Model

The idealisation of flow in the linear section of a regenerative pump is made such that the flow equations of the model can be solved by numerical methods with the aid of a digital computer.

Here the model is presented in general terms regarding the impeller and channel designs so that it may be applied to pumps of arbitrary designs. The specifications of the impeller geometry and detailed procedures of solving the model are given in later chapters.

2.1.1 The two sections of a pump

A regenerative pump may be divided into two regions:

1) The ports and stripper region and

2) The linear section.

These are now described in full.

1) The ports and stripper region

As shown in Fig. (2-1), this section of the pump is enclosed within the smaller of the pumps two sectors. It comprises the inlet and the discharge ports and the stripper between them. This region may take about 20% of the pump circumference. The larger part of it is occupied by the stripper whose function is to seal the channel between the two ports. It will be shown in chapter 3 that the required effectiveness of such a seal together with the number of impeller blades decide the angle of the stripper sector.

Although the pattern of flow through the clearances between the stripper and the impeller can be approximated by a simple leakage flow model, the pattern of flow in the inlet and discharge ports regions is exceedingly complex and there is no simple way of specifying it in detail. This is why this section of the pump is referred to as the "non-linear" section.

2) The linear section

In general terms this section can be described as that part of the pump which contains the channel, i.e. from the inlet port to the discharge port, see Fig. (2-1). In this section energy is transferred from the impeller to the fluid. The total head of the fluid increases continuously from the beginning of this section downstream to its end. Fig. (2-2) reproduces typical experimental measurements of the head variation of the fluid as it circulates through the pump at different flow rates, Ref. (7). It can be seen that the head rise per unit angle $(\partial H/\partial \theta)$ is essentially constant in this region. This experimental fact is a basic element in the analysis developed here.

In the rest of this work the term linear section is used to refer to that part in which the fluid head increases continuously in the direction of the impeller rotation and in which the gradient $(\partial H/\partial \theta)$ is essentially constant. This definition may not include parts of the channel in the vicinity of the two ports.

2.1.2 Hypothesis of operation

The fluid in the linear section of the pump follows streamlines approximating qualitatively to toroidal helices as shown in Fig. (2-3). Their projections on to a meridional plane are assumed to form closed

loops. The fluid, while traversing from the inlet to the discharge port, circulates repeatedly between the impeller and the channel. At the discharge port it either leaves the pump or else it may be trapped between the impeller blades and the stripper and get carried over to the inlet region.

Energy is transferred from the impeller to the fluid each time it enters the blade passages. In addition to the familiar centrifugal head imparted to it, the fluid also gets carried downstream against the tangential pressure gradient in the pump. Thus while being subject to the motion dictated by the centrifugal forces on it, a fluid particle is simultaneously pumped to a higher energy level by tangential displacement. The centrifugal head imparted to the fluid each time it passes through the impeller is only a part of the total energy it receives. The pump, therefore, is not merely a centrifugal device.

In the channel, where there are no moving parts, the fluid not only receives no energy input but also loses energy due to the frictional losses it encounteres. At the lower part of the working section where the fluid leaves the channel and enters the impeller incidence or shock losses are bound to occur.

Terms Relating to the Hypothesis of Operation

The following terms are introduced to help make a quantitative description of the pump operation, referring to Fig. (2-3):-

The flow cycle:

In one complete flow cycle a fluid particle travels through the impeller from point (1) to point (2) and travels in the channel from point (2) to point (3) where it re-enters the impeller. The flow path in each flow cycle is actually an open-ended three dimensional trajectory. However, its projection onto a meridional plane is assumed to be a closed loop. Hence on a meridional cross section points (1) and (3) are the same point.

The push (θ_i):

It is the angular displacement through which a fluid particle is pushed downstream by the impeller in one flow cycle.

The throw (θ_c):

It is the angular displacement through which a fluid particle travels while in the channel in one flow cycle. The name conveys the idea that the impeller throws the fluid into the channel.

The carry (θ_n):

It is the net angular displacement through which the fluid is carried downstream in one flow cycle from point (1) to point (3). Then:

$$\theta_n = \theta_i + \theta_c \tag{2.1a}$$

Let: θ_{pc} = angular displacement covered in the peripheral channel per flow cycle.

θ_s = angular displacement covered in the side channel per flow cycle.

Then: $$\theta_n = \theta_i + \theta_{pc} + \theta_s \tag{2.1b}$$

The circulatory flow (Q_c):

In the linear section it is assumed that the flow in its re-entrant motion circulates about a circumferential axis of rotation, see Fig. (2-3). In an r-θ plane through the centre of circulation the axis of rotation is a circle of radius (R_m) which is to be determined in the analysis. On a meridional section the axis is seen as Point (C), located on the outer edge of the impeller blades, see section (4.7).

Consider any plane surface (S), as shown in Fig. (2-3), extending from the wall to the centre of circulation (C) and extending over the full circumferential length of the linear section. The circulatory flow (Q_c) is the total flow through such a surface, i.e.

$$Q_c = \int_S V_m \, dS \tag{2.2}$$

where S is the surface defined above and (V_m) is the meridional velocity of the flow.

2.1.3 Aspects of the pumping action

As the circulatory flow passes through the impeller, its angular momentum in the direction of the shaft rotation is increased by virtue of the work of the impeller. At the same time the impeller carries the fluid downstream against a tangential pressure gradient. Thus energy, additional to the commonly understood Euler head, is imparted to the fluid, unlike the case in conventional centrifugal pumps where the tangential pressure gradient is essentially zero.

In the channel the fluid flows against the tangential pressure gradient. To maintain the pressure gradient the angular momentum of the fluid drops continuously after it leaves the impeller. However, since the radial co-ordinates (r) changes along a streamline, the drop of angular momentum does not necessarily cause a continuous drop in the tangential velocity (V_θ) of the fluid in the channel. On the other hand conditions may be such that the tangential velocity in the channel decreases to the extent that reversed flow is produced in parts of the channel. In a particular pump the behaviour of the tangential velocity of the flow depends mainly on the pressure gradient ($\partial P/\partial\theta$) and the flow path of the fluid. Longer streamlines are more likely to have a reverse flow than shorter ones both because of the relatively longer time spent under the influence of the tangential gradient and the larger frictional losses due to the longer flow path.

According to the model the longest streamlines are those in the outer most streamtube which is in touch with the solid walls. The length of the streamline reduces to zero at the centre of circulation. The losses are also expected to drop from a maximum at the wall to zero at the centre of circulation.

2.1.4 Basic assumptions

The model used to represent the flow field in the linear section incorporates the following basic assumptions

1) The flow is steady (i.e. $\frac{\partial}{\partial t} = 0$)

2) The fluid is incompressible (i.e. ρ = constant)

3) Body forces are negligible compared with the pressure forces on the flow.

4) All processes taking place in the system are adiabatic.

5) There are no end effects due to the suction and discharge ports: the analysis applies only to the linear part of the working section where there are no end effects.

6) The tangential pressure gradient is constant throughout the linear section (i.e. $\frac{\partial P}{\partial \theta}$ = constant).

7) The velocity field is axi-symmetric everywhere in the linear section (i.e. $\frac{\partial \bar{V}}{\partial \theta} = 0$).

Assumptions (1) - (5) are normal practice in the analysis of rotor-dynamic machines. Assumption (6) is corroborated experimentally as mentioned in section (2.1.1) and shown in Fig. (2-2). However, a comment must be made about assumption (7).

In a rotor which changes the energy level of a fluid the blade force in the whirl direction maintains a pressure difference between the leading and trailing surfaces of the blade. Consequently, a circulation is set up round each blade with the effect of reducing the velocity relative to the blade on the leading surface and increasing it on the trailing side. Thus in any rotor the velocity does change in the tangential direction from one blade to the next. In ref. (22) a mathematical treatment is given to prove that the velocity field must vary in the tangential direction in any rotor which changes the energy level of the fluid.

If, however, the number of blades approaches infinity, the space between them approaches zero. The blade loading will be infinitely small and the change of velocity between the blades approaches zero. The path of the fluid is limited to the mean surfaces of the blades without a relative motion perpendicular to these surfaces. The relative velocity ($\bar{W}$) will be parallel to the blade surface everywhere, i.e. at any point in the impeller:

$$\bar{W} \times d\bar{S} = 0 \qquad (2.3)$$

where $\bar{W}$ = relative velocity of fluid to impeller at any location

$d\bar{S}$ = an element of blade surface at that location.

When the blade surface lies entirely in the meridional plane, i.e. $d\bar{S} = dS\hat{i}_\theta$, then from the above relation the tangential component (W_θ) of the relative velocity is zero everywhere.

Although a flow can not be axi-symmetric in a real rotor, assumption (7) is normal practice in the analysis of rotodynamic machines. In the channel of a regenerative pump where there are no moving parts and no transfer of energy to the fluid, this assumption should be more compatible with the real situation than is the case inside the impeller. Hence the velocity field is assumed axi-symmetric in the entire linear section.

At the exit from the blades the effect of slip is accounted for using an empirical slip model as is the normal practice in the analysis of turbomachines.

The above seven assumptions will be used in the following derivations.

2.2 Equations of Flow

The motion of the fluid in the linear section is described with reference to a cylindrical system of co-ordinates: r, θ and z, see Fig. (2-4). In this system of co-ordinates the velocity field ($\bar{V}$) at any point is:

$$\bar{V} = V_r \hat{i}_r + V_\theta \hat{i}_\theta + V_z \hat{i}_z \tag{2.4}$$

It is convenient to define another orthognal co-ordinate system: m, n, and θ as shown in Fig. (2-4). The co-ordinates (m) are the generatrices of the stream surfaces along which the total velocity ($\bar{V}$) is assumed to lie and there are no velocity components in the (n) direction normal to these surfaces. Then:

$$\bar{V} = V_m \hat{i}_m + V_\theta \hat{i}_\theta \tag{2.5}$$

The circulatory velocity ($\bar{V}_m$) is that component of the toal velocity which is parallel to the r-z plane. Since the axi-symmetric approach is adopted for the velocity field, the r-z plane will be referred to as the 'meridional plane' and the subscription (m) is used to refer to it. ($\bar{V}_m$) will be referred to as the circulatory velocity or the

meridional velocity and it is given by:

$$\bar{V}_m = V_r \hat{i}_r + V_z \hat{i}_z \tag{2.6}$$

Similarly the velocity of the fluid relative to the impeller is:

$$\bar{W} = W_r \hat{i}_r + W_\theta \hat{i}_\theta + W_z \hat{i}_z \tag{2.7}$$

or $$\bar{W} = W_m \hat{i}_m + W_\theta \hat{i}_\theta \tag{2.8}$$

2.2.1 The equations of flow in the channel

1) The equation of motion:

In this analysis the fluid properties are assumed to be expressable by uniform continuous functions so that the general equation of absolute flow:

$$\frac{D\bar{V}}{Dt} = \frac{\partial \bar{V}}{\partial t} + (\bar{V}.\bar{\nabla})\bar{V} = -\frac{\bar{\nabla}P}{\rho} + \bar{f} - \bar{\nabla}(gz) \tag{2.9}$$

holds at any point in the channel. Using assumptions (1) - (3) of section (2.1.4) the above equation reduces to the form:

$$(\bar{V}.\bar{\nabla})\bar{V} = -\bar{\nabla}\left(\frac{p}{\rho}\right) + \bar{f} \tag{2.10}$$

Introducing assumption (7) and using the cylindrical system of co-ordinates defined in Fig. (2-4), the above equation can be expanded into its three components:

$$V_r \frac{\partial V_r}{\partial r} + V_z \frac{\partial V_r}{\partial z} - \frac{V_\theta^2}{r} = -\frac{1}{\rho}\frac{\partial p}{\partial r} + f_r \tag{2.11a}$$

$$V_r \frac{\partial V_\theta}{\partial r} + V_z \frac{\partial V_\theta}{\partial z} + \frac{V_r V_\theta}{r} = -\frac{1}{\rho}\,\frac{1}{r}\frac{\partial p}{\partial \theta} + f_\theta \tag{2.11b}$$

$$V_r \frac{\partial V_z}{\partial z} + V_z \frac{\partial V_z}{\partial z} = -\frac{1}{\rho}\frac{\partial p}{\partial z} + f_z \tag{2.11c}$$

The friction force ($\bar{f}$) can be related to the velocity gradients in a simple manner only for special types of flows. The viscosity and the density of the fluid are here assumed constant, then the friction force ($\bar{f}$) is given by:

$$\bar{f} = \nu \bar{\nabla}^2 \bar{V} \tag{2.12}$$

where (ν) is the kinematic viscosity of the fluid.

This equation is valid for turbulent as well as laminar flow. However, for turbulent flow the dependent variables all vary as functions of time. If time-averaged variables are used, equation (2.12) does not hold for turbulent flows. In practical terms, therefore, it holds only for laminar, incompressible flow with constant viscosity. However, for two-dimensional flow, like the one considered here, an eddy viscosity (ε) may be defined to account for the turbulent momentum exchange such that the viscous and turbulent effects can be combined in the relation:

$$\bar{f} = (\nu + \varepsilon)\ \bar{\nabla}^2\ \bar{V} \tag{2.13}$$

This relation can then be used if time-averaged flow parameters are used. However, up to now there is no data available regarding the losses in regenerative pumps to enable this eddy viscosity to be evaluated. As a first approximation its value may be assumed constant throughout the channel and its magnitude may be fixed from data from similar machines.

The forms of the equations of motion of invicid, laminar and turbulent flow models are as follows:

(a) Invicid flow field:

With zero viscosity, equation (2.12) gives zero frictional forces everywhere and hence equation (2.11) reduces to:

$$V_r \frac{\partial V_r}{\partial r} + V_z \frac{\partial V_r}{\partial z} - \frac{V_\theta^2}{r} = -\frac{1}{\rho}\frac{\partial p}{\partial r} \tag{2.14a}$$

$$V_r \frac{\partial V_\theta}{\partial r} + V_z \frac{\partial V_\theta}{\partial z} + \frac{V_r V_\theta}{r} = -\frac{1}{\rho}\frac{\partial p}{\partial \theta} \tag{2.14b}$$

$$V_r \frac{\partial V_z}{\partial r} + V_z \frac{\partial V_z}{\partial z} = -\frac{1}{\rho}\frac{\partial p}{\partial z} \tag{2.14c}$$

(b) Laminar flow field:

The friction force in a laminar flow field is given by equation (2.12) where in the cylindrical system of co-ordinates:

$$\bar{\nabla}^2 = \frac{\partial^2}{\partial r^2} + \frac{1}{r}\frac{\partial}{\partial r} + \frac{1}{r^2}\frac{\partial^2}{\partial \theta^2} + \frac{\partial^2}{\partial z^2} \tag{2.15}$$

Introducing this expression for $\bar{\nabla}^2$ into equation (2.12) and using the axi-symmetric assumption, the following expressions are obtained for the three components of the friction force:

$$f_r = \nu\left[\frac{\partial^2 V_r}{\partial r^2} + \frac{1}{r}\frac{\partial V_r}{\partial r} + \frac{\partial^2 V_r}{\partial z^2} - \frac{V_r}{r^2}\right] \tag{2.16a}$$

$$f_\theta = \nu\left[\frac{\partial^2 V_\theta}{\partial r^2} + \frac{1}{r}\frac{\partial V_\theta}{\partial r} + \frac{\partial^2 V_\theta}{\partial z^2} - \frac{V_\theta}{r^2}\right] \tag{2.16b}$$

$$f_z = \nu\left[\frac{\partial^2 V_z}{\partial r^2} + \frac{1}{r}\frac{\partial V_z}{\partial r} + \frac{\partial^2 V_z}{\partial z^2}\right] \tag{2.16c}$$

In the analysis developed here the tangential pressure gradient $\frac{\partial p}{\partial \theta}$ is an input parameter to be declared to represent any desired operating condition of the pump. Accordingly when the total change of pressure (dp) between two locations is to be evaluated, f_θ of equation (2.16b) does not need to be evaluated. This great simplification can be seen more clearly from the pressure difference between two points:

$$p_2 - p_1 = \int_1^2 dp = \int_1^2 \frac{\partial p}{\partial r}\,dr + \int_1^2 \frac{\partial p}{\partial \theta}\,d\theta + \int_1^2 \frac{\partial p}{\partial z}\,dz \tag{2.17}$$

Then: $$p_2 - p_1 = \int_1^2 \frac{\partial p}{\partial r}\,dr + \frac{\partial p}{\partial \theta}\,\Delta\theta + \int_1^2 \frac{\partial p}{\partial z}\,dz \tag{2.18}$$

Only the first and last terms on the RHS of this equation and the tangential displacement ($\Delta\theta$) need to be evaluated. To evaluate the first and last terms on the RHS of equation (2.18) equations (2.11a) and (2.11c) are to be used. Hence the expressions for (f_r) and (f_2) given by equations (2.16a) and (2.16c) respectively must be evaluated. From the inspection of these two expressions it can be seen that they can be completely determined if the velocities (V_r) and (V_z) are known continuous functions of (r) and (z) and if (V_θ) is also known.

(c) Turbulent flow field:

The expansion of the frictional force ($\bar{f}$) of equation (2.13) is the same as that of equation (2.12) except that the kinematic viscosity (ν)

is replaced by $(\nu + \varepsilon)$. Then the three components of the frictional force in turbulent flow are obtained by equations (2.16) when this replacement is made.

The way the pressure difference between two points may be determined in this flow is the same as that described above for laminar flow.

2) The equation of continuity:

The equation of continuity in the channel is obtained from the general form of the continuity equation in cylindrical system of co-ordinates:

$$\frac{\partial \rho}{\partial t} + \frac{1}{r}\frac{\partial (\rho r V_r)}{\partial r} + \frac{1}{r}\frac{\partial (\rho V_\theta)}{\partial \theta} + \frac{\partial (\rho V_z)}{\partial z} = 0 \qquad (2.19)$$

by using assumptions (1), (2) and (7). The result is:

$$\frac{1}{r}\frac{\partial (r V_r)}{\partial r} + \frac{\partial V_z}{\partial z} = 0 \qquad (2.20)$$

3) The energy equation:

The general energy equation for absolute, adiabatic incompressible flow along a streamline is given by, see ref. (22):

$$\frac{\partial}{\partial t}\left(\frac{V^2}{2}\right) dt + d\left(\frac{p_s}{\rho}\right) = dt\ \bar{V}.\bar{f} \qquad (2.21)$$

where p_s, the total or stagnation pressure of the fluid, is given by:

$$p_s = p + \rho\frac{V^2}{2} + \rho g z \qquad (2.22)$$

and $\bar{f}$ is the friction force and $(dt\ \bar{V}.\bar{f})$ is the work of friction along a distance $(dt V)$ along the streamline covered in time (dt) by the fluid travelling with velocity $(\bar{V})$.

With assumptions (1) and (3), equation (2.21) reduces to:

$$d\left(\frac{p}{\rho} + \frac{V^2}{2}\right) = dt\ \bar{V}.\bar{f} \qquad (2.23)$$

There is no simple way of determining the work of friction $(dt\ \bar{V}.\bar{f})$ by analytical methods. It is usually estimated by applying the

experimentally established empirical formulations of losses in conduits. The energy equation is more conveniently put in the integrated form:

$$\frac{p_2 - p_1}{\rho} = \frac{V_1^2 - V_2^2}{2} - gh_f \qquad (2.24)$$

where gh_f is the energy lost per unit mass of fluid because of friction between point (1) and point (2) along the same streamline. Methods of estimating this quantity will be discussed later in the chapter. Now if it is assumed that it can be estimated and that $(P_2 - p_1)$ can be evaluated from the equations of motion as described above, then (V_2) can be computed if (V_1) is known.

Routines for solving the flow in the channel will be developed in chapter (5). With their aid $(p_2 - p_1)$ and (V_1) are estimated and (gh_f) is estimated by methods developed in section (2.3) so that equation (2.24) can be used to calculate (V_2) step-wise along streamlines in the channel.

2.2.2 The equations of flow in the impeller

The axi-symmetric approach adopted here reduces the actual three dimensional motion to two dimensional motion. Consequently the fluid relative motion $(\bar{W})$ in the impeller can be analysed with reference to an absolute system of co-ordinates because it has no variation due to the impeller motion. Therefore the same absolute system of co-ordinates is used for both the channel and impeller flows.

It will be shown in Chapter (4) that the velocity $(\bar{W})$ of the fluid inside the impeller can be determined directly if the meridional component $(\bar{W}_m)$ and the blade shape are known without the need to solve the flow equations in the impeller. It will also be shown in Chapter (4) that the method of solving the flow model developed here is based on assuming a function to give the meridional component $(\bar{W}_m)$ everywhere in the linear section. In this way the velocity $(\bar{W})$ is determined without explicitly involving the equations of motion in the impeller. However, these equations are used indirectly with the continuity equation later when the unrestricted law of moment of momentum will be used to determine the energy transfer from the impeller to the fluid using end conditions only. The equation of

continuity is also needed explicitly to define a stream function relationship in terms of which the meridional velocity ($\bar{W}_m$) is expressed.

1) The equation of continuity:

The general equation of continuity for relative flows is

$$\frac{\partial \rho}{\partial t} + \frac{1}{r}\frac{\partial (\rho r W_r)}{\partial r} + \frac{1}{r}\frac{\partial (\rho W_\theta)}{\partial \theta} + \frac{\partial (\rho W_z)}{\partial z} = 0 \qquad (2.25)$$

Using assumption (1), (2) and (7) of section (2.1.4), the continuity equation in the impeller is obtained from this equation as:

$$\frac{1}{r}\frac{\partial (r W_r)}{\partial r} + \frac{\partial W_z}{\partial z} = 0 \qquad (2.26)$$

This equation differs from equation (2.20) only in that the velocity components are relative and absolute respectively. The absolute velocity ($\bar{V}$) in the impeller is related to the relative motion ($\bar{W}$) by the equation:

$$\bar{V} = \bar{W} + \bar{\omega} \times \bar{r} \qquad (2.27)$$

where $\bar{\omega}$ is the angular velocity of the impeller and ($\bar{r}$) is the position vector of the location considered. In turbomachines:

$$\bar{\omega} \times \bar{r} = \omega\, r\, \hat{i}_\theta$$

Hence: $V_r \hat{i}_r + V_\theta \hat{i}_\theta + V_z \hat{i}_z = W_r \hat{i}_r + (W_\theta + \omega_r)\hat{i}_\theta + W_z \hat{i}_z$

From which:

$$V_r = W_r \qquad (2.28a)$$

$$V_z = W_z \qquad (2.28b)$$

Thus equations (2.26) and (2.20) are in fact identical. However, inside the impeller the blades take up part of the flow area, and this must be deduced from the total area by applying a blockage factor (or

an area restriction factor) (B) to the equation of continuity. Introducing the blockage factor into equation (2.20), it becomes:

$$\frac{1}{r}\frac{\partial}{\partial r}(rBV_r) + \frac{\partial}{\partial z}(BV_z) = 0 \qquad (2.29)$$

This equation can then be used both in the impeller where in general $B = B(r, z)$ and in the channel where there are no blades present and (B) is equal to unity. The blockage factor (B) is derived in chapter (4).

2) Power input by the impeller

The energy input by the impeller to the fluid can be determined by applying the angular momentum equation, as for rotodynamic machines with no tangential pressure gradient, and then adding the energy needed to support the tangential pressure gradient existing in the pump.

Consider any stream tube as shown in Fig. (2.5). The thickness (dn) in the n-direction is taken small enough that the fluid properties along a mean streamline in the tube can be used for the entire fluid in that stream tube.

With the assumptions that the flow is steady with negligible body forces; and if both the velocity and the pressure fields are axi-symmetric, the energy input per unit mass of flow per flow cycle is given by the Euler equation:

$$e_i' = \omega (R_2 V_{\theta 2} - R_1 V_{\theta 1}) \qquad (2.30)$$

However, there is a tangential pressure gradient $\frac{\partial p}{\partial \theta}$ against which the fluid must be pushed. In doing so the impeller imparts a specific energy (e_i'') to the fluid in addition to that given by equation (2.30), where:

$$e_i'' = \frac{1}{\rho}\frac{\partial p}{\partial \theta}\Theta_i \qquad (2.31)$$

where:

$\frac{1}{\rho}\frac{\partial p}{\partial \theta}$ = the tangential energy gradient per unit mass.

θ_i = the tangential displacement in one flow cycle defined as the push in section (2.1.2).

The specific energy transfer per flow cycle is therefore given by:

$$e_i = \omega(R_2 V_{\theta 2} - R_1 V_{\theta 1}) + \frac{1}{\rho} \frac{\partial p}{\partial \theta} \theta_i \qquad (2.32)$$

This change of fluid energy across the impeller in one flow cycle is also obtained by a more comprehensive derivation of flow equations for regenerative pumps given in Appendix (A). Note that since the flow field is here assumed incompressible, equation (A.38) of that appendix should be identical with equation (2.32) above.

The power input by the impeller to the fluid per streamtube is given by:

$$dP_i = \rho dQ_c \, \omega(R_2 V_{\theta 2} - R_1 V_{\theta 1}) + \frac{1}{\rho} \frac{\partial p}{\partial \theta} \theta_i \qquad (2.33)$$

where:

dP_i = power input to all the fluid in a streamtube extending along the tangential length of the linear section.

dQ_c = the circulatory flow through the streamtube.

The total power input by the impeller is, therefore, given by:

$$P_i = \sum_{j=1}^{k} \rho \, dQ_c (U_2 V_{\theta 2} - U_1 V_{\theta 1} + \frac{1}{\rho} \frac{\partial p}{\partial \theta} \theta_i)_j \qquad (2.34)$$

where (k) is the number of streamtubes in the entire section and (j) is a counter.

With assumption (4) of section (2.1.4) the process of energy addition to the fluid is adiabatic. Hence the power input by the impeller must be equal to the increase in the total energy of the fluid per unit time. Part of this energy is inevitably converted from a mechanical form to thermal energy due to the frictional forces in the flow. This thermal energy is considered to be lost since the flow is incompressible.

Let gh_ℓ be the specific energy lost in a streamtube in the linear section. Then the useful specific energy rise of the fluid in the linear section is, for any streamtube, given by:

$$e_f = e_i - gh_\ell \tag{2.35}$$

where (e_i) is given by equation (2.32). The net useful power gained by the fluid across the linear section is therefore:

$$P_f = \sum_{j=1}^{k} \rho \, dQ_c (U_2 \, V_{\theta 2} - U_1 \, V_{\theta 1} + \frac{1}{\rho} \frac{\partial p}{\partial \theta} \theta_i - gh_\ell)_j \tag{2.36}$$

The efficiency (η_ℓ) of the process of energy transfer from the impeller to the fluid in the linear section of the pump is defined by the equation:

$$\eta_\ell = \frac{P_f}{P_i} \tag{2.37}$$

where P_i and P_f are given by equations (2.34) and (2.36) respectively.

2.3 Major Losses in the Linear Section

Fluid approaching the impeller from the channel all along the linear section may be forced to change direction of flow abruptly on entering the impeller. Consequently shock or incidence losses occur. Viscosity and turbulence generate shear stresses within any flow field where there are velocity gradients and momentum exchanges. As a result frictional losses occur.

These are considered to be the two major loss generating phenomena in the linear section. There are also secondary losses which will be discussed separately.

The method of calculation adopted here is such that the losses calculated along a particular streamtube are assumed to affect the flow in that streamtube only. The limitations of this approach are discussed in section (2.3.6).

2.3.1 Incidence or shock losses

For the approaching fluid to form minimum eddies and hence to dissipate minimum energy in the blade intake region, the fluid relative flow angles (β_3) must be closely similar to the blade angles (β_1) everywhere in that region.

Theoretically, all losses which could be avoided by way of design could be avoided at the design point. However, even at this point, assumptions are made regarding some details of the actual flow, e.g. regarding the pre-whirl in the approaching flow caused by the viscous drag and the internal secondary circulation: these are impeller effects which cannot be known exactly. Due to the assumption made in this regard, there cannot be a complete match between the flow angles and the blade angles everywhere.

At off-design conditions, severe incidence shock losses are to be expected.

There are two incidence loss models which have been widely used:

1) A constant pressure shock loss proposed by Wallace (25).

2) A loss model based upon the tangential component of kinetic energy destroyed proposed by Futral and Wasserbauer (26) and others (27)-(29); and referred to in the literature as the NASA model.

Both of these models were extended by Wallace and Whitfield (30) so as to cover all possible off-design conditions, i.e. positive and negative incidence. They presented comparisons of the two models and found little difference between them over a wide range of conditions.

The kinetic energy incidence loss model (26)-(29) is used extensively for the prediction of the incidence losses in incompressible flows (31). By this method the incidence loss is given by the square of the change in the tangential component of the fluid velocity relative to the member being approached. The specific energy loss at the entrance to the impeller is thus given, for any streamtube, by:

$$gh_i = \frac{1}{2} (W_{\theta 1} - W_{\theta 3'})^2 \qquad (2.38)$$

where, for any streamtube:

gh_i = specific energy loss in shock.

$W_{\theta 1}$ = relative tangential velocity of fluid just inside the impeller.

$W_{\theta 3'}$ = relative tangential velocity of fluid just outside the impeller.

2.3.2 Skin friction losses

Usually impeller flows have high Reynolds number and the skin friction losses in the blade passages are estimated by applying the experimentally established formulations of losses in conduits of turbulent flows. Since an explicit solution of the equations of motion is not needed in the impeller as mentioned in section (2.2.2), these models are used without the need to solve the corresponding equations of turbulent motion.

However, the solution of the equations of motion and the energy equation together is necessary in the channel. Although turbulent loss models can be used to estimate the losses (gh_f) of the energy equation (2.24), there is no simple way of determining the equivalent frictional force ($\bar{f}$) of equation (2.13) in a consistent manner for use in the solution of the equations of motion (2.11). Complete consistency in writing the flow equations in the channel can be maintained only if an invicid flow model is assumed. Yet consistency may also be approximately maintained when turbulent loss models are used if the eddy viscosity (ε) can be appropriately estimated by experimental means similar to those used to establish the friction factor of those loss models.

Empirical friction factor:

In fully developed flows in straight conduits the specific energy loss due to friction is found to be given by, see ref½ (21):

$$gh_f = \frac{L}{D_h} \frac{V^2}{2} f \qquad (2.39)$$

where:

gh_f = the energy lost per unit mass of fluid.

L = the length of the flow path.

D_h = the hydraulic diameter of the conduit, defined by the equation:

$$D_h = \frac{\text{cross sectional area of conduit}}{\text{the wetted perimeter of the solid boundary in contact with the wall}} \tag{2.40}$$

V = the average total velocity of the flow parallel to the axis of the conduit.

f = the friction factor which is determined analytically for symmetrical laminar flows only and experimentally for other flows. In general:

$$f = f(Re, \frac{k_s}{D_h}) \tag{2.41}$$

where:

Re = the Reynolds number $(= \frac{V D_h}{\nu})$

k_s = the average height of protrusion of surface roughness.

$\frac{k_s}{D_h}$ = the relative surface roughness.

For completely hydraulically rough flows Nikuradses corrected form of TH. von Karman empirical correlation of the friction factor for straight conduit is, see ref. (21):

$$f = \frac{1.0}{(4.0 \log_{10} (\frac{2 D_h}{k_s}) + 3.48)^2} \tag{2.42}$$

An equation which correlates the whole transition region from hydraulically smooth to completely rough flow was established by Colebrook and White (32):

$$1/\sqrt{f} = 3.48 - 4 \log_{10} \left[\frac{k_s}{2 D_h} + \frac{18.7}{Re\sqrt{f}} \right] \tag{2.43}$$

This equation is used instead of equation (2.42) when the flow regime is not completely rough, i.e. when the friction factor also depends on Reylond number. However, for Re $\rightarrow \infty$, equation (2.43) transforms into equation (2.42).

The applicability of the concept of the hydraulic diameter is assumed to hold when the flow is solved along streamtubes.

2.3.3 Losses in the blade passages

A flow in a rotating passage formed by two adjacent blades is not unlike that in a stationary conduit if the relative parameters are used instead of the absolute ones.

a) Hydraulic diameter of inner steamtubes:

Considering any streamtube (j) as shown in Fig. (2.6) its cross sectional area (a) at any location is approximately given by:

$$a = (\frac{2\pi r}{Z} - t)\ dn \qquad (2.44)$$

where:

r = radial co-ordinate of the location.

Z = number of blades of impeller.

t = blade thickness at that location.

dn = streamtube meridional thickness perpendicular to its generatrices.

Although (dn) may vary with both (r) and (z), it can be assumed constant throughout the tube because its variation is usually very small.

Since the wetted perimeter is (2 x dn), the hydraulic diameter of the tube at any location (r) is:

$$D_h = (\frac{2\pi r}{Z} - t)\ /2.0 \qquad (2.45)$$

b) Hydraulic diameter of the outer most streamtube:

The streamtube in contact with impeller hub and the channel wall is referred to as the outer most, or just the outer, streamtube, see Fig. (2.6). Its wetted perimeter differs from those of the inner tubes and hence its hydraulic diameter is given by:

$$D_h = (\frac{2\pi r}{Z} - t)\ dn/(2dn + \frac{2\pi r}{Z} - t) \qquad (2.46)$$

c) Losses along a streamtube:

Along any flow path dL, as shown in Fig. (2.6), the skin friction loss is given by:

$$d(gh_b) = \frac{dL}{D_h} \frac{W^2}{2} f \tag{2.47}$$

where:

$d(gh_b)$ = specific energy loss along the tube in the blade-passage.

W = average relative velocity over that path.

The specific loss encountered in a streamtube from point (1) to point (2) is given by:

$$gh_b = \sum_{j=1}^{k} \frac{dL}{D_h} \frac{W^2}{2} f \tag{2.48}$$

where:

gh_b = total specific energy loss in a streamtube in the blade passages.

k = number of steps taken along the tube from point (1) to point (2).

A simpler method of determining (gh_b) is by using the average parameters for the flow path from point (1) to point (2) without the need for the summation of equation (2.48).

Note that flows in blade passages, like those in diffusers, are usually not fully developed: the flow area varies, the velocity profile varies and there is an adverse pressure gradient which may cause rapid boundary layer growth and possible separation. Strictly speaking, therefore, losses in such flows cannot be accurately estimated by the above correlations for fully developed flows.

However, since in regenerative pumps the blade height is usually small compared with the impeller radius and these variations are not profound, it is permissible to use the fully devloped flow formulations to estimate the losses: particularly since the results represent first approximations only.

2.3.4 Losses in the channel

Losses due to the circulatory flow (V_m) in the channel are estimated separately from those due to the tangential motion (V_θ).

(i) Losses due to the circulatory flow

(a) Inner streamtubes:

Consider any inner streamtube in the channel as shown in Fig. (2.7). The cross sectional area(a) of the tube is given by:

$$a = \theta_p \, r \, dn \tag{2.49}$$

where:

θ_p = the angle of the sector comprising the linear section.

r = radial co-ordinate of the location where the cross section is considered.

dn = the streamtube thickness in the n-direction. It can be estimated by equation (2.45).

The wetted perimeter of the streamtube is given by:

$$\text{wetted perimeter} = 2dn$$

Then the hydraulic diameter is

$$D_h = \theta_p \frac{r}{2.0} \tag{2.50}$$

(b) The outer streamtube:

The wetted perimeter of this streamtube, see Fig. (2.7), is given by:

$$\text{wetted perimeter} = 2dn + \theta_p \, r$$

Then
$$D_h = \theta_p \, rdn/(2dn + \theta_p \, r) \tag{2.51}$$

Along a meridional flow path (dL) the loss due to the circulatory flow is givey by:

$$d(gh_m) = \frac{dL}{D_h} \frac{V_m^2}{2} f \tag{2.52}$$

and the specific energy loss encountered in a streamtube from point (2)

to point (3), see Fig. (2.7), is given by:

$$gh_m = \sum_{j=1}^{k} \frac{dL}{D_h} \frac{V_m^2}{2} f_j \qquad (2.53)$$

where:

gh_m = specific energy loss in a streamtube in the channel due to the meridional motion (V_m) only.

dL = step length along the streamtube.

k = number of steps along the streamline from point (2) to point (3).

Unlike the case in the blade-passages, the energy loss ($d(gh_m)$) along each of the steps taken along a streamtube must be evaluated and used as an integral part of the step-wise solution of the flow equation as will be shown in detail in chapter (5).

(ii) Loss due to the tangential motion

(a) Inner streamtubes:

It can be seen from Fig. (2.7) that, with respect to the tangential motion, the inner streamtubes have no wetted perimeters if they are considered independently from the outermost streamtube. This leads to a tangential loss distribution which is zero everywhere and finite at the outer streamtube. Such apparent anomaly may provide a degree of flexibility in deciding the shape of the loss distribution across the flow as discussed in section (2.3.6). In that section it is also shown that such a situation can be avoided if required by using an average hydraulic diameter for all streamtubes.

(b) The outermost streamtube:

Referring again to Fig. (2.7), the cross sectional area of the outermost streamtube with respect to the tangential flow is approximately given by:

$$a = dn\, L' \qquad (2.54)$$

where:

L' = the mean length of the tube meridional cross section from

point (2), in the direction of the meridional flow, to point (1) at the inlet to the impeller.

dn = the meridional width perpendicular to the streamtube generatrices.

The wetted perimeter is equal to the perimeter of the channel. Then the hydraulic diameter is:

$$D_h = dn\ L'/L \tag{2.55}$$

where usually $L' \simeq L$ and hence

$$D_h = dn \tag{2.56}$$

This equation shows that care must be taken in choosing the width (dn) of the outer streamtube: very small (dn) may lead to exceeding exaggerated loss in the outer tube, see section (2.3.6).

Along a flow path (dL) in the tangential direction the loss will be:

$$d(gh_t) = \frac{dL}{D_h} \frac{V_\theta^2}{2} f \tag{2.57}$$

V_θ = average tangential velocity along the path (dL).

The total loss due to the tangential motion in the streamtube from point (2), impeller exit, to point (3), impeller inlet, is given by:

$$gh_t = \sum_{j=1}^{k} \frac{dL}{D_h} \frac{V_\theta^2}{2} f \tag{2.58}$$

The summation is done step-by-step while the step-wise solution along the tube is carried out.

2.3.5 Total losses along a streamtube:

The losses encountered along a streamtube in one complete flow cycle are:

(i) the shock loss due to incidence onto the impeller.

(ii) the skin friction loss in the blade passages: the total relative velocity is assumed parallel to the blade surface (axi-symmetric approach).

(iii) the skin friction loss in the channel: it is broken down into meridional loss and tangential loss.

Therefore the sum of the specific energy loss in any streamtube is given by:

$$gh_\ell = gh_i + gh_b + gh_m + gh_t \qquad (2.59)$$

where (gh_ℓ) stands for the specific energy loss in a particular streamtube in the linear section and has been introduced earlier in section (2.2.2) and used in equation (2.35). The terms on the RHS of equation (2.59) are given by equations (2.38), (2.48), (2.53) and (2.58) respectively.

2.3.6 Discussion of skin loss method

There is no simple analytical method of determining the manner in which the losses in the linear section are distributed, although there is little doubt that they must vary continuously across the whole flow. Fig. (2.8a) shows some possible trends of loss distributions across a section in which only (r) is assumed to vary from the centre of circulation (c) to the wall of the channel. Yet these losses have been presented above as though their occurence in each of the streamtubes is independent of that in the neighbouring tubes. By this approach the losses are estimated by analogy with the flow in conduits and, since the streamtubes are discrete, this means a discontinuous loss variation. However, this approach can still be valid if the discrete distribution of the calculated losses approximate that of the actual losses.

Moreover, an apparent anomaly arises out of the fact that the shapes of the streamtubes which are treated as conduits depends upon the number of streamtubes into which the flow is divided. In particular the streamtube next to the impeller hub and the channel wall will of necessity have a much larger wetted area than the other tubes because the latter are in contact with the blades alone. The wetted area of the former is almost independent of its assumed meridional width while the small wetted areas of the inner tubes are directly proportional to their assumed meridional width. Thus while the hydraulic diameters of the inner tubes will remain almost constant, the relatively small

hydraulic diameter of the outer tube will be proportional to its assumed meridional width. Then for a particular velocity distribution, the size of the calculated losses in the outer tube will depend upon its assumed meridional width; while those in the other tubes will be more or less the same. Therefore a very exaggerated loss distribution can result if the flow is divided into many streamtubes.

Fig. (2.8) shows diagrams of the type of loss distribution which can result from the use of this method. Although this method allows a degree of control over the shape of the loss distribution, it also presents an opportunity and a challenge to the investigator. However, the trend of the actual loss distribution in these pumps is not published and hence the necessary comparisions required by this method cannot be made.

At this stage of the development of the flow model it has been judged best to use the type of distribution resulting from the following simple method:

The hydraulic diameter (D_h) is taken to be the same for all streamtubes. Its value is calculated, using the methods described above, considering that the whole flow constitutes that in a single conduit. Then the flow can be divided into any number of tubes for analysis. The specific losses per unit length of flow-path along the different streamtubes will be proportional to the square of the velocity along them, because the friction factor (f) will be the same for all streamtubes too.

Although this approach does not have a mechanism for altering the shape of the loss distribution, it does have the following advantages:

1) For a given geometry the loss distribution is a function of the square of velocity along the different streamtubes. Thus the distribution will not have an exaggerated shape if the velocity distribution is smooth.

2) Although the wall effect is distributed throughout the whole fluid, the streamlines close to the wall do suffer a higher loss since they have a larger meridional velocity in these pumps. This is as would be expected in reality.

2.4 Secondary Losses in the Linear Section

There are three recognised secondary losses in the linear section which will be discussed in turn:

(i) losses due to changes of flow area.

(ii) losses due to secondary circulation resulting from the pressure gradients between the blades.

(iii) losses due to secondary flows resulting from the curvatures of the fluid path.

(i) Effect of change of flow area:

Sudden flow area changes occur on entry to and exit from the impeller because of the finite blade thickness. Such discontinuities cause eddies to be generated and consequent energy loss.

It is considered here however, that the blade thickness at the entry and exit regions is small enough to make these losses insignificant compared with the major losses: this is in line with the assumption that the meridional velocity ($\bar{V}_m$) has no discontinuities. This assumption applies to the blade edges only: it does not mean that the blade thickness is ignored elsewhere.

(ii) Secondary circulation:

The pressure gradients between the leading and the trailing sides of the blades produce secondary or eddy circulations which are superimposed upon the main flow. Within a blade passage this has the effect of increasing the relative velocity on the trailing side and reducing it on the leading side. This has the following effects (33) - (36):

(a) the boundary layer build up at the trailing side increases and subsequently the frictional losses in the blade passage are increased.

(b) the mean direction of the fluid leaving the impeller is modified: instead of following the direction of the blade surface, as assumed by the axi-symmetric approach, the fluid flows rather in a direction which deviates backwards with respect to the positive direction of rotation. This means that its absolute tangential

velocity is less than that which it would be if this phenomenon did not occur. This approach corresponds to that usually applied to centrifugal machines.

As mentioned in section (2.3), it is assumed that the blade passages are short and the effect on the boundary layer growth is not significant such that the losses in the passages can be estimated using the formulation of section (2.3). However, the reduction of the absolute tangential velocity at the impeller exit is corrected by using a slip factor, see chapter (4).

(iii) Effect of curvature of flow path:

Since the streamtubes are by necessity curved, the influence of their curvatures must be included in the formations of losses for straight conduits which were considered in section (2.3). The losses along a streamtube have been resolved into losses associated with the meridional motion and losses associated with the tangential motion. The radius of curvature of the fluid path which affects the former losses is that of the streamline projection onto a meridional plane; and that which affects the latter losses is the radial co-ordinate of the location with respect to the pump axis.

Both measurements and theoretical calculations of the influence of curvature on turbulent and laminar flows have been carried out by many investigators, (21), (41) - (43). In curved pipes particles near the flow axis which have a higher velocity are acted upon by a larger centrifugal force than the slower particles near the wall. This leads to the emergence of a secondary flow which is directed outwards in the centre region and inwards towards the centre of curvature near the wall, see ref. (21).

However, the velocity profile in each of the streamtubes considered here is qualitatively different from that in a closed conduit. In a streamtube the velocity is axi-symmetric and almost uniform in the meridional plane because the meridional width of the tube is small. Moreover, the strong circulatory flow which is mostly radially inwards in the channel over-rides the centrifugal effects due to the tangential motion of the fluid there.

It is judged therefore that the correlations for accounting for the influence of curvature in closed conduits (21), may not be applied for flows in the streamtubes considered here. In the absence of the appropriate methods of estimating the influence of the streamtube curvature, such influence is at present ignored.

2.5 Estimation of the Eddy Viscosity

In the method of solution developed in chapter (4) the flow is solved along streamlines. This allows the use of the energy equation in the following form, see equation (2.21):

$$\frac{1}{\rho}(p_2 - p_1) = \frac{1}{2}(V_1^2 - V_2^2) + \int_1^2 dt\, \bar{V}\, \bar{f}$$

between any two points along the streamline, where the frictional force ($\bar{f}$) in the two dimensional velocity field considered here is given by equation (2.13) with $\frac{}{} = 0$:

$$f_r = (\nu + \varepsilon)\left[\frac{\partial^2 V_r}{\partial r^2} + \frac{1}{r}\frac{\partial V_r}{\partial r} + \frac{\partial^2 V_r}{\partial z^2} - \frac{V_r}{r^2} \right]$$

$$f_\theta = (\nu + \varepsilon)\left[\frac{\partial^2 V_\theta}{\partial r^2} + \frac{1}{r}\frac{\partial V_\theta}{\partial r} + \frac{\partial^2 V_\theta}{\partial z^2} - \frac{V_\theta}{r^2} \right]$$

$$f_z = (\nu + \varepsilon)\left[\frac{\partial^2 V_z}{\partial r^2} + \frac{1}{r}\frac{\partial V_z}{\partial r} + \frac{\partial^2 V_z}{\partial z^2} \right]$$

where:

ε = the eddy viscosity introduced to account for the turbulent motion by Renolds (45).

To evaluate the loss term ($\int_1^2 dt\, \bar{V}\, \bar{f}$) between two points, the three components f_v, f_θ and f_z of the frictional force ($\bar{f}$) must be known along the path between the points.

In the method of solution in chapter (4) the meridional velocity ($\bar{V}_m$) and its derivatives will be assumed known everywhere. Then f_r and f_z can be evaluated everywhere if $(\nu + \varepsilon)$ is known. However, f_θ cannot be evaluated because (V_θ) and its derivatives are unknown. Thus the

evaluation of the loss term by integrating $dt\ \bar{V}\ \bar{f}$ is not possible. Instead it has been assumed that the loss can be estimated using the empirical loss models of closed conduits as discussed in section (2.3).

This is not the end of the problem because the frictional force ($\bar{f}$) also appears in the equation of motion (2.11) which must be solved together with the energy equation so that the two unknowns (p_2 and $V_{\theta 2}$) can be obtained. The equation of motion is used to obtain the pressure difference $\frac{1}{\rho}(p_2 - p_1)$ by using the partial derivatives of the pressure given by the three components of the equation as follows:

$$\frac{1}{\rho}(p_2 - p_1) = \int_1^2 \frac{1}{\rho}\frac{\partial p}{\partial r}\,dr + \int_1^2 \frac{1}{\rho}\frac{\partial p}{\partial \theta}\,d\theta + \int_1^2 \frac{1}{\rho}\frac{\partial p}{\partial z}\,dz \qquad (2.60)$$

where:

$$\frac{1}{\rho}\frac{\partial p}{\partial r} = -\ V_r\frac{\partial V_r}{\partial r} + V_z\frac{\partial V_r}{\partial z} - \frac{V_\theta^2}{r} - f_r \qquad (2.61a)$$

$$\frac{1}{\rho}\frac{\partial p}{\partial \theta} = -\ V_r\frac{\partial V_\theta}{\partial r} + V_z\frac{\partial V_\theta}{\partial z} + \frac{V_r V_\theta}{r} - f_\theta \qquad (2.61b)$$

$$\frac{1}{\rho}\frac{\partial p}{\partial z} = -\ V_r\frac{\partial V_z}{\partial r} + V_z\frac{\partial V_z}{\partial z} - f_z \qquad (2.61c)$$

It has been mentioned above that f_r and f_z can be evaluated if $(\nu + \varepsilon)$ is known because V_r and V_z and their derivatives are assumed known everywhere. Then the first and last integrals on the RHS of equation (2.60) can be evaluated if (ε) is known for a particular fluid. The evaluation of the second integral does not require that the RHS of equation (2.61b) be evaluated because $\frac{1}{\rho}\frac{\partial p}{\partial \theta}$ is assumed to be a known constant everywhere. The problem therefore reduces to finding the eddy viscosity (ε) of the flow everywhere to be used in the (r) and (z) components of the equation of motion such that the resulting frictional force should be approximately the same as that which is implicitly used in the empirical model for estimating the loss term in the energy equation. Thus consistency will be approximately maintained in expressing the frictional forces both in the energy equation and in the equation of motion.

Since the empirical models used to estimate the loss term in the energy equation are basically correlated from experimental measurements on circular pipe flows, eddy viscosity (ε) obtained on basis of similar experimental results should be used in the equation of motion so that consistency is reasonably maintained.

In ref. (21) the variation of (ε) over the cross section of a circular pipe is given on the basis of measured results. The variation is such that it has not been possible to describe it by a plausible hypothesis, see ref. (21). However, from that variation the average value of the parameter, $\left(\frac{\varepsilon}{RV\sqrt{\frac{1}{2}f}} \right)_{av}$, which can be assumed to apply approximately for the entire flow in the pipe is about 0.06, R being its radius.

Since the concept of hydraulic diameter has been generally verified for turbulent flow, see ref. (21), the variation of (ε) in non-circular conduits may be assumed to be similar to that in a circular pipe if the hydraulic diameter is used instead of the pipe radius, i.e.

$$\frac{\varepsilon}{2D_h V\sqrt{\frac{1}{2}f}} = 0.06 \qquad (2.62)$$

V = average velocity in the conduit.
f = friction factor defined earlier in section (2.3).

This equation relates the eddy viscosity (ε) in an approximate manner to the hydraulic diameter (D_h) and the friction factor (f) which are used to estimate the frictional losses in the energy equation. From this approximation (ε) is proportional to the velocity (V); since (D_h) and (f) are considered constant for the entire flow. The specific friction loss (gh) was found earlier to be proportional to the square of the velocity along the tube. Therefore (gh) is proportional to the product (ε V) as would be expected.

This approach, in which an average value of (ε) is assumed to apply over the entire section, is dictated by the lack of data regarding the distribution of (ε) across the flow in the pumps. Also that flow cannot be represented by the simple flow in circular pipes and hence

the distribution of (ε) across a flow in a circular pipe cannot be used as it is to represent that in the pump. A similar averaging process however, has also been used in estimating the energy losses (gh). This is about the nearest approach which could be made to reasonable consistency at this stage.

2.6 Summary

A flow model is developed to represent the flow in the linear section of a regenerative pump; the linear section being that part of the pump where the tangential gradient of the fluid head ($\partial H/\partial \theta$) is essentially constant.

A hypothesis is made regarding the operation of the pump and related terms are introduced. The general aspects of the flow are discussed. Seven basic assumptions are made to simplify the flow equations which are written for the flow inside the impeller and in the channel. A relationship for the power input by the impeller to the fluid is developed (also see Appendix A); and the corresponding useful fluid power gained in the linear section is written by defining a specific energy loss. The major losses in the section are considered to be the incidence and the skin friction losses and formulae are developed to estimate them.

Secondary losses due to changes of flow area, secondary circulation and fluid path curvature are discussed and generally considered insignificant compared to the major losses.

The problem of maintaining consistency in writing the equation of motion, in which the frictional forces are expressed using an eddy viscosity, and the energy equation, in which the loss term is estimated using empirical pipe loss models, is discussed. A degree of consistency is believed to have been achieved by using an average value of the eddy viscosity obtained from measurements of flows in circular pipes because the loss formulations used in the energy equation are basically from the same source.

To complete the modelling of pump flow, the performance of the non-linear section of the pump is discussed in the next chapter.

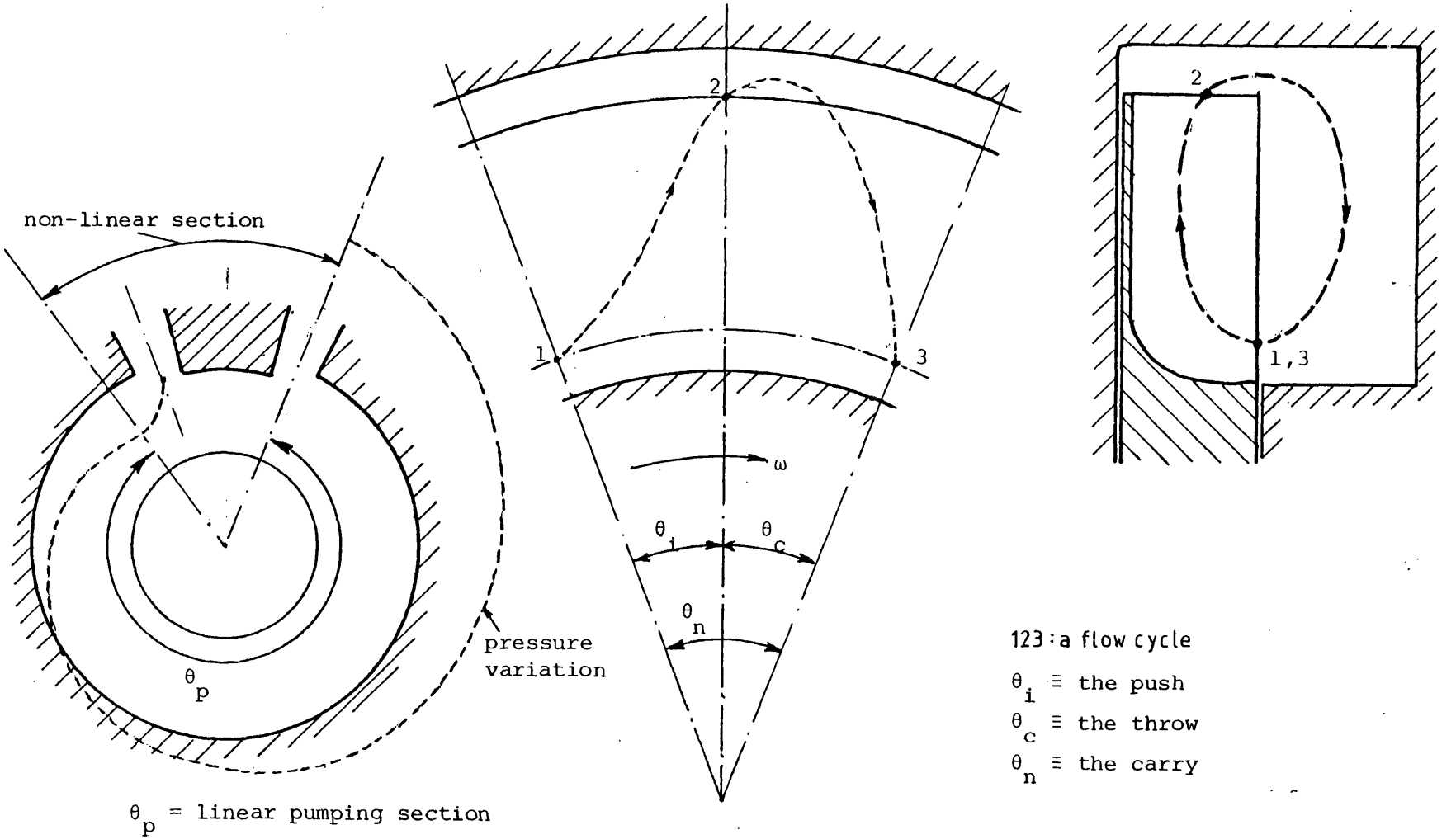

Fig. (2.1): Diagrams defining terms relating to the hypothesis of operation

Fig. (2.1)

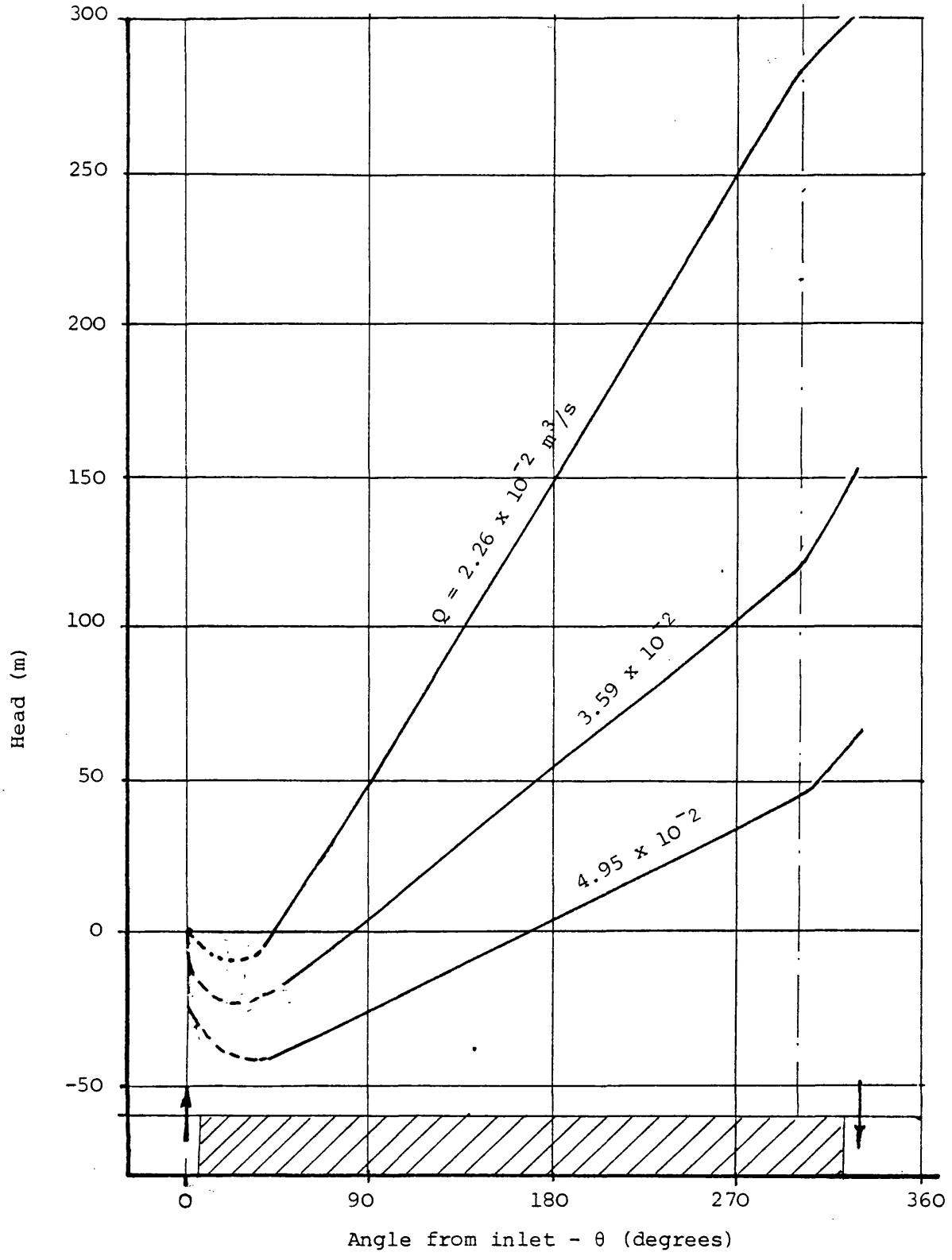

Fig. (2.2): Typical head distribution at various flow rates (reproduced from ref. (7))

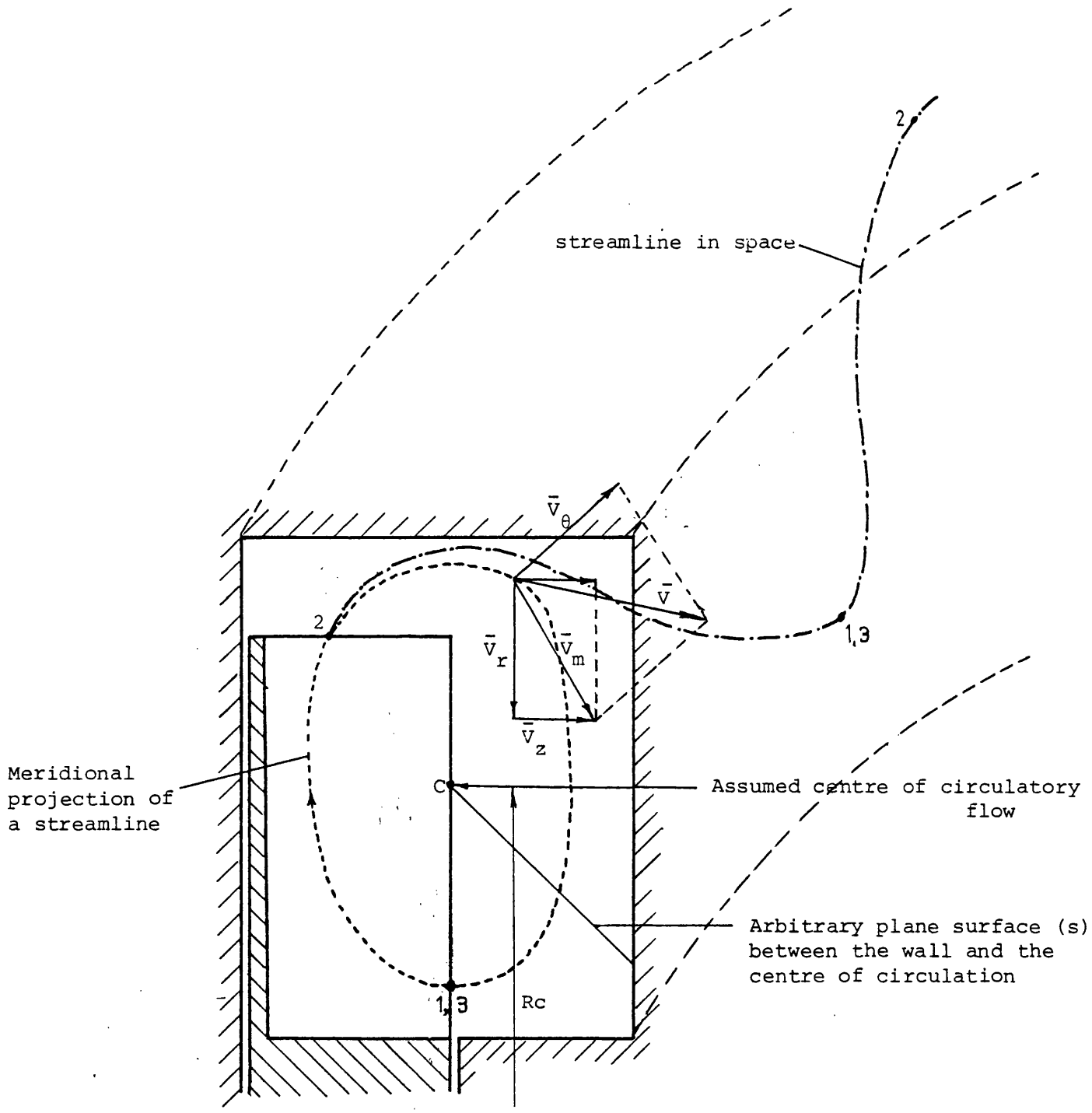

Fig. (2.3): A streamline and a flow cycle 123

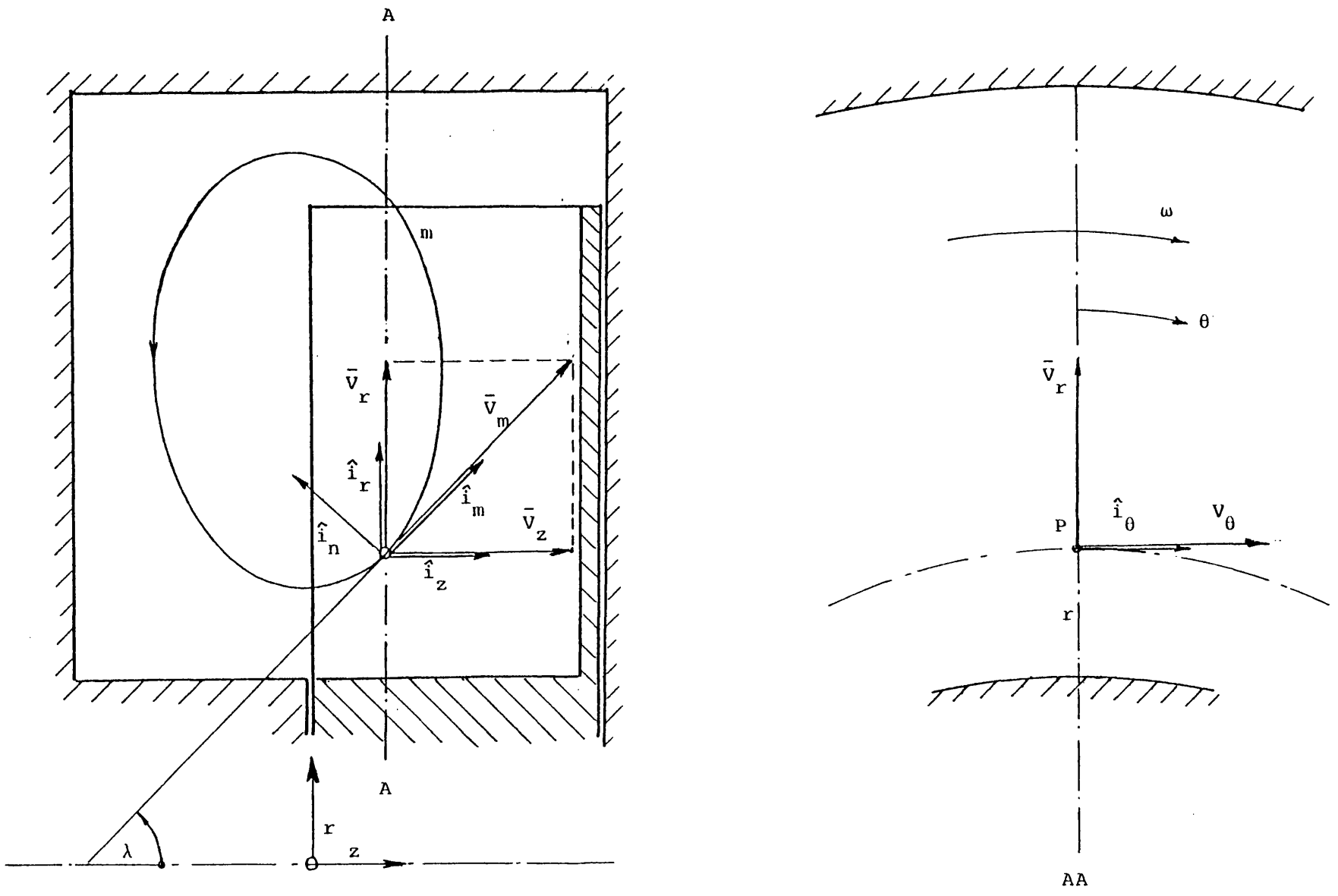

Fig. (2.4): A diagram defining the co-ordinate systems

Fig. (2.4)

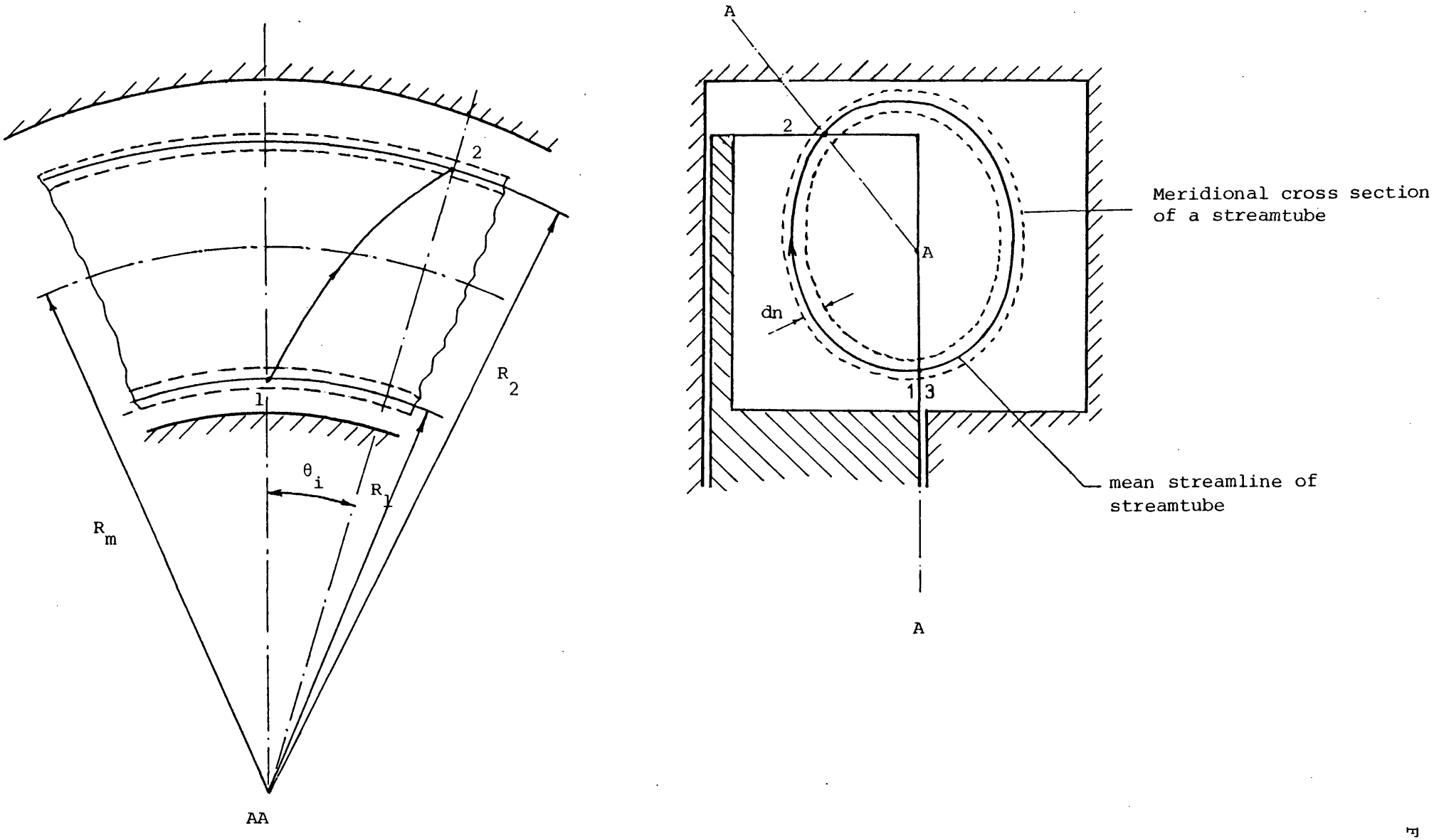

Fig. (2.5): Streamtube and its mean streamline

Fig. (2.5)

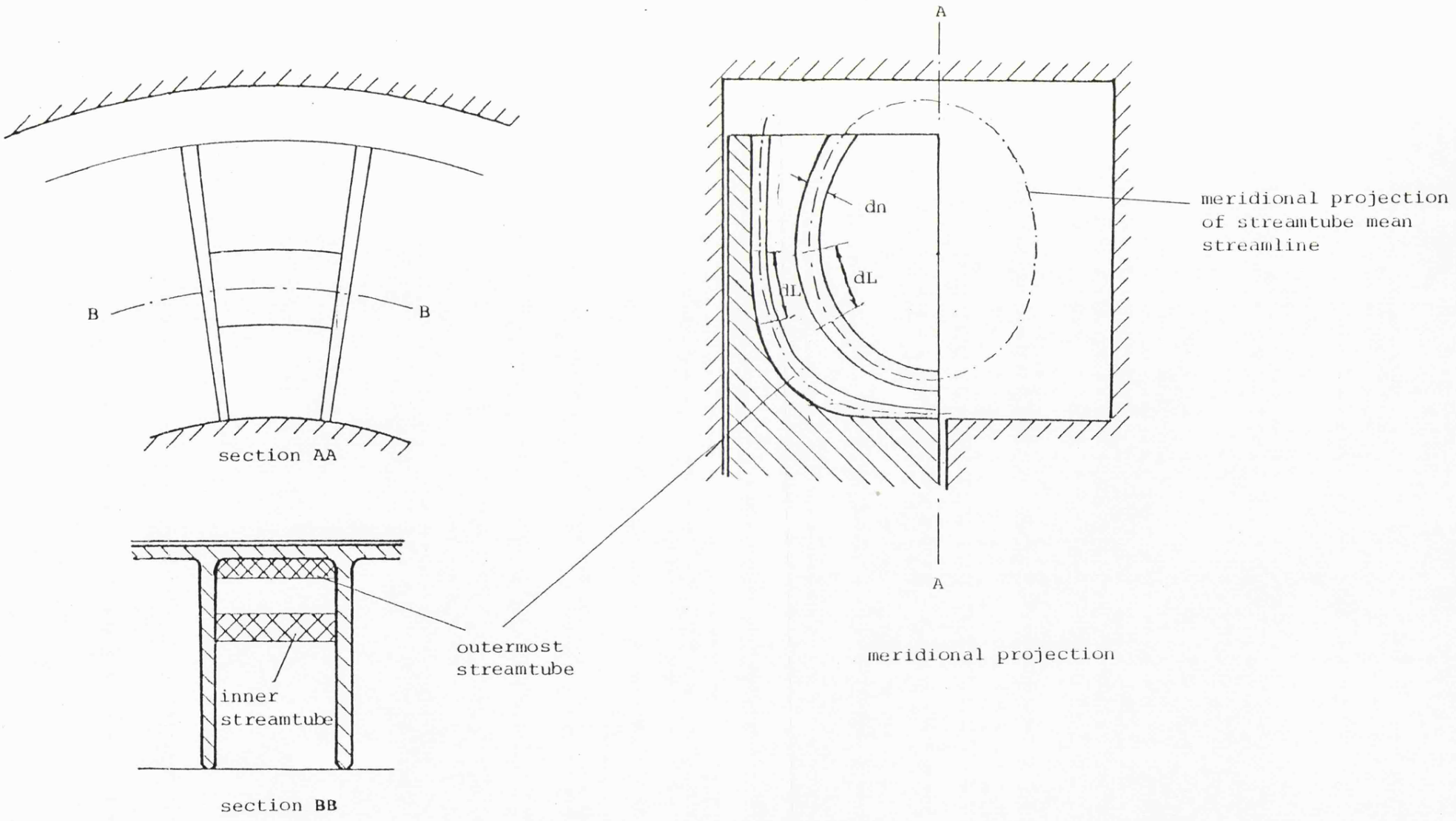

Fig. (2.6): A diagram for estimating the hydraulic diameters of streamtubes inside the impeller

Fig. (2.7)

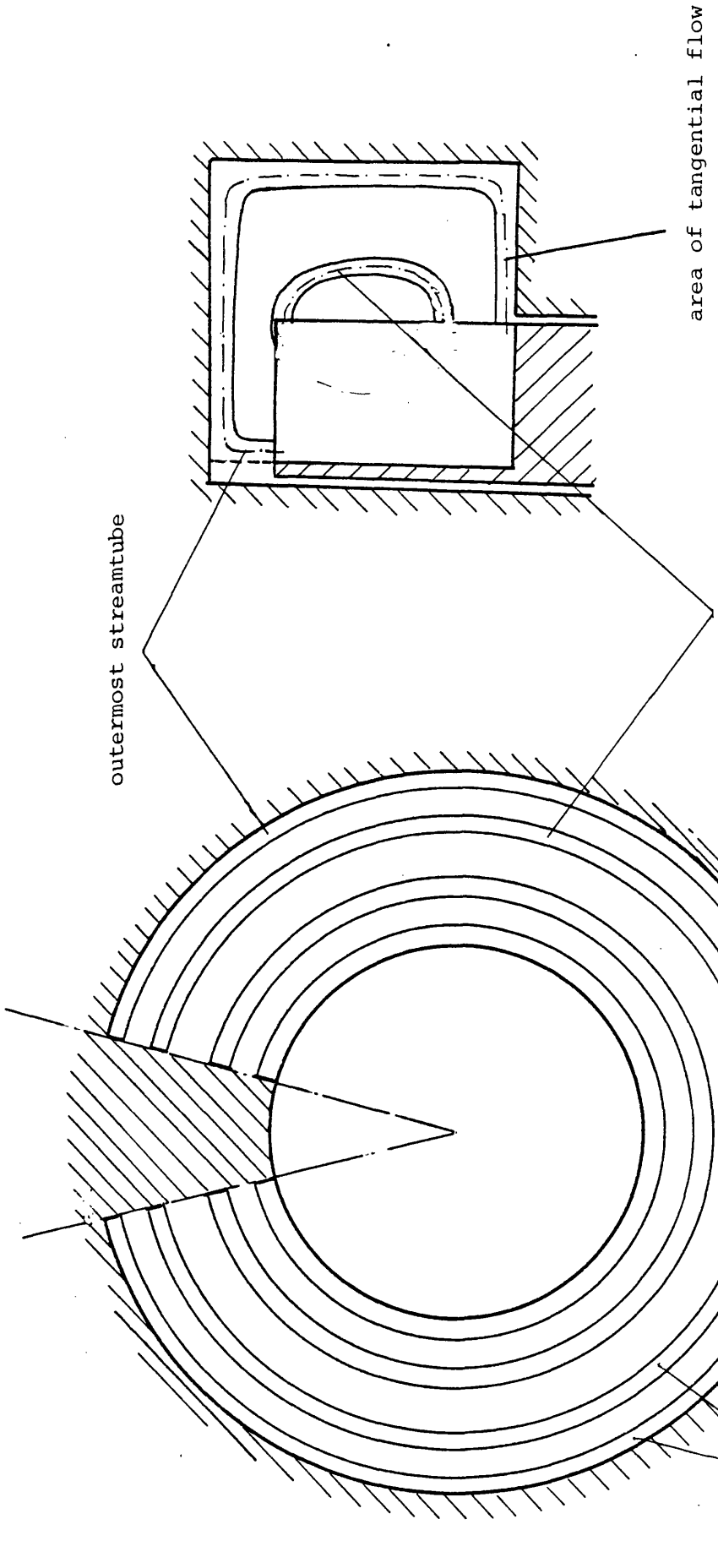

Fig. (2.7) : A diagram for estimating the hydraulic diameters of streamtubes in the channel

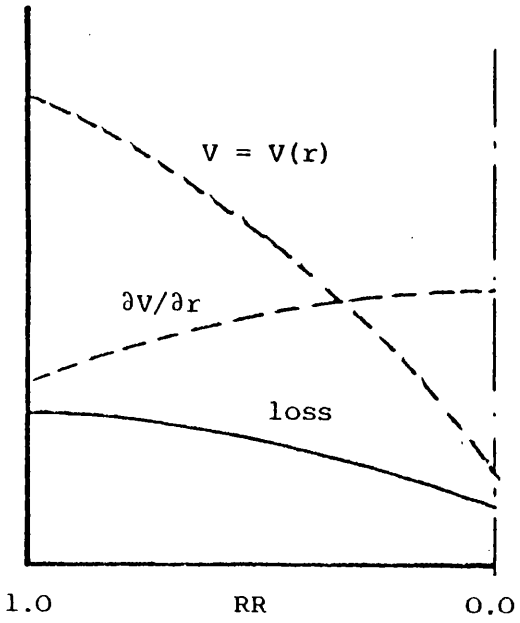

(a) Expected trend of loss distribution

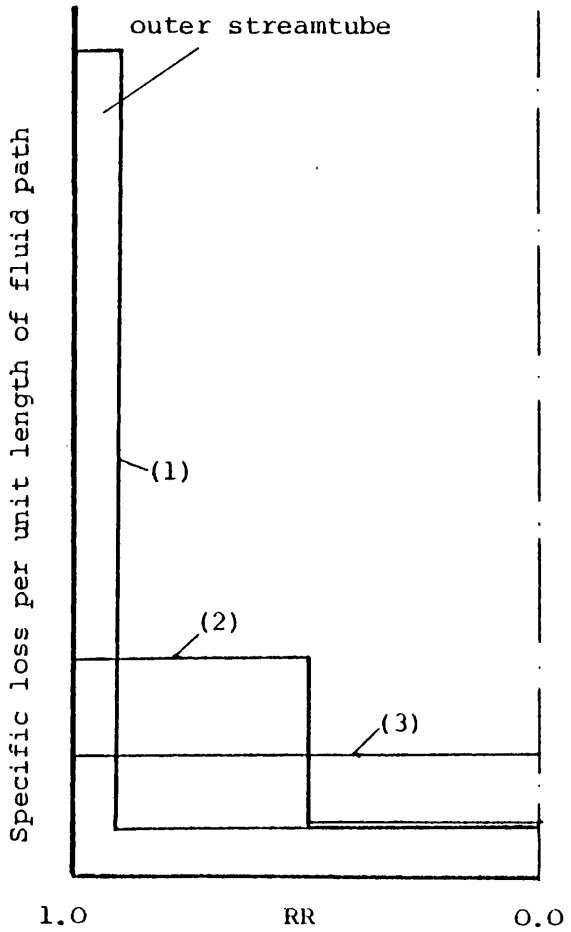

(1) Flow divided into a large number of streamtubes

(2) Flow divided into two streamtubes

(3) Entire flow considered in one streamtube

(b) Types of loss distribution when the hydraulic diameter is computed separately for each streamtube (velocity assumed uniform)

Fig. (2.8): Sketches of types of loss distribution

3. ANALYSIS OF THE NON-LINEAR SECTION

This chapter is concerned with the estimation of the losses in the inlet and the discharge ports, the carry-over losses and the leakage losses. It also deals with the estimation of the disc frictional loss, the pump discharge flow rate and the formulation of the performance relationships.

The head across the pump, its flow rate and the shaft power requirement are the three main parameters required to establish its overall performance. Since the head is normally determined from the inlet flange to the discharge flange, losses in the inlet and discharge regions must be estimated and deducted from the head gained by the fluid in the linear section to obtain the net head rise across the pump. Power losses in bearings, stuffing boxes and disc friction must be included in the shaft power requirement. Leakage of fluid through the stripper clearances from the high pressure side to the low-pressure side constitutes a further loss in the pump. The fluid trapped in the blade pockets and carried-over through the stripper and the consequent power loss in this process must also be estimated.

Formulae are written which may be used to determine the head, discharge, efficiency and power, so that the performance may be calculated at a constant speed.

3.1 Losses In The Ports Regions

The design of the inlet and discharge ports of a regenerative pump is mainly dictated by the need to preserve its self-priming characteristics. A pump which is to be properly self-priming requires that the ports be narrower than the channel in the radial direction. Their circumferential widths are also limited by the requirement to make the effective pumping section as long as possible. Consequently the two ports are usually narrow ducts and the flow through them is accompanied by considerable energy losses.

Furthermore, although the impeller starts to affect the fluid in the channel immediately after the stripper, the mechanism of energy transfer becomes fully established only at the beginning of what has been defined as the linear section where the useful energy of the fluid starts to increase. Over the entry region, from the stripper to

the beginning of the linear section, there is a considerable drop in the fluid total head, see Fig. (3.1b) and Fig. (3.2). The flow is undeveloped over this region and hence the head loss is unavoidable although it can be reduced by properly locating the inlet port with respect to the stripper, see ref. (1).

3.1.1 Qualitative assessment

Fig. (3.1b) is a reproduction from ref. (7) of typical experimental curves of the fluid head against the tangential distance from the point at which it enters the pump to the point at which it leaves. (Numbers on the curves refer to pressure taps indicated in Fig. (3.1a). It can be seen from Fig. (3.1b) that both losses in the inlet port, from point 1 to point 3, and in the discharge port, from point 11 to point 2, are functions of the discharge flow rate. The losses are considerably larger at larger flow rates than at small flow rates as is the case in all closed conduits.

The flow from the suction point 3 to point 4 is maintained by a continuous drop in the pressure because the velocity remains essentially constant and the energy transfer from the impeller starts to become effective only at point 4. Therefore the suction pressure at point 3 must be higher than the pressure at point 4. At the latter point the energy input by the impeller just starts to exceed the losses and the total head of the fluid begins to increase. When the flow rate is small the energy loss in the entry region is also small, see Fig. (3.2). However, it becomes more remarkable as the discharge increases.

Thus the losses in the inlet port and in the entry region are both functions of the discharge flow rate. Similar losses occur in the discharge region, although the effect of the losses in the entry region on the internal flow are greater. These losses are usually assumed to depend on two factors:

1) The rate of the discharge flow

2) The location, geometry, dimensions and orientation of the ports with respect to the channel, the barrier and the impeller.

Qualitatively, the dependence of the losses on the first factor has

been sufficiently clarified by experimental tests examples of which are reproduced in Fig. (3.1b). Nevertheless, the effects of the second factor have not been equally sufficiently explained. Senoo (1) tested a pump to investigate the effect of the inlet port location with respect to its distance downstream of the stripper. By varying the position of the port circumferentially he found that the pump performance could be considerably improved by placing the inlet port sufficiently downstream from the stripper such that the fluid approaching from the inlet port entered the pumping passage at a point where the flow pattern was fully established.

However, a functional relationship between the port location and the corresponding entry loss has not even been qualitatively established. Moreover, investigations on the effects of the geometry, dimension and orientation of the ports on the losses have not been reported in the literature.

3.1.2 Quantitative estimation

Losses in the inlet and discharge regions are estimated using empirical relationships correlated from experimental data. However, the available experimental data in the literature have been reported with reference to the discharge flow rate only without reference to the other factors, see section (3.1.1) above. It may therefore be permissible at this stage to assume that the head loss in the ports regions is a function of the pump flow rate only. This makes it possible to establish one formula for the total loss in the ports regions because the flow rate is the same in both regions.

Like in all closed conduits, the loss in the ports regions may be approximated by the following relation:

$$gh_p = K'_p Q^2 \qquad (3.1)$$

where:

Q = the pump discharge flow rate.

K'_p = a constant to be determined from experimental data.

gh_p = specific energy loss in the ports.

If such a functional relation is correlated from experimental data for a particular design, it may not be equally applicable to other designs. Yet it may be sufficiently accurate to use in a first approximation calculation if the ports settings are not greatly different. An example is given in the following:

In Table (3.1) the head losses in the inlet and discharge regions at various flow rates of a 0.48 m diameter pump are produced from experimental curves given in ref. (7). The impeller speed is 1000 rev/min and the pump is of the STA-Rite TH-7 design-configuration 4.

Flow rate (Q) $(m^3/s) \times 10^2$		2.265	3.596	4.955
Head loss (h_p) (m)	Inlet region	3.05	21.95	42.67
	Discharge region	12.19	18.29	30.48
	Total	15.24	40.24	73.15

Table (3.1): Entry and discharge losses at various flow rates

Fig. (3.3) shows graphically the experimental data of Table (3.1). Also shown in the figure is a plot of the relationshp of equation (3.1) based on the same data. The constant K_p' is found to be equal 29.2×10^4, the pumped fluid being air.

Using non-dimensional parameters, equation (3.1) can be written as:

$$\psi_p = K_p \phi^2 \qquad (3.2)$$

where:

$\psi_p = gh_p/(\omega^2 D^2)$

$\phi = Q/(\omega D^3)$

K_p = the port loss coefficient to be determined experimentally

Equation (3.2) may be used to estimate the total loss in the entry and discharge regions of geometrically similar pumps.

3.2 Leakage Losses

The clearances between the impeller and the casing cannot be reduced below a minimum to avoid accidental rubbing and the risk of seizure. Fluid, therefoer, leaks from the high-pressure side to the low pressure side. In particular the operation of a regenerative pump is extremely sensitive to the impeller-stripper clearance because of its low-discharge and the high pressure difference across the stripper seal.

The effect of the impeller drag also contributes to the recirculation losses through the stripper because the drag is in the same direction as that of the pressure drop, see Fig. (3.4). However, in the linear section of the pump the impeller drag opposes the leakage caused by the pressure difference. Although the two opposing effects may not exactly neutralise each other in the linear section, it is assumed in this analysis that the resultant leakage is insignificant compared to the other losses.

Thus only the leakage through the stripper clearances is considered. This leakage is partly due to the pressure difference across the stripper and partly to the drag of the impeller.

3.2.1 Leakage due to pressure difference

For a particular fluid the leakage rate due to the pressure difference across the stripper depends on the magnitude of the pressure difference, the size of the clearance and the number of blades in the stripper region at the same time, see Fig. (3.5).

The blades within the stripper are considered to act as a series of submerged orifices. An orifice coefficient C_d, introduced to account both for orifice area contraction and reduction in velocity due to friction, is assumed constant and the same for all orifices. Then since the clearance area is the same for all orifices, continuity requires that the pressure difference across each of the orifices is the same and is given by, see Fig. (3.5):

$$\Delta\psi_\ell = \frac{\psi_\ell}{Z_s} \tag{3.3}$$

where:

$\Delta\psi_\ell$ = non-dimensional head across each orifice.

ψ_ℓ = non-dimensional head across the linear section

Z_s = number of blades within the stripper at any one time.

Applying the energy equation across an orifice, the effective velocity of leakage is obtained from the equation:

$$V_\ell = C_d\ \omega D \sqrt{\frac{2\psi_\ell}{Z_s}} \tag{3.4}$$

C_d = orifice coefficient

V_ℓ = effective velocity of leakage.

V_ℓ is the same everywhere in the stripper region. Actually it is the velocity relative to the blade. The corresponding kinetic energy $\frac{V_\ell^2}{2}$ of the fluid emerging from any of the orifices is assumed to be completely dissipated in turbulence in the receiving fluid.

In a pump which has a one-sided impeller, the leakage due to the pressure difference through the radial clearance C_r is, see Fig. (3.5):

$$\phi_{\ell r} = C_d\ C_r\ (X_b + C_a)\ \frac{1}{D^2} \sqrt{\frac{2\psi_\ell}{Z_s}} \tag{3.5}$$

and that through the axial clearnace C_a is:

$$\phi_{\ell a} = C_d\ C_a\ (R_o - R_i)\ \frac{1}{D^2} \sqrt{\frac{2\psi_\ell}{Z_s}} \tag{3.6}$$

where:

ϕ_ℓ = non-dimensional leakage flow rate.

C_r = clearance in the radial direction between the impeller and the stripper

C_a = clearance in the axial direction.

The leakage through the clearance between the casing and the impeller disc in the stripper sector below R_i is assumed negligibly small.

The stripper can form an effective seal between the two ports only if there is at least one blade within it at any one time. In fact the

more the blades within it at any one time, the better the sealing effect, see equations (3.5) and (3.6). The effectiveness of the seal can be increased by one or more of the following:

1) increasing the circumferential extent of the stripper.

2) increasing the number of blades of the impeller.

3) increasing the blade thickness at the edges.

Although the performance of the pump is greatly affected by the amount of the leakage, these three meausres have countering disadvantages of significance comparable to that of the leakage, namely: that the first option results in a reduction in the working section of the pump and the second and third options result in excessive losses in the impeller. A compromise must therefore be made.

3.2.2 Leakage due to the impeller drag

The edges and tips of the rotating blades have a dragging effect on the fluid in the stripper clearances. The rate of recirculation of fluid due to this effect can be estimated by assuming a linear variation of the velocity of the fluid in the clearances from zero at the stripper walls to a maximum at the blade edges, see Fig. (3.5). Thus the fluid dragged by the impeller tip is given by:

$$\phi_{\ell t} = C_r \frac{1}{4D^2} X_b \tag{3.7}$$

and that dragged at the blade edge is given by

$$\phi_{\ell e} = C_a \frac{1}{4D^2} \frac{R_o}{2} \tag{3.8}$$

The total leakage rate through the stripper clearances is therefore given by the sum of:

$$\phi_\ell = \phi_{\ell r} + \phi_{\ell a} + \phi_{\ell t} + \phi_{\ell e} \tag{3.9}$$

i.e.

$$\phi_\ell = \frac{1}{4D^2}\left[C_r X_b + C_a \frac{R_o}{2}\right] + C_d \frac{1}{D^2}\sqrt{\frac{2\psi_\ell}{Z_s}}\left[C_r (X_b + C_a) + C_a(R_o - R_i)\right] \tag{3.10}$$

Usually $C_r = C_a = C$; then:

$$\phi_\ell = \frac{C}{4D^2}\left[\left(X_b + \frac{R_o}{2}\right) + 4\,C_d\sqrt{\frac{2\psi_\ell}{z_s}}\,(X_b + R_o - R_i)\right] \qquad (3.11)$$

Thus the leakage is directly proportional to the leakage area and the square root of the pressure difference across the linear section and inversely proportional to the number of blades within the stripper at any one time.

3.3 The Carry-over Loss

At the discharge port region the fluid in the channel is forced by the closing stripper seal to flow out, except for the part of it which leaks to the low-pressure side and which has been considered in the previous section.

The fluid between the blades when they are entering the stripper is trapped and carried through to the low-pressure side. Since the swept volume of the blades is comparable to the volume of the channel, this carried-over fluid is usually a significant part of the total fluid energized by the impeller. When trapped, it is at the highest energy level attained by the fluid in the pump. When the blade cells are in the inlet region that same fluid is at the lowest energy level in the pump. There are, however, apparantly different ideas as to what actually happens between these two ends of this carry-over process.

Wilson, Santalo and Oelrich (7) considered in their analysis of the pump that the trapped fluid performed a turbine work on the impeller and they assumed that the losses involved were negligible. In other words they assumed that the losses due to the carry-over process are negligible.

Sixsmith (24) considered that the carried-over fluid remained essentially at its high pressure state until the blade cell opened into the low pressure inlet region where it expanded in a mixing process. Part of the trapped fluid then escaped from the blade cells and expanded by throttling and the rest expanded adiabatically. Thus although no turbine work was recognised, part of the energy of the carried-over fluid was considered to be converted into kinetic energy at the inlet region via the adiabatic expansion process.

Therefore both Wilson (7) and Sixsmith (24) considered that part of the energy imparted to the trapped fluid was recovered. However, the difference between the two schools of thought lies mainly in answers to the following:

1) How big is the recovered part of the energy of the carried-over fluid.

2) By what mechanism is it recovered?

Convincing answers to these questions could perhaps be obtained from a detailed analysis of the carry-over process; but no attempt has been made in this wrok to perform such an analysis. However, there is an alternative way of judging the efficiency of the energy-recovery in such a process. It is as follows:

The carry-over losses do not affect the head generated by the pump, although they affect the power requirement and the overall efficiency of the pump. Thus the prediction of the characteristic curve $H = H(Q)$ can be made without the carry-over loss being known. Then, if the predicted head-discharge relation agrees with the experimental one, the efficiency of the process of recovering energy from the carried-over fluid may be determined by matching the predicted overall efficiency with the experimental one.

This method is a practical way of shedding light on the carry-over process, although it answers the first question only. However to improve the efficiency of the process, a thorough analysis may be required

Reference may be made to the contribution made by Sixsmith (24) with regards to the carry-over losses. He reported that the carry-over losses may be reduced by almost a factor of two by a multi-stage de-compression through ports in one of the side walls of the stripper. The expelled fluid is returned to the linear working section through ports evenly spaced along its length.

3.3.1 Estimation of the carry-over

It is assumed that the blade passages are completely full with fluid when they enter the stripper region.

Referring to Fig. (3.6), the total annular volume of the impeller between R_i and R_o is:

$$v_t = \pi(R_o^2 - R_i^2)\ X_b \tag{3.12}$$

The volume of the blades is given by:

$$v_b = (R_o - R_i)\ X_b\ t_{av}\ Z \tag{3.13}$$

where

t_{av} = average blade thickness

Z = number of blades

There may be part of the impeller, about the hub-root corner of it, which is not machined to the same axial width as the rest of it, see Fig. (3.6). A factor may be introduced to account for this so that the actual volume of the blade pockets is given by:

$$V_a = K(v_t - v_b) \tag{3.14}$$

where

v_a = actual volume of blade pockets

v_t = total annular volume of impeller

K = a factor to account for the unmachined part of the impeller.

Alternatively the volume of the unmachined part may be estimated by the following approximation, see Fig. (3.6):

$$v_\ell = \frac{\ell}{2} X_b \quad 2\pi(R_i + \frac{\ell}{4}) - t_{av} Z) \tag{3.15}$$

where:

ℓ = radial distance, as shown in the figure, equal to the height of a triangle whose area is approximately equal to the meridional area S_ℓ of the unmachined part. Then:

$$v_a = v_t - v_b - v_\ell \tag{3,16}$$

The non-dimensional volumetric flow rate of the fluid carried-over is given by:

$$\phi_{co} = \frac{N}{60} \frac{v_a}{\omega D^3} \tag{3.17}$$

The corresponding power is given by:

$$\bar{p}_{co} = \psi_{\ell} \phi_{co} \tag{3.18}$$

An efficiency of the carry-over energy recovery is defined by the following:

$$\bar{p}_{re} = \eta_{co} \bar{p}_{co} \tag{3.19}$$

where

$\bar{p}_{re}$ = power recovered from the carried-over fluid

η_{co} = efficiency of the carry-over process. Provisionally it may be assumed to have any value between zero and 100%. Its value will be varied systematically in order to assess its importance according to the method discussed in section (3.3) above.

3.4 Estimation Of The Pump Flow Rate

The total tangential flow rate through a meridional cross section in the linear section is composed of the tangential flow rate in the channel and the tangential flow rate within the impeller. The latter has been referred to as the carry-over flow rate. Then:

$$\phi_t = \phi_{tc} + \phi_{co} \tag{3.20}$$

where:

ϕ_t = total tangential flow in the linear section

ϕ_{tc} = tangential flow in the channel

ϕ_{co} = carry-over flow rate

Part of the tangential flow in the channel recirculates as leakages,

as discussed earlier. The rest forms the pump discharge flow rate, i.e.

$$\phi = \phi_{tc} - \phi_{\ell} \tag{3.21}$$

where

ϕ = the pump discharge flow rate.

To evaluate ϕ, the tangential flow in the channel must be determined. Two methods may be used:

1) Numerical integration method:

The tangential flow rate in the channel can be determined directly from the equation:

$$Q_{tc} = \int_A V_\theta \, dA \tag{3.22}$$

A = total area of a meridional cross section in the channel.

The evaluation of this surface integral requires V_θ to be known over the entire channel meridional cross section. However, V_θ can be known at discrete points only since the solution of the flow is made at discrete points along streamlines. Only numerical integration can therefore be used. By averaging the tangential velocities obtained within a small area of the meridional section, the flow rate through the area is approximately given by:

$$d\dot{Q}_{tc} = V_{av} \, dA$$

dA = area of a cell

$V_{\theta dv}$ = average tangential velocity in the cell.

If the entire meridional section of the channel is meshed with cells, the tangential flow Q_{tc} is given by the summation:

$$Q_{tc} = \sum_{j=1}^{K} V_{\theta av} \, dA \tag{3.23}$$

The accuracy of this method depends largely on the size of the cell in the mesh. If the number of cells is increased, the accuracy of

the summation is theoretically improved. However, this requires the flow to be solved along a larger number of streamlines because each cell must have at least one streamline passing through it. Also the number of points considered along each streamline must be increased so that each cell gets at least one point of solution within its boundary. Thus it can be seen that this method is demanding in terms of computation requirements. An alternative method is to determine the tangential flow from the circulatory flow rate as follows:

2) Circulatory flow method:

Referring to Fig. (3.7), an arbitrary steamtube j is considered in which a fluid particle is assumed to start a flow cycle at point 1. That particle completes that flow cycle at point 3 which is θ_{nj} radians downstream of point 1 but at the same r and z. Any other particle in the same streamtube between points 1 and 3 that starts a flow cycle in the same plane z = constant will complete its flow cycle downstream from point 3. This follows because the velocity field is assumed axi-symmetric. Therefore all the meridional flow dQ_c through that streamtube between points 1 and 3 must pass downstream through the meridional cross section θ = constant at point 3. But the flow which crosses that surface (S_θ) is the tangential flow in that tube both within the impeller and in the channel, i.e.

$$dQ_{t_j} = d\psi_j \theta_{n_j} \tag{3.24}$$

where

$d\psi_j$ = the circulatory flow rate per unit angle in streamtube j

θn_j = the net tangential displacement in one complete cycle in it.

Similarly, the tangential flow in the channel only along a streamtube is given by:

$$dQ_{tc_j} = d\psi_j \, \theta_{c_j} \tag{3.25}$$

where

θ_{c_j} = the tangential displacement in the channel only in one complete cycle of streamtube j.

From equation (3.24) the total tangential flow rate through the entire meridional section is obtained by the summation:

$$Q_t = \sum_{j=1}^{K} d\psi_j \, \theta_{nj} \tag{3.26}$$

From equation (3.25), the total tangential flow rate through the channel is given by:

$$Q_{tc} = \sum_{j=1}^{K} d\psi_j \, \theta_{cj} \tag{3.27}$$

Note that the carry-over flow rate can also be obtained using equations (3.26) and (3.27) in equation (3.20). The comparison of the result with that obtained by equation (3.17) may provide a means of judging how accurately the flow is represented by a stream function ψ and how accurately it is solved for θ_n and θ_c.

3.5 Disc Friction Losses

The pressures of the fluid in which regenerative impellers discs rotate are not axially symmetrical. Investigation of the losses associated with the rotation of a disc in such situations have not been published in the literature. It has therefore been decided to use the correlations established for estimating friction torque on enclosed discs rotating in a fluid with axi-symmetric pressure field.

By correlating experimental measurements carried out on enclosed discs rotating in fluid within an axi-symmetric chamber, Daily and Nece (46) have developed relations for the friction torque for four flow regimes. For a single wet-wall, the disc torque is estimated by the relation:

$$M = C_m \frac{1}{4} \rho \, \omega^2 \, r_o^5 \tag{3.28}$$

where

M = torque due to friction on the disc

C_m = torque coefficient depending on the flow regime

ω = angular speed of disc

r_o = outer radius of disc (inner radius assumed zero).

$$C_m = \frac{3.7(S/r_o)^{0.1}}{Re^{0.5}} \quad \text{for } Re < 3 \times 10^5 \tag{3.29}$$

$$C_m = \frac{0.0102(S/r_o)^{0.1}}{Re^{0.2}} \quad \text{for } Re > 3 \times 10^5 \tag{3.30}$$

where

S = axial clearance between the disc and the wall

$Re = \frac{\omega r_o^2}{\nu}$

The corresponding disc friction power is given by:

$$P_d = \omega M \tag{3.31}$$

3.6 Overall Performance Relations

Pumps are normally run at constant speed, while the delivery head and the discharge are altered by throttling the delivery valve. Interest therefore attaches to the variation of head, efficiency and power with the discharge flow rate. The results of a particular test may be made available for a different speed or for a homologeous pump of different absolute dimensions by using the non-dimensional quantities which are defined here as follows:

$$\text{Non-dimensional head } (\psi) = \frac{gH}{\omega^2 D^2} \tag{3.32}$$

$$\text{Non-dimensional discharge } (\phi) = \frac{Q}{\omega D^3} \tag{3.33}$$

$$\text{Non-dimensional power } (\bar{P}) = \frac{P}{\rho \omega^3 D^5} \tag{3.34}$$

The overall efficiency of the pump is defined by

$$\eta = \frac{\psi \phi}{\bar{P}} \tag{3.35}$$

where

ψ = head across the pump

ϕ = the pump discharge flow rate

$\bar{P}$ = shaft power.

The overall performance of a pump can therefore be represented by the three curves: $\psi = \psi(\phi)$, $\bar{p} = \bar{p}(\phi)$ and $\eta = \eta(\phi)$, which will be considered in turn.

Head (ψ) vis Discharge (ϕ):

The net head ψ across the pump is given by:

$$\psi = \psi_\ell - \psi_p \tag{3.36}$$

where

ψ_ℓ = fluid useful head rise produced across the linear section

ψ_p = head lost to friction in the inlet and discharge regions.

It is given by equation (3.2).

The head ψ_ℓ imparted to the fluid in the linear section is given by:

$$\psi_\ell = \frac{\bar{p}_f}{\phi_t} \tag{3.37}$$

where

$$\bar{p}_f = \frac{p_f}{\rho\omega^3 D^3} \tag{3.38}$$

$$\phi_t = \frac{Q_t}{\omega D^3} \tag{3.39}$$

where

p_f = fluid useful power gained in the linear section given by equation (2.36)

Q_t = total tangential flow rate through the entire pumping passage, given by equation (3.20) or equation (3.26).

The corresponding volumetric discharge flow rate (ϕ) of the pump is computed using equation (3.21). The head-discharge relationship can then be established as:

$$\psi = \psi(\phi) \tag{3.40}$$

It may be mentioned that whatever happens in the stripper region does

not affect the relation expressed by equation (3.40). Although the discharge ϕ is directly affected both by the amount of leakage through the stripper clearances and the amount of the fluid carried-over, neither the head across the pump ψ nor the head across the linear section ψ_ℓ are affected by these parameters.

Power ($\bar{P}$) vis Discharge (ϕ):

The required power input to the pump shaft is given by:

$$P = P_i + P_b + P_d - P_{re} \tag{3.41}$$

where

P = total shaft power input

P_i = power input by the impeller to the fluid in the linear section. It is obtained from equation (2.34)

P_b = power absorbed in bearings and packages. It is usually found to be in the range of 1% to 8%, see ref. (35)

P_d = power absorbed in overcoming disc frictional forces. It is given by equation (3.31)

P_{re} = power recovered from the fluid carried-over through the stripper. It is given by equation (3.19).

The power discharge relationship:

$$\bar{P} = \bar{P}\ (\phi) \tag{3.42}$$

can then be determined. Using the definition of equation (3.35), the efficiency-discharge relationship:

$$\eta = \eta(\phi)$$

can also be determined using equation (3.40) and (3.42).

3.7 The Entry Length of the Pumping Passage

It has been shown earlier that the pressure of the undeveloped flow in the entry region to the pumping passage falls further from the entry port discharge pressure to a minimum value at a location θ_{in} degrees downstream, see Fig. (3.1b) and Fig. (3.2). The pressure then increases continuously and essentially at a constant rate up to the discharge port. The rest of the passage along which the flow head increases is the effective pumping passage (θ_p) which is referred to as the linear section.

The value of θ_{in} has been found experimentally by several investigators to depend upon the flow rate, although the manner in which it does so has not been conclusively determined.

According to the experimental tests reported by Senoo (1), see Fig. (3.2), θ_{in} increases considerably with the increase of the discharge flow rate. From his findings the ineffective p rt is practically zero at the smallest flow rate. At large flow rates θ_{in} may reach up to 27% of the angle between the inlet and the discharge ports.

On the other hand Wilson's (7) experimental results, which are reproduced in Fig. (3.1b), show that the development length, contrary to the trend reported by Senoo, decreases with the increase of the flow rate. As a percentage of the passage from the inlet port downstream to the discharge port, the ineffective part drops from about 15% at the smallest of the three flow rates reported to about 7% at the largest flow rate.

The disagreement between the two experimental findings seems to suggest that factors other than the flow rate may be involved in determining the entry length of the passage. These may include the shape of the region itself and those of the impeller and channel.

A common factor between the two sets of results is the fall in pressure immediately following the entry port and the subsequent linear gradient of increasing pressure. The pressure fall is presumably associated with the establishment of the fully developed flow pattern, during which process additional flow losses seem likely to occur. It is difficult to see what factors will govern these losses, although it

may be supposed that a large flow rate might require more channel length for its organisation than a small flow rate. Even at zero net channel flow rate some reorganisation is still necessary in order to recombine that part of the flow passing through the stripper with that remaining in the channel. Therefore losses may be expected in this region even at zero net flow rate.

However, in the absence of conclusive experimental results regarding the entry length it is here assumed to be independent of the flow rate. This assumption is a mid-way compromise between the two sets of experimental results referred to above. Based on those results it may be reasonable to assign a value of about 10% of the pumping passage to the ineffective part.

3.8 Cavitation

As explained before, the undeveloped flow in the entry region experiences a pressure drop as the fluid approaches the linear section from the suction point. The pressure gradient changes to positive at the beginning of the linear section as the energy added by the impeller exceeds the losses. The lowest pressure in the pump is therefore at the region where the sign of the pressure gradient changes from negative to positive, see Fig. (3.8).

Senoo (1) found from experimental tests that at relatively large speeds and large flow rates the discharge did not increase even when the head was reduced. He also found that under those conditions the pressure gradient was not uniform along the pumping passage: whereas there was hardly any pressure gradient along the low pressure part of the passage described above, there was a remarkable pressure increase along a relatively short length of the passage at its end, see Fig. (3.8). Since the flow rate is the same along the pumping passage, the pressure gradient must be constant if the impeller work on the fluid is uniform along the passage. The conclusion therefore was that the impeller work was not uniform along the passage under those conditions.

The explanation is that since the minimum pressure of the liquid is limited by its vapour pressure; and since the flow rate in the entry region is maintained by the drop of pressure there, the maximum flow rate must be decided by the suction pressure. When the discharge

increases to a certain value, the minimum pressure in the pump, which occurs just where the linear section starts, drops down to the vapour pressure. Cavitation starts to occur there. Bubbles are formed in the liquid. They obstruct the transfer of energy from the impeller to the liquid. Since the vapour pressure can not decrease at a particular temperature, the flow rate does not increase even if the head across the pump is decreased. The flow rate decides the energy gradient in the linear section. If the head across the pump is further decreased, the ineffective length of the pumping passage increases. The length of the ineffective part, where the liquid flows together with bubbles of vapour without its pressure being increased, should indicate the rate of growth of the bubbles and their subsequent rate of collapse. The effective part of the pumping passage starts after enough bubbles have collapsed so that the obstruction to the energy addition to the liquid is no longer effective. Along the effective part the head of the fluid increases at a rate comparable to that at the conditions of maximum discharge under normal running conditions, see Fig. (3.8).

In this analysis the effects of cavitation are not incporated. It is simply assumed that pumps in which flows are to be analysed by this method run under normal working conditions.

3.9 Summary

In order to determine the over-all performance of a pump, formulae have been developed for the discharge, head, power and efficiency at a constant impeller rotational speed.

Formulae have been written for the estimation of the leakage through the stripper clearances, the flow rate of the carry-over and the tangential flow rate in the channel and within the impeller. The discharge flow rate of the pump is obtained by deducting the leakage losses from the channel tangential flow. The sum of the tangential flows in the channel and within the impeller together form the total flow rate through the working section. That part within the impeller is unavoidably carried back through the stripper to the inlet region.

An expression for the losses in the entry and discharge regions has been correlated from experimental data from the literature. The head across the pump is obtained by deducting these losses from the head

across the linear section. An expression for the latter was established in Chapter 2.

The shaft power is expressed as the sum of the total power input by the impeller to the fluid in the linear section and the mechanical losses.

Provision is made that part of the power of the fluid carried over may be recovered in one form or another. Such an undetermined behaviour of the carry over process is dealt with by introducing a carry over efficiency the importance of which will be assessed later.

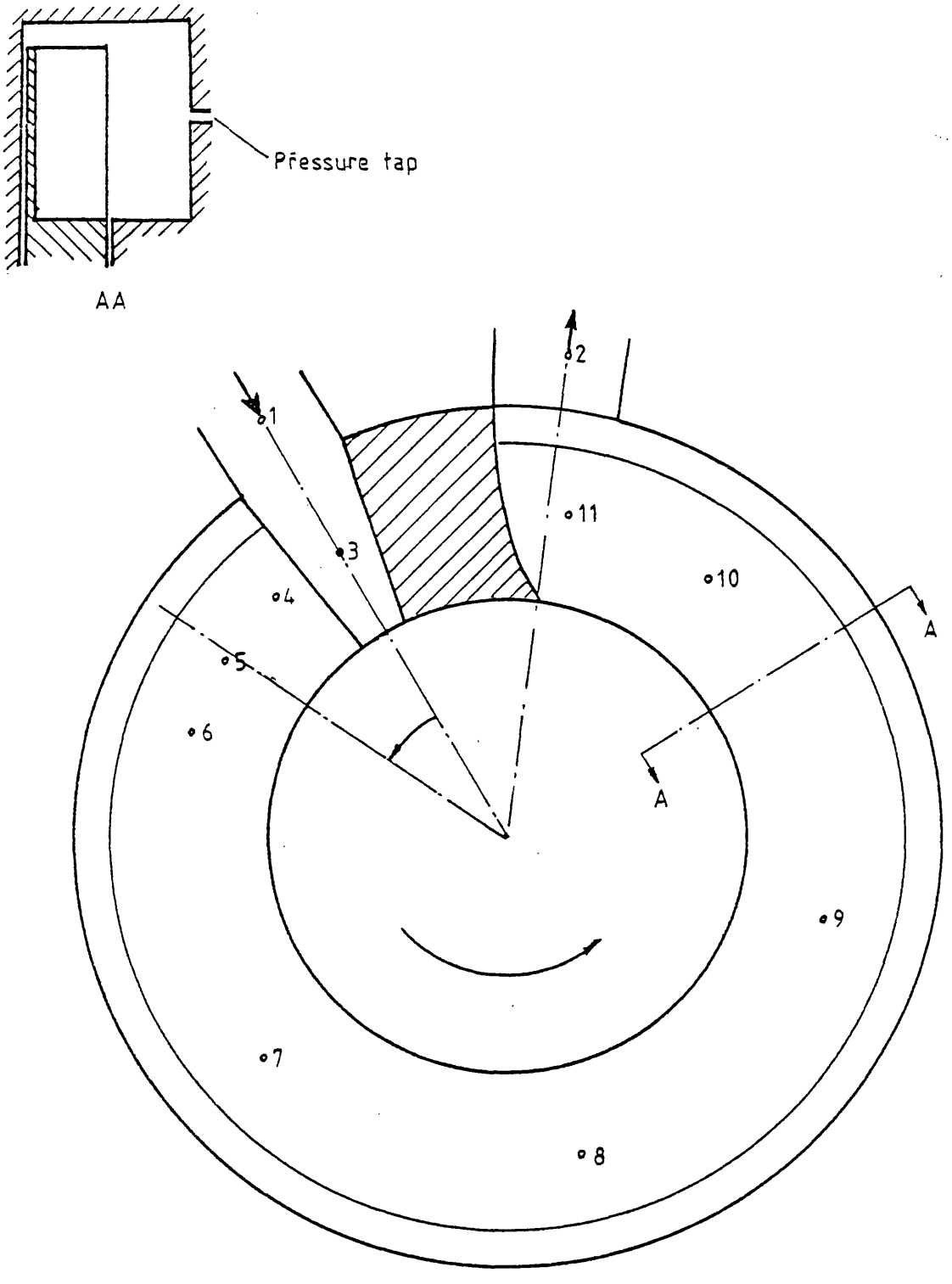

Fig. (3.1a): Schematic diagram of a Regenerative Pump with pressure taps indicated by numbers referred to in Fig. (3.1b) (reproduced from ref. (7))

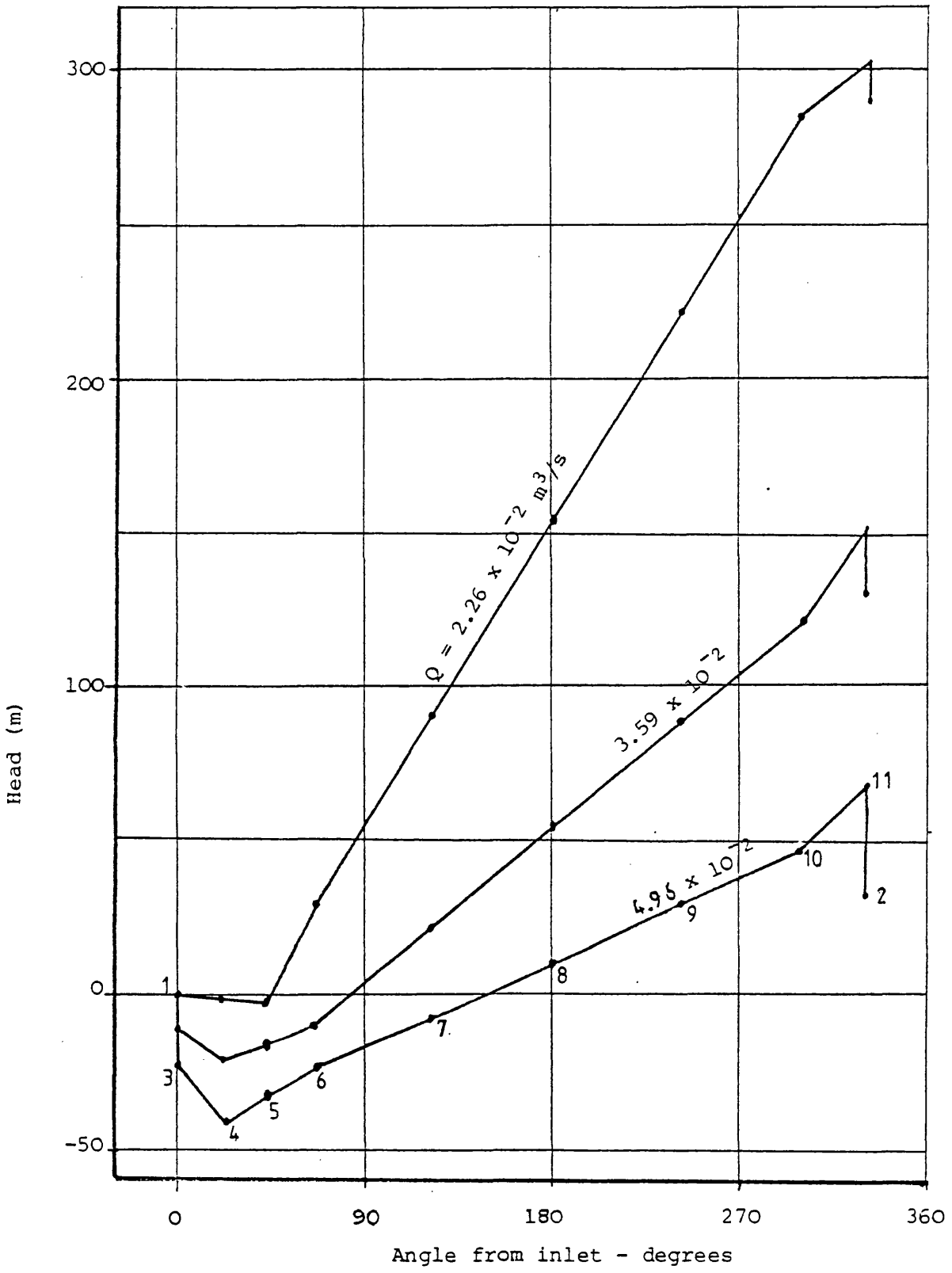

Fig. (3.1b): Head losses in inlet and discharge regions for different flow rates

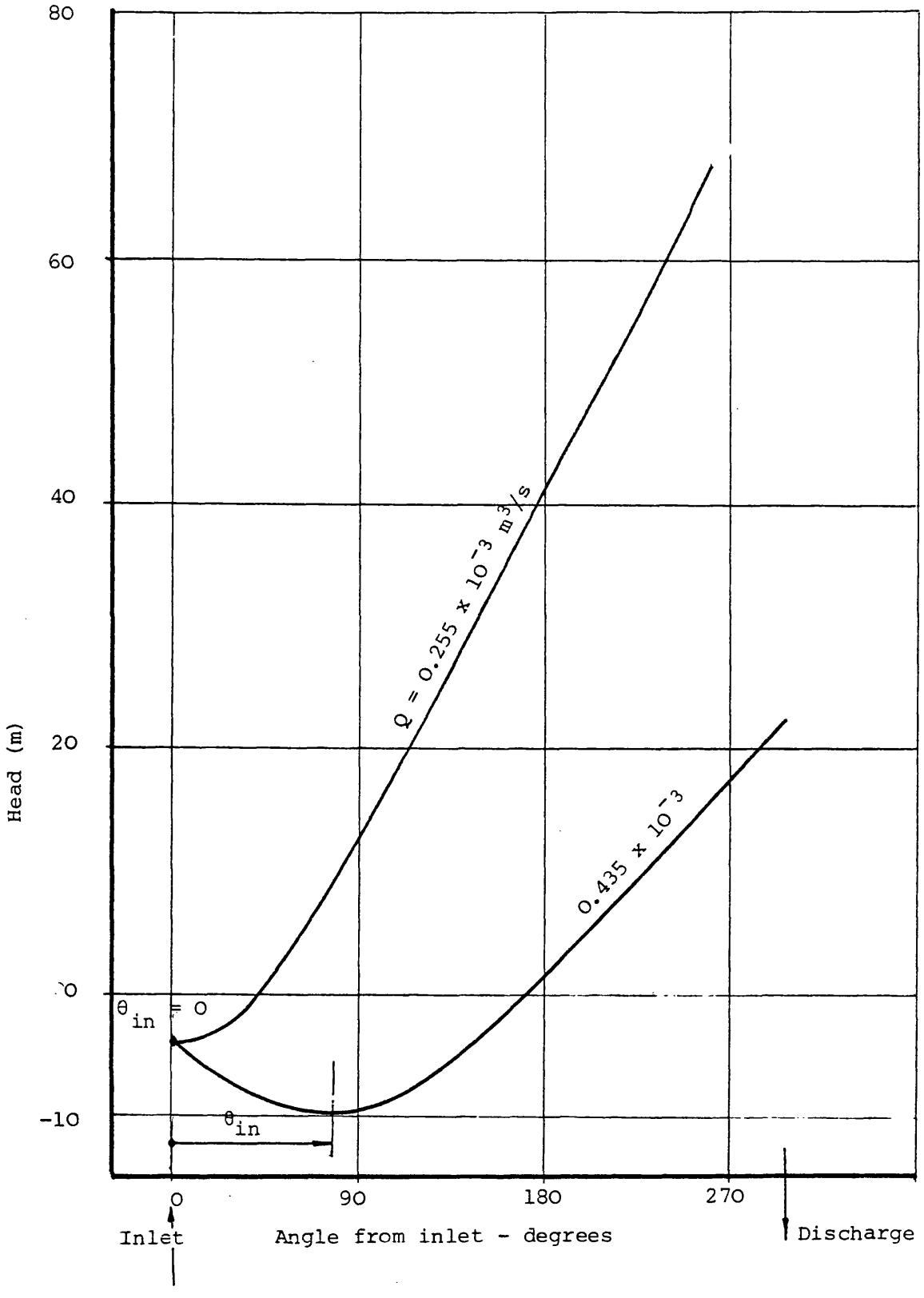

Fig. (3.2): Effect of flow rate on entry losses downstream from the suction point (reproduced from ref. (1))

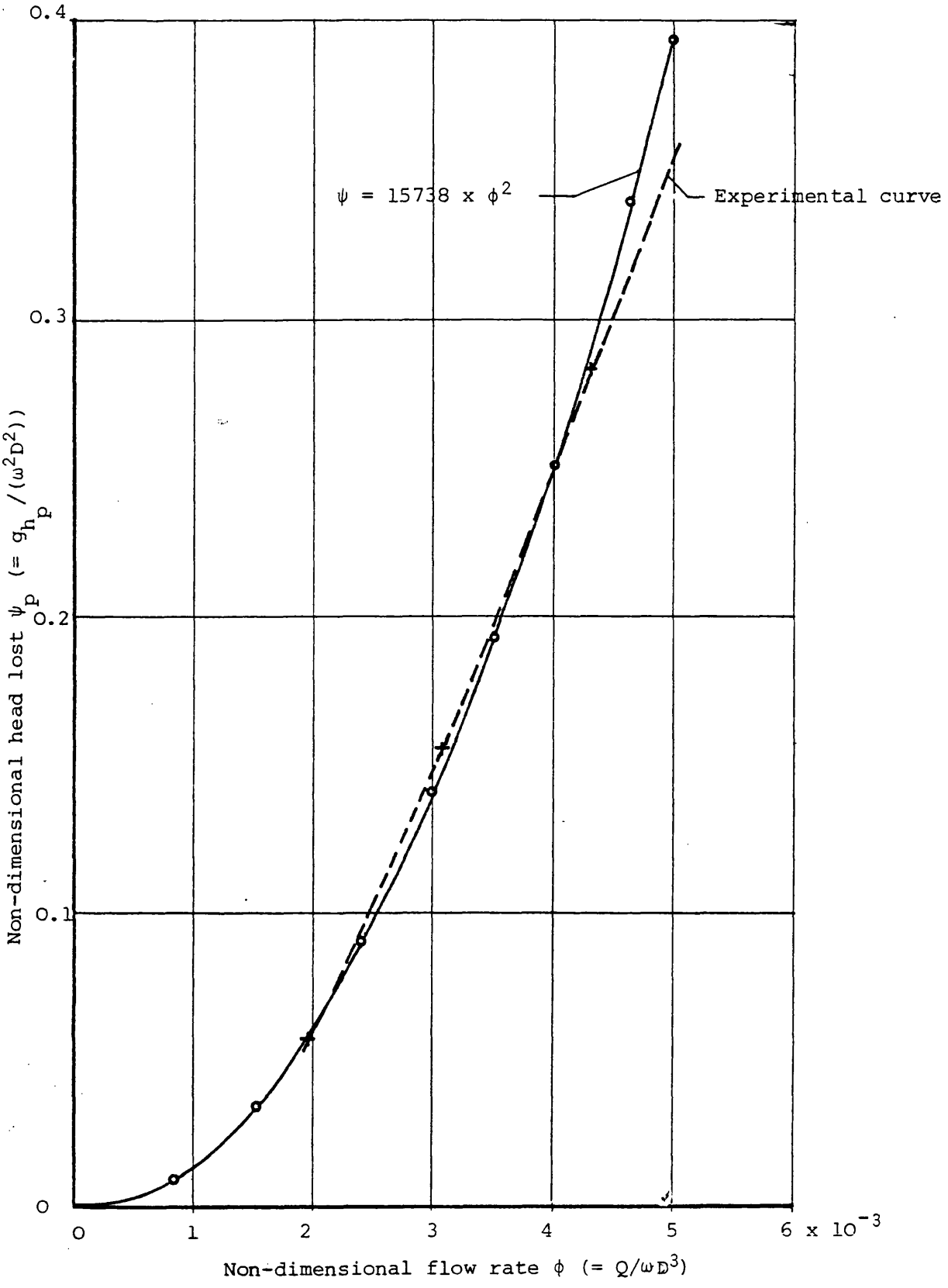

Fig. (3.3): Typical head loss in entry and discharge region against the flow rate (Data from ref. (7))

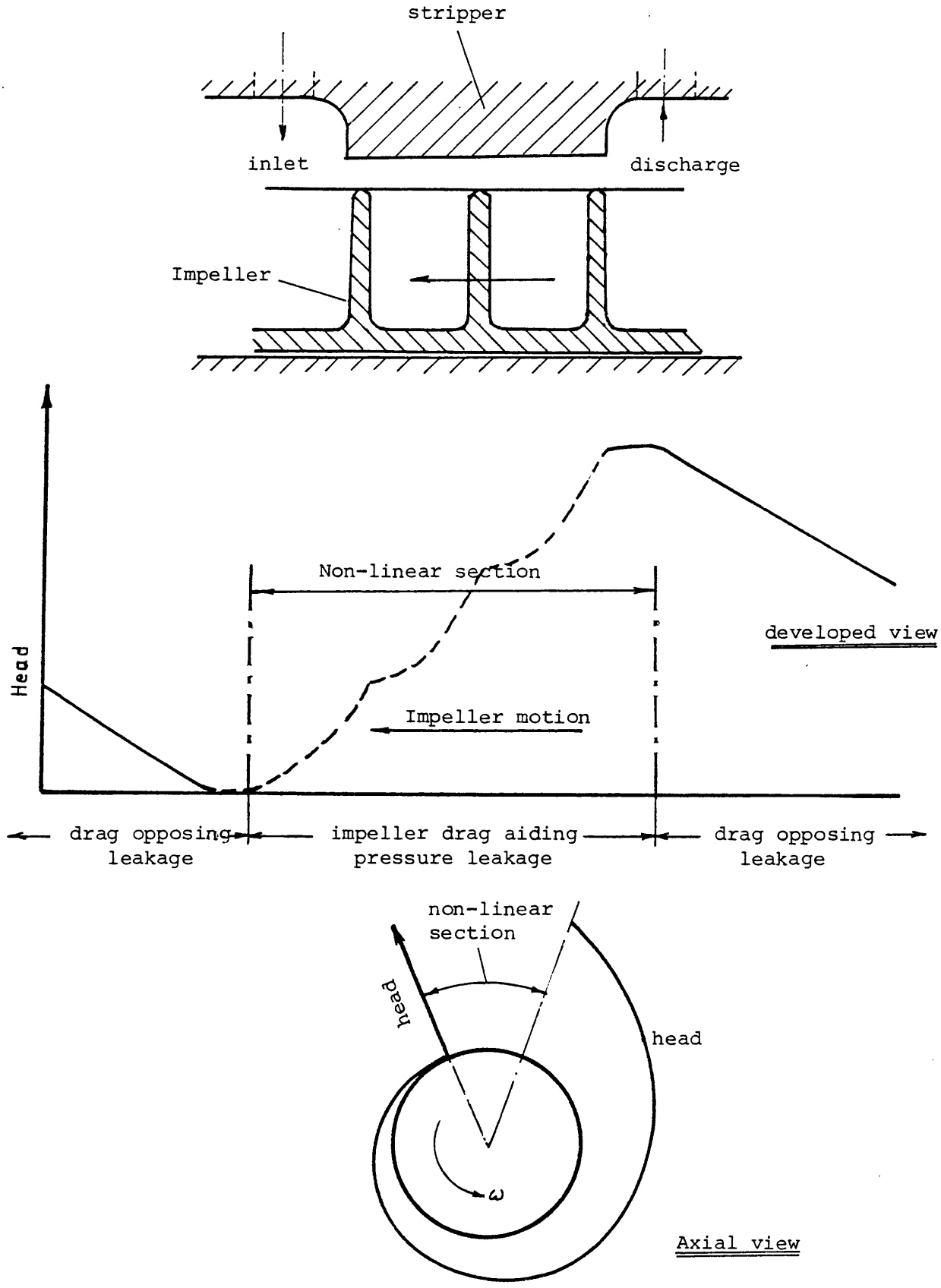

Fig. (3.4): Schematic diagram of the circumferential pressure variation in a pump in relation to the impeller drag effect

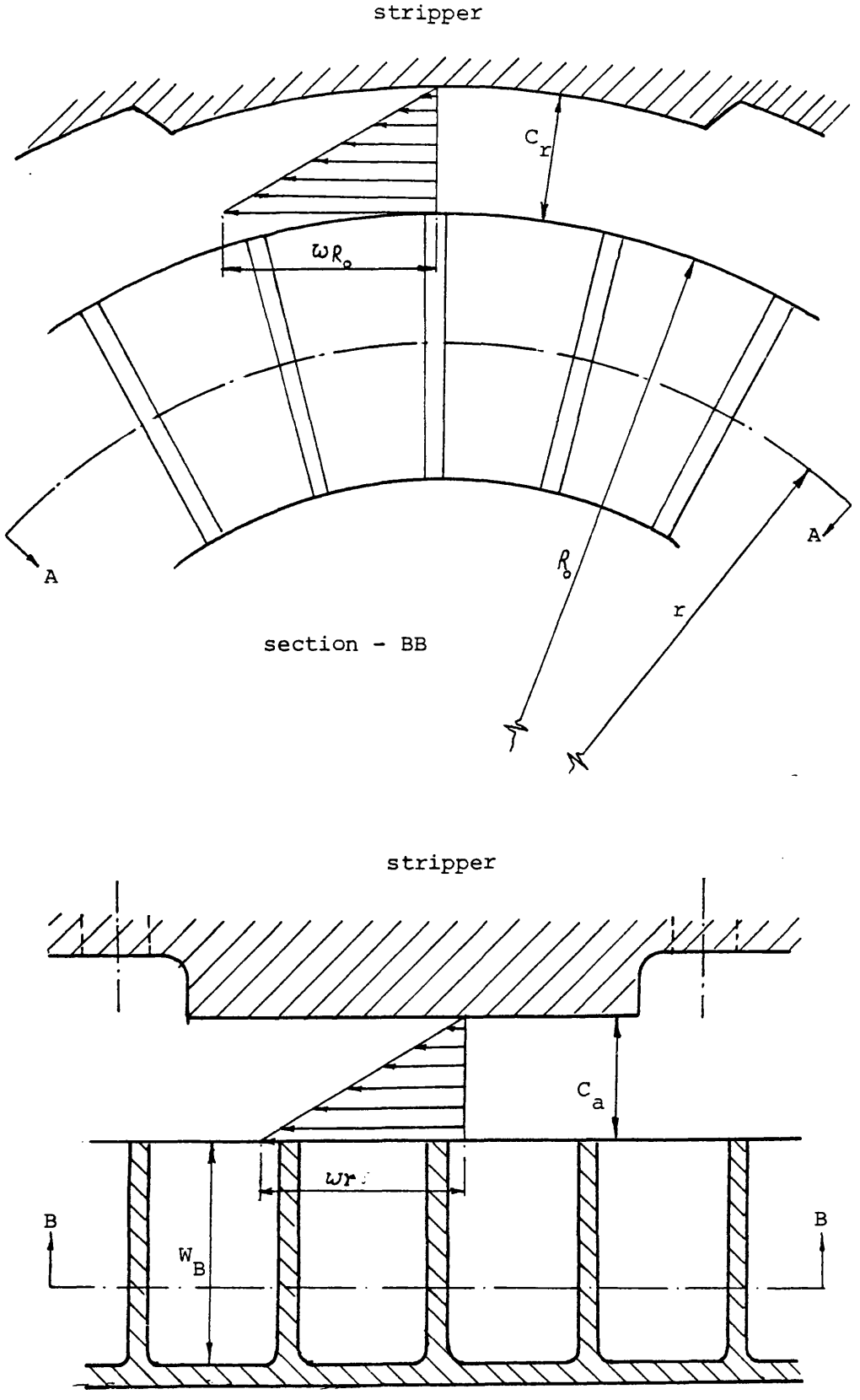

Fig. (3.5): Idealisation of leakage through impeller-stripper clearances due to pressure difference and drag. (Drawing not to scale)

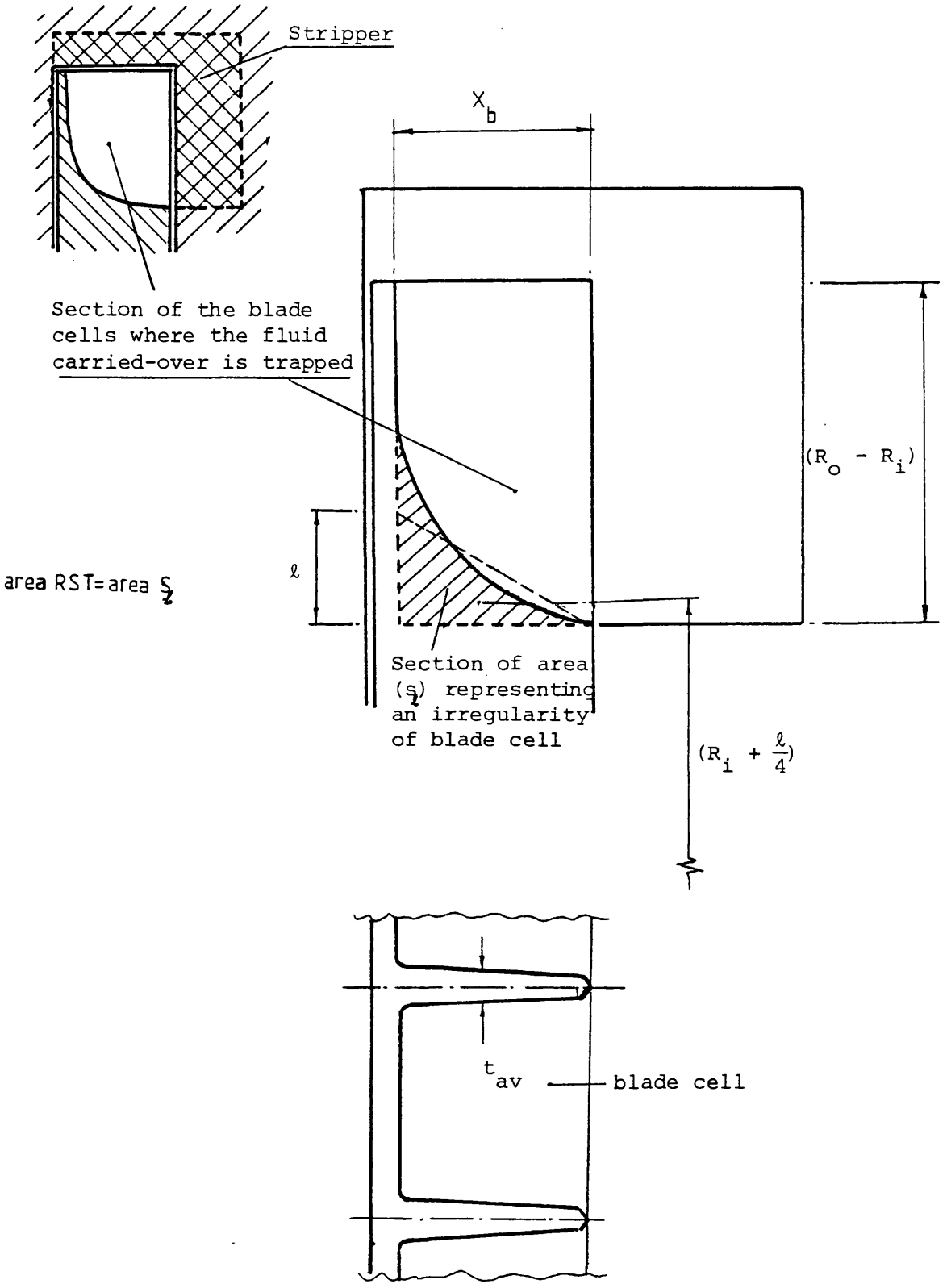

Fig. (3.6): A sketch for estimating the volume of the blade pockets.

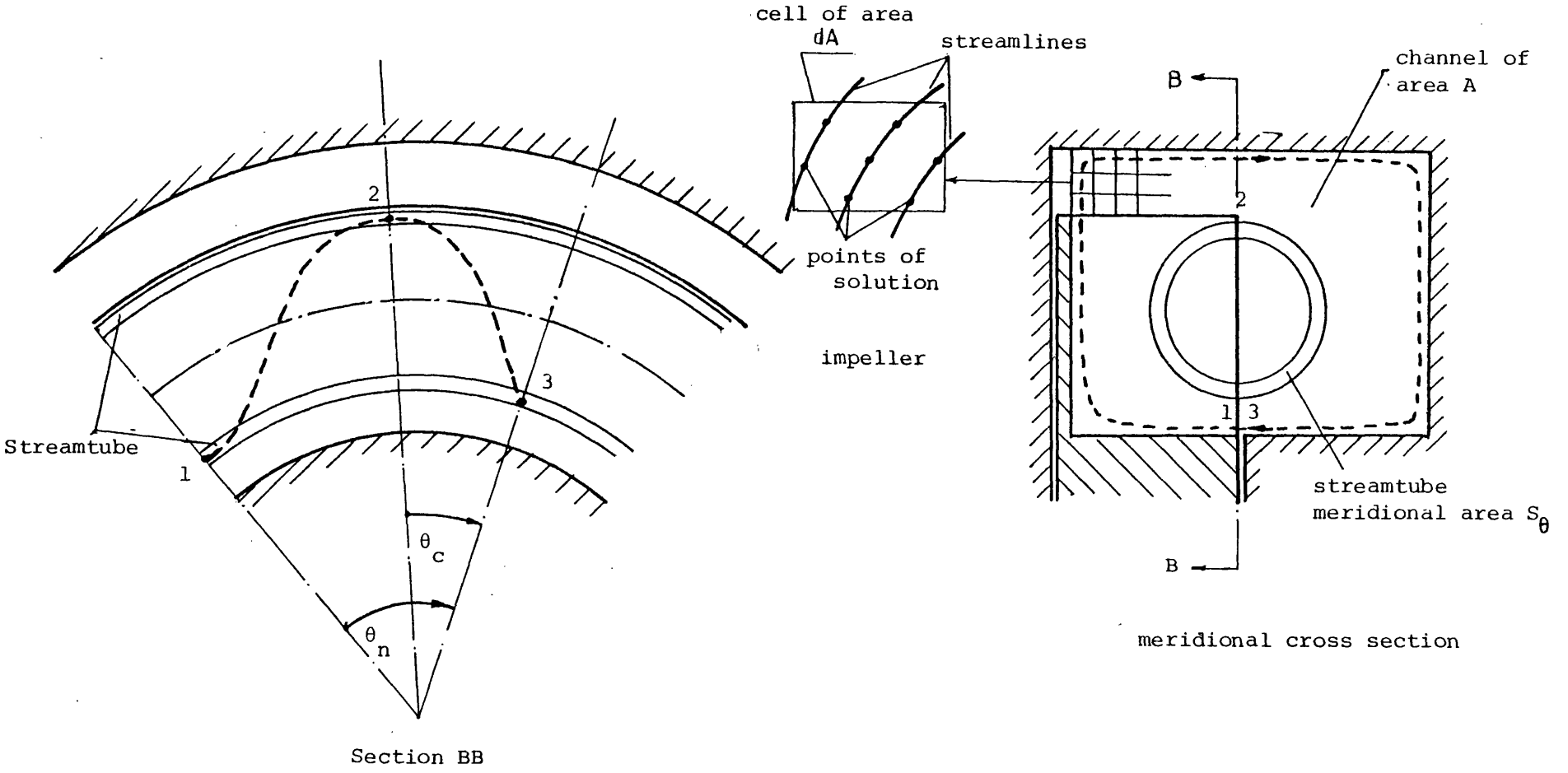

1 to 2: inside the impeller
2 to 3: in the channel

Fig.(3.7) Schematic diagram for calculating the pump flow rate

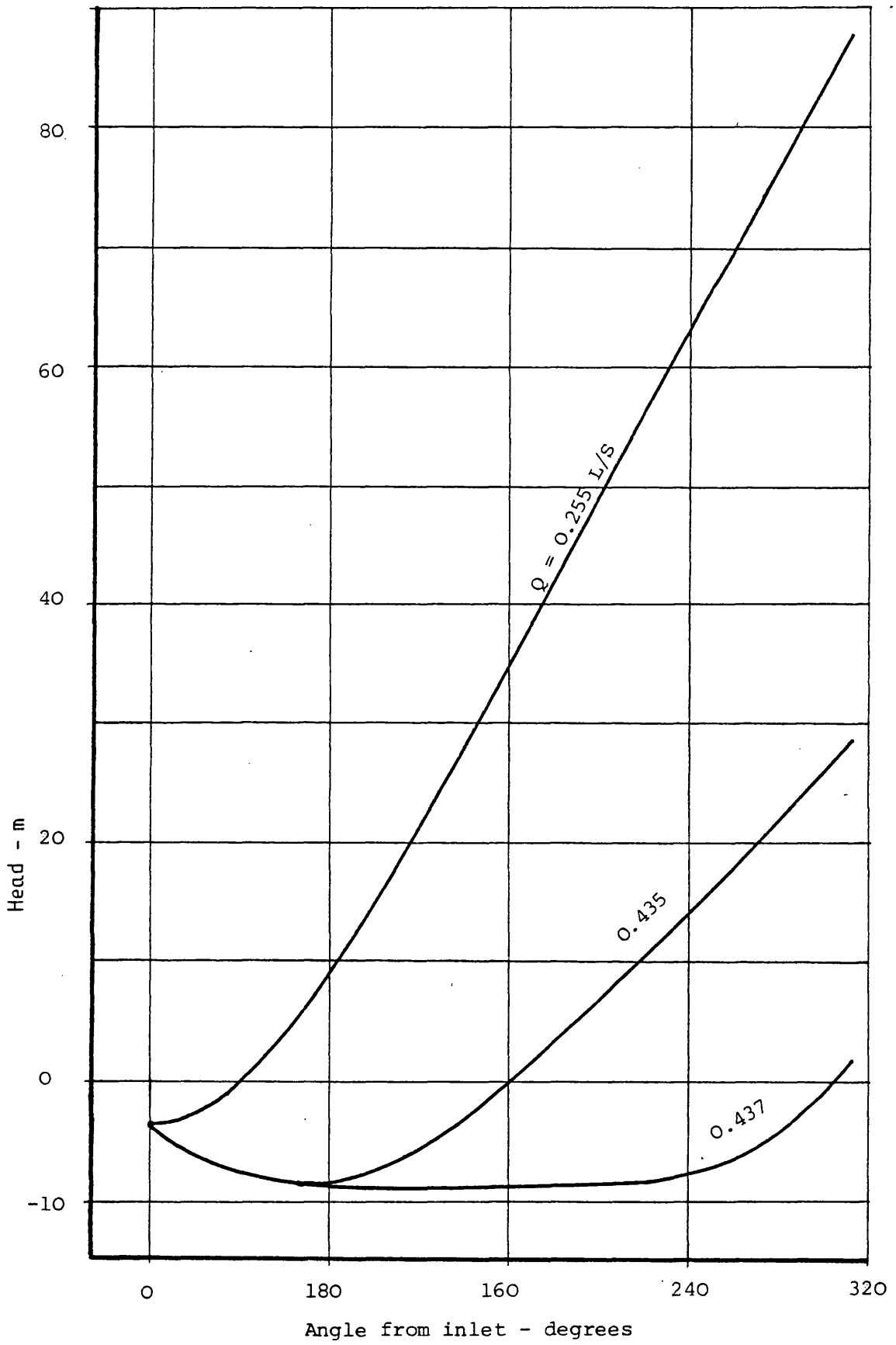

Fig. (3.8) Cavitation effects on the head variation in the pumping passage (reproduced from ref. (1))

4. METHOD OF SOLUTION

In this chapter a scheme is developed for solving the flow model. The method is direct in that it is based on a given blade shape and a given impeller-channel configuration rather than the inverse method of calculation, where a blade shape and an impeller-channel arrangement are established for prescribed velocity and pressure distribution.

The solution of the flow is based on the concept that the meridional velocity of an axi-symmetric velocity field can be represented by a stream function. The concept arises from the use of the equation of continuity for an axi-symmetric velocity field and does not involve further assumptions regarding the nature of the flow.

A procedure is developed by which the equation of a stream function can be determined such that it approximately represents the meridional velocity field. The procedure involves a solution of the flow along streamlines and the use of an energy balance between conditions at the beginning and at the end of flow cycles.

The established stream function can then be used in a further phase of the solution for the prediction of the overall performance characteristics of the given pump. Although in both the first and the second parts of the solution the flow is solved in the linear section, the second phase incorporates, in addition, the models described in Chapter 3 for the estimation of the performance of the components of the non-linear section.

Provision is made that blades of constant blade angles and constant radial deviations can be dealt with. However, in principle, the method could accommodate more complex blade designs by properly extending the routine specifying the geometry.

The tangential velocity at the exit from the impeller is estimated using a conventional slip model. The details of the numerical techniques of the solution will be discussed in Chapter 5.

4.1 Specification of Geometry

Two conditions limit the range of pump geometrical arrangements that can be analysed by the method developed here. These are:

1) That the flow models presented in Chapters 2 and 3 should reasonably represent the flow in the pump.

2) That a stream function relationship $\psi = \psi(r, z)$ should be obtainable such that it satisfies the boundary conditions of the pump meridional cross section.

Within these limits the method should enable in principle the performance of a pump of arbitrary blade shape to be predicted.

With regard to the impeller-channel configuration, the method is here discussed with explicit reference to pumps whose linear sections have rectangular meridional cross sections as shown in Fig. (4.1).

4.1.1 Common types of impeller blade

Impellers of regenerative pumps in common use up to now include the so called paddle wheel type where both the blade angle (β_0) and the angle of the radial deviation (ε) are zero everywhere on the blade, see Fig. (4.2a). Other impellers are of the claw-type where the blade is radial and the blade angle (β_0) is constant everywhere, see Fig. (4.2b).

In turbomarchinery radial blading is usually chosen since it has two major advantages over non-radial blading:

1) It generates lower level of stress than a non-radial blade in high speed machines.

2) It is simpler to manufacture.

However, the rotational speeds of regenerative pumps are on the low side (the highest reported speed is 6000 rev/min) and the blade span is usually short. Hence radial deviations, where they are advantageous with respect to the impeller hydraulic performance, may not constitute serious structural problems. As for the second reason, it should not be a criterion for deciding upon the type of blade at the stage of theoretical investigation. It should be possible therefore to consider blades of any shape rather than to adhere to the practical considerations favouring radial blading.

4.1.2 Specification of blade geometry

The following is based on the specification of blade geometry due to Vavra (22).

Referring to Fig. (4.3) and Fig. (4.4), the geometry of a blade of arbitrary shape can be described in the following way:

Definitions of parameters at any point (P):

$\hat{i}_1$: a unit vector in the direction of the relative velocity $\bar{W}$. It is tangent to the curve of intersection of the stream surface and the blade surface, since with the axi-symmetric approach the relative velocity is assumed to be along the blade surface.

$\hat{i}_2$: a unit vector tangent to the curve θ = constant.

$\hat{i}_3$: a unit vector tangent to the curve of intersection of the plane.

z : constant with the blade surface.

δ : the angle between $\hat{i}_n$ and $\hat{i}_2$ measured positibe from $\hat{i}_n$ to $\hat{i}_2$ in the direction of $\bar{\omega}$.

β : the angle between the tangent to the stream surface generatrice and the direction of the relative velocity. Hence it is also the blade angle when measured on the stream surface from $\hat{i}_m$ to $\hat{i}_1$ positive in the direction of rotation.

λ : the angle between the tangent to the stream surface genetratice m and the axis of the pump, i.e. it is the angle between the vectors $\hat{i}_m$ and $\hat{j}$ and is measured from the positive direction of $\hat{j}$.

ε : the angle between $\hat{i}_3$ and $\hat{i}_r$. This is the deviation of the blade surface from the radial direction and is measured from $\hat{i}_r$ to $\hat{i}_3$ positive in the direction of rotation.

α : the angle of the absolute flow velocity $\bar{V}$ measured on the stream surface from $\hat{i}_m$ to the vector $\bar{V}$.

If a stream function is declared to represent the meridional velocity field, the stream surface geneatrices m and the stream surface angles λ are readily obtained everywhere.

The manner in which the angle λ varies in a machine indicates whether the machine is of the axial, radial or mixed flow type, see Fig. (4.5). If for example the angle λ is zero everywhere, then the stream surface are concentric cylinders and the flow is purely axial. In conventional rotors the angle generally varies from zero to 90 degrees. However, in regenerative pumps λ varies through the full 360 degrees although part of this occurs in the channel, see Fig. (4.5).

For a given blade shape, the relative flow angle β at any location inside the impeller is a function of the stream surface angle λ only. Vavra (22) has shown that for a given blade with a constant radial deviation, the variation of the blade angle with the angle λ is given by the expression:

$$\beta = \beta_o \cos(\lambda) + \varepsilon \sin(\lambda) \qquad (4.1)$$

where at any location, β_o is the blade angle measured on a cylindrical surface co-axial with the machine axis. β_o at a point may be zero, negative or positive; and it may be constant or varying over the blade surface as may the angle of deviation ε.

However, in this work it is assumed that β_o and ε are both constant everywhere on the blade surface as is usually the case with regenerative pump blades, see Fig. (4.2). Thus with these two angles known, the flow angle β can be computed everywhere from equation (4.1) if a stream function is declared so that λ may be determined.

In general a blade geometry is completely specified if the angles β_o and ε are specified everywhere on the blade surface.

Various investigators used different methods for the specification of these angles.

The structure of the programs described in this work allows any specification method to be incorporated instead of taking constant blade angles.

4.1.3 Correction for finite thickness of blades

The effect of the blade thickness can be accounted for by reducing the flow areas by the amount which is taken up by the blades.

Let dA be an elemental area perpendicular to the meridional velocity and dA_e be that part of it which is the effective flow area such that:

$$dA_e = dA - \text{area taken up by the blades}$$

Then $W_m' \, dA = W_m dA_e$

where:

W_m' = the meridional velocity if the blade thickness is zero.

W_m = the actual meridional velocity.

Defining a blockage factor or an area restriction factor by:

$$B = \frac{dA_e}{dA} \tag{4.2}$$

then $$W_m = \frac{1}{B} W_m' \tag{4.3}$$

An expression for the blockage factor B can be derived from first principles using the blade angles already defined in section (4.1.2). It has been shown by many workers (e.g. Vavra (22)) that this is given by,

$$B = 1.0 - \frac{Zt}{2\pi r \cos(\beta)} \sqrt{1.0 + \sin^2(\beta) \tan^2(\delta)} \tag{4.4}$$

where β and δ are as defined in section (4.1.2) and:

Z = the number of impeller blades

t = the blade thickness at any location measured perpendicular to the blade surface.

r = the radial distance of the location from the axis of the pump.

The angle δ is related to the blade shape and the stream surface angle λ by the following expression:

$$\tan(\delta) = \tan \lambda - \frac{\tan \varepsilon}{\tan \beta \cos \lambda} \qquad (4.5)$$

A special case is when the relative flow angle β is zero everywhere. Equation (4.4) then reduces to the following:

$$B = 1.0 - \frac{zt}{2\pi r} \qquad (4.6)$$

Using equations (4.5), (4.4) and (4.3) the actual meridional velocity can readily be computed at any point if the blade number, blade thickness and blade shape are known.

4.2 Effect of Slip

As mentioned in section (2.4), the pressure difference between any two adjacent blades of an impeller causes a tendency for a secondary circulation about each blade such that the fluid leaving the impeller deviates from the path prescribed by the blade surface backwards with respect to the positive direction of rotation. The result is that the fluid tangential velocity is less than that which would be expected from the velocity vector diagram based on the outlet blade angle. In order to allow for the reduction in the ideal tangential velocity, a slip factor (σ) is usually introduced which is defined as follows:

$$V_{\theta 2} = \sigma V_{\theta 2i} \qquad (4.7)$$

where:

σ = slip factor.

$V_{\theta 2}$ = the actual tangential velocity at the exit from the impeller.

$V_{\theta 2i}$ = the fluid exit tangential velocity which would be expected from an impeller with an infinite number of blades. With such an impeller the flow angle and the blade angle are identical everywhere.

Wiesner (39) reviewed the many correlations available in the literature for calculating the slip factor. Ferguson (44) has compiled values of slip factor found from several theories for a number of blade angles and blade numbers and compared them with known experimental values. He found that for radial vaned impellers the expression given by Stanitz (37) agreed very well with experimental observations. Stanitz's

expression for slip factor is:

$$\sigma = 1.0 - \frac{0.63\ \pi}{Z(1.0 - \phi_2 \tan(\beta_2))} \tag{4.8}$$

where:

Z = number of blades

$\phi_2 = V_{f2}/U_2$

$V_{f2} = V_r$ at the tip of the impeller

$= V_Z$ at the vertical edge of the impeller

β_2 = the blade angle at the exit from the impeller

With the ideal velocity $V_{\theta 2i}$ from equation (4.9) and the slip factor from equation (4.8), the tangential velocity $V_{\theta 2}$ at the exit from the impeller can be computed readily by equation (4.7), but see Chapter 6 and Appendix A regarding special effects in regenerative machines.

4.3 Basis of the Method

The method of solving the flow in the linear section is based on the assumption that a stream function relationship $\psi = \psi(r,z)$ can be established to approximately represent the meridional velocity $\bar{V}_m = \bar{V}_m(r,z)$ at any operating condition of a given pump.

Theoretically, the meridional velocity of an axi-symmetric velocity field can be represented by a stream function. In practical terms, however, it may not always be possible to determine such a function explicitly. For example:

1) The flow field may be too complex to be represented by a simple function or it may require for its representation a relationship that needs too many unknown parameters to be determined.

2) The wall boundary of the meridional cross section may be such that a simple stream function cannot be found which will satisfy the boundary conditions.

Practically, therefore, the applicability of the analysis is subject to the following expectations:

1) The meridional cross section should have a regular shape so that its boundaries can be defined by a simple function. An example of this is the rectangular section shown in Fig. (4.1).

2) It is to be expected that, using a simple function, the representation of the meridional velocity field may be only approximate.

The solution in the linear section is required to determine only the velocity and the pressure distributions. Since the flow is assumed incompressible, other flow parameters can be derived from these.

4.3.1 Impeller solution

In the impeller the axi-symmetric approach greatly simplifies the situation: from Fig. (4.4) it can be seen that the relative tangential velocity is given by:

$$W_\theta \hat{i}_\theta = W_m \tan(\beta)\, \hat{i}_\theta \tag{4.9}$$

Since the total velocity is the sum of the tangential and the meridional velocities, there is:

$$\bar{W} = W_m \tan(\beta)\, \hat{i}_\theta + W_m\, \hat{i}_m \tag{4.10}$$

Thus the problem of determining the velocity field inside the impeller reduces to finding the meridional component $\bar{W}_m$ of the flow.

With the velocity field $\bar{W}$ known, the circulatory flow dQ_c and the impeller angular push θ_i can be determined for any streamtube and hence the power input by the impeller to the fluid, given by equation (2.34), can be evaluated and so is the pressure distribution if required. The losses in the blade passages can also be estimated if the velocity is known.

4.3.2 Channel solution

In the channel if the meridional velocity $\bar{V}_m$ is known everywhere, the equation of motion and the energy equation can be solved along streamlines, starting by the known conditions at the exit from the impeller.

Thus the tangential velocity V_θ and the static pressure p can be

estimated at discreet points along streamlines as will be shown in Chapter 5.

Subsequently, the pump discharge flow rate and the skin frictional losses in the channel and the losses across the incidence at the entry to the blades can be evaluated.

Therefore the task of solving the flow in the linear section, both in the impeller and in the channel, is essentially that of determining the appropriate meridional velocity $\bar{V}_m$ under the given tangential pressure gradient $\frac{\partial p}{\partial \theta}$.

4.4 The Stream Function

In Fig. (4.6) a meridional section in the linear section of a typical pump is shown. The stream function ψ is a measure of the circulatory flow rate Q_c and it is convenient to take $\psi = 0$ at the channel wall. It has its maximum value at the centre of circulation C. At any point between the wall and the centre c the circulatory flow is defined as the meridional flow rate through any surface extending from the wall to the point considered.

Referring to Fig. (4.6), an elemental circulatory flow is given by:

$$dQ_c = V_r dz\, r d\theta - V_z dr\, r d\theta \qquad (4.11)$$

Since the velocity field is assumed axi-symmetric, the circulatory flow is consequently a function of r and z only.

The stream function is defined as the circulatory flow per unit angle i.e.

$$d\psi = dQ_c/d\theta \qquad (4.12)$$

Then from equation (4.11):

$$d\psi = rV_r\, dz - rV_z dr \qquad (4.13)$$

Curves ψ = constant are the generatrices of stream surfaces or the meridional projection of streamlines, i.e.

$$\psi = \text{constant} \tag{4.14}$$

is a family of the closed curves which are the meridional projections of the true streamlines in r, θ and z co-ordinates.

Since ψ is a function of r and z only, its total differential is given by:

$$d\psi = \frac{\partial \psi}{\partial r} dr + \frac{\partial \psi}{\partial z} dz \tag{4.15}$$

By comparing equation (4.13) with equation (4.15), the following expressions are obtained for the meridional components of the velocity:

$$V_r' = \frac{1}{r} \frac{\partial \psi}{\partial z} \tag{4.16a}$$

$$V_z' = -\frac{1}{r} \frac{\partial \psi}{\partial r} \tag{4.16b}$$

Introducing the blockage factor B defined in section (4.1.3), the corrected meridional velocity components are obtained as follows:

$$V_r = \frac{1}{B} \frac{1}{r} \frac{\partial \psi}{\partial z} \tag{4.17a}$$

$$V_z = -\frac{1}{B} \frac{1}{r} \frac{\partial \psi}{\partial r} \tag{4.17b}$$

The stream function $\psi = \psi(r,z)$ defined by equation (4.13) can be shown to satisfy the equation of continuity. The basic characteristics of the function are:

1) It is a single-valued continuous function of r and z only.

2) It satisfies the equation of continuity and the boundary condition of the meridional cross section.

3) Physically, it is the circulatory flow per unit angle; hence it has the dimensions of volume flow per unit time per unit angle.

4) It represents the meridional velocity at any point by equation (4.17).

If, for a given pump and a specified tangential pressure gradient $\frac{\partial P}{\partial \theta}$, a stream function relationship $\psi = \psi(r,z)$ is declared, then the meridional velocity $\bar{V}_m$ is in effect also declared everywhere in the linear section. According to the provisions of the previous section, this means that all the flow field inside the impeller is effectively defined while that in the channel is partially defined but requires V_θ to be determined.

On the basis of this conclusion, general stream function relationships which have the basic characteristics listed above are now examined and methods are developed to determine explicitly the appropriate forms under the operating conditions.

4.4.1 General stream function relationships

Different stream function relationships $\psi = \psi(r,z)$ can be written in general forms for the same impeller-channel configuration such that they all satisfy the boundary conditions of the meridional cross section. However, only by using a digital computer can it be decided whether or not a simple form of function can possibly be extracted from a more general form to approximate the meridional velocity of a given pump under a chosen tangential pressure gradient. The reason for this is that to test a particular function it is necessary to solve the flow iteratively along streamlines using finite difference approximations.

The following general forms of stream function relationships are considered so that simpler versions of them can be obtained and examined more closely:

1) Algebraic Stream function

The following continuous algebraic surface equation satisfies the boundary conditions according to the notation in Fig. 4.7a):

$$\psi = \sum_{j=1}^{k} A_j (1.0 - RR^{a_j})^{b_j} (1.0 - ZZ^{c_j})^{d_j} \qquad (4.18)$$

where j refers to the term number in a series of k-terms. A, a, b, c and d are constants. RR and ZZ are the non-dimensional radial and axial co-ordinates respectively, measured from the centre of circulation c as shown in Fig. (4.7a).

2) Trignometric Stream Functions:

a) The following relationship satisfies the boundary conditions of the section according to the notation shown in Fig. (4.7b):

$$\psi = \sum_{j=1}^{k} A_j \left(\sin(RR^{a_j}\,\pi)\right)^{b_j} \left(\cos\left(ZZ^{c_j}\,\frac{\pi}{2}\right)\right)^{d_j} \qquad (4.19)$$

where:

$$RR = \frac{r - R_i}{R_o - R_i}$$

b) The following function satisfies the boundary conditions of a meridional section according to the notations shown in Fig. (4.7a):

$$\psi = \sum_{j=1}^{k} A_j \left(\sin\left(RR^{a_j}\,\frac{\pi}{2}\right)\right)^{b_j} \left(\cos\left(ZZ^{c_j}\,\frac{\pi}{2}\right)\right)^{d_j} \qquad (4.20)$$

A function which has k terms will have 5k + 1 constants to be determined. Considering one term only of any of the above three series there are six independent constants to be determined: the coefficient A, the four indices a, b, c and d, and the radius R_m of the centre of circulation. However in the case of the function expressed by equation (4.19) R_m is not independent of the index a; therefore it will have five constants only to determine.

4.4.2 A one-term function

The non-dimensional form of a single term function of the type of equation (4.18) is:

$$\bar{\psi} = \frac{\psi}{A} = (1.0 - RR^a)^b \cdot (1.0 - ZZ^c)^d \qquad (4.21)$$

Consider the following two equations which represent sections through the surface of the stream function:

A section RR = 0 is given by:

$$\bar{\psi} = (1.0 - ZZ^c)^d \qquad (4.22)$$

A section ZZ = 0 is given by:

$$\bar{\psi} = (1.0 - RR^{a})^{b} \tag{4.23}$$

To obtain an idea of the types of surfaces that can result from the use of different values of the indices, these sections are plotted for selected values of the indices a, b, c and d and are shown in Fig. (4.8) and Fig. (4.9). It can be seen that a remarkable change of surface shape can be effected by changing the values of the indices.

Since these curves are obtained by varying only two indices of the function out of six available variables, it is considered that a one-term function will be sufficient to give any surface which may be required for a first approximation representation.

Hence in the rest of this work the stream function used will have the following simple form:

$$\psi = A(1.0 - RR^{a})^{b} \ (1.0 - ZZ^{c})^{d} \tag{4.24}$$

Where A is the stream function coefficient which is a constant and equal to the maximum value of the function which occurs at the centre c where RR = ZZ = 0. a, b, c and d are constant indices and RR and ZZ are the non-dimensional co-ordinates defined in Fig. (4.7a).

It can be mentioned that a similar trignometric function from equation (4.20) will give the same results. However, a function from equation (4.19) is one degree of freedom less because it does not include the constant R_m at all.

4.5 The Centre of Circulation

Although the circulatory flow itself has been verified experimentally by several workers as shown in Chapter 1, there is no published experimental work with regard to the location of its centre c.

Regarding the stream function, the centre c is the location where the function is maximum, i.e.

$$\frac{\partial \psi}{\partial r} = \frac{\partial \psi}{\partial z} = 0 \tag{4.25}$$

However, this condition is satisfied at any point where RR and ZZ are chosen to be zero, see equation (4.24). Therefore, as far as the stream function is concerned, equation (4.25) cannot be used to determine the centre of circulation. It is determined by fixing the two axes ZZ = RR = 0.

The Axis ZZ = 0:-

Due to the centrifugal force, the relative flow inside the impeller will be mainly radially outwards. On the other hand, the centrifugal effect on the channel flow arising from its tangential motion is relatively weaker compared to the flow emerging from the impeller into the channel. The circulatory flow in the channel will therefore be mainly radially inwards. Accordingly, it is assumed that the centre c lies along the vertical edge of the blades. The axis ZZ = 0, which will be used in the stream function equation, is thus defined with respect to the meridional cross section.

The Axis RR = 0:-

The centre of circulation c is at a radius R_m from the axis of the machine, see Fig. (4.7a). It is assumed that the radius R_m will not be greater than the outer radius of the impeller; since if the flow is to be maintained, all the fluid must be presumed to pass through the impeller, i.e.

$$R_m < R_o \tag{4.26}$$

The circulatory flow in regenerative pumps is not unlike that in fluid couplings and torque converters if the turbine element in these machines is imagined to be replaced by the side channel. In the analysis of fluid couplings and torque converters, see ref. (47), the meridional velocity is usually assumed to be either constant or linearly varying with the distance from the centre c of circulation, see (a) and (b) of Fig. (4.10).

Applying the principle of continuity, the radius R_m is obtained in these two cases as follows:

a) When the meridional velocity is assumed constant along the distance

from the centre in a meridional section, see Fig. (4.10a):

$$R_m = \frac{R_o^2 + R_i^2}{2} \tag{4.27}$$

b) When a linear variation is assumed, Fig. (4.10b):

$$R_m = \frac{2}{3} \frac{(R_o^3 - R_i^3)}{(R_o^2 - R_i^2)} \tag{4.28}$$

Some workers on regenerative pumps, for example Pfleiderer (8), used the linear average of the outer and inner radii of the section for the radius R_m:

$$R_m = \frac{1}{2} (R_o + R_i) \tag{4.29}$$

This average has also been used for R_m in fluid couplings, see ref. (47).

The above three equations clearly give different values of R_m. There is no indication as to which one of them best approximates the actual location of the centre of the meridional flow. However, for all the above results it will be observed that:

$$R_m \geqslant \frac{1}{2} (R_o + R_i) \tag{4.30}$$

Since, in the approach developed here, R_m may be declared to have an arbitrary value, like any of the other stream function parameters, its determination must be seen as an integral part of the determination of the stream function relationship.

However, the range in which R_m is searched for is considerably narrowed by employing the limits expressed by equations (4.26) and (4.30). Summarising, it is assumed that:

$$R_o > R_m > \frac{1}{2} (R_o + R_i) \tag{4.31}$$

4.6 Preliminary Investigations

To establish the stream function of equation (4.24) to represent the flow at a given operating condition in a given pump it is required to determined the coefficient A, the four indices a, b, c and d and the radius R_m since the rest of the parameters R_o, R_i, X_c and X_b involved in the function are assumed to be known dimensions of the pump.

Each of the first five parameters can have any positive value in the range from zero to infinity and the function will still satisfy all the characteristics of section (4.4). The routine for determining the appropriate values of the parameters is considerably simplified by examining the main features of the velocity profiles, resulting from using arbitrary values for the four indices a, b, c and d, against the following expectations:

1) The meridional velocity should be zero at the centre of circulation because a fluid particle cannot have two opposite motions at the same time and place.

2) At the wall the velocity should strictly speaking be zero. However, boundary layer-type solutions are not considered here. The flow is solved along stream tubes and the boundary layer region is assumed to be negligibly small compared to the meridional width of a stream tube so that the velocity at the wall can, in practical terms, be assumed finite. This approach is resorted to in analysis of hydraulic couplings and torque converters as well as in these pumps.

These expectations provide only a means for narrowing the ranges of values that the four indices may assume. They do not provide a mechanism for determining the appropriate values of these parameters because they deal only with end conditions of the velocity profile. The complete shape of the profile can only be determined by solving the flow.

Furthermore, such a preliminary study does not provide any guide to the values of the coefficient A or the radius R_m. Therefore, the non-dimensional form of the stream function, equation (4.21), will be used in this examination.

From equation (4.17) and equation (4.21) and referring to Fig. (4.7a), the following expressions are obtained for the meridional components of the velocity, ignoring the blockage:

$$V_r = \frac{1}{r} (1.0 - RR^a)^b \; d \; (1.0 - ZZ^c)^{d-1} \; (-cZZ^{c-1}) \; \frac{1}{X} \qquad (4.32a)$$

$$V_z = - \frac{1}{r} (1.0 - ZZ^c)^d \; b(1.0 - RR^a)^{b-1} \; (-aRR^{a-1}) \; \frac{1}{Y} \qquad (4.32b)$$

where X and Y are non-dimensionalising lengths. Referring to Fig. (4.7a):

In sector I: $X = X_c$, $Y = R_o - R_m$, $RR = \frac{r - R_m}{Y}$, $ZZ = \frac{Z}{X_c}$ (4.33I)

In sector II: $X = X_c$, $Y = R_m - R_i$, $RR = \frac{R_m - r}{Y}$, $ZZ = \frac{Z}{X_c}$ (4.33II)

In sector III: $X = X_b$, $Y = R_m - R_i$, $RR = \frac{R_m - r}{Y}$, $ZZ = \frac{|Z|}{X_b}$ (4.33III)

In sector IV: $X = X_b$, $Y = Ro - R_m$, $RR = \frac{r - R_m}{Y}$, $ZZ = \frac{|Z|}{X_b}$ (4.33IV)

A small computer program has been written which computes the velocity profile along any section from the centre c to the wall for various combinations of a, b, c and d. Excerpts from the results obtained along a section Zz = 0 are shown in Fig. (4.11) to Fig. (4.18).

Although the velocity profiles are labelled as V_z against RR, they also represent the profiles V_r vis ZZ. The expected end conditions mentioned above are the same for both velocities. Therefore, instead of repeating the same plots and the same findings, it is taken that in this preliminary study:

$$a = c \qquad (4.34a)$$

and

$$b = d \qquad (4.34b)$$

Conclusions which may be drawn from these profiles are as follows:

1) Both indices a and c must be greater than unity if the velocity at the centre is to be zero. In Fig. (4.11) and Fig. (4.12) the velocity at the centre is infinite because a = c < 1.0. In Fig. (4.13), a = c = 1.0 and the velocity is finite at the centre. In Fig. (4.14) to Fig. (4.18) the necessary condition of zero velocity at the centre is met. Then the following conclusions are made regarding the magnitudes of a and c:

$$a > 1.0 \tag{4.35a}$$

$$c > 1.0 \tag{4.35b}$$

2) Indices b and d greatly affect the magnitude of the velocity next to the wall. It can be seen from Fig. (4.11) to Fig. (4.15) that if these two indices are less than unity, the velocity at the wall is infinite irrespective of the magnitudes of the other indices. While if they are greater than unity, the velocity at the wall is zero, see Fig. (4.16) and Fig. (4.17) as examples; and if they are equal to unity, the velocity at the wall is finite, see Fig. (4.18).

Since infinite velocities cannot occur, the only possible ranges of values of b and d are as follows:

$$b > 1.0 \tag{4.36a}$$

$$d > 1.0 \tag{4.36b}$$

However, with the introduction of the second expectation discussed above, it may be concluded with a reasonable degree of certainty that both b and d could be equal to unity. i.e.

$$b = 1.0 \tag{4.37a}$$

$$d = 1.0 \tag{4.37b}$$

Equations (4.35), (4.36) and (4.37), which summarize the useful results obtained from this study, will be used as a guide in the search for stream function parameters.

4.7 Determination of the Stream Function Parameters

To determine the values of the indices, the radius R_m and the coefficient A, the following procedure is used:

a) Select a value for $\partial p/\partial\theta$.

b) Select arbitrary values for R_m, a, b, c, d and A.

c) Compute the flow, along a streamline, through the impeller and channel, leading to a determination of the pressure increase and the peripheral angle turned through in a single cycle.

d) Compare the pressure increase with that implied by the peripheral angle and the chosen value of $\partial p/\partial\theta$.

e) Vary A until this comparison is satisfactory.

f) Repeat the steps (c) to (e) for other streamlines.

g) Since A should be constant across the section, repeat steps (b) to (f) until A is the same for all streamlines.

This process will now be described in more detail.

4.7.1 Flow cycles on gH-θ plane:

The variation of fluid energy along a flow cycle can be described on an energy (gH) - angular displacement (θ) plane as shown in Fig. (4.19).

By definition the tangential pressure gradient is constant. i.e.

$$\frac{\partial p}{\partial \theta} = \text{constant} \tag{4.38a}$$

Then, with the axi-symmetric assumption, there is also:

$$\frac{\partial (gH)}{\partial \theta} = \text{constant} \tag{4.38b}$$

where H is the fluid total head defined by:

$$gH = \frac{p}{\rho} + \frac{V^2}{2} \tag{4.38c}$$

i.e. The gradient of the energy variation in the peripheral direction

is also constant. Then the energy variation along any curve r = constant - z = constant is represented by a straight line in the plane gH - θ. However, the variation of gH with θ along streamlines may assume various shapes depending on flow conditions and the path of the streamline.

a) The flow cycle 123'3:

Referring to Fig. (4.19), consider the flow along a streamline starting at point (1) just inside the impeller and passing to point (2) at impeller exit and going from there through the channel to point (3') just outside the impeller before passing to point (3) just inside the impeller again. Points (1) and (3) have the same r_1 and z_1 co-ordinates, but different values of θ. Therefore the line L joining (1) and (3) has a slope $\partial(gH)/\partial\theta$. The path 123'3 describes a flow cycle.

From (1) to (2) the head rises due to the work done by the impeller. The fluid leaves the impeller at (2) and is thrown forward into the peripheral pressure gradient. As it moves forwards it exchanges its kinetic energy for potential energy and its peripheral velocity V_θ is reduced.

Depending upon the rapidity of the meridional motion the value of V_θ achieved at point (3') could either still be positive or zero or in the opposite direction to that of the impeller motion.

As the fluid re-enters the impeller (passing from (3') to (3)) it suffers a loss of energy depending upon the way it approaches the impeller blade edge.

b) Losses in a flow cycle:

The ideal flow cycle corresponding to the cycle described above is indicated by the path 145 in Fig. (4.19). The losses encountered in the actual cycle are also indicated. The ideal energy variation along the peripheral curve r_1 = constant - z_1 = constant is shown by the line M.

The angular displacement of the cycle 123'3 is composed of θ_i in the impeller and θ_c in the channel. The head input in the impeller is composed of Euler head ($gH_4 - gH_8$) and the head $\theta_i \frac{\partial(gH)}{\partial\theta}$ imparted due

to the tangential energy gradient.

The losses in the cycle are $(gH_4 - gH_2)$ in the impeller passages, $(gH_6 - gH_3)$ in the channel and $(gH_{3'} - gH_3)$ across the impeller leading edge.

The increase in the fluid specific energy is given by:

$$\Delta(gH)_a = (gH_3 - gH_1) \tag{4.39}$$

Such energy gain per flow cycle may be different in different streamlines in common with the other parameters.

c) An assumed flow cycle:

Referring to Fig. (4.20), assume an operating condition is represented by the slope $\partial(gH)/\partial\theta$ of the line L. Assume that the solution of the flow along a streamline using arbitrary values for the stream function parameters (A, a, b, c, d and R_m) results in a flow cycle represented by the path 1ABc in the figure; while 123'3 is the actual flow cycle under that condition but it is not known at the present.

The cycle 1ABc is referred to as the computed or the assumed cycle because it is obtained on the basis of assumed stream function parameters. The computed net head rise according to this cycle is:

$$\Delta(gH)_c = gH_c - gH_1 \tag{4.40}$$

It can be seen from Fig. (4.20) that the assumed meridional velocity does not have its proper value because the end point c on the cycle does not lie on the line L the slope of which has been used as an input parameter for the solution itself.

A solution has been determined when the terminal point of the cycle falls on line L. In these circumstances:

$$\Delta(gH)_c = \theta_n \frac{\partial(gH)}{\partial\theta} \tag{4.41}$$

where:

$\Delta(gH)_c$ = computed energy rise in a cycle. It is obtained by solving

the flow using an assumed stream function.

θ_n = net peripheral angle turned through in the cycle. It is computed on the same basis as $\Delta(gH)_c$.

$\theta_n \frac{\partial(gH)}{\partial\theta}$ = actual energy rise in a flow cycle if θ_n has the proper value. In such case it is also equal to $(gH)_a$ given by equation (4.39). In all cases it is referred to by $\Delta(gH)_\theta$ because it is computed on basis of θ_n, i.e.

$$\Delta(gH)_\theta = \theta_n \frac{\partial(gH)}{\partial\theta} \tag{4.42}$$

Generally the discrepancy (Δ) between the assumed and the actual cycles can be expressed by:

$$\Delta = \left|1.0 - \frac{(gH)_\theta}{(gH)_c}\right| - 100\% \tag{4.43}$$

The magnitude of this discrepancy provides a measure of the incompatibility between the assumed meridional velocity field and the actual one.

4.7.2 Approach to solution

In principle, a complete solution can be obtained by studying n streamlines and using the end of cycle incompatability mentioned above to correct each of the n unknown parameters of a selected stream function.

However, there is no guarantee that a solution even exists in the case of any given surface and selected value of $\partial p/\partial\theta$. A complete solution is possible if the function is capable of representing the flow exactly. This cannot be guaranteed.

However, it is to be expected that such solutions can be approached sufficiently closely for practical purposes. This has been shown to be the case using the simple six-parameter stream function used here.

A procedure which is compatible with the nature of approximate representation of flow is that which is based on comparing results obtained using different sets of values of the parameters and selecting the set which produces the best representation.

The amount of work involved is greatly reduced if the number of variables is reduced from six to four: this allows the search for a solution to be carried in a single plane rather than in a multi-dimensional space. It is, therefore, helpful, but not necessary, to reduce the unknown indices to two.

From the preliminary studies presented in section (4.6) it has been shown that, from the expected condition of finite velocity at the wall:

$$b = d = 1.0 \tag{4.44}$$

Alternatively, a similar simplification can be achieved by taking:

$$a = c \tag{4.45a}$$

and

$$b = d \tag{4.45b}$$

This is obtained by inspecting the preliminary results given by equations (4.35), (4.36) and (4.37).

Either of these options reduces the number of unknowns indices to two. The procedure described in the following subsection is presented on the understanding that one of them is used: no matter which one. However, the procedure can be extended to allow the inclusion of an arbitrary number of parameters.

A further simplification can be achieved if both equations, (4.44) and (4.45), are utilised together. Then the search for a solution will be involving only three unknowns:

$a(=c)$, A and R_m

4.7.3 Outline of procedure

The following are the steps used in seeking a solution, see the flow diagram of Fig. (4.21).

1) Declare a value of R_m in the range given by equation (4.3).

2) Declare an operating condition of the given pump by declaring a value for $\partial p/\partial\theta$.

3) Select arbitrary values for the indices on basis of the results of the preliminary studies.

4) Select a streamtube.

5) Declare a value for A and solve the flow along the streamtube to obtain the flow parameters in a complete flow cycle 1ABC of Fig. (4.20). There may or may not be a suitable solution which results in a positive computed head rise. If a positive value of $\Delta(gH)_c$ is obtained, continue to step (6); otherwise vary the value of A. If there is no positive head obtained for all values of A, then the combination of the other five parameters is not appropriate to represent the flow.

One or more of these values are altered until a solution gives a positive head.

6) Use the end of cycle incompatability, measured by equation (4.43), to correct the value of A. Typical plots of $\Delta(gH)_c$ and $\Delta(gH)_\theta$ against A' are shown in Fig. (4.22), while the other parameters are being kept constant. A' is the non-dimensional coefficient given by:

$$A' = \frac{A}{\omega D^3} \tag{4.46}$$

an A_m is the matching value of A, see Fig. (4.22).

7) Repeat steps (4) to (6) for other streamlines and obtain their matching values A_m.

A particular set of values of the parameters R_m, a, b, c and d will in general result in different values of A_m for each streamline. This means that the coefficient of the stream function varies across the meridional section. This contradicts the assumption that A is a constant made when the stream function was differential to obtain the meridional velocity V_r and V_z and their derivatives.

The variation of A_m across the section can be measured by the following ratio:

$$A_R = \frac{A_{m(max)}}{A_{m(min)}} \tag{4.47}$$

$A_{m(max)}$ = the maximum of the values of A_m of all streamlines.

$A_{m(min)}$ = the minimum of the values of A_m.

A_R = a measure of the degree of variation of A_m across the meridional section.

A_m = the matching value of the coefficient A for a streamline, see Fig. (4.22).

The best representation is achieved by a stream function for which the matching coefficients A_m of all streamlines have the same value, i.e. when there is:

$$A_R = 1.0 \tag{4.48}$$

Equation (4.48) provides a criterion for selecting the most suitable stream function.

For particular values of R_m and $\partial p/\partial\theta$, the guide given by equation (4.48) is used to determine the most suitable set of values of the four indices. Fig. (4.23) shows typical variations of A_R against a (= c) for fixed values of b (= d). (i.e. the expectation expressed by equation (4.45) is used in this graph.

From such curves, a map which depicts the ratio A_R as a set of contours can be plotted, as shown in Fig. (4.24), for the purpose of determining the values of a (= c) and b (= d) which correspond to the minimum variation of A_m across the meridional section. Although there is not necessarily a position on the map where the ideal condition of equation (4.48) is obtained, A_R may achieve a minimum value $A_{R(min)}$ approximating unity.

An important conclusion is drawn from results of the type shown in Fig. (4.23). Out of all the curves b = d = constant, the curve b = d = 1.0 is found, in most cases, to be the one which results in the minimum value of the ratio A_R. This confirms the expectation expressed in equation (4.44). According to this finding, equation (4.44) will be used in the rest of this work.

This suggests the use of a map of contours of A_R, as shown in Fig. (4.25), to determine the values of a and c which correspond to $A_{R(min)}$, rather than assuming a = c. However, from results of A_R plotted against a for fixed values of c, see Fig. (4.26), it may be found in some cases that for all the curves c = constant, the minimum ratio $A_{R(min)}$ occurs at points where c = a. The second expectation, equation (4.45), is therefore also confirmed in such cases. Generally, however, a and c may not be equal, see Fig. (4.25).

Summarising: take indices b = d = 1.0 in all cases and determine the values of the indices a and c from a map of contours of the degree of mismatching between streamlines (A_R) on an a - c plane as shown in Fig. (4.25). A less accurate way of determining the best values of a and c is by assuming a = c and determining their value from a single curve as shown in Fig. (4.27).

8) Repeat the above process from step (2) for different operating conditions ($\partial p/\partial \theta$) to cover the working range of the given pump and obtain the best degree of matching between streamlines ($A_{R(min)}$) at each of them.

The effect of the magnitude of the tangential pressure gradient on the 'best degree of matching obtained' may be noticeable if the less elaborate approach of assuming a = c is adopted, see Fig. (4.28). However, better and less different 'best degrees of matching' at the different operating points can be obtained from maps of contours as explained earlier.

9) Repeat the above procedure for other values of the radius of the centre of meridional circulation R_m. Plot the 'best degree of matching obtained', $A_{R(min)}$, against R'_m for the different pressure gradients considered, as shown in Fig. (4.29).

From such curves, the value of R'_m which corresponds to the best of the 'best degrees of matching' may be obtained for each of the pressure gradients.

In many cases it has been found that more or less the same value of R'_m is the best for all working conditions, see Fig. (4.29). In such cases one value is used for the radius of the centre of meridional

circulation at all working condition. Otherwise, different values of R_m may be used at different pressure gradients.

Thus R_m, which is an integral part of the stream function, is logically determined, together with the indices, by a procedure which is designed to satisfy a basic condition required in the stream function relationship: the condition that the variation of the coefficient (A) should be minimum, if not possible to have it constant, over the meridional section.

10) Using the values of R_m obtained as above, determine the corresponding values of the indices a, b, c and d at the different pressure gradients required. Then use these as input data in the second phase of the solution to predict the performance of the pump.

4.8 Summary

A scheme for solving the flow model has been developed with explicit reference to pumps having rectangular meridional cross sections.

In specifying the geometry, it is assumed that the blades have blade angles and radial deviations which are constant everywhere.

A conventional slip factor is selected for estimating the tangential velocity of the fluid at the exit from impeller.

A mathematically simple stream function relationship, which satisfies the boundary conditions of the meridional cross section, has been selected for the purpose of approximating the meridional velocity field. A preliminary study is carried out on the function to limit the range of parameter values to receive detailed study.

Procedures for establishing the values of the parameters of the function are then developed and presented in detail. Their determination requires the aid of digital computer.

The numerical techniques and the programs generated for solving the flow are discussed in the next chapter.

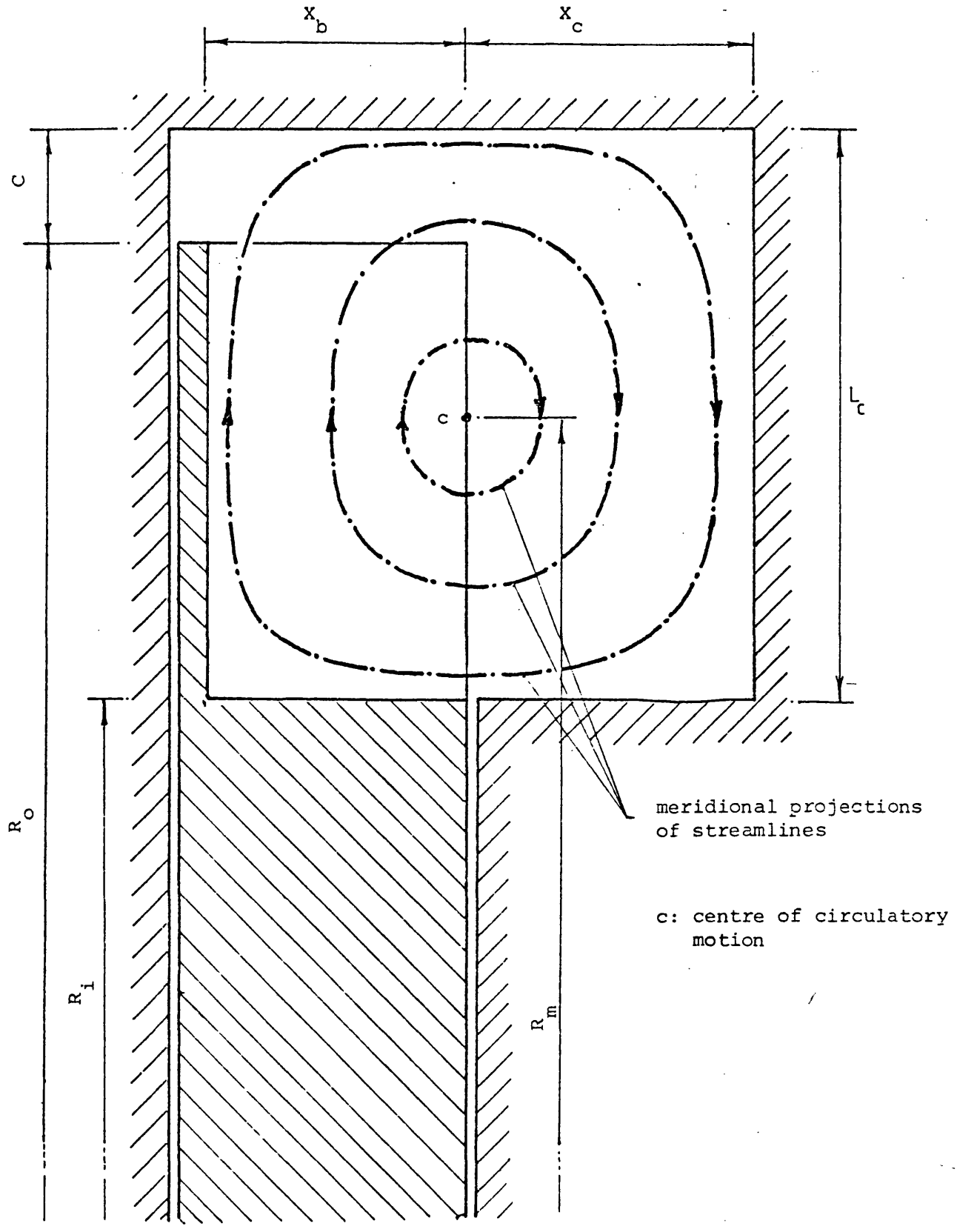

Fig. (4.1): Meridional cross section of idealised rectangular impeller-channel configuration

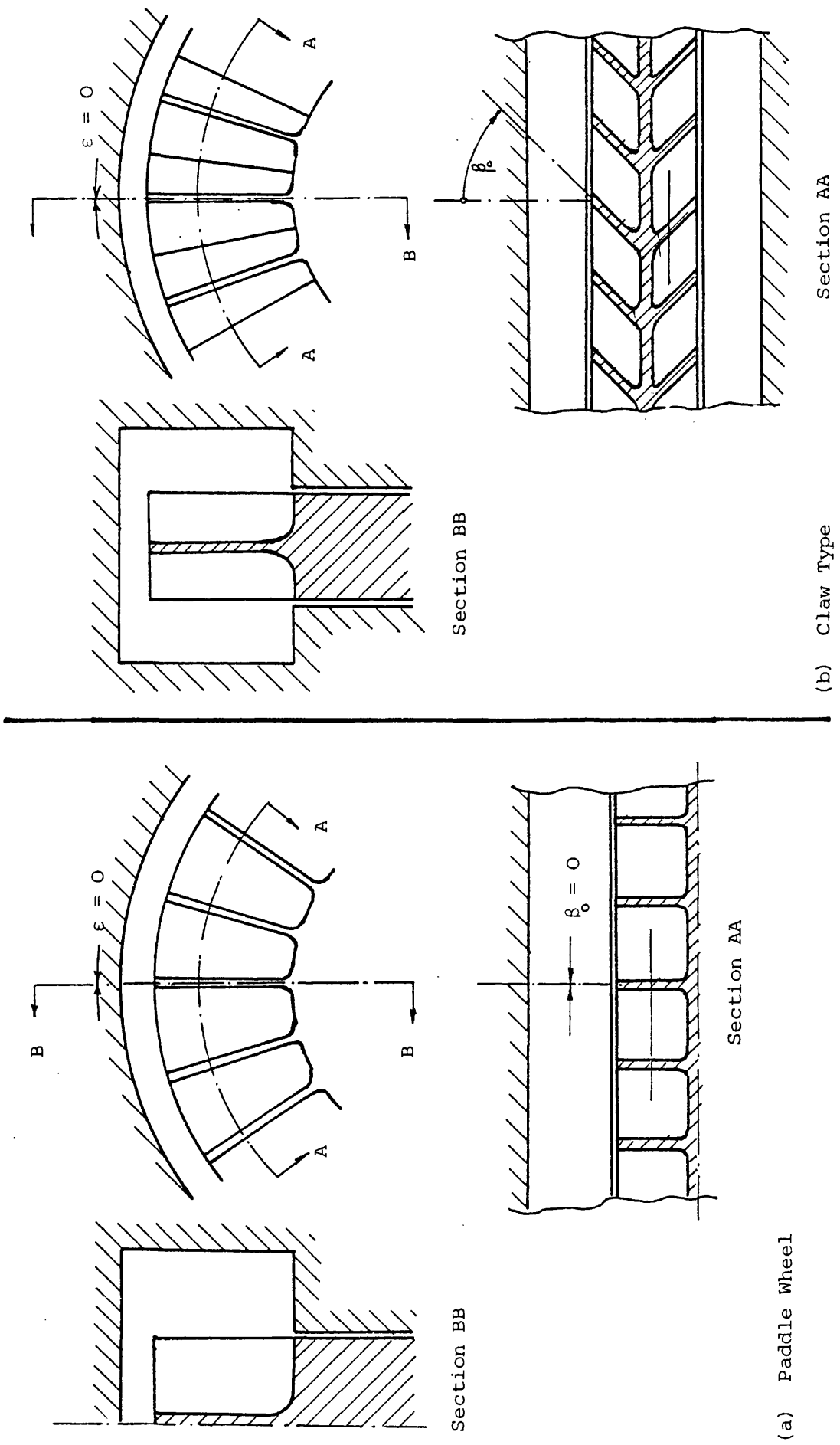

Fig. (4.2): Common Types of Regenerative Impeller

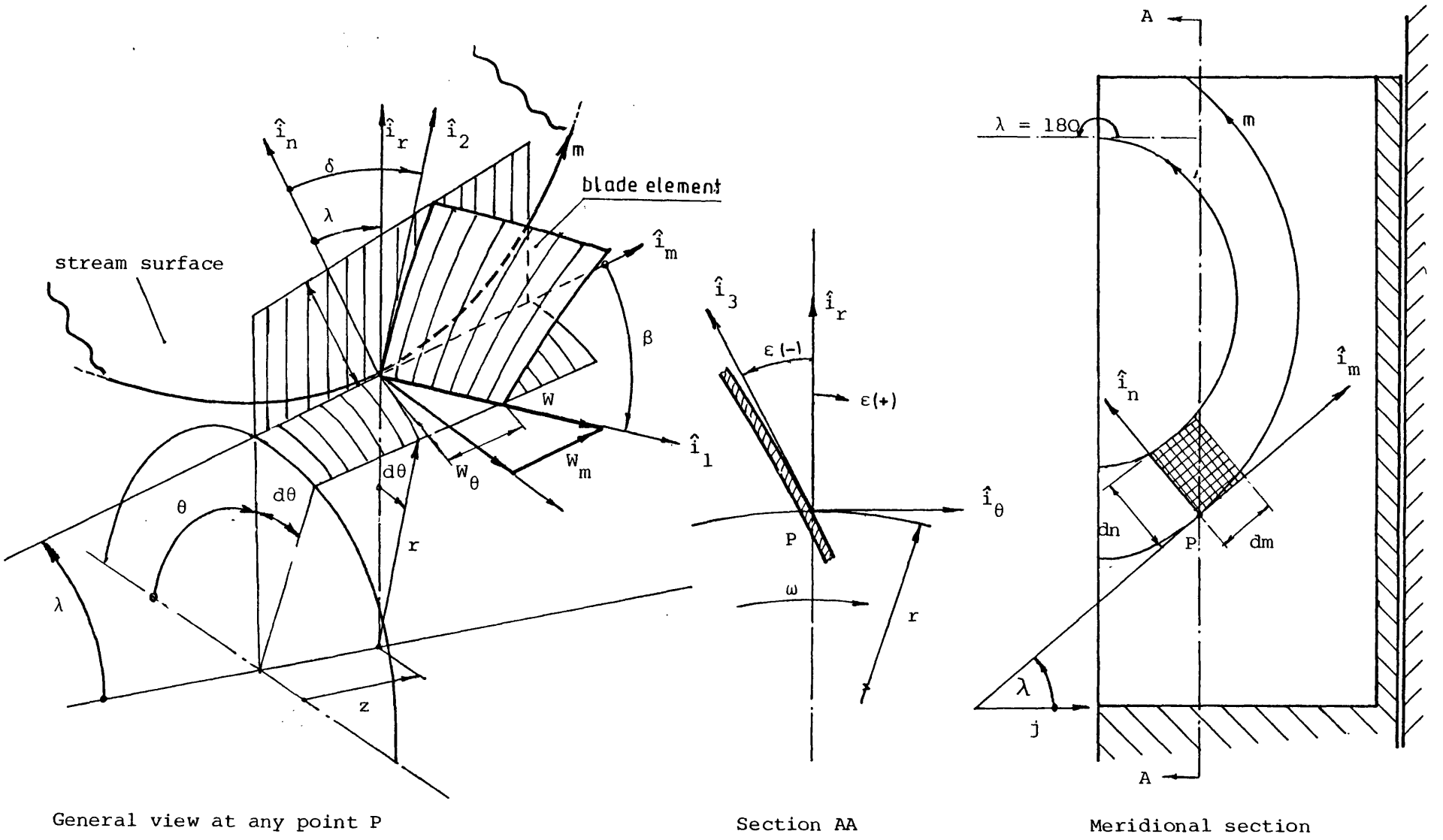

General view at any point P | Section AA | Meridional section

Fig. (4.3): Views of blade element and stream surfaces for definition of β, ε, λ and δ (adapted from Vavra (22))

Fig. (4.3)

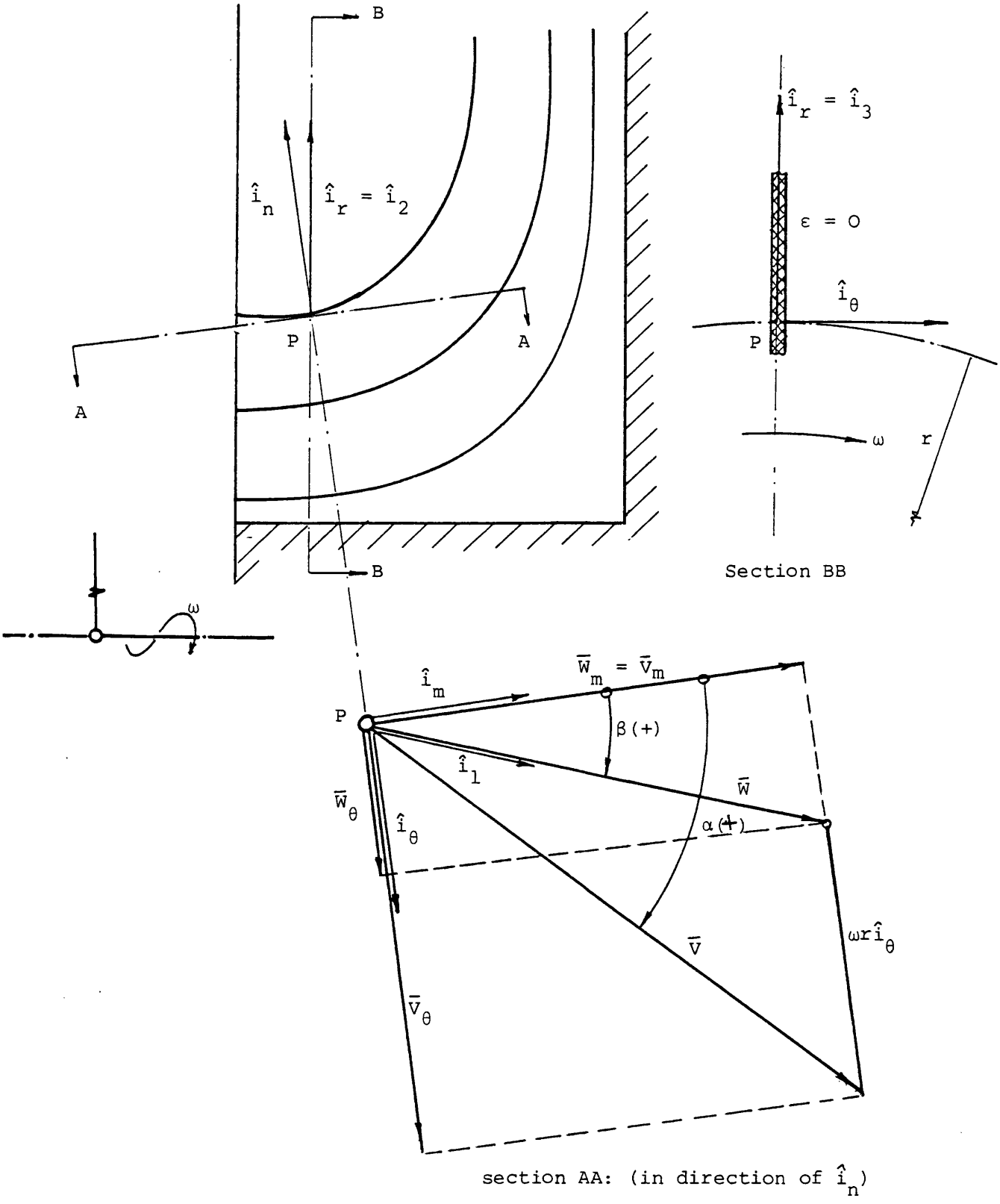

Fig. (4.4): Flow conditions at point on radial element of blade and positive directions of measurement

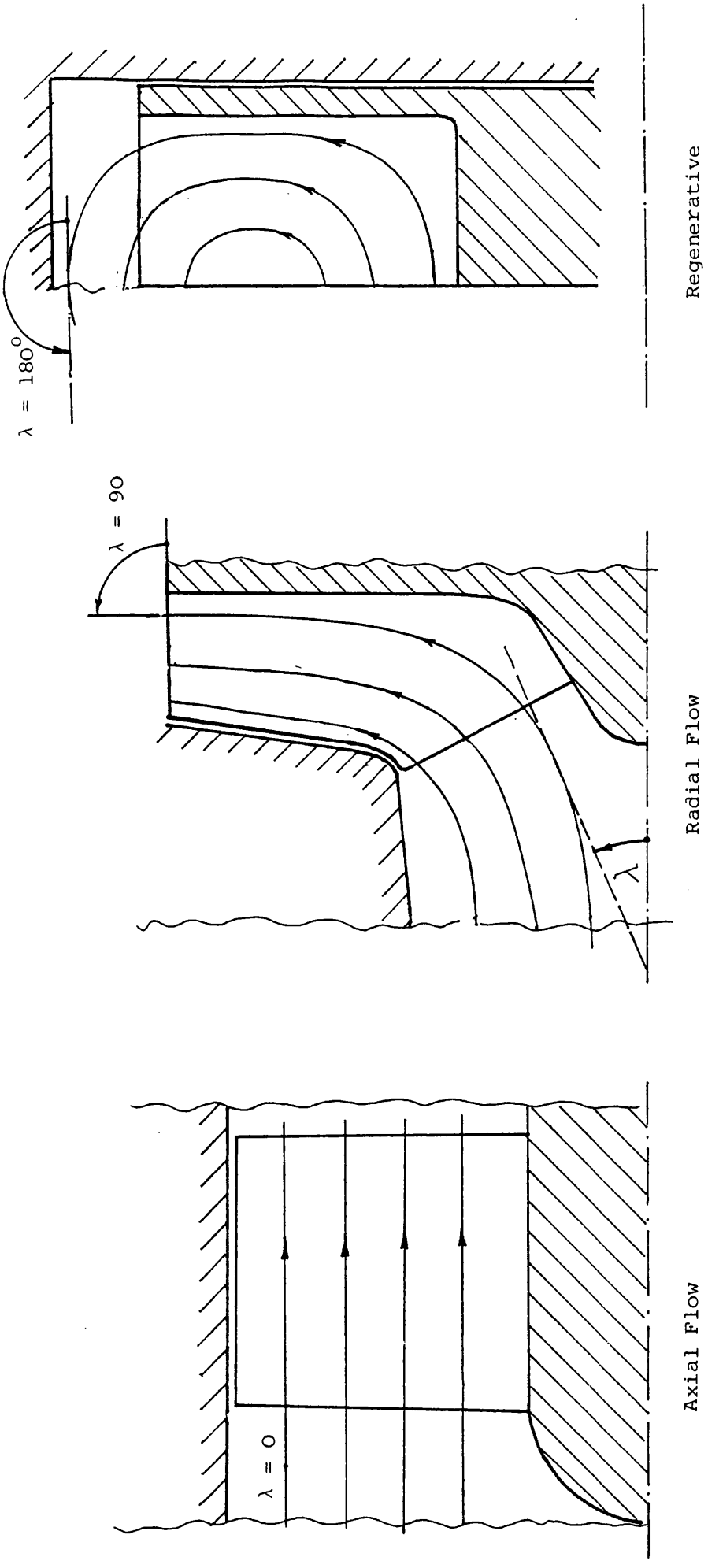

Fig. (4.5) Variation of angle λ in different types of pump

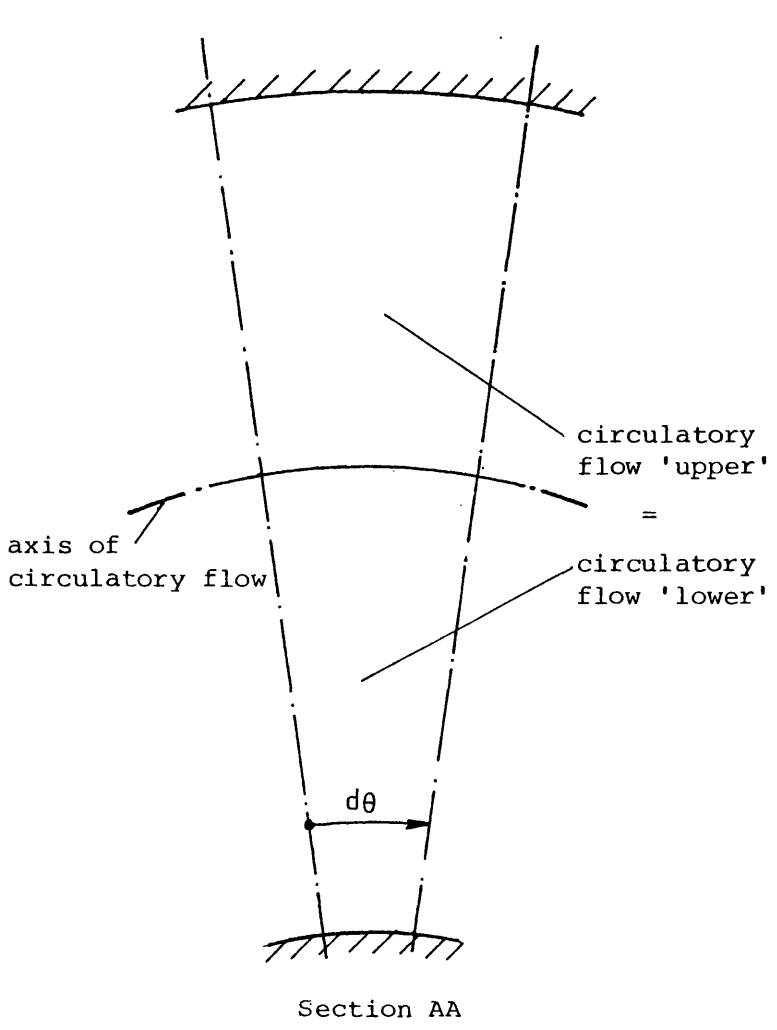

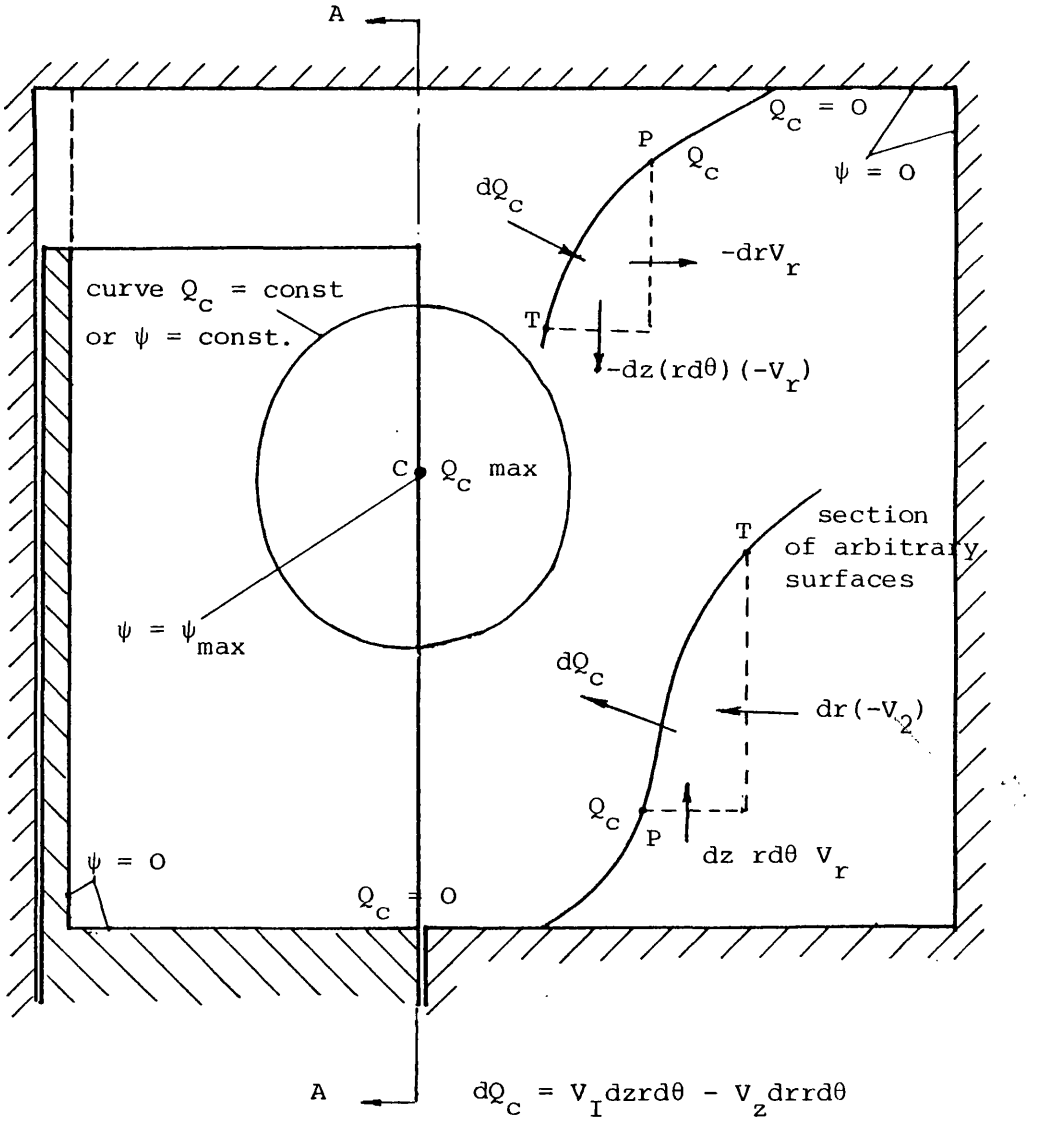

Fig. (4.6): Stream function definition

Fig. (4.6)

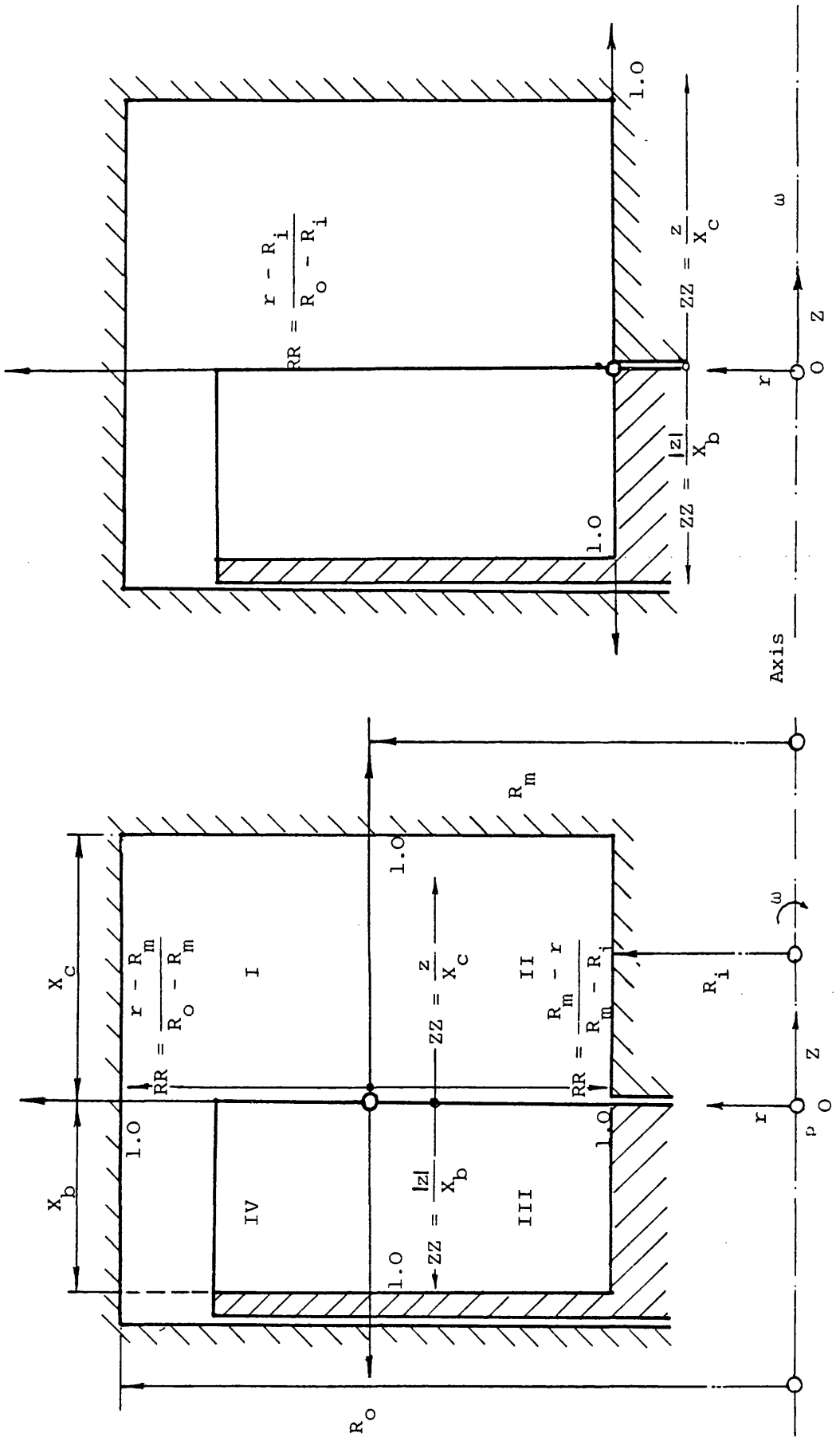

(a) equation (4.18), (4.20)

(b) equation (4.19)

Fig. (4.7): Co-ordinates used in defining the stream function relationships

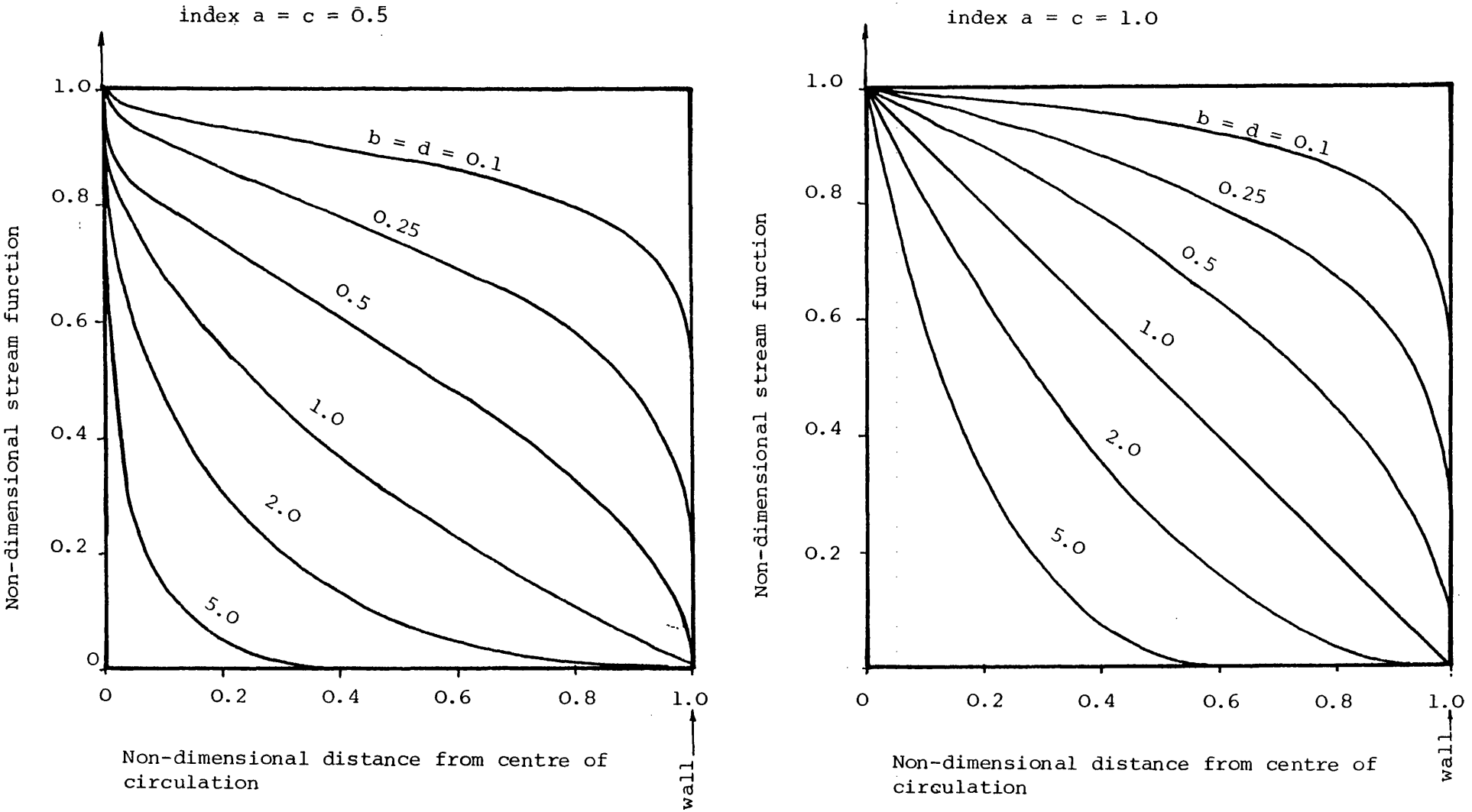

Fig. (4.8): Sections across stream function surface for various values of indices

Fig. (4.8)

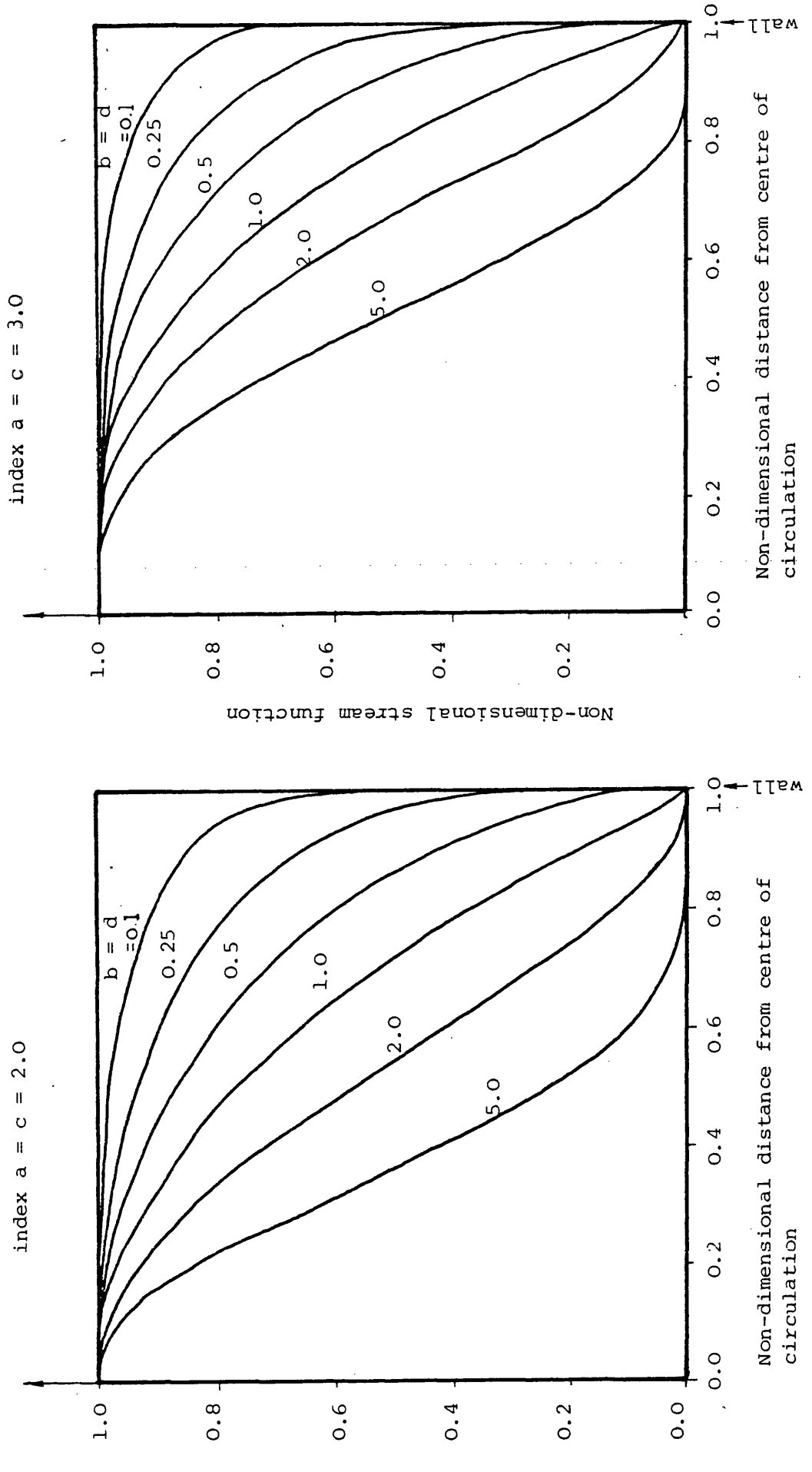

Fig. (4.9): Sections across stream function surface for various values of indices

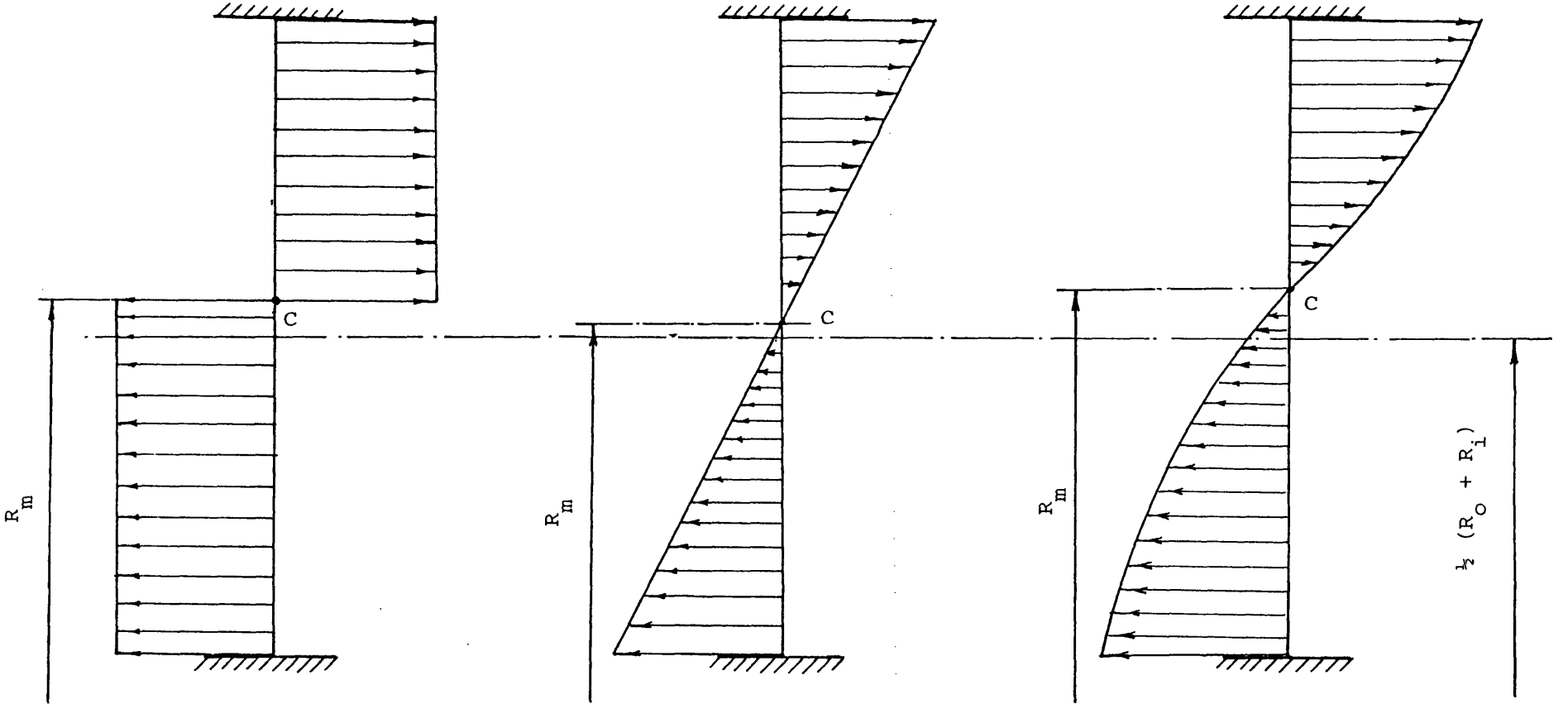

(a) Constant velocity profile (b) Linearly varying (c) Varying non-linearly (regenerative pumps)

Fig. (4.10): (a) & (b) Commonly assumed velocity profiles in fluid couplings and torque converters compared with that proposed for regnerative pumps (c)

Fig. (4.11)

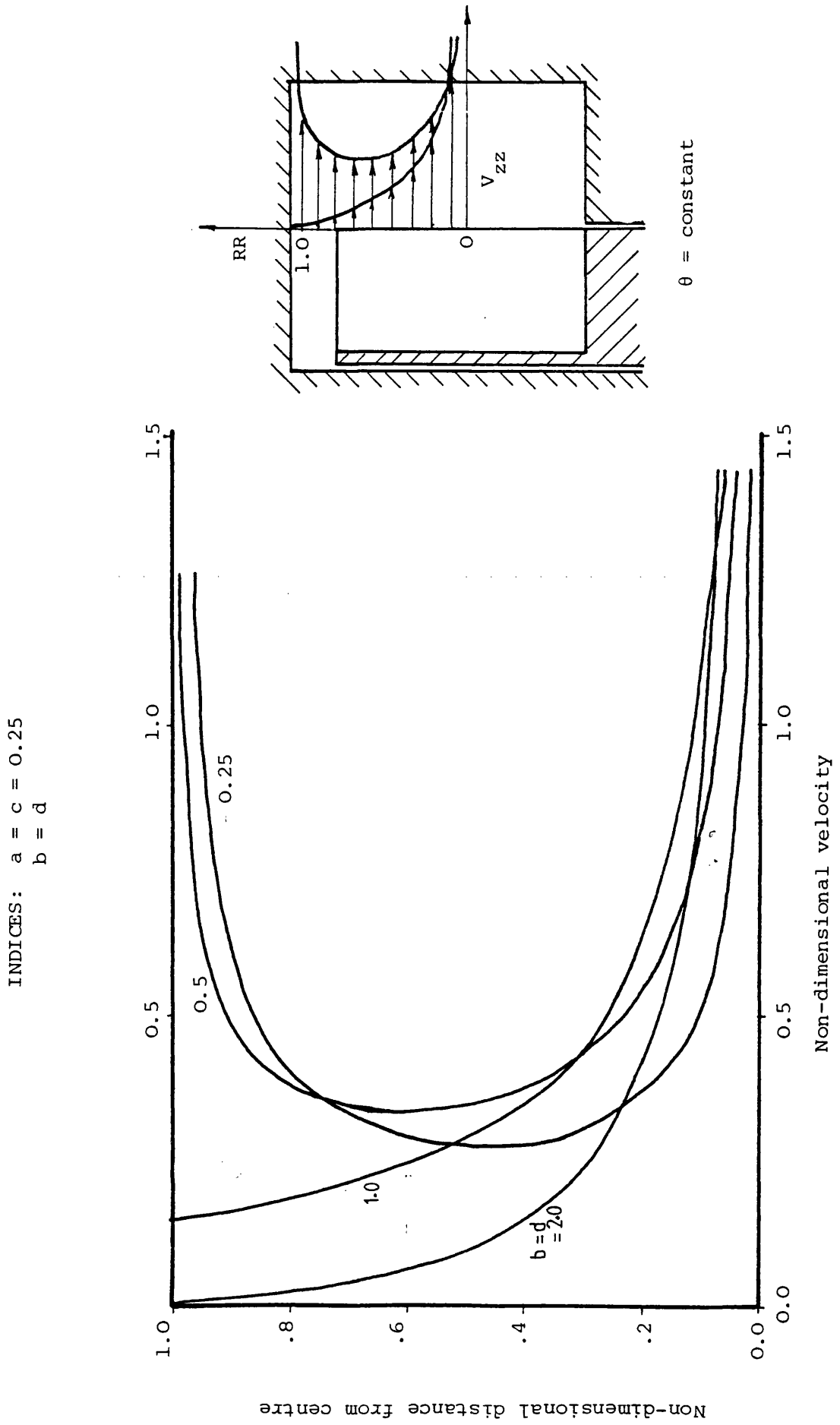

Fig. (4.11): Unacceptable types of meridional velocity profile (e.g. at centre V = ∞)

INDICES: a = c = 0.5
b = d

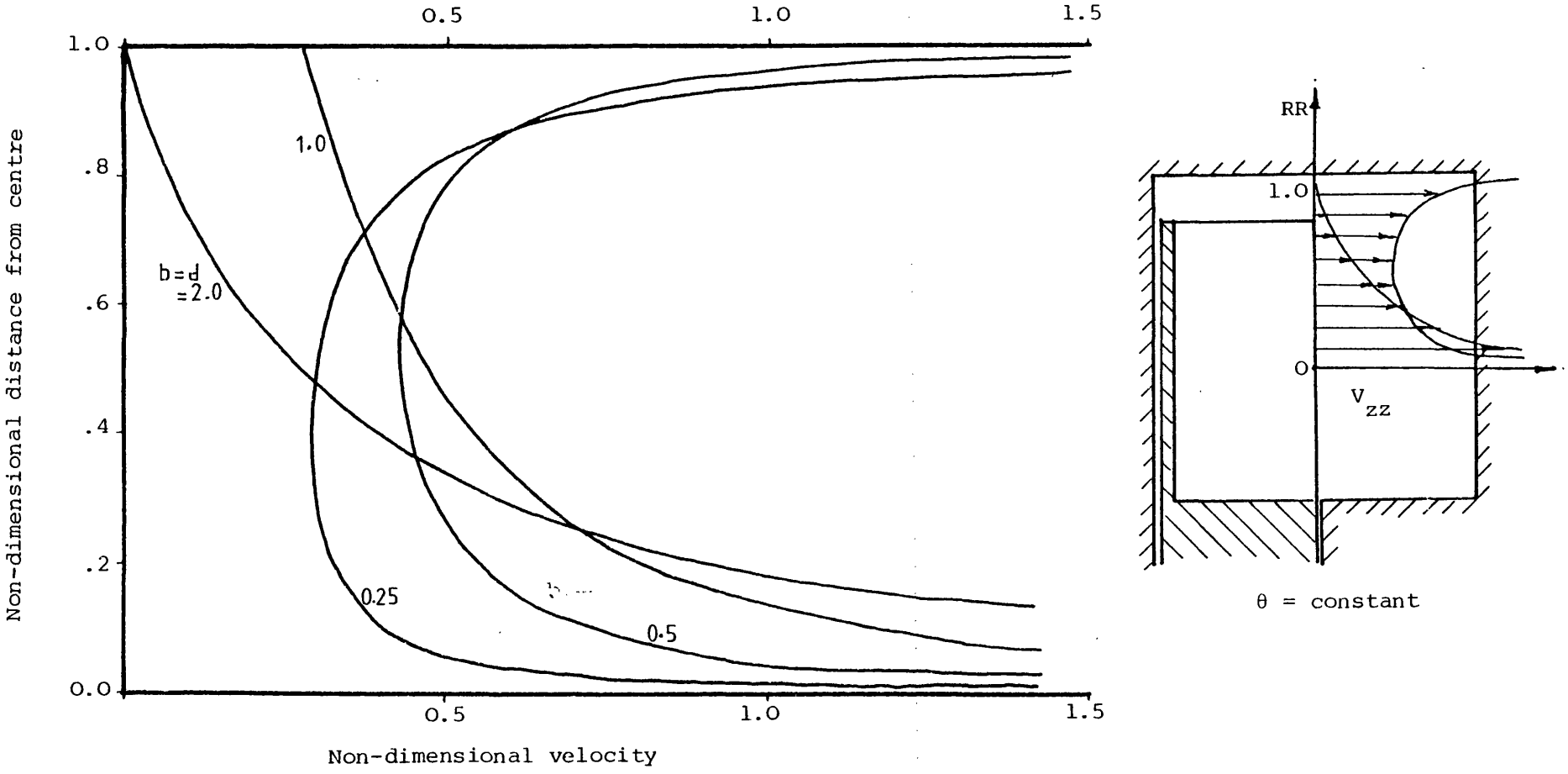

Fig. (4.12): Unacceptable types of meridional velocity profile (e.g. at centre V = ∞)

Fig. (4.12)

Fig. (4.13)

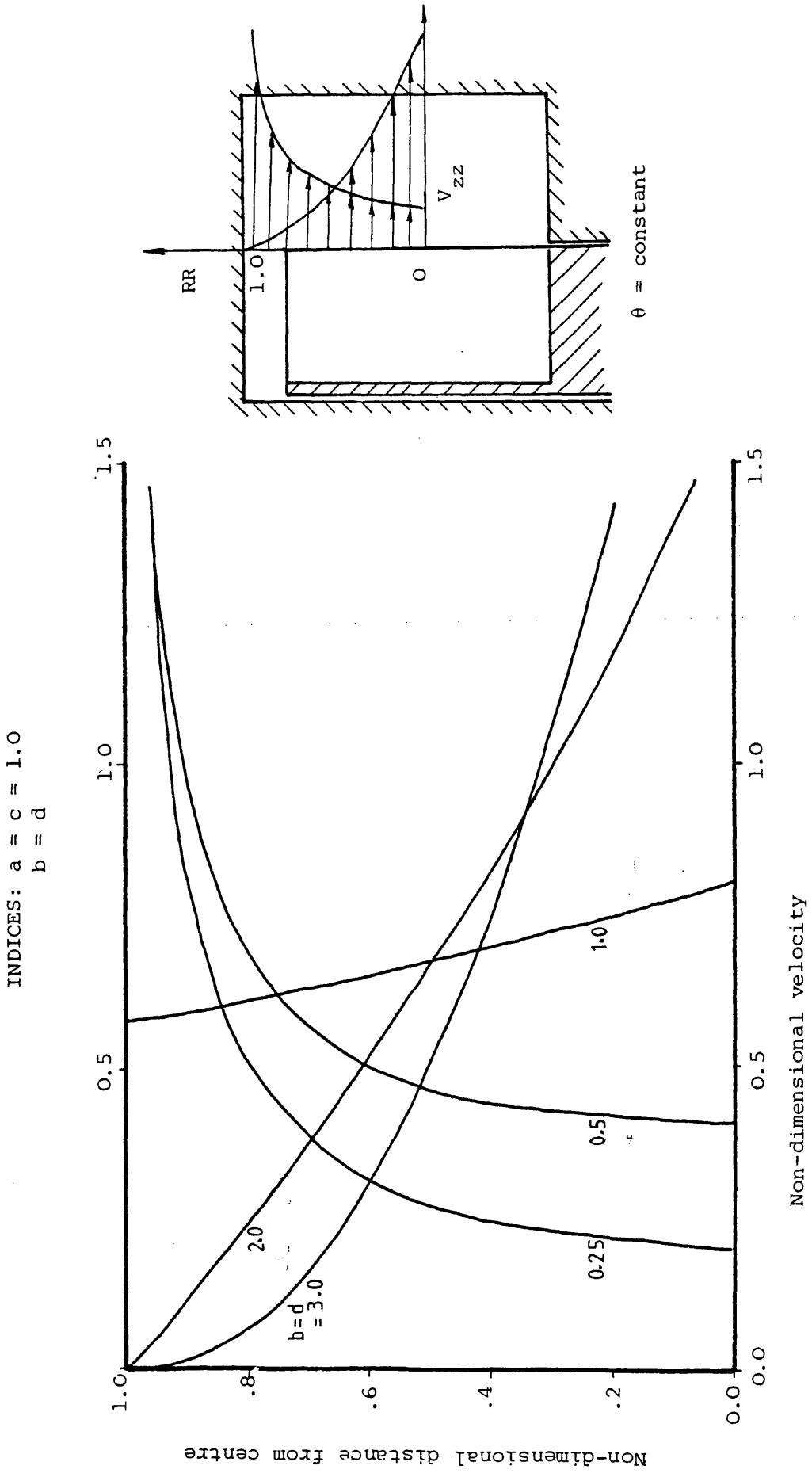

Fig. (4.13): Unacceptable types of meridional velocity profile ($V \neq 0$ at centre)

Fig. (4.14)

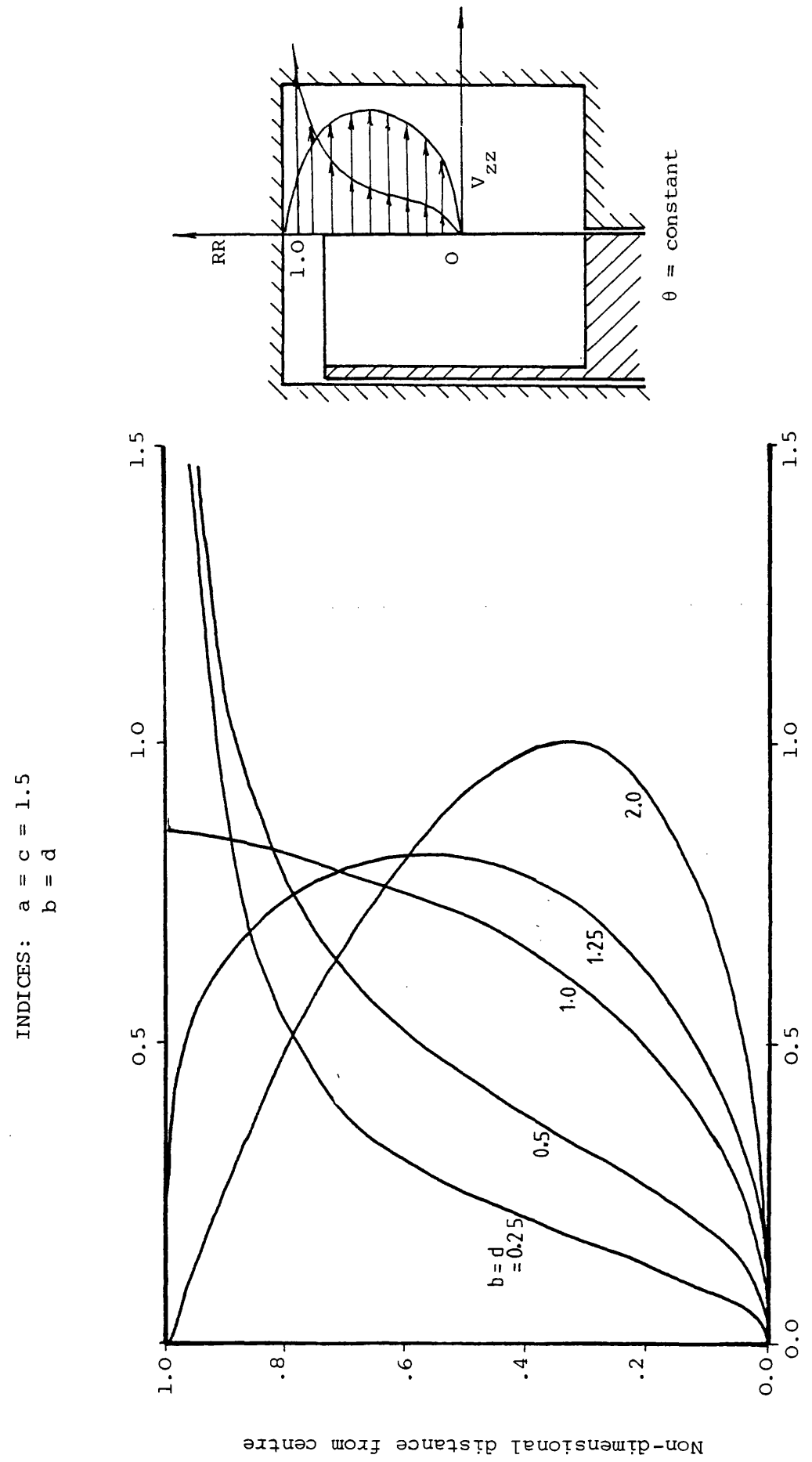

Fig. (4.14): Effect of b, d on meridional velocity profiles which have a required zero value at centre

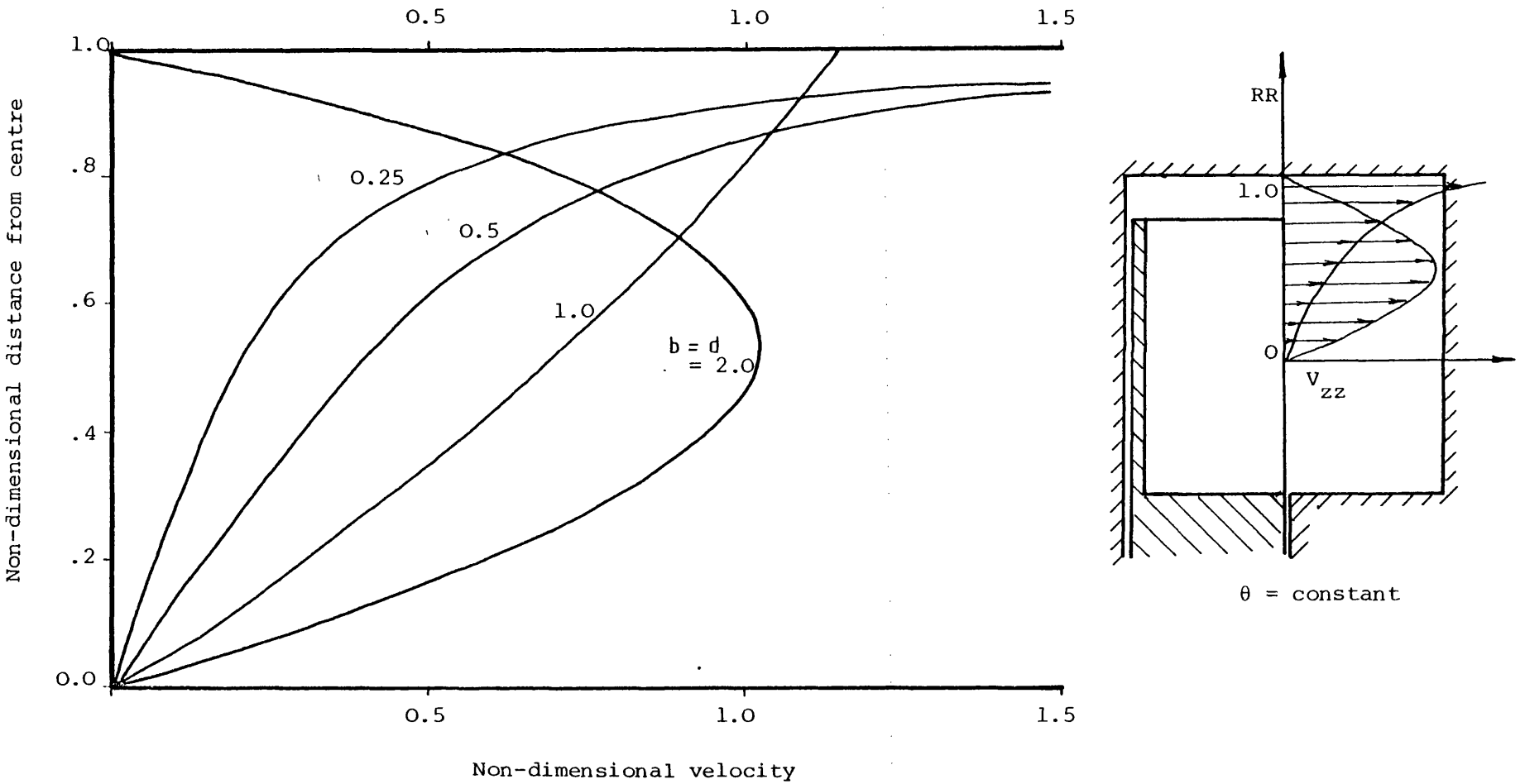

Fig. (4.15): Effect of band d on acceptability of meridional velocity profiles (compare with Fig. (4.14) to see effect of a and c)

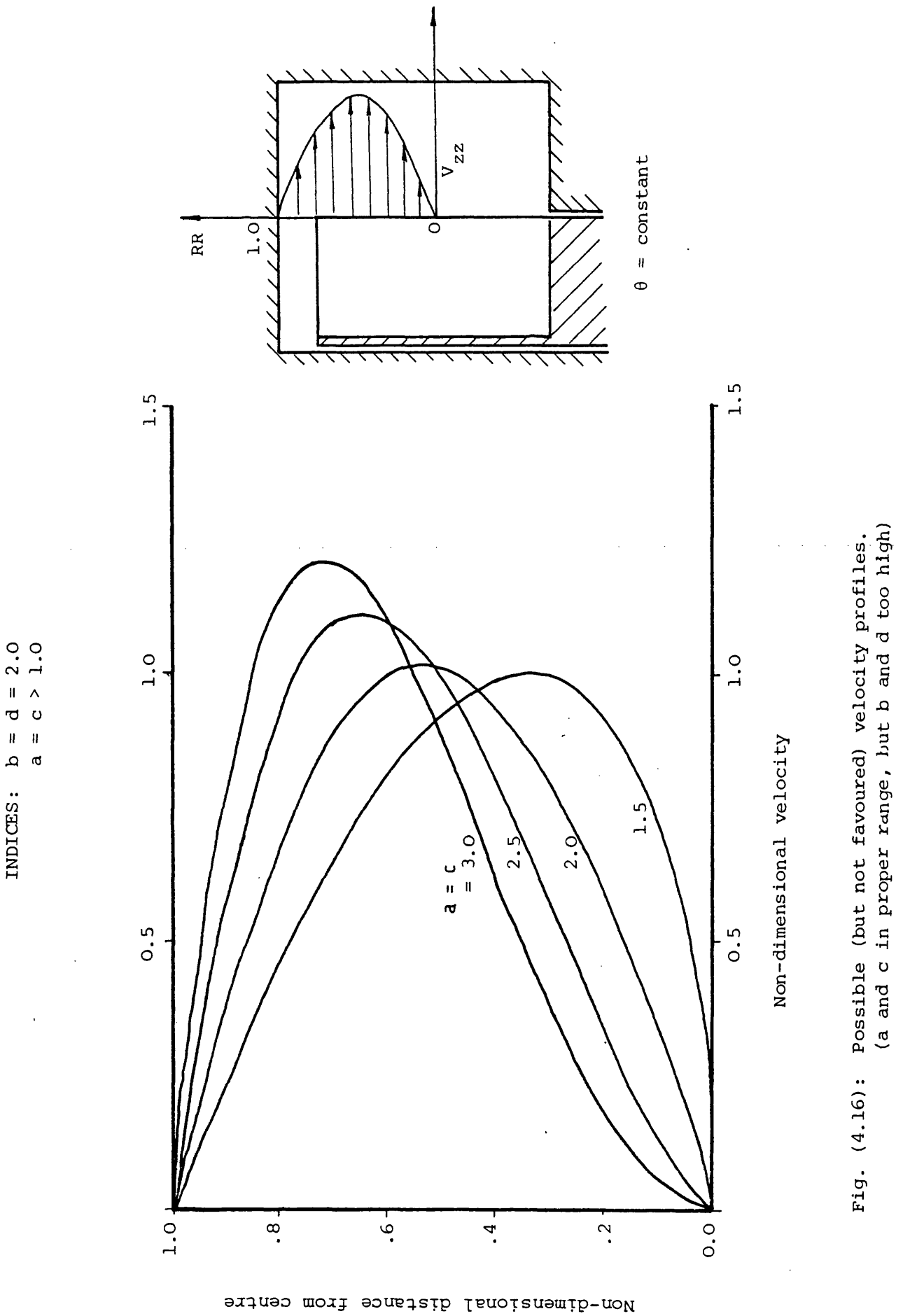

Fig. (4.16): Possible (but not favoured) velocity profiles.
(a and c in proper range, but b and d too high)

INDICES: b = d = 1.5
a = c > 1.0

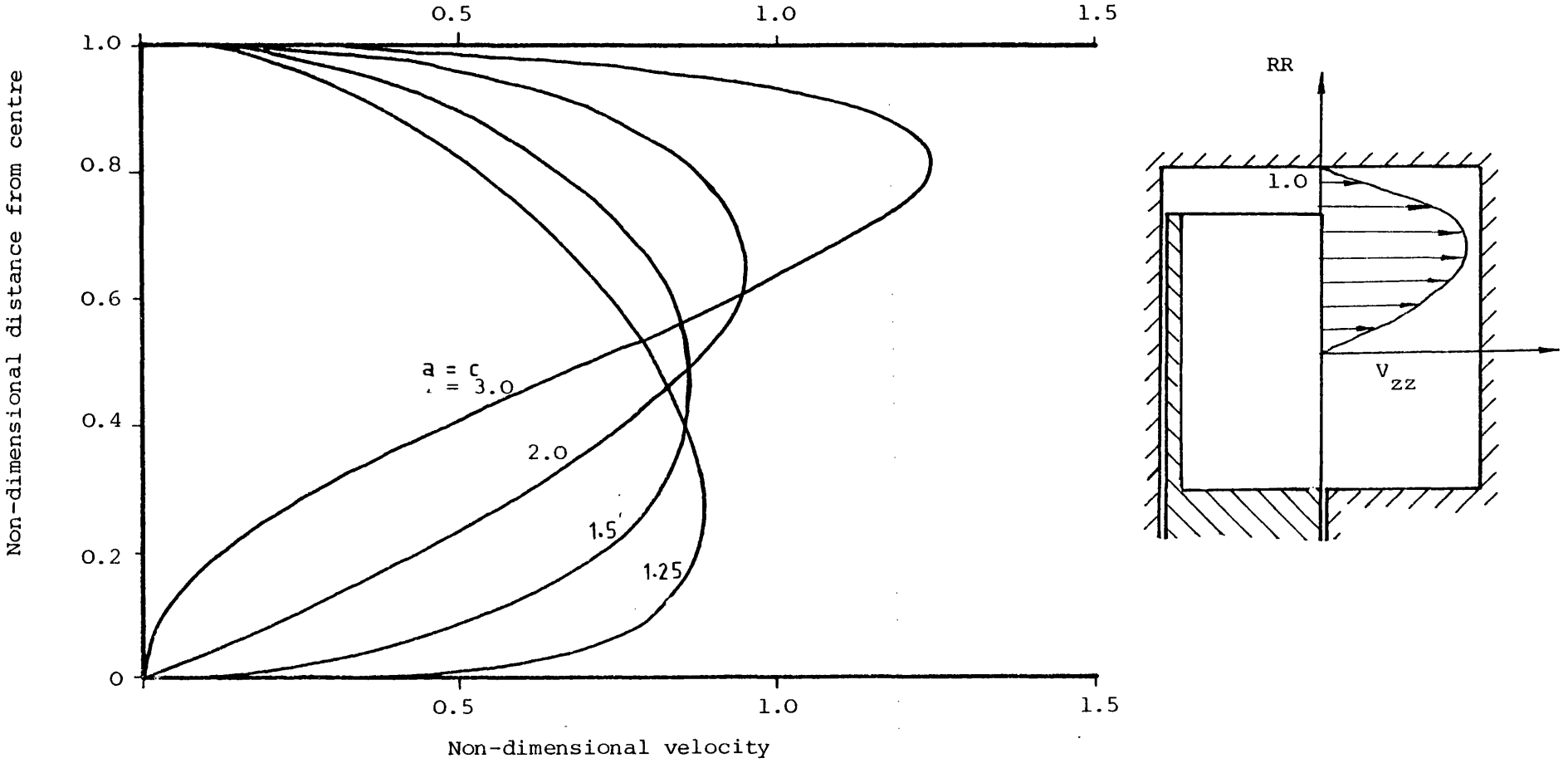

Fig. (4.17): Possible (but not favoured) velocity profiles b and d > 1.0 as in Fig. (4.16), compare with Fig. (4.18)

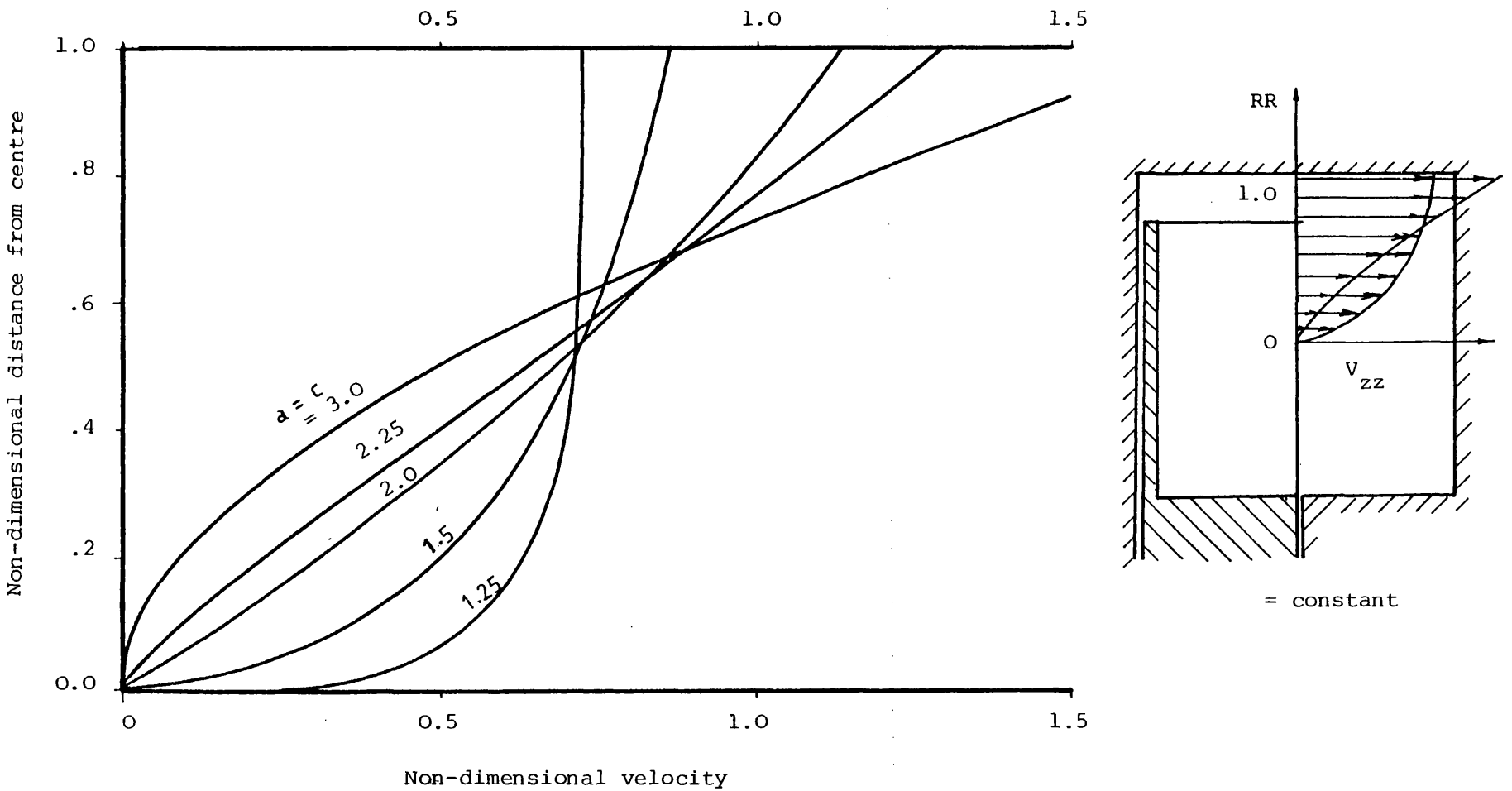

Fig. (4.18): Favoured meridional velocity profiles and corresponding values of indices

Fig. (4.18)

123'3 = computed cycle at converging conditions

145 = ideal cycle to show losses

pump: STA-RITE TH-7

stream function parameters: A' = 0.00818
a = c = 2.0
b = d = 1.0
R_m = 0.7

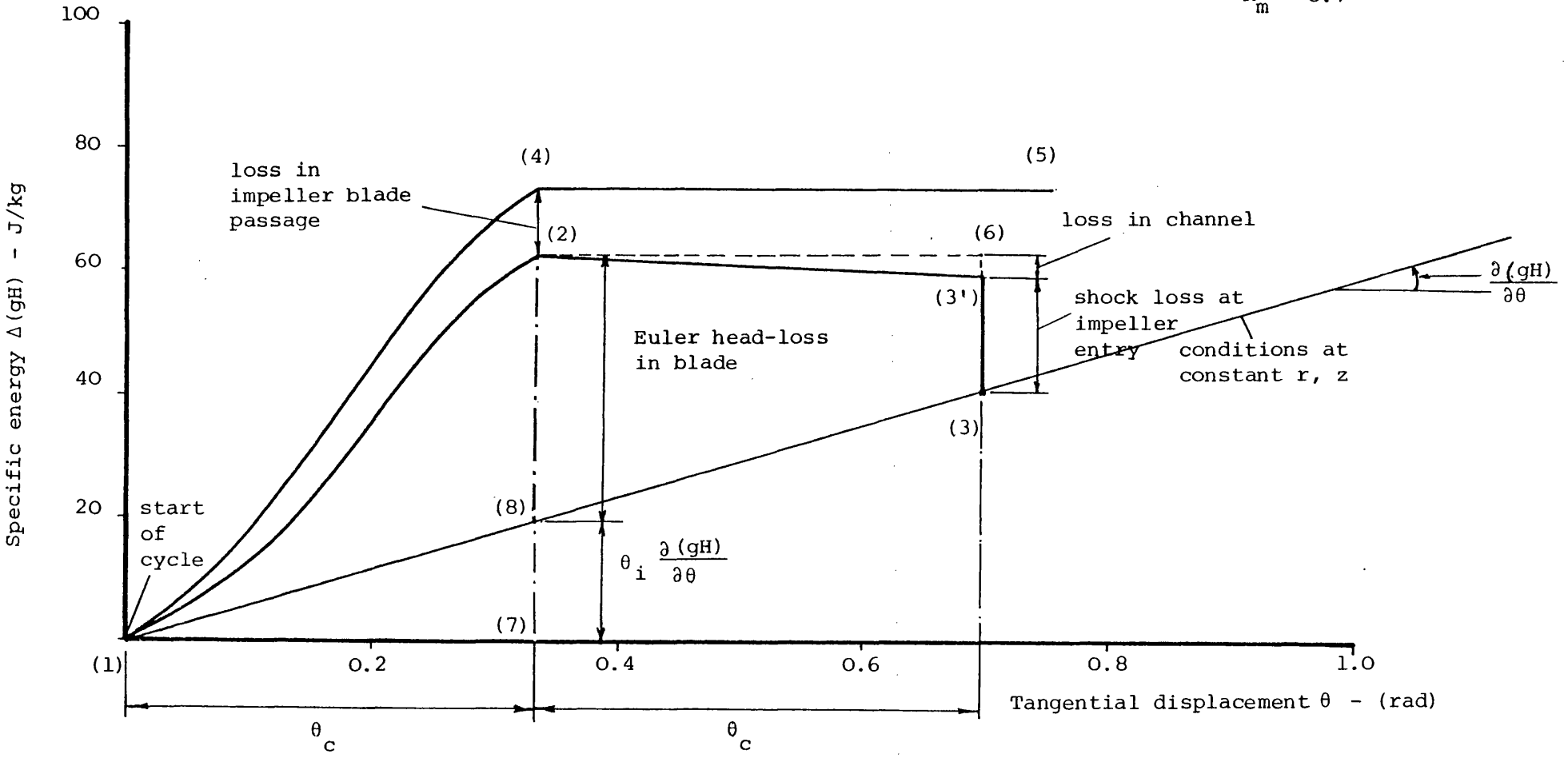

Fig. (4.19): Typical flow cycle along a streamline

Fig. (4.19)

Fig. (4.20)

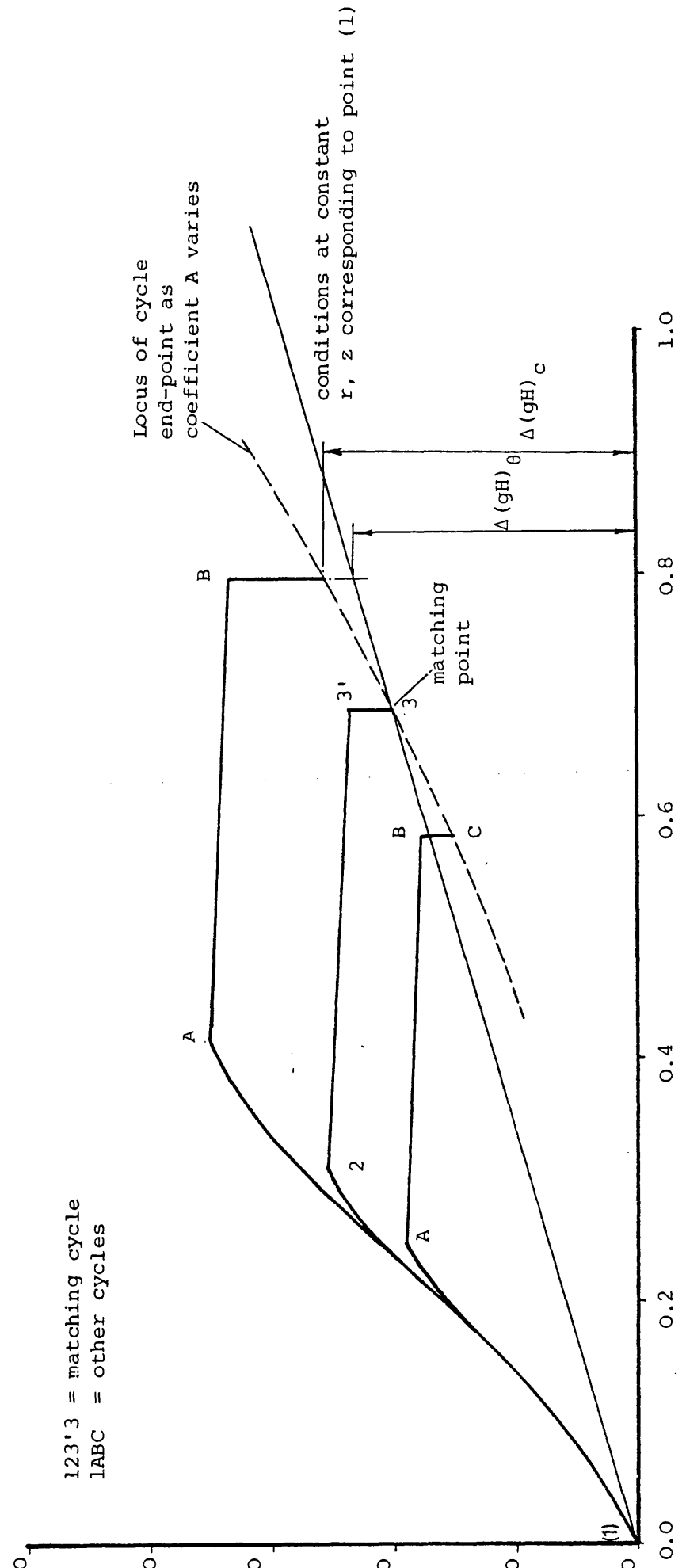

Fig. (4.20): Computed cycles with various values of 'A' showing matching conditions

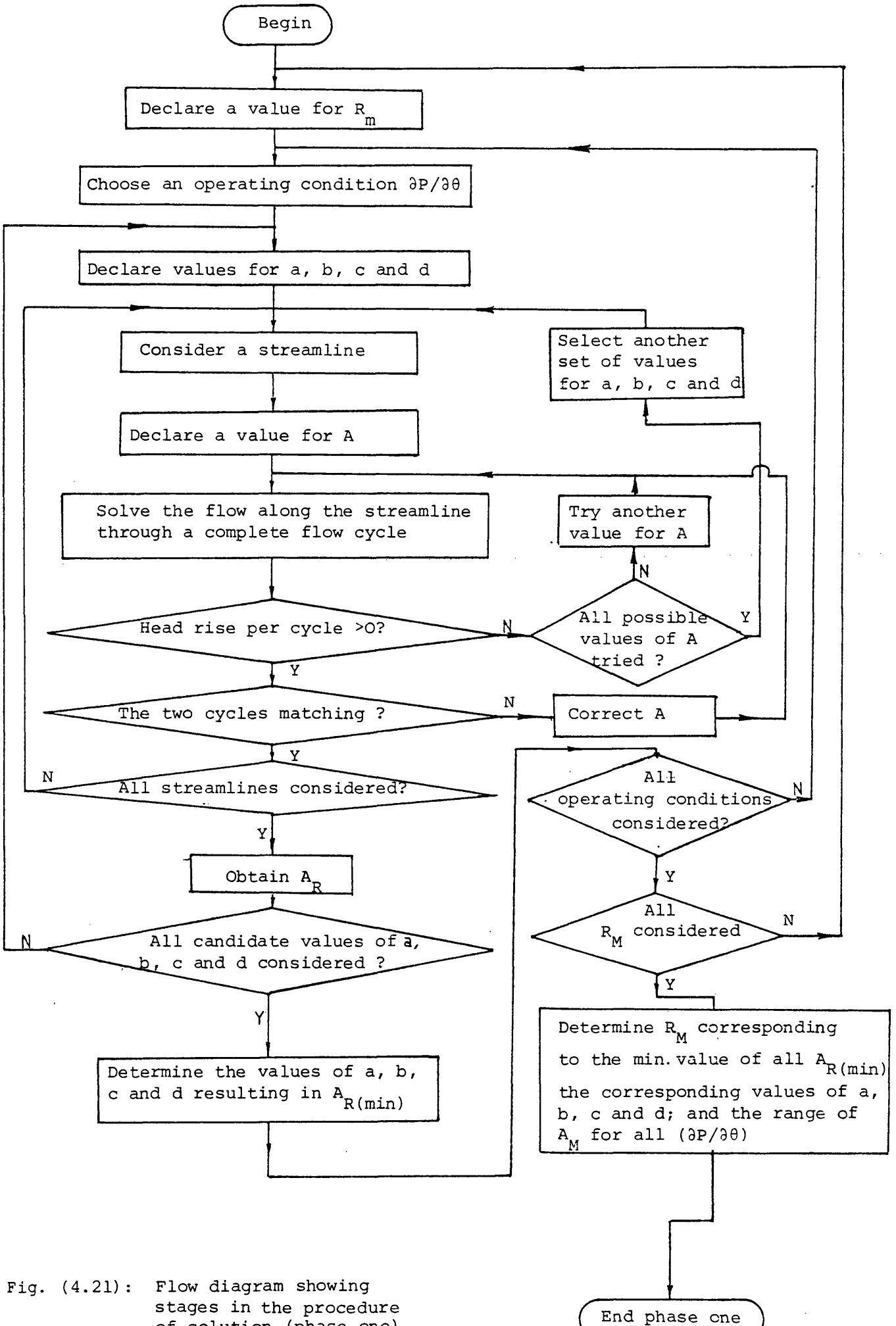

Fig. (4.21): Flow diagram showing stages in the procedure of solution (phase one)

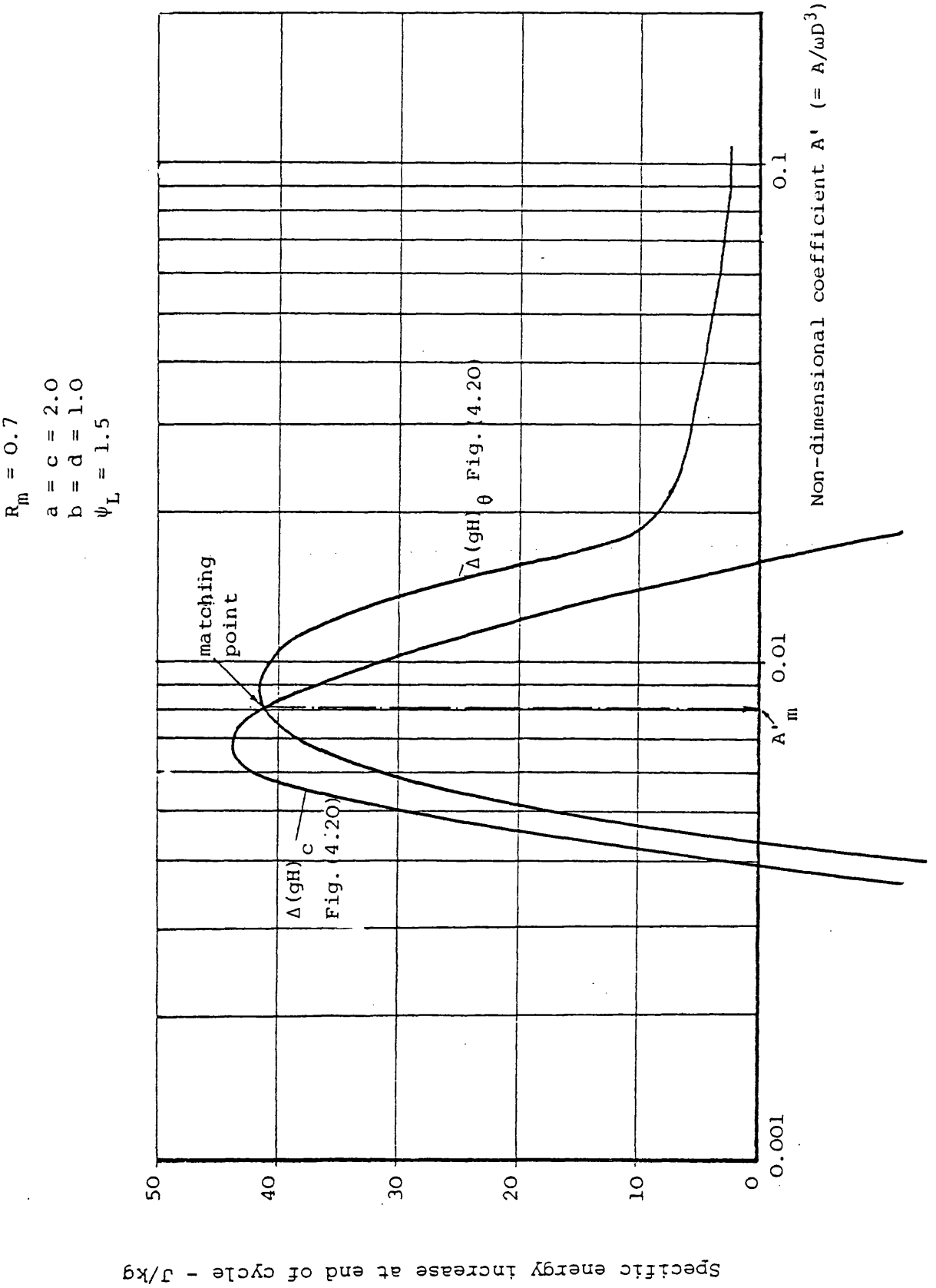

Fig. (4.22): Variation of computed head rise in a flow cycle with stream function coefficient A'.

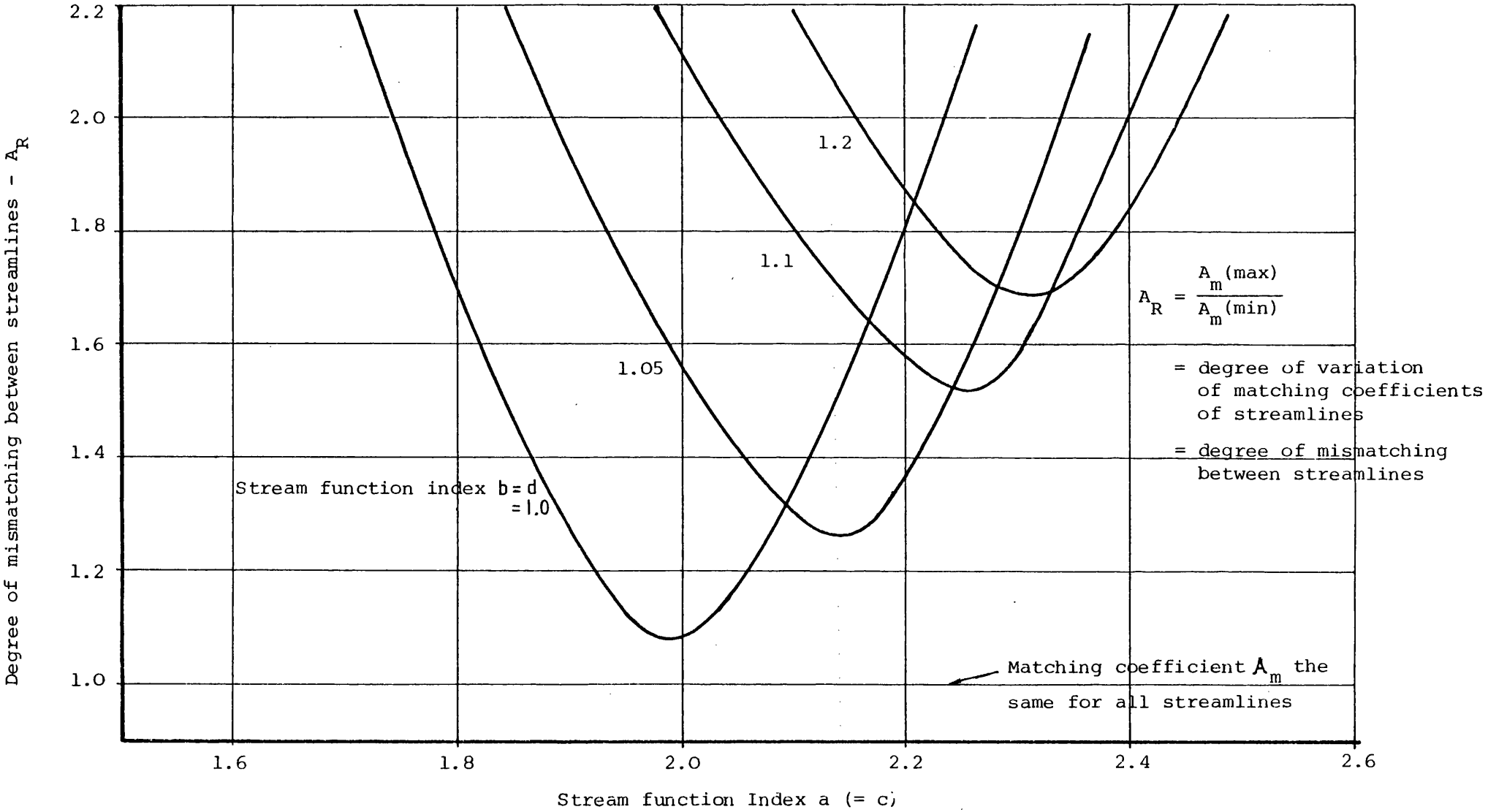

Fig. (4.23): Degree of mismatching between streamlines against indices a = c for various values of indices b = d

Fig. (4.23)

(see Fig. (4.23))

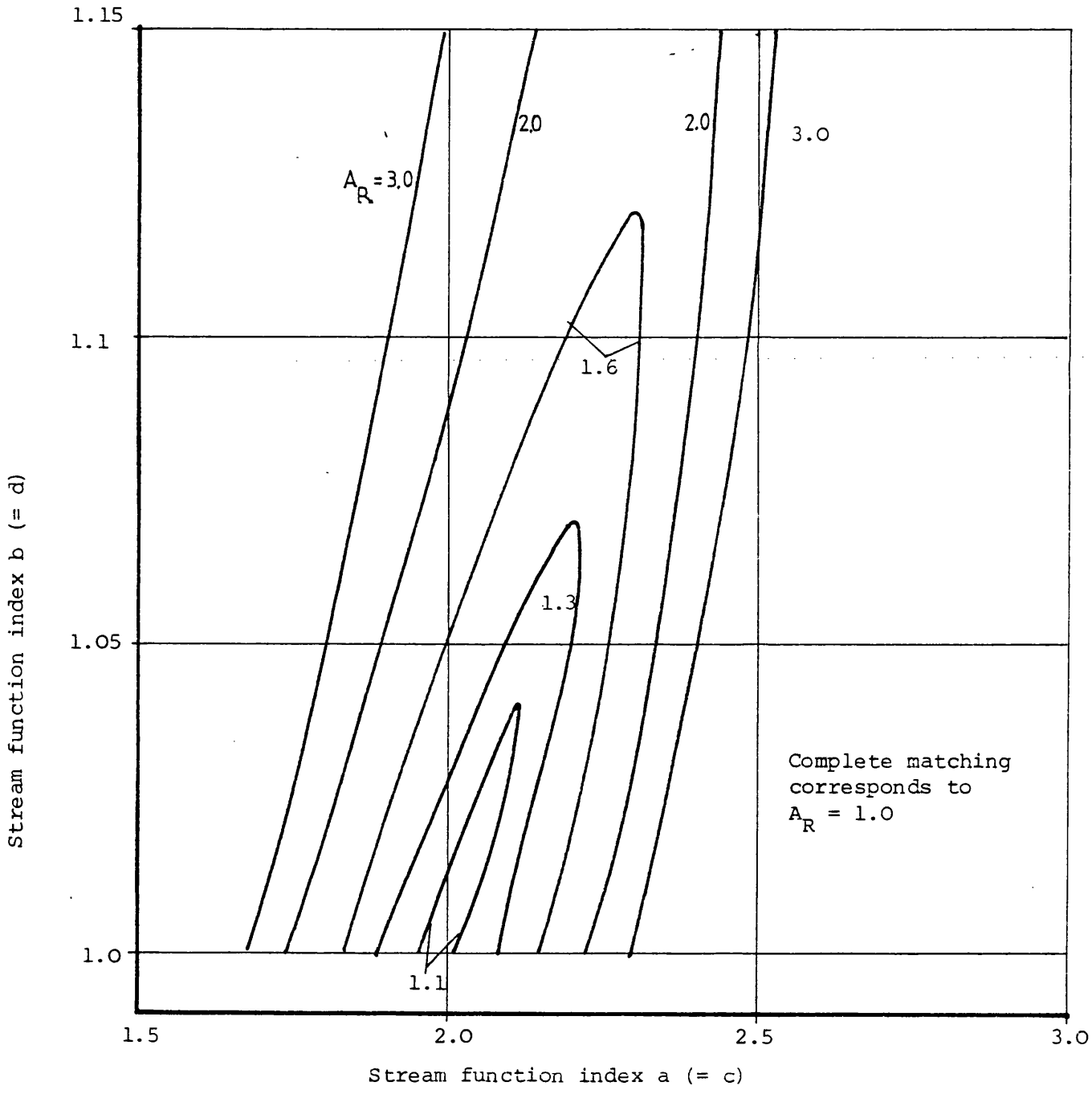

Fig. (4.24): Contours of degree of mismatching between streamlines on plane of indices of stream function

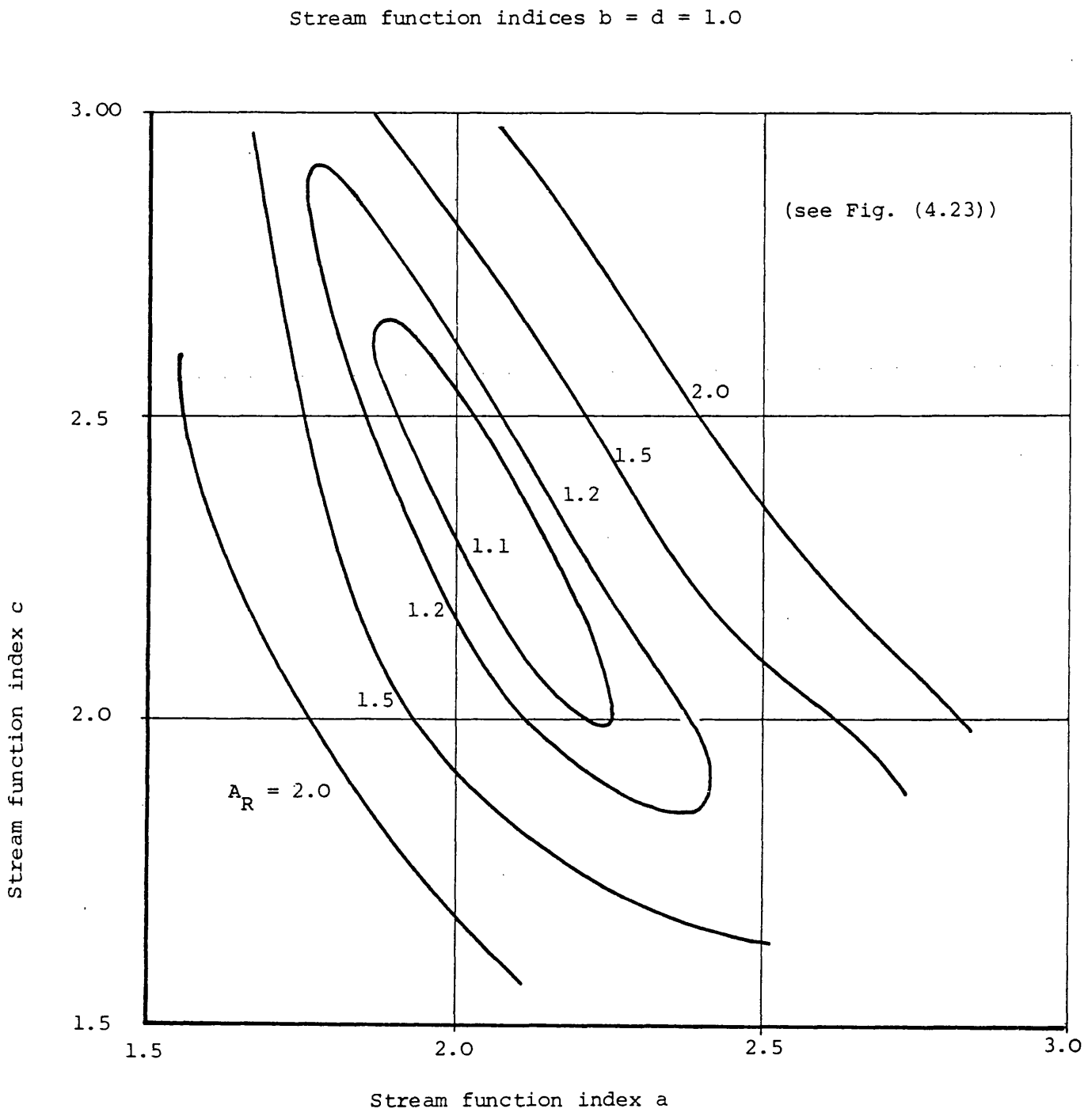

Fig. (4.25): Degree of mismatching between streamlines at various values of indices a, c.

Pump: STA-RITE TH-7 - (3.0)
Non-dimensional head across linear section (ψ_L) = 0.5
Indices b = d = 1.0
R'_m = 0.7

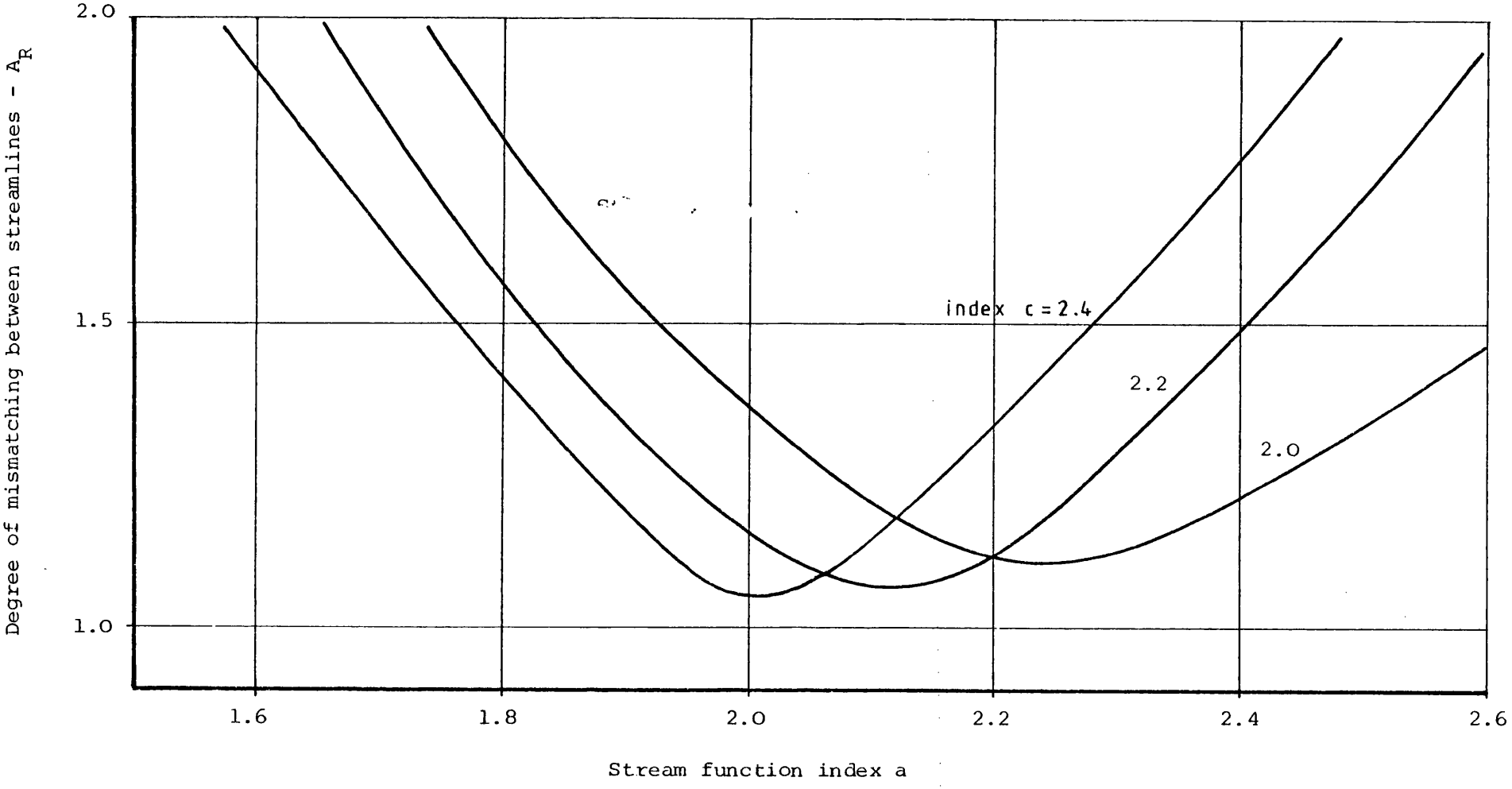

Fig. (4.26): Degree of mismatching between streamlines against index a for fixed values of index c (b = d - 1.0)

Fig. (4.26)

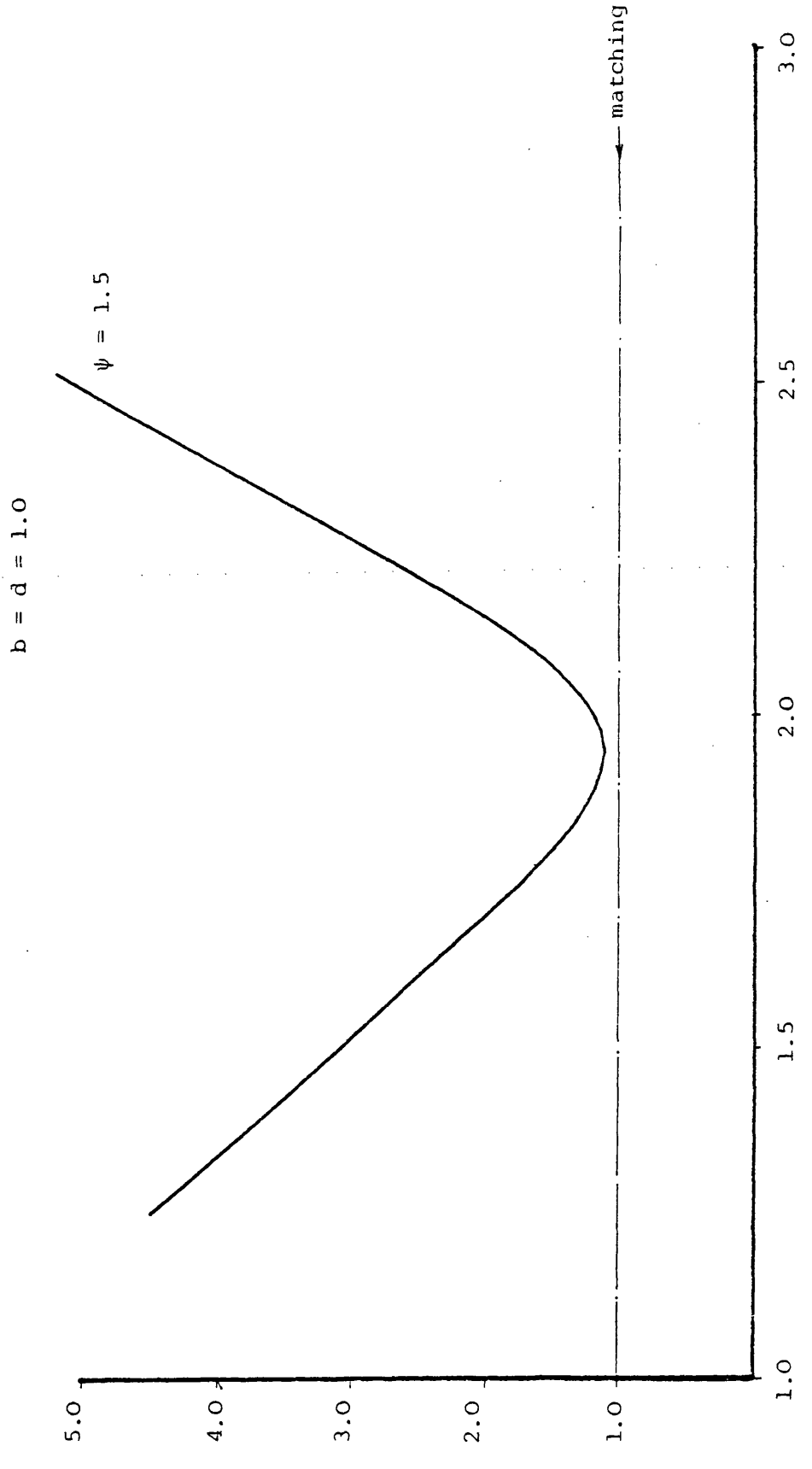

Fig. (4.27): Degree of mismatching between streamlines against index a (= c) for d = d = 1.0

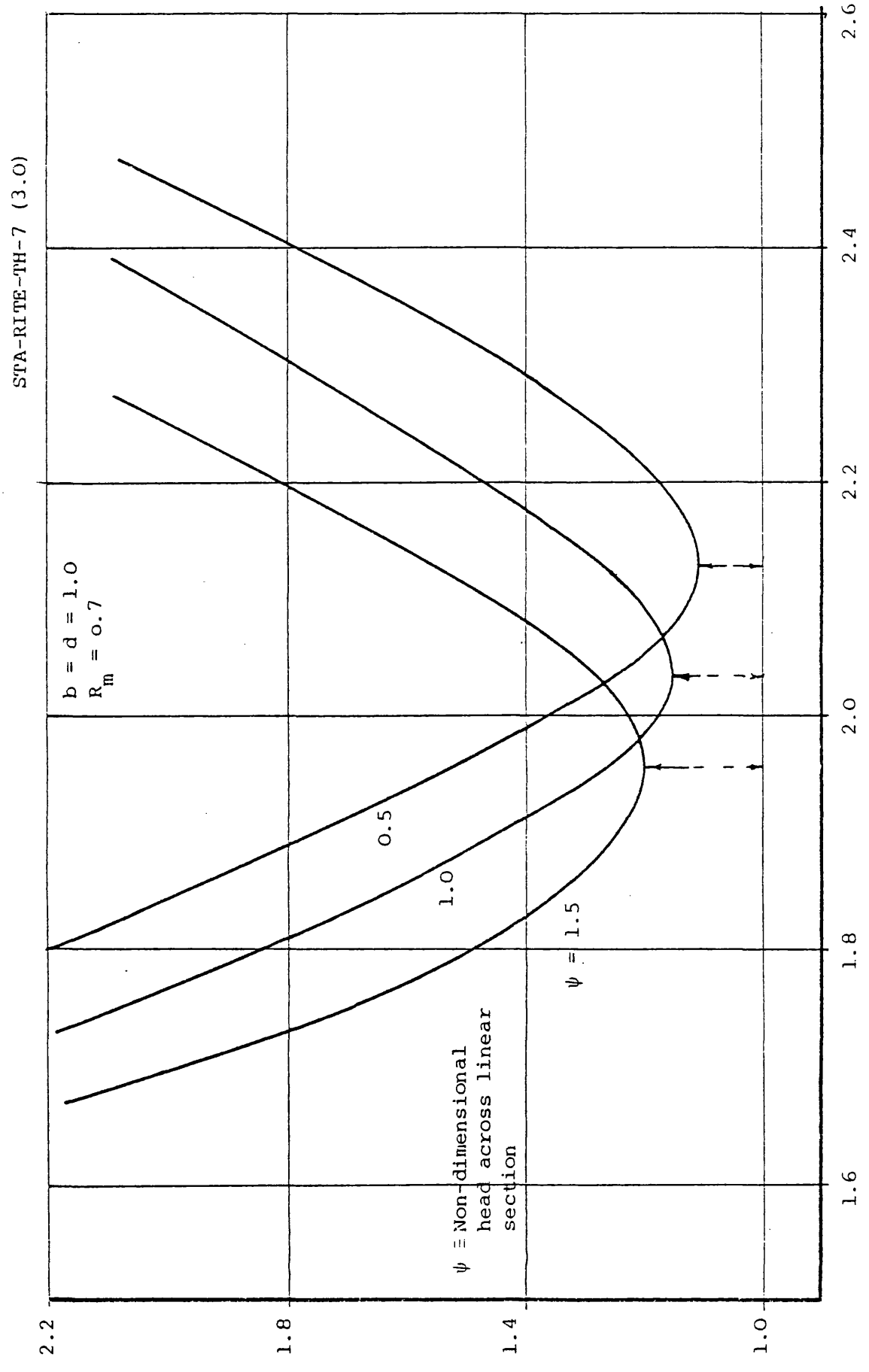

Fig. (4.28): Effect of circumferential pressure gradient on degree of mismatching between streamlines.

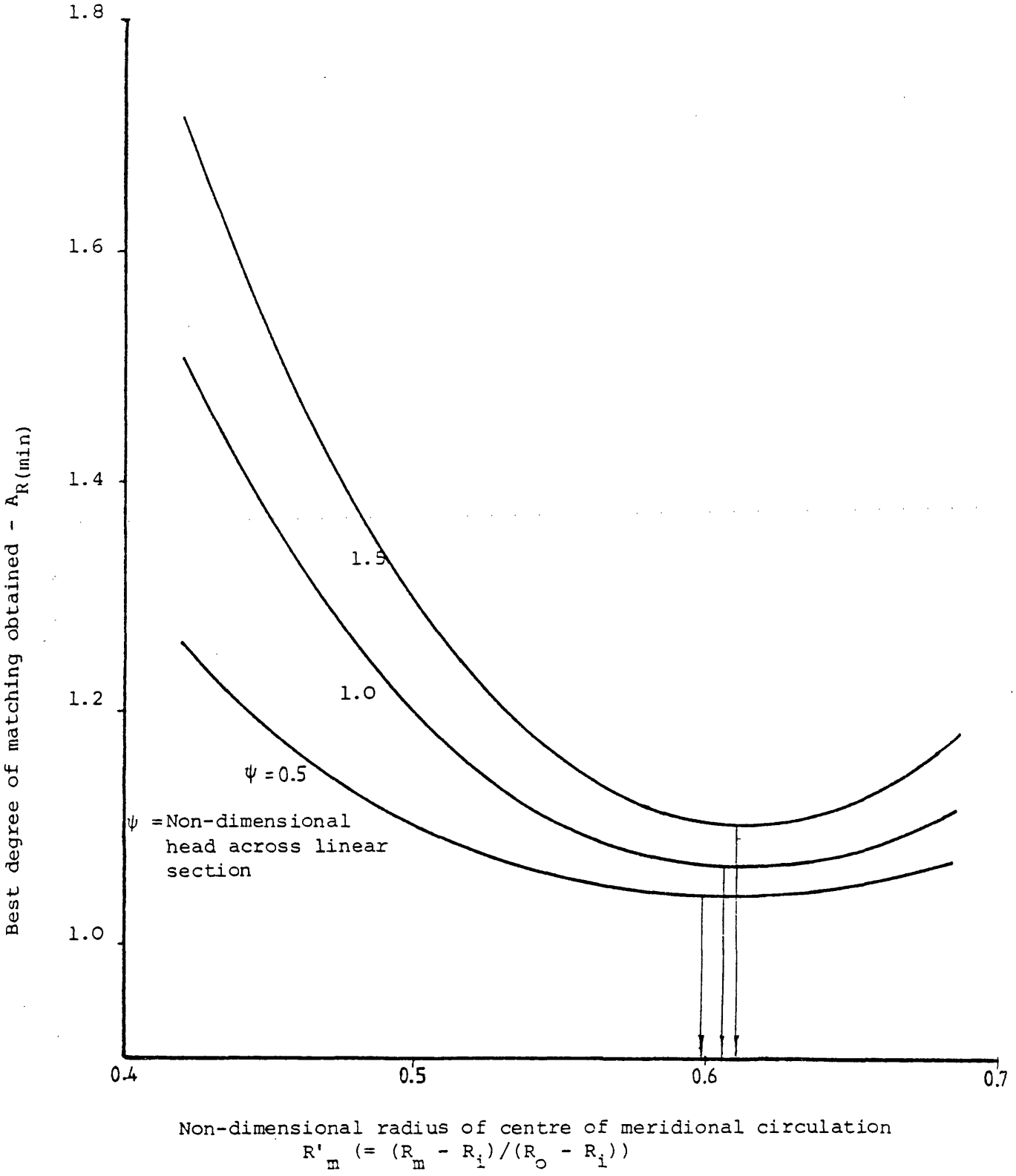

Fig. (4.29): Best degree of matching obtained against radius of centre of meridional circulation

5. NUMERICAL METHODS AND COMPUTER PROGRAMS

Numerical methods are used to solve the flow equations and since the flow has an arbitrary set of boundary conditions the solution is necessarily an iterative one. Furthermore, the method described in Chapter 4 for establishing appropriate streamfunction equations for the representation of the meridional velocity requires the flow to be solved several times, using experimental streamfunction relationships. Thus, a computer is the only practical means of performing the iterations required.

Computer programs written in FORTRAN IV have been prepared for carrying out the solution of the flow. These programs and the basic numerical methods used in them for solving the flow equations are described in this chapter.

The programs are described with the aid of general flow diagrams and complete FORTRAN IV listings are given in Appendix C. A fully documented copy of all the computer programs is available in the School of Engineering Computer Library at the University of Bath.

5.1 Sequence of Using Programs

The computer programs are basically used to calculate the velocity and pressure of the flow along streamlines. Using suitable iteration methods and the procedure given in section (4.7.3), appropriate streamfunction equations are then obtained to represent the meridional velocity field. Employing these functions, the performance characteristics of the pump are predicted.

In principle it is possible to arrange a single computer program such that it performs the iterations required to establish the streamfunctions and predicts the performance of the pump all in one run. However, it was shown in Chapter 4 that it is required to plot various graphs so that the appropriate streamfunction parameters may be obtained. Various sets of computed results are required and the entire job may prove to be complex when accommodated in a single program.

To avoid unnecessary complications, the solution is done in two phases using two main programs.

The first program (REGEF) is used for establishing the streamfunction equations. It is the source which provides the data for the procedure described in Chapter 4. It provides information about the flow when any set of the six parameters of the streamfunction A, a, b, c, d, and R_m is assumed. These data are used, externally to the program, to plot the necessary graphs, according to the scheme outlined in section (4.7.3), from which the appropriate streamfunction equations are determined. Thus the first phase of the solution is completed.

The program does not deal with the overall performance of the pump. Thus, it incorporates the flow model in the linear section only.

The second program (CHARA) uses the streamfunction equations determined in the first phase of the solution to directly solve the flow and predict the overall performance characteristics of the pump. It deals, therefore, with the flow in all parts of the pump: in the linear section, in the ports regions and within the stripper region.

5.2 Scheme of Solution

Although the pressure field is not axi-symmetric, it is assumed that the tangential pressure gradient $\partial p/\partial \theta$ is constant throughout the linear section. Then, if the pressure is determined at a point $P_1(r_1, z_1, \theta_1)$, it can directly be computed at any other point $p_2(r_1, z_1, \theta_2)$ in the linear section. On the other hand, the velocity field is assumed to be axi-symmetric. Thus, the flow conditions in the linear section may be investigated on an arbitrary meridional plane. Therefore the solution of the flow field is accomplished by solving the flow through a complete flow cycle along each of the streamtubes into which the flow may be divided. A flow cycle may be started on an arbitrary meridional plane, see Fig. (2.3).

The flow equations are solved at discreet points on the flow cycles. The first point of solution is the streamline exit point from the impeller blades. This is chosen because the flow conditions at it are directly estimated using a slip factor model and the assumed streamfunction equation as will be shown in section (5.3.2). These conditions are then used to solve for the flow conditions at the next solution point which is a close neighbouring location on the streamline at a step length chosen as demanded by the numerical

method used. These latter conditions are in turn used to solve for those at the next point and so on until the flow cycle is completed. Another streamtube is then considered and so on until all streamtubes are solved. The method is further described in the following sub-sections.

5.2.1 Pressure difference in the channel

Since the pressure is a three-dimensional point function which can be expressed as:

$$p = p(r, \theta, z) \tag{5.1}$$

the pressure difference between any two points 1 and 2 on the same streamline is given by, see Fig. (5.1):

$$\frac{p_2 - p_1}{\rho} = \int_1^2 \frac{1}{\rho} \frac{\partial p}{\partial r}\, dr + \int_1^2 \frac{1}{\rho} \frac{\partial p}{\partial \theta}\, d\theta + \int_1^2 \frac{1}{\rho} \frac{\partial p}{\partial z}\, dz \tag{5.2}$$

Alternative paths may be chosen along which the integration may be performed, such as:

$$\frac{p_2 - p_1}{\rho} = \int_1^5 \frac{1}{\rho} \frac{\partial p}{\partial r}\, dr + \int_5^6 \frac{1}{\rho} \frac{\partial p}{\partial \theta} + \int_6^2 \frac{1}{\rho} \frac{\partial p}{\partial z}\, dz \tag{5.3}$$

However, the same difficulties are encountered in trying to perform the integrations irrespective of the path followed and basically the same techniques are employed. Therefore equation (5.2) will be used to explain the method.

Expressions for the partial derivatives on the RHS of equation (5.2) are obtained from the three components of the equation of motion (B-8) to (B-10) as follows:-

$$1) \quad \int_1^2 \frac{1}{\rho} \frac{\partial p}{\partial r}\, dr = -\int_1^2 (\nu + \varepsilon)\left(\frac{\partial^2 V_r}{\partial r^2} + \frac{1}{r}\frac{\partial V_r}{\partial r} + \frac{\partial^2 V_r}{\partial z^2} - \frac{V_r}{r^2}\right) dr$$

$$- \int_1^2 \left(V_r \frac{\partial V_r}{\partial r} + V_z \frac{\partial V_r}{\partial z}\right) dr$$

$$- \int_1^2 \frac{V_\theta}{r}\, dr \tag{5.4}$$

Using an assumed streamfunction equation, all the terms of the first and second integrals of the above equation can be expressed in terms of the independent variable r. However, the manner in which V_θ varies with r is not known and hence the last integral of the equation cannot be performed by merely specifying a streamfunction equation.

Furthermore, by inspecting the type of expressions which will result from substituting expressions from appendix B for the terms in the first and second integrals, it can be seen that analytical integration is not possible because of the complexity of the functions. Numerical integration is therefore bound to be used.

By some methods the integration is approximated by a quadrature formula of the following type:

$$\int_1^2 \frac{1}{\rho}\frac{\partial p}{\partial r}\,dr \simeq \sum_{i=1}^{k} \frac{1}{2}\left[\left(\frac{1}{\rho}\frac{\partial p}{\partial r}\right)_1 + \left(\frac{1}{\rho}\frac{\partial p}{\partial r}\right)_2\right]\Delta r \qquad (5.5)$$

where k is the number of intervals into which the range $|r_2 - r_1|$ is divided.

However, if the two points are close enough so that the numerical integration is performed in one interval, there is from equation (5.5):

$$\int_1^2 \frac{1}{\rho}\frac{\partial p}{\partial r}\,dr \simeq \frac{1}{2}\left[\left(\frac{1}{\rho}\frac{\partial p}{\partial r}\right)_1 + \left(\frac{1}{\rho}\frac{\partial p}{\partial r}\right)_2\right]\Delta r \qquad (5.6)$$

This kind of approximation is used here for two reasons:

a) Either the integrals are too complex to perform analytically or the functions to be integrated are unknown.

b) Iteration methods can be used to estimate the unknown functions (e.g. V_θ in the last integral of equation (5.4)) when this approximation is used.

By the same reasoning there is also:

$$2)\quad \int_1^2 \frac{1}{\rho}\frac{\partial p}{\partial z}\,dz \simeq \frac{1}{2}\left[\left(\frac{1}{\rho}\frac{\partial p}{\partial z}\right)_1 + \left(\frac{1}{\rho}\frac{\partial p}{\partial z}\right)_2\right]\Delta z \qquad (5.7)$$

3) $$\int_1^2 \frac{1}{\rho}\frac{\partial p}{\partial \theta}\, d\theta = \frac{1}{\rho}\frac{\partial p}{\partial \theta}(\theta_2 - \theta_1) \qquad (5.8)$$

since $\frac{1}{\rho}\frac{\partial p}{\partial \theta}$ = constant.

Summarising: the pressure difference between two close points on the same streamline in the channel is approximated by the equation:

$$\frac{p_2 - p_1}{\rho} = \frac{1}{2}\left[\left(\frac{1}{\rho}\frac{\partial p}{\partial r}\right)_1 + \left(\frac{1}{\rho}\frac{\partial p}{\partial r}\right)_2\right]\Delta r + \frac{1}{\rho}\frac{\partial p}{\partial \theta}\Delta\theta + \frac{1}{2}\left[\left(\frac{1}{\rho}\frac{\partial p}{\partial z}\right)_1 + \left(\frac{1}{\rho}\frac{\partial p}{\partial z}\right)_2\right]\Delta z \qquad (5.9)$$

5.2.2 Tangential velocity in the channel

The energy equation integrated between any two points on the same streamline in the channel is given by:

$$\frac{p_2 - p_1}{\rho} + \frac{V_2^2 - V_1^2}{2} + gh = 0 \qquad (5.10)$$

where gh is the specific energy loss between the two points due to friction.

Since the flow conditions at point 1 are known and the meridional velocity at point 2 is directly computed using the assumed stream-function equation, equations (5.9) and (5.10) can be solved simultaneously for $V_{\theta 2}$ and p_2. However, gh, $\left(\frac{\partial p}{\partial r}\right)_2$ and $\Delta\theta$ are all functions of $V_{\theta 2}$. Therefore, the solution can only be done iteratively.

Using an estimate of $V_{\theta 2}$, equation (5.9) can be evaluated and the loss gh can be estimated. These are then substituted into equation (5.10) and the resulting error is calculated from the following equation:

$$\left(\frac{p_1}{\rho} + \frac{V_1^2}{2} - gh\right) - \left(\frac{p_2}{\rho} + \frac{V_2^2}{2}\right) = \text{error} \qquad (5.11)$$

A procedure is developed by which the estimate of $V_{\theta 2}$ is iteratively corrected until the error reduces to a prescribed level, see section (5.3.4).

5.2.3 Tangential velocity in the impeller

In section (4.3.1) it was shown that the velocity field inside the impeller is known if a meridional velocity field is assumed. This simplification was made possible because of the axi-symmetric assumptions. The tangential velocity in the impeller is then given by:

$$V_\theta = V_m \tan\beta + \omega r \qquad (5.12)$$

which is directly computed using the blade angles β_o and ε, the stream-function and the impeller speed.

5.2.4 Pressure distribution in the impeller

The net increase in the fluid head between any two points 1 and 2 on the same streamline inside the impeller is given by, see equation (2.36):

$$\Delta(gH) = (U_2 V_{\theta 2} - U_1 V_{\theta 1}) + \frac{1}{\rho}\frac{\partial p}{\partial \theta}\Delta\theta - gh \qquad (5.13)$$

where gh is the specific energy loss between the two locations which is estimated by the methods of section (2.3.3). Then using equation (5.12), $\Delta\theta$ can be estimated, and equation (5.13) evaluated and the static pressure at point 2 obtained.

The subroutines and the details of the techniques used to execute the above scheme will now be discussed.

5.3 Main Subroutines

In the two programs introduced earlier, there is a section which deals with the solution along a selected streamline for a complete flow cycle. The calculations in this section are done with the aid of subroutines which are considered in the following in the order of their first use in the programs.

5.3.1 The meridional velocity (MOTION)

At any point in the channel or inside the impeller the meridional velocity components V_r and V_z and their derivatives, which appear in the equation of motion, are evaluated directly from the equations given in Appendix B using subroutine MOTION. The subroutine requires

the following input information:

1) The meridional co-ordinates of the point

2) Values of the parameters of a specified streamfunction equation

3) The blockage factor B and the manner in which it varies within the impeller.

The necessary differentials of the streamfunction are directly determined according to the relations derived in Appendix B. These derivatives are then used with the co-ordinates of the given point to determine V_r, V_z, $\frac{\partial p}{\partial z}$ and all the terms of $\frac{\partial p}{\partial r}$ which do not include V_θ, see Appendix B. However, when the flow is solved in the impeller the partial derivatives of the pressure are not required.

All the calculations in MOTION are carried out without iteration. A general flow diagram for the subroutine is shown in Fig. (5.2) and a Fortran listing of it is given in Appendix C.

5.3.2 Conditions at exit from impeller (FIRST)

The r and z co-ordinates of the impeller inlet and exit of a streamline are obtained by solving the equation of the meridional projection of the streamline:

$$F(r, z) = 0 \tag{5.14}$$

simultaneously with the meridional projection of the impeller blades. Equation (5.14) is obtained from the streamfunction equation.

The velocity head at exit:

The stream surface meridional angle λ, Fig. (4.3), is computed from the equation:

$$\tan \lambda = \frac{V_r}{V_z} \tag{5.15}$$

The flow angle at the exit is then computed from equation (4.1) and the corrected value of the tangential velocity is consequently estimated as explained in section (4.2).

The pressure at the exit:

When solving the flow along a streamline, interest centres on the variation of the pressure rather than on its absolute value. It is therefore convenient to take the static pressure at the exit from the impeller to be zero on each streamline.

However, when the variation of pressure over the entire meridional plane is required, a zero pressure datum can be taken at one streamline exit from the impeller: the pressure at exit points of other streamlines is subsequently estimated using the meridional partial derivatives of the pressure which are determined by subroutine MOTION.

The calculations of the conditions at this first point of the flow cycle are carried out in subroutine FIRST. A flow diagram of the computations is given in Fig. (5.3).

5.3.3 Steping along a streamline (STREAM)

Points of solution along a streamline are located using subroutine STREAM.

The first point in a flow cycle is determined as explained in section (5.3.2). Using the co-ordinates of this point and the step-length to be taken to the next solution point, equation (5.14) of the streamline is solved to locate the position of the latter.

The step-length is defined as the meridional distance between any two neighboruing solution points on the same streamline and is given by:

$$\Delta s = \sqrt{\Delta r^2 + \Delta z^2} \qquad (5.16)$$

where Δr and Δz are the radial and the axial distances respectively between the two points.

By solving for the tangential velocity at the second point, the tangential displacement $\Delta\theta$ is also determined. The three-dimensional path of the streamline is followed by combining Δr, Δz and $\Delta\theta$.

The location of the second point on the meridional plane is obtained by specifying the magnitude of the step Δs. Then one of the two meridional co-ordinates, whichever is changing faster than the other at the point considered, is used to locate point 2 as follows:

Assume that co-ordinate r changes faster than z at the point considered. Put $r_2 = r_1 + \Delta s$ and solve equation (5.14) for z_2. Compare the distance between the two points with the specified one and correct r_2 accordingly.

If the condition is imposed that the meridional distance between the two points should be equal or less than the specified Δs, experience shows that the condition is met by the above procedure in a maximum of two iterations.

Alternatively, the location of the second point can be made directly in one step if Δs is meant to be equal to the change in the magnitude of the co-ordinate which changes faster at the point. Iteration is not then needed.

Choice of the step length Δs:

It is chosen on the basis of two considerations:

1) That it should be less than the minimum diameter of the meridional projection of the streamline being followed.

2) That approximation of the type of equation (5.9) should result in a reasonable degree of accuracy.

The role of Δs in determing the accuracy may be judged by fixing all the other parameters needed to calculate a particular flow along a particular streamline while Δs is varied. Flow parameters such as the net increase of specific energy per flow cycle, the tangential velocity at the inlet to the impeller, etc., may then be plotted against Δs. Variations of the types shown in Fig. (5.4) are usually obtained. When the step length is on the larger side, computed parameters tend to change with the change in Δs; while they attain almost constant values in the range of small Δs. The step length at which a computed parameter starts to settle to a constant value is chosen.

A general flow diagram for subroutine STREAM is shown in Fig. (5.5). The subroutine is used for stepping along the streamline where the non-dimensional co-ordinate RR decreases, i.e. in sectors I and III of Fig. (4.7a). A similar subroutine POINT 2 is used where RR increases, i.e. in sectors II and IV of Fig. (4.7a).

5.3.4 The tangential velocity (SECOND)

An iteration method is used in subroutine SECOND for the determination of the tangential velocity V_θ in the channel. Iteration is necessary for the solution of equations (5.9) and (5.10), as mentioned earlier, because not only $V_{\theta 2}$ and p_2 are unknown, but also gh, $(\frac{\partial p}{\partial r})_2$ and $\Delta\theta$ require $V_{\theta 2}$ to be known so that they can be evaluated. An estimate of $V_{\theta 2}$ is therefore used first to compute the following:

1) The frictional loss gh_t between the two points considered due to the tangential motion. This is estimated using equation (2.57).

2) The pressure difference of equation (5.9). This requires the tangential displacement $\Delta\theta$ to be known.

The angular displacement $\Delta\theta$:

To estimate the circumferential movement of a particle between the points, the time taken by the particle to travel from point 1 to point 2 is utilized. The streamline equation is:

$$\frac{dr}{V_r} = \frac{rd\theta}{V_\theta} = \frac{dz}{V_z} \tag{5.17}$$

$$\Delta t = \int_1^2 \frac{dr}{V_r} = \int_1^2 \frac{rd\theta}{V_\theta} = \int_1^2 \frac{dz}{V_z} \tag{5.18}$$

where the integration has to be performed along the streamline.

Although $\frac{1}{V_r}$ and $\frac{1}{V_z}$ can be expressed as functions of r and z respectively, using the relations derived in appendix B, the integration can only be performed numerically. Following the approach adopted in section (5.2.1), there is:

$$\Delta t \simeq \frac{1}{2}\left(\frac{1}{V_{r1}} + \frac{1}{V_{r2}}\right)\Delta r \tag{5.19}$$

$$\Delta t \simeq \frac{1}{2}\left(\frac{1}{V_{z1}} + \frac{1}{V_{z2}}\right)\Delta z \tag{5.20}$$

$$\text{and} \quad \Delta t \simeq \frac{1}{2}\left(\frac{r_1}{V_{\theta 1}} + \frac{r_2}{V_{\theta 2}}\right)\Delta\theta \tag{5.21}$$

Also from equation (5.18) there is:

$$\Delta\theta = \int_1^2 \frac{V_\theta}{r}\, dt \tag{5.22}$$

which may be approximated by:

$$\Delta\theta \simeq \frac{1}{2}\left(\frac{V_{\theta 1}}{r_1} + \frac{V_{\theta 2}}{r_2}\right)\Delta t \tag{5.23}$$

In each flow cycle there are two points where V_r is zero; and other two points where V_z is zero. Hence equations (5.19) and (5.20) together should provide an unfailing means of estimating the time interval. This is then substituted in equation (5.23) to estimate $\Delta\theta$. Equation (5.21) gives almost the same result as equation (5.23), but it is bound to fail when one or both of the tangential velocities is zero.

The iteration for $V_{\theta 2}$

Equation (5.11) is conveniently put in the following form:

$$gH_a - gH_b = \text{error} \tag{5.24}$$

where gH is the fluid head defined by equation (4.48c) and:

$$gH_a = gH_1 - (gh_m + gh_t) \tag{5.25}$$

$$\text{and} \quad gH_b = \frac{p_2}{\rho} + \frac{V_2^2}{2} \tag{5.26}$$

gH_1: is the total head at point 1. It is known from section (5.3.2).

gh_m: is the specific friction loss between the two points due to the meridional motion, estimated by equation (2.52).

gh_t: specific friction loss due to the tangential motion, from equation (2.57).

gH_b: is the total head at point 2 computed using the estimate of $V_{\theta 2}$. It is composed of a constant part and a part which is a function of $V_{\theta 2}$, i.e.

$$gH_b = press2 + f(V_{\theta 2}) \tag{5.27}$$

where:

$$press2 = \frac{p_1}{\rho} + \frac{1}{2}\left[\left(\frac{1}{\rho}\frac{\partial p}{\partial r}\right)_1 + Term2\right]\Delta r + \frac{1}{2}\left[\left(\frac{1}{\rho}\frac{\partial p}{\partial z}\right)_1 + \left(\frac{1}{\rho}\frac{\partial p}{\partial z}\right)_2\right]\Delta z + \frac{v_{m2}^2}{2} \tag{5.28}$$

$$f(V_{\theta 2}) = \frac{v_{\theta 2}^2}{2}\left[1.0 + \frac{\Delta r}{2r}\right] + \frac{1}{\rho}\frac{\partial p}{\partial \theta}\,\Delta\theta \tag{5.29}$$

Term2 = all the terms of $\frac{1}{\rho}\frac{\partial p}{\partial r}_2$ except $\frac{v_{\theta 2}^2}{r}$, see equation (B.8)

The function given by equation (5.29) takes the sign of $V_{\theta 2}$ if the latter is positive. However, it may have a positive, a zero or a negative value if $V_{\theta 2}$ is negative because $\Delta\theta$ is then negative while the first term on the RHS is always positive.

Fig. (5.6) shows a schematic diagram of the specific energy gH plotted against the estimate of the tangential velocity at any point 2 when the conditions are such that $f(V_{\theta 2})$ is positive irrespective of the sign of the estimate of $V_{\theta 2}$. Two curves are to be considered: curve 'a' which represents the variation of gH_a computed by equations (5.25); and curve 'b' which represents equation (5.27). The energy equation (5.10) is satisfied only at the point of intersection of these two curves, and the value of $V_{\theta 2}$ which corresponds to this point is the required value.

Referring to Fig. (5.6), any value of $V_{\theta 2}$ may be taken to be the first estimate. However, a convenient choice is the value of $V_{\theta 1}$. After gH_a and gH_b are calculated and the corresponding error is obtained from equation (5.24), the next estimate of $V_{\theta 2}$ may be obtained by solving the following equation for $V_{\theta 2}$:

$$\frac{p_2}{\rho} + \frac{V_2^2}{2} = gH_a \tag{5.30}$$

and the iteration is continued until the error reduces to a prescribed level.

The way in which the iteration proceed is shown schematically in Fig. (5.6). Whether an estimate is lower or higher than the proper value, it can be seen that the iteration rapidly leads to a satisfactory convergence: it usually takes two or three iterations only to reduce the error to a reasonably low level; for most cases three iterations were sufficient for the relative error to be less than 0.001.

The same applies when conditions are such that $f(V_{\theta 2})$ of equation (5.29) is a negative quantity. Such conditions are shown in Fig. (5.7).

By determining the tangential velocity at point 2, all the other flow conditions at that point are also determined. Point 2 is then referred to as the new point 1 and a step is taken to a new point 2 using sub-routine STREAM or POINT2, see section (5.3.3).

This procedure is repeated until the flow cycle has been followed to its last point in the channel which is referred to point 3' in Fig. (4.19). The flow now passes into the impeller via the discontinuity 3'3 encountered at the leading edge. The shock losses are estimated using the model selected in section (2.3.1).

The flow inside the impeller is solved directly using the methods of sections (5.2.3) and (5.2.4). Since there is no iteration involved in determining the tangential velocity in the impeller, the total head imparted to the fluid per flow cycle can be calculated from equation (5.13) by taking point 1 at the impeller inlet and point 2 at its exit and estimating the tangential displacement from the following equation:

$$\theta_2 - \theta_1 = \int_1^2 d\theta = \int_1^2 \frac{V_\theta}{rV_r}\, dr = \int_1^2 \frac{V_\theta}{rV_z}\, dz \qquad (5.31)$$

where the integrations have to be performed along the streamline. The evaluation of these integrals requires V_θ of equation (5.12) to be expressed as a function of r or z only along the streamline. Again numerical integration is bound to be used. Therefore, the step-wise numerical solution is preferred because, in addition, it provides data about the pressure variation in the impeller.

The flow cycle calculations are completed when its exit from the impeller is reached again.

A general flow diagram for subroutine SECOND, in which the above calculations are carried out, is shown in Fig. (5.8).

5.3.5 The matching coefficient (MATCH)

The solution of a flow cycle described above is carried out assuming a value for the streamfunction coefficient A. From the solution, the computed energy gradient may not match the assumed energy gradient in the linear section as explained in detail in section (4.7.1). The necessary correction is made according to steps (5) and (6) of the procedure given in section (4.7.3).

Similar to Fig. (4.22), Fig. (5.9) shows typical plots of the computed energy rise per flow cycle $\Delta(gH)_c$ and the corresponding energy rise per flow cycle $\Delta(gH)_\theta$ computed using the assumed energy gradient, see equations (4.41) and (4.42) respectively. The incompatibility between the two energy gradients is measured by the discrepancy given by equation (4.43) and graphically, it is given by the vertical distance between the two curves. Subroutine MATCH is used in the search for the matching value of the coefficient A_m as will be described now.

Experience shows that the coefficient value is always less than unity, and since it cannot be negative, there is the following broad range:

$$0.0 < A < 1.0 \tag{5.32}$$

Referring to Fig. (5.9), it can be seen that the matching value of the coefficient lies between a minimum and a maximum, i.e.

$$A_{min} < A < A_{max} \tag{5.33}$$

where:

A_{min} = coefficient value which results in zero $\Delta(gH)_\theta$

A_{max} = coefficient value which results in zero $\Delta(gH)_c$ while $\Delta(gH)_\theta$ is positive.

When A is less than A_{min}, both $\Delta(gH)_c$ and $\Delta(gH)_\theta$ are negative; and when A is more than A_{max}, only $\Delta(gH)_c$ is negative: these flow conditions are unacceptable.

The first estimate of A may be any value in the range given by equation (5.32). If the conditions at the end of a cycle solution are within the acceptable range, i.e. within the range in which both energy rises are positive, the solution is tested for matching; and is used in making the next estimate of A if the test is not satisfactory. Otherwise, it is rejected and the value used for A is taken as a new lower limit if (gH) is negative, and as a new upper limit if it is positive, see Fig. (5.9).

When two positive solutions are made, the next value of A is obtained by linear interpolation or extrapolation by solving for the intersection of two straight lines drawn as shown in Fig. (5.9). However, the controlling effect of the two limits is still used if such solution results in a value of A outside the limits.

It can be seen from Fig. (5.9) that at the end of any cycle solution, whether it is within the acceptable range or not, the value of A used can be identified as greater or less than the matching value: when $\Delta(gH)_\theta < \Delta(gH)_c$, it is less and vice versa. This provides a means for continuously updating the limits of the coefficient A such that the range in which matching occurs is narrowed after each solution. This guarantees a convergence if a matching condition exits. A failure to converge would almost certainly mean that there are no matching conditions because the values of the set of the other five parameters of the stream function equation are not appropriate for representing the flow conditions. Experience shows that, in the average, 5 iterations for the matching coefficient are sufficient for a reasonable convergence to be achieved if a suitable choice of these parameters is made. The average number of iterations usually required to reduce the relative discrepancy between the two energies to less than 0.001 is about 8 iterations.

5.4 Main Programs

These are programs REGEF and CHARA which were introduced in section (5.1). Both programs require the following input data:

1) The dimensions and the geometry of the impeller and the channel. These include the number of blades, the blade angles β_o and ε and the blade thickness everywhere on the surface of the blade.

2) The stream function equation to be used to represent the merdional velocity.

3) The values of the circumferential pressure gradients $\frac{\partial p}{\partial \theta}$. These represent chosen operating conditions of the pump.

However, program CHARA requires, as additional input information, those data about the performance of the non-linear section which have been discussed in chapter 3. Among these are the port loss coefficient and the stripper and side-plate clearances.

Both programs use the same set of subroutines, and the same techniques, for solving the flow along streamlines. These have been described in detail in the previous sections of this chapter.

The output from both programs is presented in tabular form. However, the programs could easily be extended to present the output in graphical form if required. The amount of information about the flow which may be printed is controlled by input parameters. There are two main levels of volume of output:

1) A basic output which includes the flow conditions at selected locations (e.g. at inlet to and exit from the impeller). These include the velocity components, the static pressure and the total head. Also given are the specific losses per flow cycle (i.e. losses in the blade passages, in the channel and at the entry to the impeller blades) and the tangential displacements in the impeller and in the channel per flow cycle.

2) A more detailed output in which the flow conditions are printed at all points of solution along any selected flow cycle. This type of output can be used for plotting maps of pressure and velocity fields.

In the following the overall structures of the two programs are described.

5.4.1 Program REGEF

The purpose of this program is to provide data for establishing appropriate stream function equations for representing the meridional velocity fields. Thus, the program is written such that it gives results of solutions of the flow at selected circumferential pressure gradients $\frac{\partial p}{\partial \theta}$ using different combinations of values of the stream-function parameters A, a, b, c, d and R_m. With these results available, the procedure of section (4.7.3) is used to obtain the appropriate functions. A general flow diagram of the program is shown in Fig. (5.10). This diagram may be viewed as an expanded section of that given in Fig. (4.21).

A value is selected for the radius R_m of the centre of circulation according to guide given by equation (4.31). A circumferential pressure gradient $\frac{\partial p}{\partial \theta}$ in the linear section of the pump is chosen. A set of values of the stream function indices a, b, c and d is chosen in the light of the results of the preliminary study of section (4.6). Now the flow model is ready to be solved along steamlines.

Using the dimensions of the meridional cross section and the radius R_m, the flow is divided by any chosen number of streamlines. Any of these may be selected for solution. Usually the solution of the flow along selected representative streamtubes gives an adequate idea of the entire flow. As an example, when the flow was divided into 10 streamtubes of equal radial width, the flow was solved in three stream-tubes only: streamtubes 1, 5 and 9; where the numbering begins from the outermost streamtube. Data from these three streamtubes were adequate for establishing the appropriate stream function relation for the flow.

The details of the actual calculations of the flow along a streamline are discussed in sections (5.2) to (5.3.5).

When all the selected streamtubes are solved, the stream function indices are changed and the procedure repeated. When this is done at all the chosen values of $\partial p/\partial \theta$, all the data required for establishing

the most appropriate stream functions are obtained for that particular R_m. The procedure is then repeated for other values of R_m. Then, externally to the program and following the procedure of section (4.7.3), the final values of the stream function parameters : R_m, a, b, c, d and the value or range of values of matching coefficient A (matching value of A may vary from one streamtube to the other) are obtained for each operating condition $\partial p/\partial \theta$. (A complete representation of the flow by the stream function is achieved if the matching value of the coefficient A is the same for all stream tubes. However, this may not always be possible to obtain using such a simple stream function equation as explained before in section (4.7.2). Slight variation of A is therefore tolerated). These are used as input data for program CHARA, see below.

The running time of program REGEF depends on many factors. Among these are the following:

1) The values of the indices a, b, c and d, and radius R_m. e.g. there is a difference in the running time when the values of these parameters are close to the appropriate values and when they are wide guesses.

2) The number of streamtubes in which the flow is actually solved. Although the flow may be divided into any number of streamtubes, running time is reduced if only selected representatives streamtubes are solved as mentioned earlier.

3) The discrepancies tolerated when iterating for the following:

   a) The tangential velocity in the channel, section (5.3.4.)
   b) The matching value of the coefficient A, section (5.3.5.)

4) The step-length between solution points along a streamline, section (5.3.3).

However, the run time should not present a problem because the required data can be collected from several runs simply by altering few input data each time.

The accuracy of convergence is only limited by practical considerations as can be seen from the way the iterations proceed in both subroutine SECOND and MATCH.

5.4.2 Program CHARA

For a given circumferential pressure gradient $\partial p/\partial \theta$, this program uses the values of the stream function parameters, obtained earlier by using program REGEF, to solve the flow and predict the performance of the pump. A general flow diagram for the program is given in Fig. (5.11).

As in program REGEF, the flow is divided into any number of streamtubes. However, the flow must be solved in each tube so that the performance of the pump can be estimated. The solution of the flow along streamtubes is carried out in exactly the same way as was described before.

In addition to solving the flow in the linear section and calculating the performance of the impeller and the channel, the prediction of the overall performance characteristics of the pump requires the following to be calculated:

1) The losses in the port regions. A port loss coefficient is used, see section (3.1).

2) The leakage through the stripper clearance, see section (3.2).

3) The carry-over losses, section (3.3).

4) The disc friction losses, section (3.5).

All these are done in this program. The program is arranged such that several operating conditions are dealt with in a single run so that the performance characteristics are predicted over the entire working range of the pump.

The run time depends on the same factors discussed earlier for program REGEF.

5.5 Summary

Two programs have been described.

1) Program REGEF which is used for providing data so that appropriate stream function parameters A, a, b, c, d and R_m are established,

externally to the program, at various conditions of circumferential pressure gradients $\partial p/\partial \theta$.

2) Program CHARA which uses the results determined in the first phase, and the models of chapter 3 for the non-linear part of the pump, to predict the overall performance characteristics at the various oeprating conditions $\partial p/\partial \theta$.

The actual calculation procedures and the subroutines used in the programs have been discussed in detail. In the next chapter these programs will be used to investigate the flow in pumps.

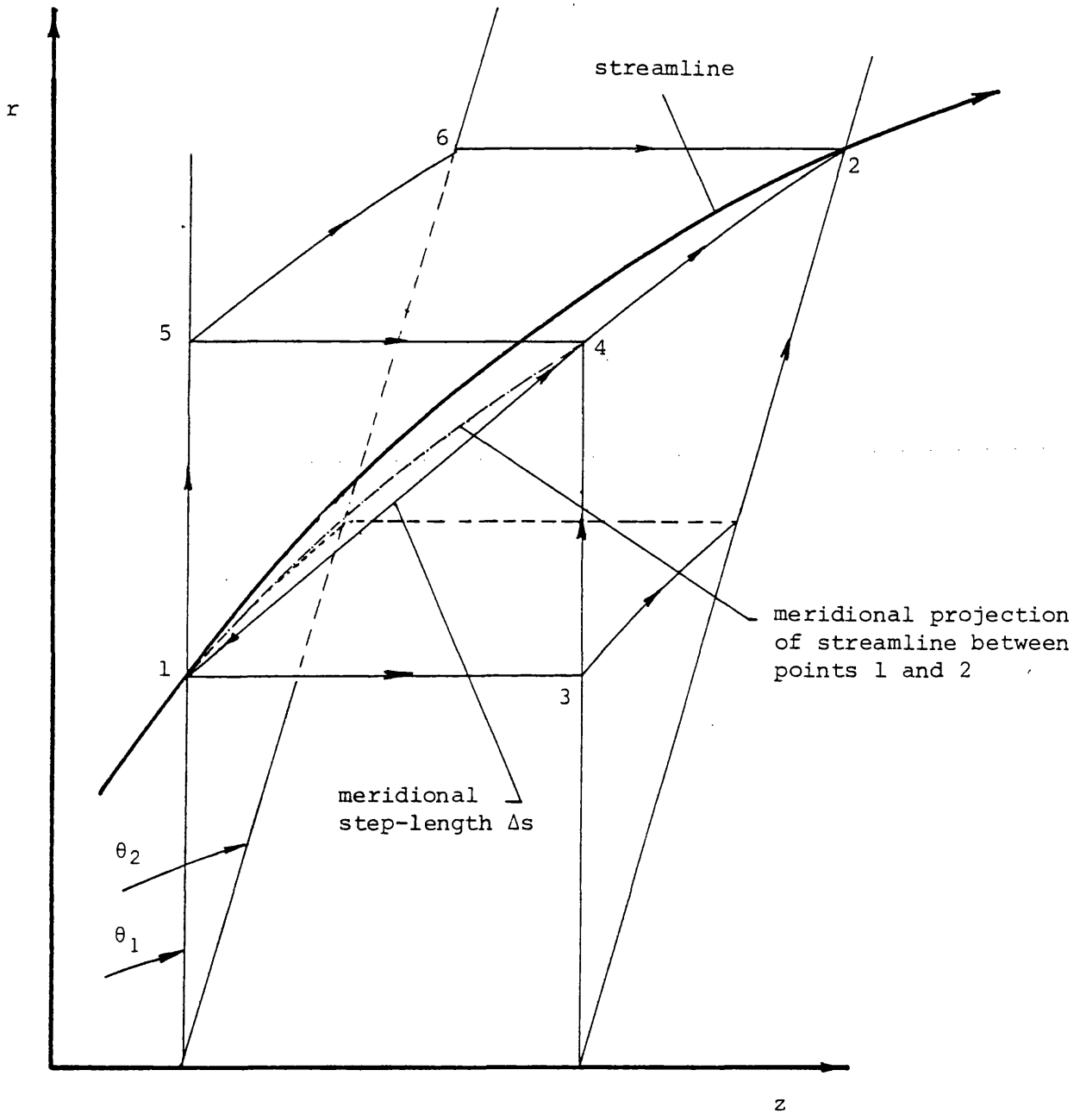

Fig. (5.1): Two neighbouring solution points on a streamline and step length Δs

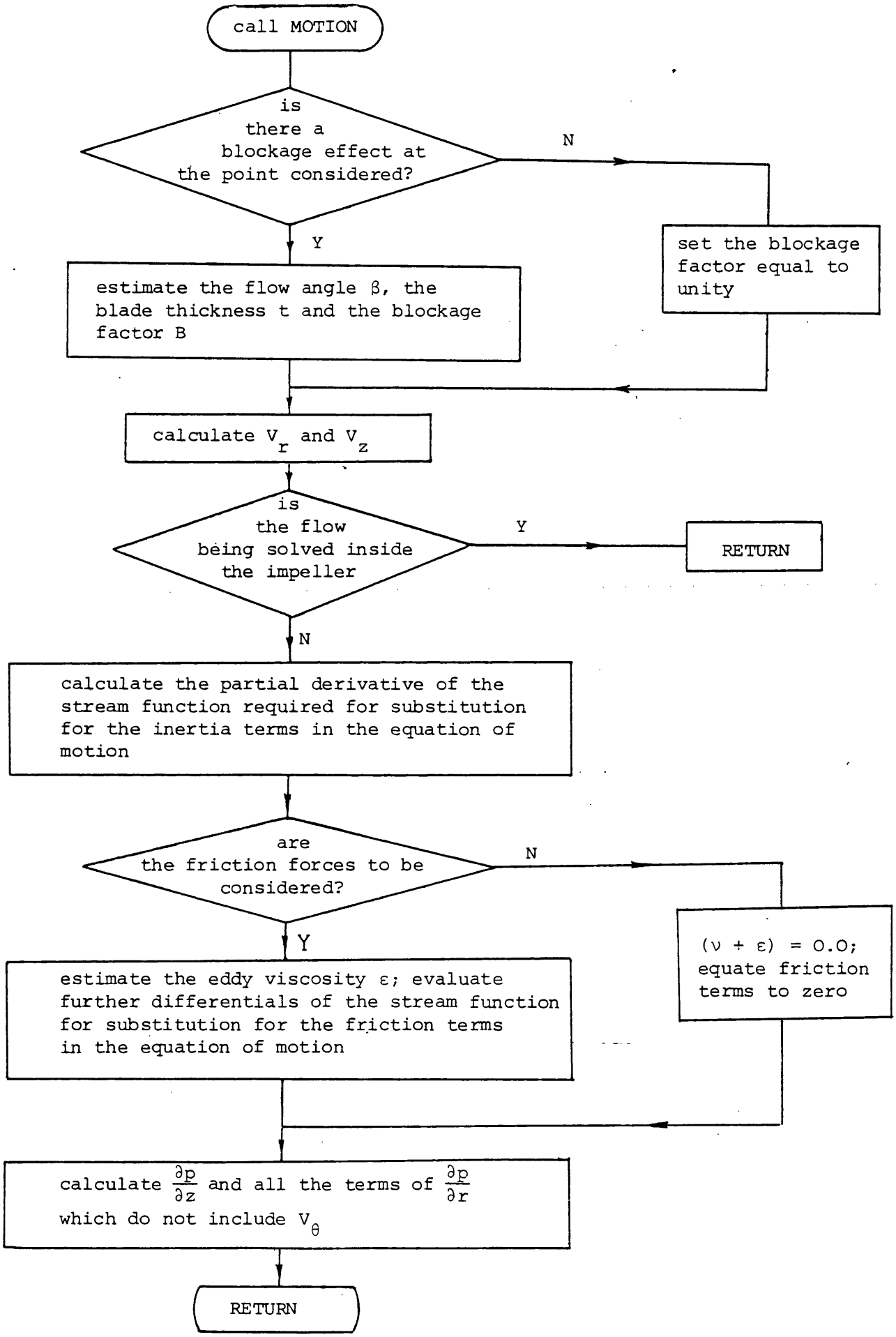

Fig. (5.2): General flow diagram for subroutine MOTION

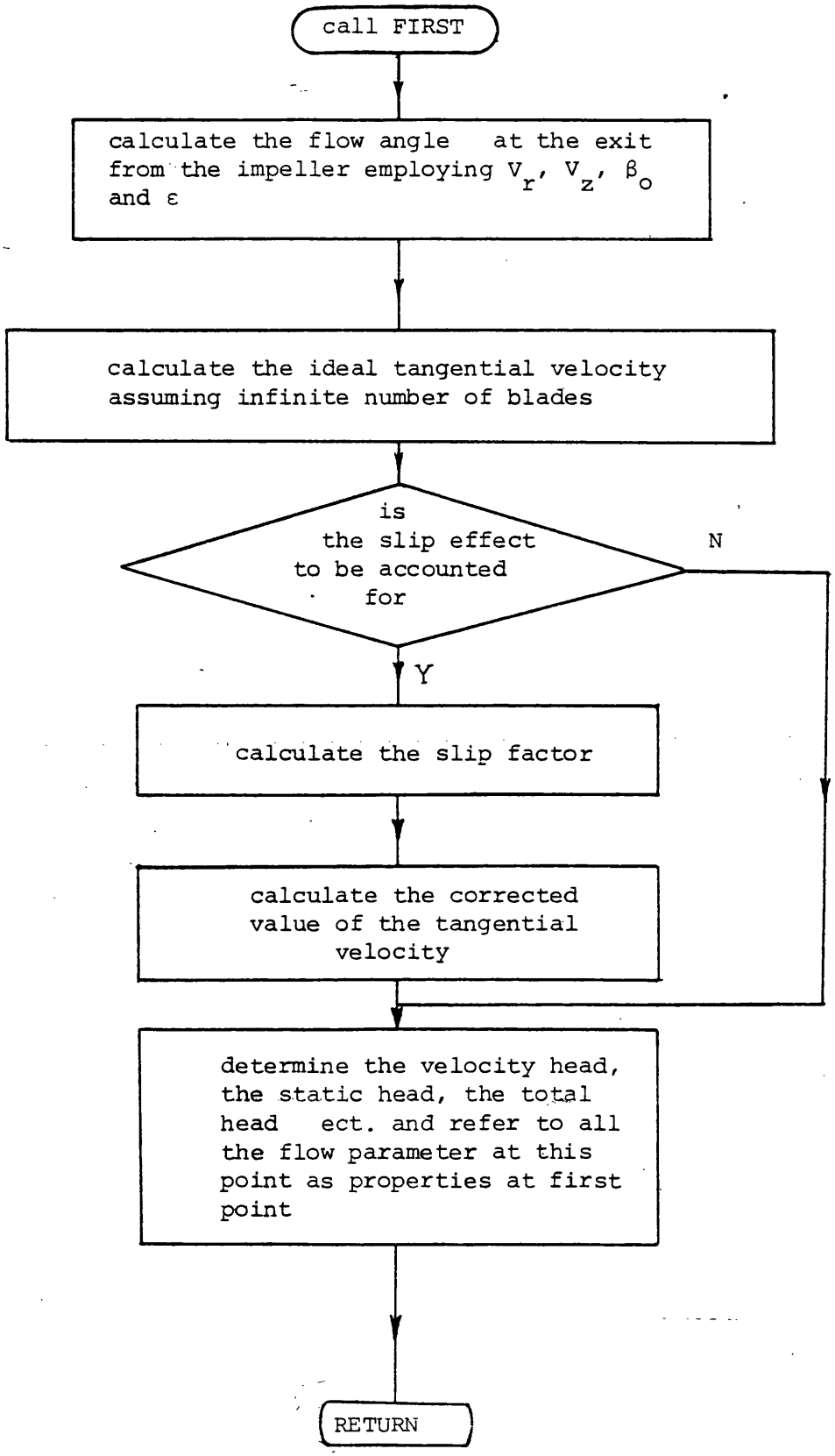

Fig. (5.3): General flow diagram for subroutine FIRST

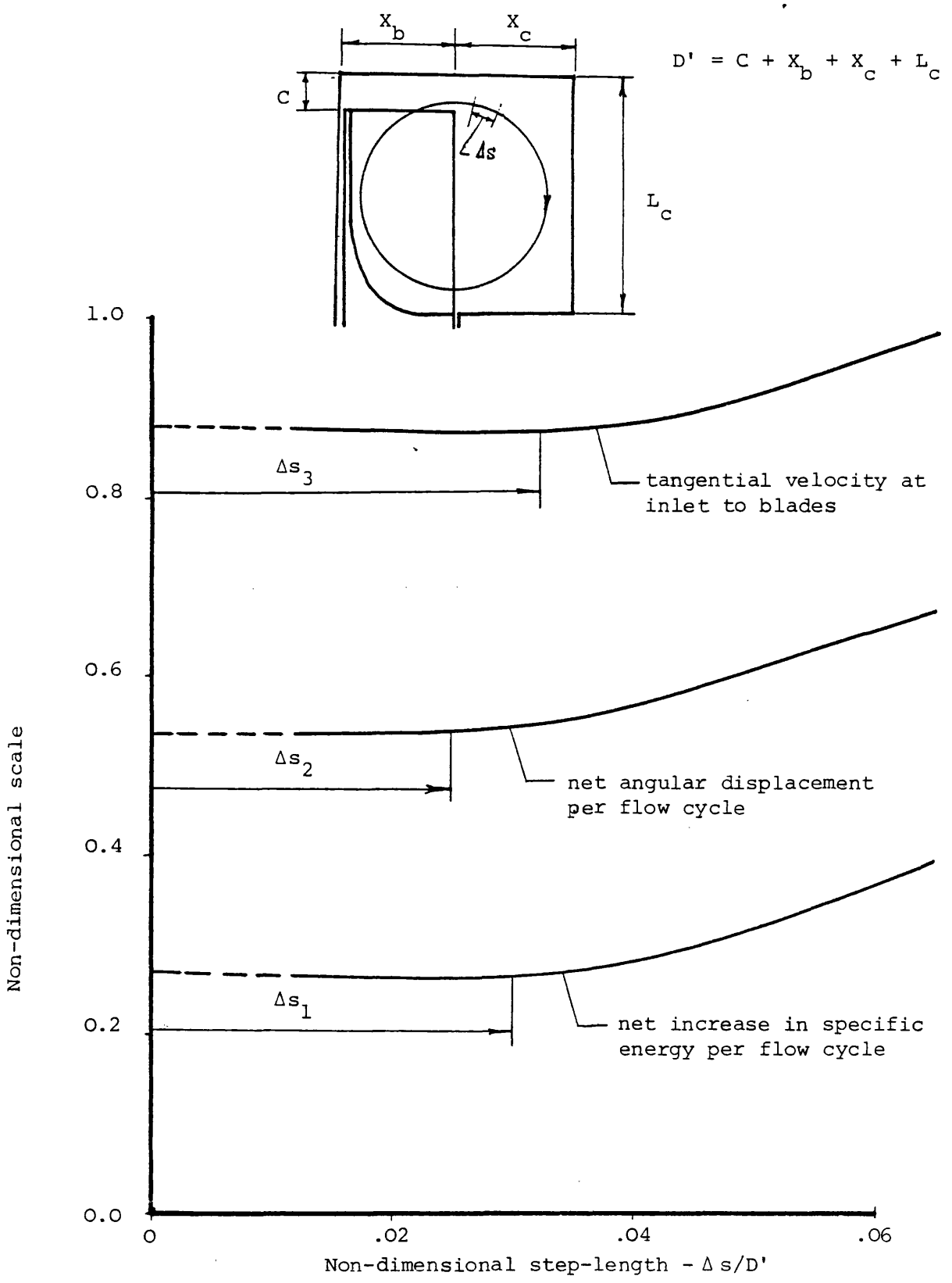

Fig. (5.4): Variation of computed flow parameters with step-length - Δs.

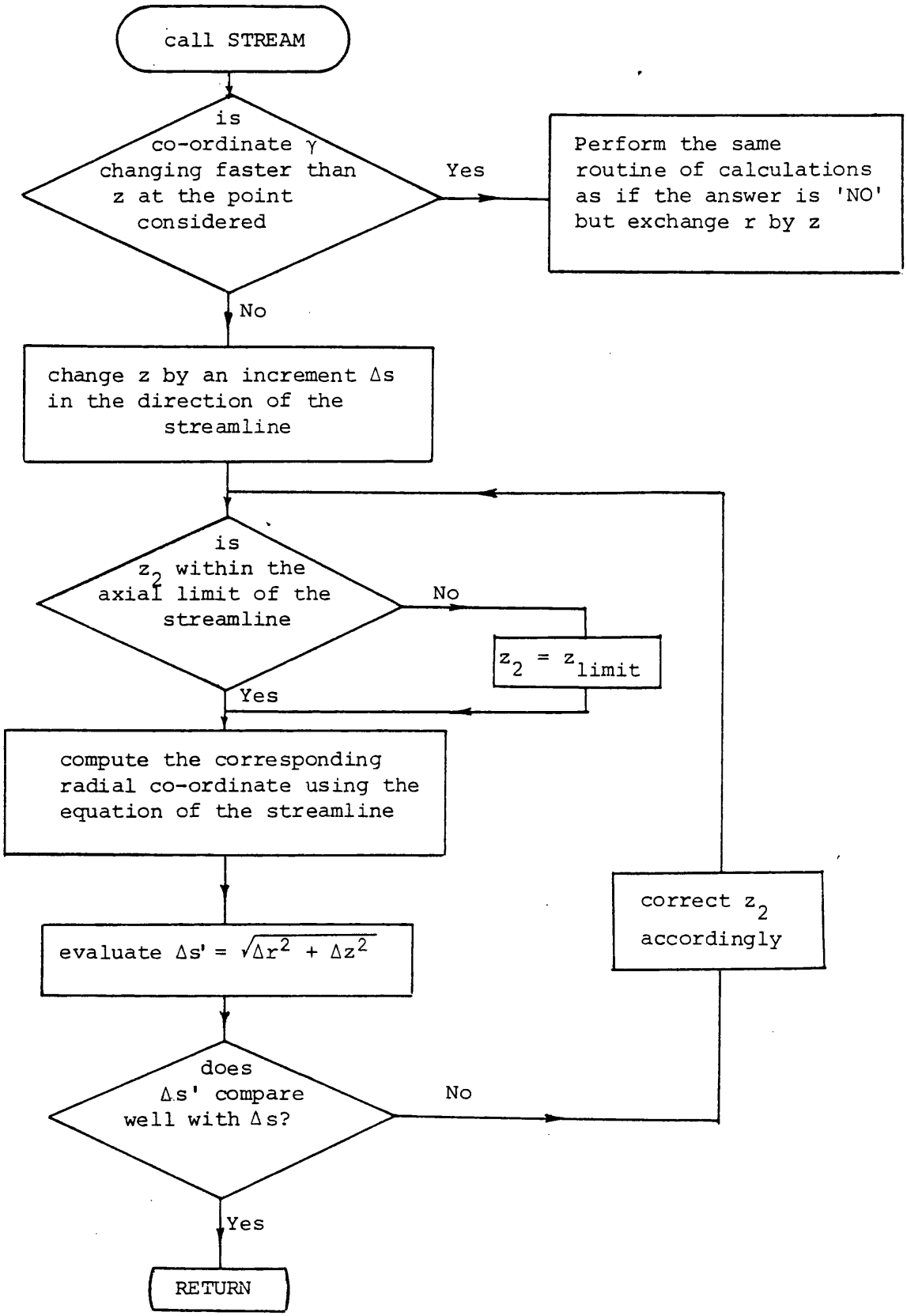

Fig. (5.5): General flow diagram for subroutine STREAM: stepping along a streamline

Fig. (5.6)

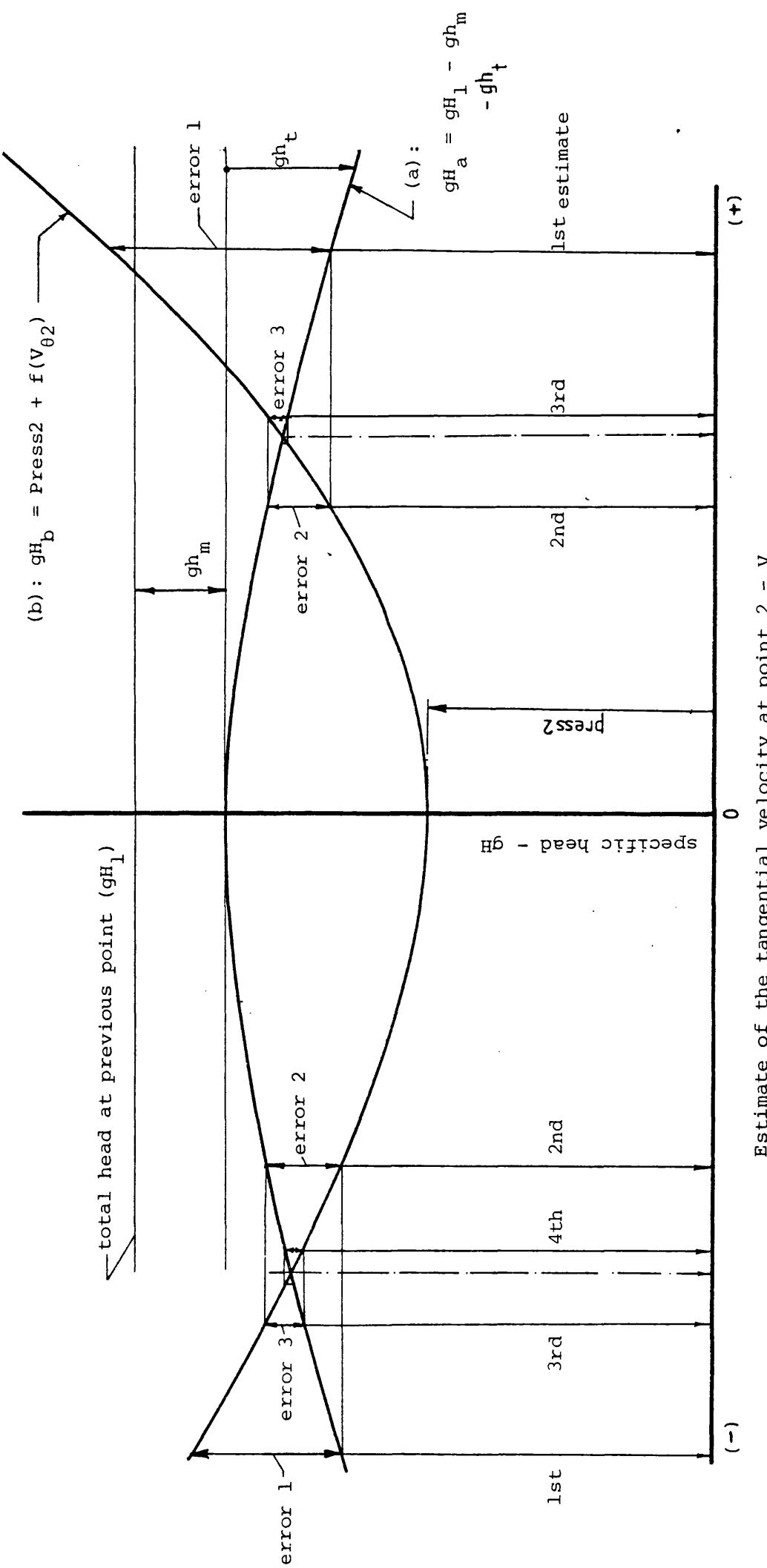

Fig. (5.6): Schematic representation of sequence of iteration for the tangential velocity at end of any step along a streamline.

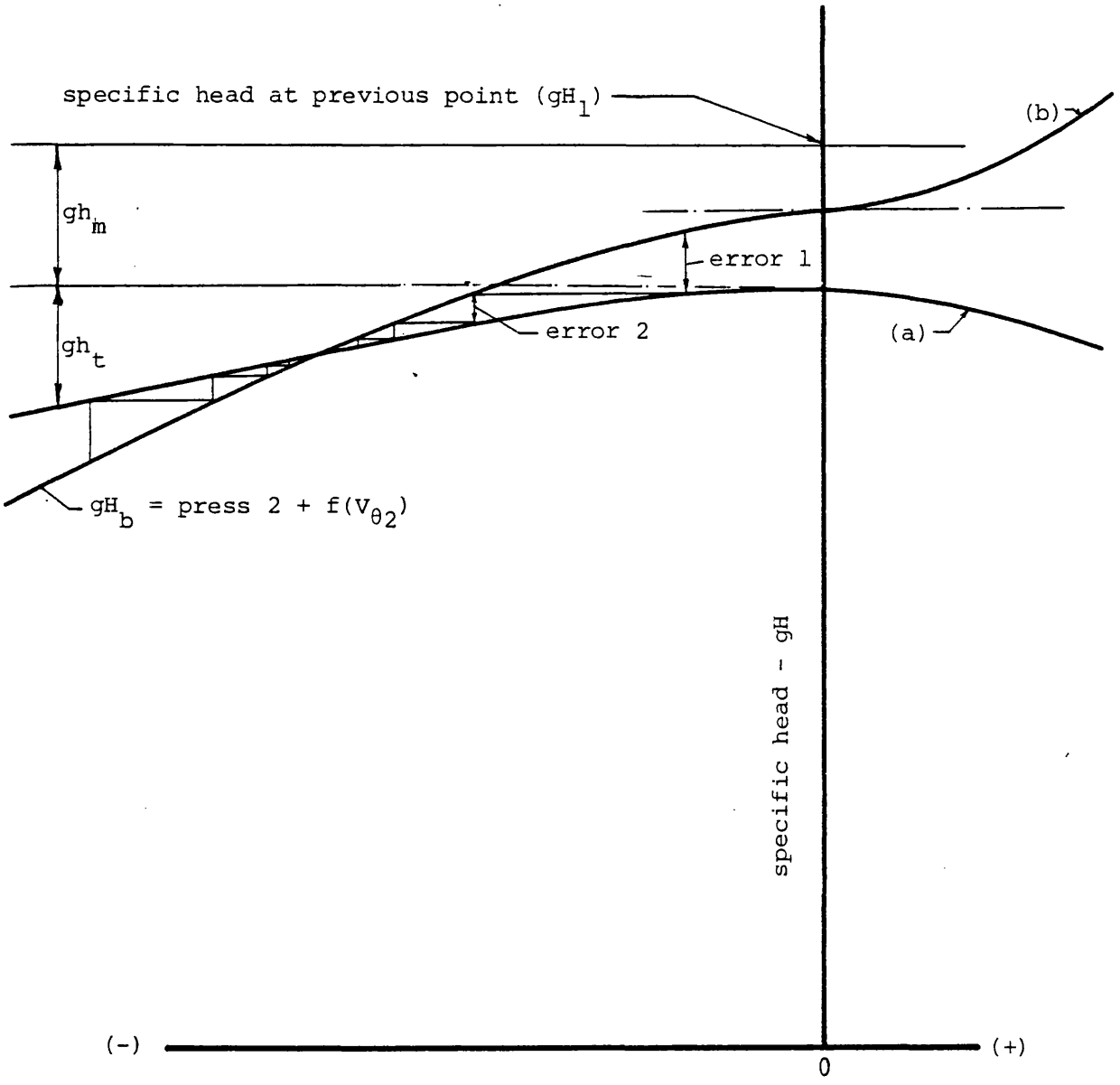

Fig. (5.7): Iterating for $V_{\theta 2}$ when $f(V_{\theta 2})$ of equation (5.27) is negative, see Fig. (5.6).

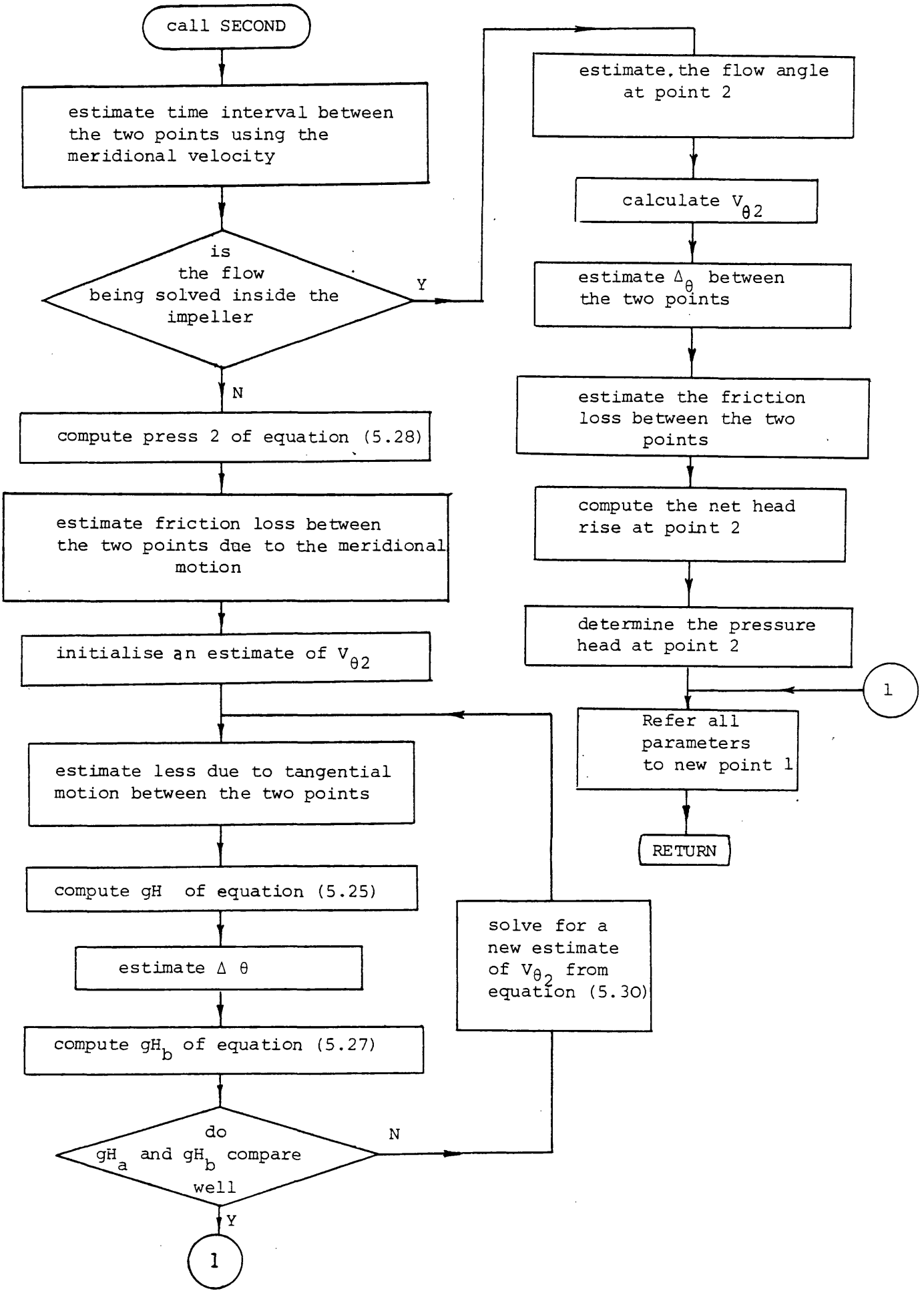

Fig. (5.8): General flow diagram for subroutine SECOND

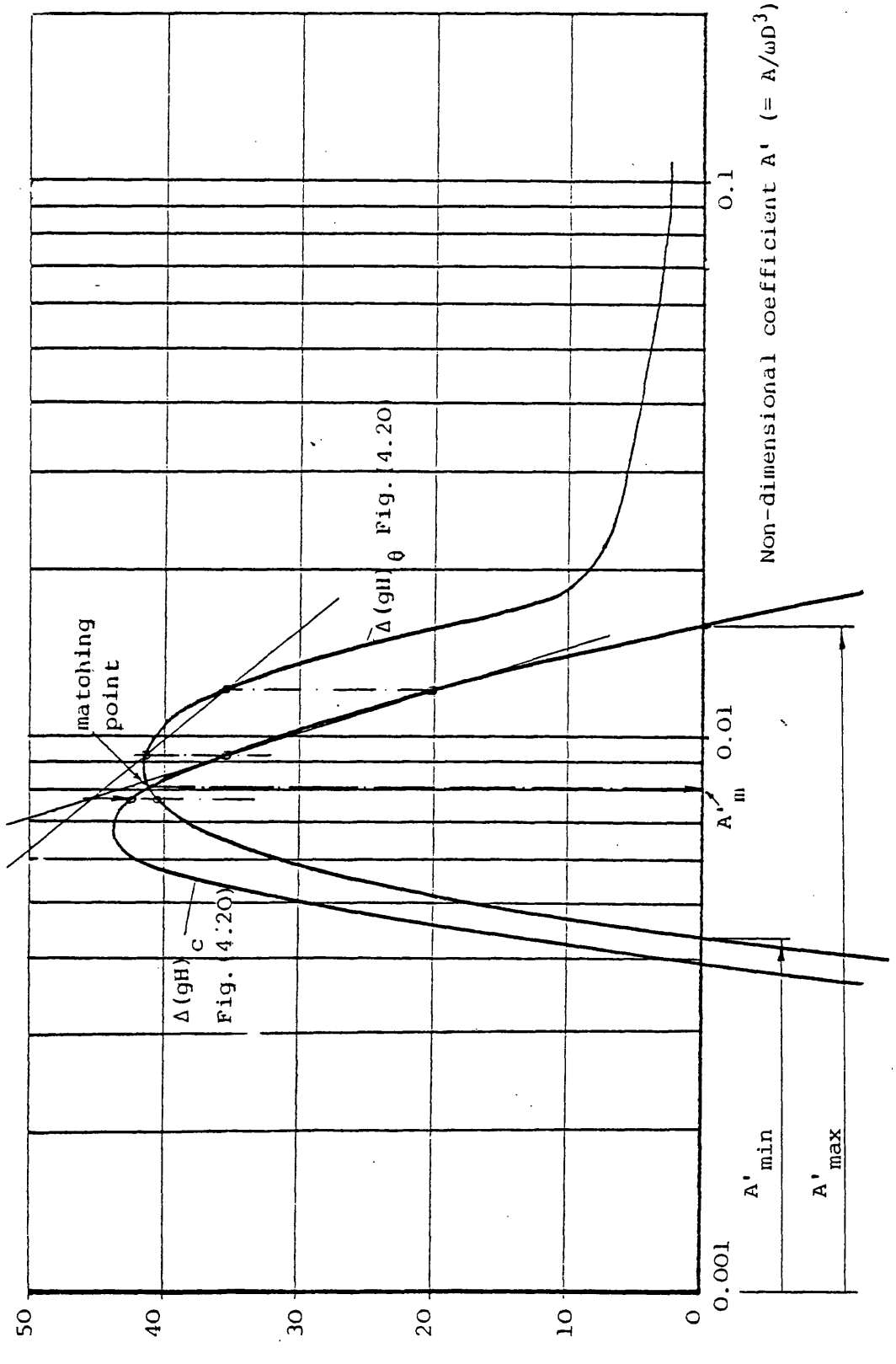

Fig. (5.9): Variation of computed head rise in a flow cycle with stream function coefficient A'.

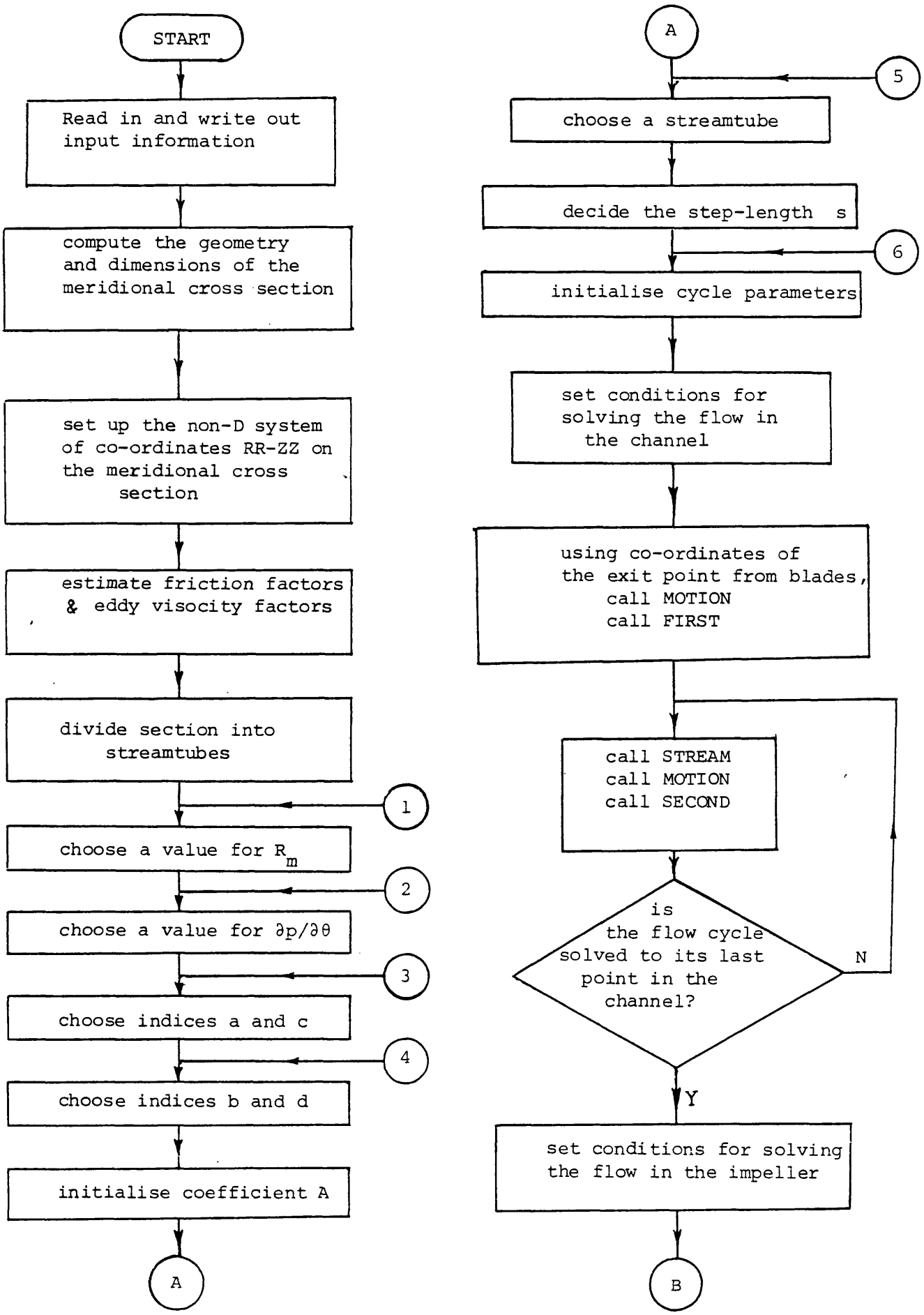

Fig. (5.10): General flow diagram for program REGEF (continued)

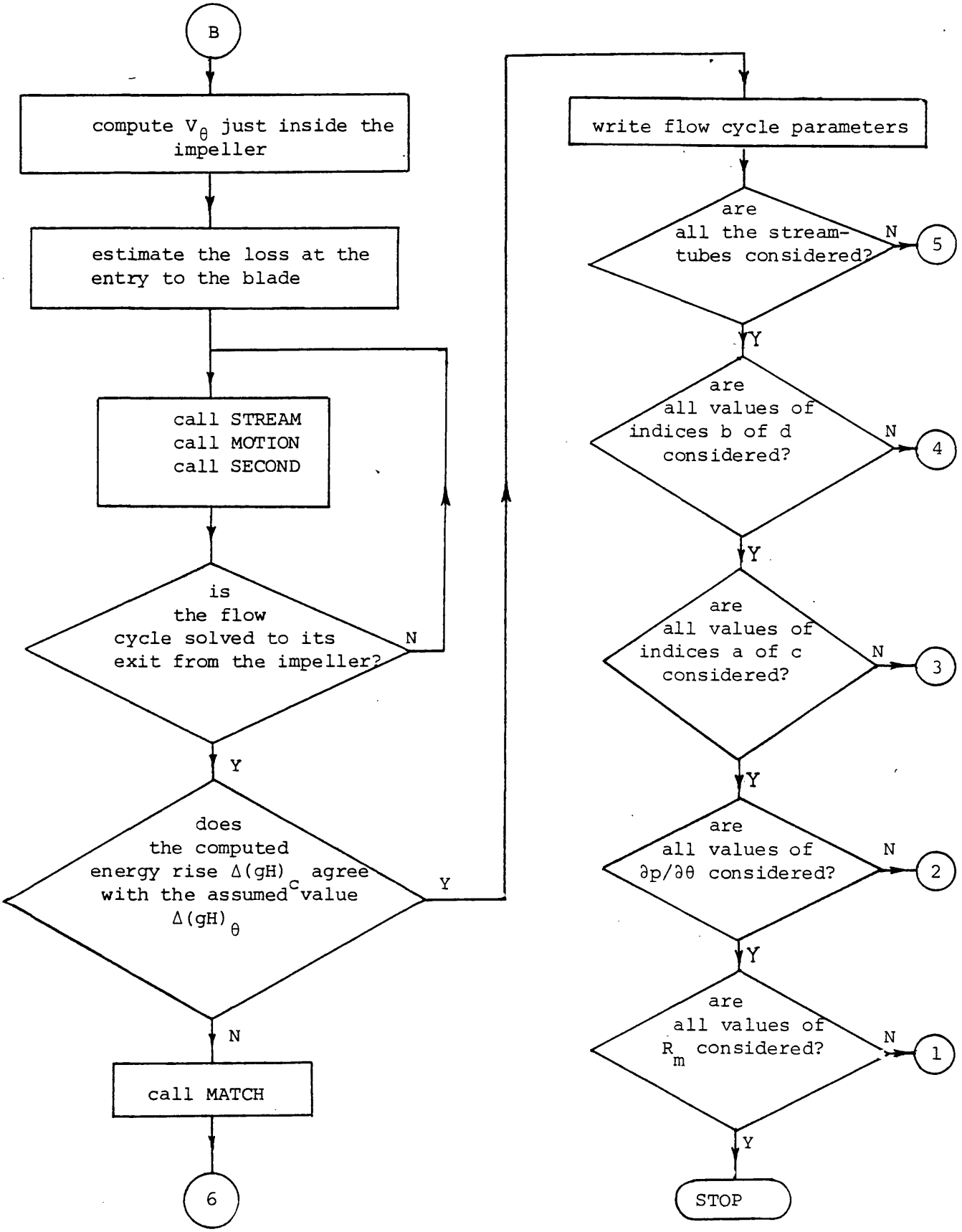

Fig. (5.10): General flow diagram for program REGEF

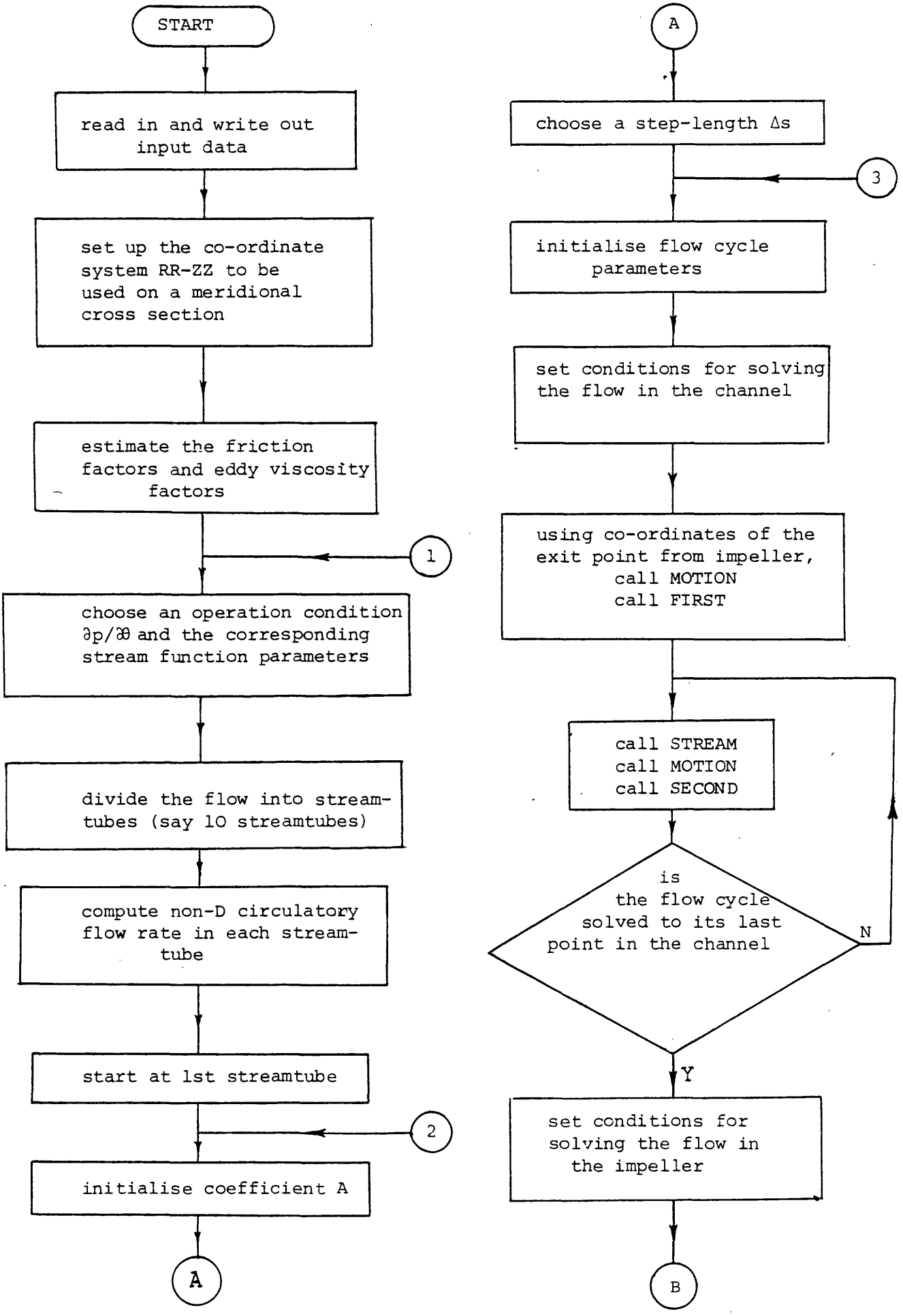

Fig. (5.11): General flow diagram for program CHARA (Continued)

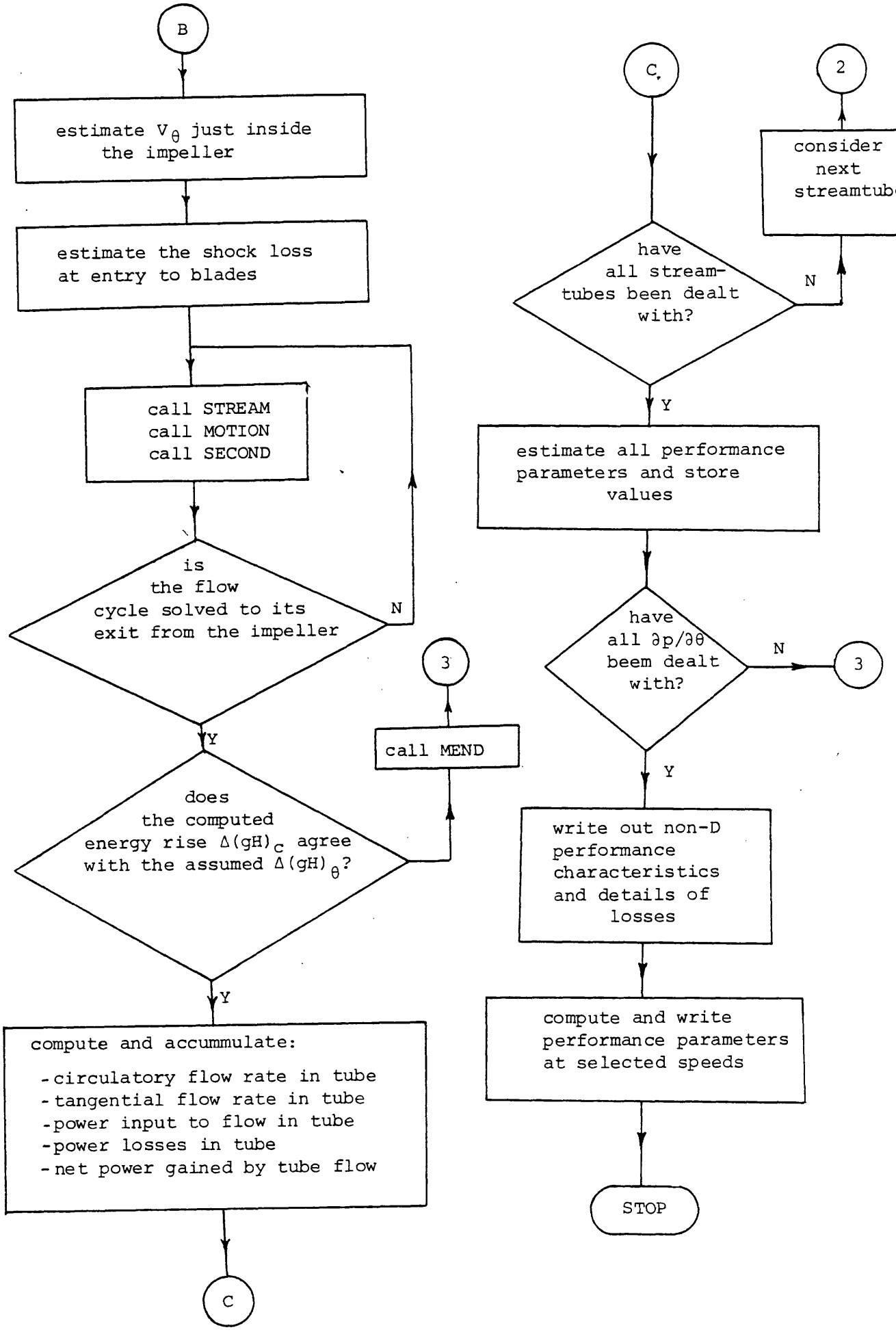

Fig. (5.11): General flow diagram for program CHARA

6. RESULTS AND DISCUSSIONS

The method described in the foregoing has been used to investigate the flow in pumps of different configurations and samples of the computed results are presented in this chapter.

First the main features of the meridional circulatory motion are discussed. These include the position of the centre, shape of profile and intensity of the circulatory motion and the manner in which these vary with the tangential pressure gradient in the pumping passage. Following this, estimates of parameters of the flow in the linear section are presented and discussed. The computed details include the absolute tangential velocity distributions in the channel and the three sources of loss: the skin friction losses in the blade passages and in the channel and the incidence losses at entry to the impeller blading. The performance characteristics are then presented in the usual way as graphs of non-dimensional parameters based on the rotational speed of 1000 rev/min, the effects of Reynolds number and compressibility being assumed negligible. Results are compared with available experimental equivalents and thence the effects of enhanced friction coefficients and slip factor are examined. Samples of computer printouts of results are included when appropriate.

6.1 Configurations Investigated

The application of the procedure described in this work requires design information about the pump to be known. This includes

a) the geometry, dimensions and number of the impeller blades

b) the dimensions of the channel and

c) the circumferential length of the active pumping section and that of the stripper seal.

These are required to calculate the internal performance. In addition to these, the port loss-coefficient has to be known so that the overall performance characteristics can be estimated and experimental results are of course needed for comparison.

Available source of data

Although a considerable amount of experimental data have been published by various investigators, most of these have been of the overall performance type. Results for the performance of the effective pumping section treated separately are meagre. An available work in which experimental results for the internal performance have been reported is that of Wilson et al (7). The experimental head-flow rate characteristic of the pumping passage was given for various configurations in that work. The other published experimental results known to the present author have been presented without specifying the internal performance separately from that of the ports; and in some cases even without specifying some of the design parameters required for the present approach. Due to the lack of a convincing method for estimating the port losses, it is to be expected that the overall performance can be predicted with only reasonable accuracy at present and Wilson's work therefore seems to be the most appropriate source of data available at this time for testing the results of the present calculations.

The experimental unit built and tested by the M.I.T. Group (7) was a larger scale model of a commercial unit known as STA-RITE TH-7 pump. They designed the unit so that various configurations of the channel could be obtained by the use of a variety of inserts with the same impeller and they reported the experimental head-flow rate characteristics of the configurations (1) to (6) listed in Table (6.1), the original model itself being referred to in that Table as configuration (0).

Assumed parameters

Some design parameters which were not given in ref. (7) have had to be assumed in the present calculations. A stripper clearance of 0.5 mm has been assumed for both the axial and radial clearances. A blade number of 44 has been assumed and the blade thickness has been assumed to vary linearly from zero at the edges to a maximum at the root accordingly to equation (B.4) of Appendix B. The thickness at the root has been taken to be 20% of the circumferential distance between two adjacent blades at the inner radius. The capacity of the inter-blade spaces to carry fluid through the stripper seal has been estimated by subtracting the volumes occupied by the blades themselves

and the various fillet radii included during the manufacturing process. This approach gave the volume of the blade pockets as 80% of that which it would be if such fillet radii were not present.

The results to be presented

The flows have been investigated at an impeller rotational speed of 1000 rev/min using the equations already derived or selected from the literature and discussed in the previous chapters. In the following, samples of the results of the computations of the flow in configuration (1) are discussed. This configuration is chosen because calculations in this case have progressed further than the rest. Although quantitatively these describe the flow in configuration (1), qualitatively they may be taken to represent all the hitherto identified major features of the flows in the other configurations investigated. Table (6.2) gives part of the information used in the calculations. Tables (6.3) to (6.6) show computer printouts of part of the results to be discussed in the following.

As mentioned in Chapter 3 the slip factor is initially taken to be a constant at a value consistent with normal practice. However, following presentation of these results together with a brief resume of the method used to obtain them, other bases of calculation are discussed.

6.2 Streamfunction and Centre of Circulation

The procedure for determing the appropriate streamfunction parameters and the position of the meridional circulation at a particular pressure gradient in the pumping passage has been described in Chapter 4. Choosing a value for the non-dimensional radius of circulation R'_m (= $(R_m - R_i)/(R_o - R_i)$), the degree of variation of the streamfunction coefficient has been plotted against the index a (= c) for various values of pressure rise as shown in Figs. (6.1) to (6.6). Each of these figures shows results obtained using a different value of the radius R'_m. In order to establish the values of the three unknown quantities R_m, A and a the flow has been divided into 10 streamtubes, and compatability conditions imposed along streamtubes 1, 5 and 9 only. As has been established in Chapter 4, the indices b and d have been taken to be equal to unity throughout. Various values of the index a (= c) have then been used and the corresponding

values of the coefficeint A have been determined for the representative three streamlines. The variation of the magnitude of the coefficient A across the flow is assumed to be measured by dividing the coefficient for streamline 1 by those of streamline 5 and 9. For each of the pressure gradients considered in any of the Figs. (6.1) to (6.6), two curve are therefore plotted: a curve showing the variation of the ratio A_1/A_5 against the index 'a', and a curve of the ratio A_1/A_9 against 'a'. The view is that when $A_1/A_5 = A_1/A_9 = 1.0$, the streamfunction coefficient can be assumed to be constant across the whole flow.

Referring to Figs. (6.1) to (6.6) it can be seen that for any of the pressure gradients the minimum variation of the coefficient A across the flow (the best matching) is obtained at the value of 'a' corresponding to $A_1/A_9 = 1.0$. At the corresponding value of a the degree of mismatching is given by the difference between the value of A_1/A_5 and unity. With $A_1/A_9 = 1.0$ it can be seen that the degree of mismatching measured by A_1/A_5 varies with the value of R'_m.

In Fig. (6.7) the degree of mismatching, (i.e. the ratio A_1/A_5 at $A_1/A_9 = 1.0$) is shown plotted against R'_m for various values of pressure rise. Since the entire solution is based on the assumption that the coefficient A is constant, the value of R'_m at which $A_1/A_5 = 1.0$ should be the centre of the meridional circulation at the particular pressure gradient. The relationship $\psi = \psi(R'_m)$ obtained by this procedure has been plotted in Fig. (6.9).

The streamfunction index 'a' corresponding to the ratio $A_1/A_9 = 1.0$ in Fig. (6.1) to (6.6) has been plotted against R'_m in Fig. (6.8) for various pressure gradients. Superimposed on these are plotted points corresponding to the appropriate values of R'_m for the different pressure rises obtained from Fig. (6.7). Thus the curve $a = a(R'_m)$ in Fig. (6.8) is obtained. Transferring the intersections of this curve with the curves ψ = constant to Fig. (6.9), the curve $\psi = \psi(a)$ is obtained.

Pressure rise - streamfunction relationship

Using values of the pressure rise ψ and the corresponding values of the radius R'_m and the index 'a' from Fig. (6.9), the corresponding values of the streamfunction coefficient A have been determined using

a version of Program REGEF. The corresponding non-dimensional values of the coefficient, i.e. $A' = A/\omega D^3$, have been plotted in the same figure, Fig. (6.9), as $\psi = \psi(A')$. This figure therefore gives a summary of the optimised streamfunction parameters A, a, and the radius of the meridional circulation R'_m which best represent the flow field at various pressure rises ψ across the pumping passage.

Pressure rise - centre of circulation relationship

Referring to Fig. (6.9), the position of the centre of the meridional circulation seems to vary with the pressure gradient in the linear section. It appears to shift slightly inwards (towards the axis of the machine) with the increase in the pressure gradient, from about $R'_m = 0.69$ at $\psi = 0.2$ to about $R'_m = 0.66$ at $\psi = 1.2$. Although there is no concrete theoretical explanation which can be given at present for this phenomenon, and indeed there is as yet no experimental proof or disproof of it, the following speculation may be made.

At high pressure gradients the intensity of the meridional circulation is stronger. This can be seen from Fig. (6.9) as the intensity of circulation is proportional to the coefficient A. On the other hand the tangential motion in the channel is of course weaker at high pressures. This means that at higher pressure gradients the circulatory motion is more able to overcome the centrifugal effect on it in the channel arising from its weaker tangential velocity. This may cause the position of the centre of meridional circulation to move slightly inwards in comparison to its position when the circulation is weaker and the tangential motion in the channel is stronger. The latter condition corresponds to low pressure gradients.

6.3 Meridional Velocity Distribution

It has been shown in Chapter 4, with the help of Figs. (4.11) to (4.18) that the shape of the profile of the meridional velocity is determined by the values of the indices a, b, c and d. Referring to Fig. (6.9) it can therefore be seen that the shape of the profile changes with the pressure rise across the pumping passage. An example is that the value of the index a varies from about 1.76 at $\psi = 1.2$ to about 1.86 at $\psi = 0.2$. Fig. (6.10) shows graphically the two velocity profiles at these two pressure rises. The profile seems to be more nearly

linear at low pressure gradients and more parabolic at high pressure gradients.

Intensity of meridional circulation

Referring to Fig. (6.9), the curve $\psi = \psi(A')$ shows that the intensity of circulation increases with the increase of the pressure gradient. The intensity, which is measured by the magnitude of the coefficient A, varies with the pressure rise ψ across the pumping section in a manner which may be expressed by the following general relationship:

$$\psi = k_1 + k_2 A^n \qquad (6.1)$$

where k_1, k_2 and n are expected to be functions of the friction losses and the rotor blading slip factor. In the absence of the friction forces no circulation is expected to take place when the pressure gradient is zero. In such ideal situation k_1 must be zero. However, in real situations even at zero pressure gradient some energy is still required to be imparted to the fluid to balance the frictional losses. Thus, even at zero pressure gradient there must still be circulatory flow and energy transfer. The curve $\psi = \psi(A')$ of Fig. (6.9) therefore intersect the axis $\psi = 0$ at a finite positive value of the coefficient A. It can be seen from the figure that the higher the pressure gradient, the faster is the circulatory motion. This means that the fluid has to spin faster and hence pass through more flow cycles at higher pressure gradients than at low pressure gradients. This is expected because the total head gained by a fluid particle in the linear section must be related to the number of times it passes through the impeller.

6.4 Tangential Velocity Distribution

An estimate of the tangential velocity distribution in the channel can be used

a) in designing the blade inlet angles so that the incidence losses may be reduced

b) to compute the head rise across the impeller and

c) to calculate the flow rate.

Fig. (6.11) shows typical plots of the tangential velocity V_θ against the angular displacement θ along streamlines in the channel for different pressure gradients; while Fig. (6.12) shows V_θ plotted against the absolute distance travelled in the channel along various streamlines. From these it can be seen that the variation of V_θ along a streamline depends on the tangential pressure gradient in the pumping passage as well as the meridional location of the streamline.

It is obvious that the fluid angular momentum is more rapidly reduced in a high pressure gradient than in a low pressure gradient. It means that the flow angular displacements in the channel θ_c are smaller at high pressures than at low ones. This is in line with the finding reported in section (6.3) that more flow cycles are executed at higher pressure gradients than at lower ones.

On the other a fluid particle following an outer streamline travels a longer distance in one flow cycle than one following an inner path. The motion is against both the friction forces and the tangential pressure gradient. At higher pressure gradients therefore reversals in the direction of the tangential velocity of the flow along outer streamlines do occur between the tip and root of the impeller as shown in Figs. (6.11) and (6.12). This characteristic of the internal flow, which was observed experimentally by Lazo and Hopkins (5). explains the large magnitude of the blade entrance losses at low flow rates, see next sections. It may be possible to reduce these losses if the blade inlet angles are designed in accordance with the distribution of the tangential velocity along the inlet edge of the blade. From these results it may be expected that a proper design of the blades should consider the use of blade inlet angles varying with radius.

Total tangential displacements

Referring to Fig. (6.13), the net tangential displacement $_n$ per flow cycle is shown plotted against the tangential pressure gradient. Like the angular throw $_c$ in the channel, $_n$ can be seen to vary in an inverse manner with the pressure gradient and it also varies from one streamline to the next at the same pressure gradient. The tangential displacements in the impeller and in the channel are shown in more detail in Fig. (6.14) at a typical pressure gradient.

The figure shows developed trajectories of streamlines, each has been started at the same meridional section and followed through a complete flow cycle.

6.5 Overall Performance

The relationship between the pressure gradient and the streamfunction parameters summarised in Fig. (6.9) has been used in program CHARA, see Chapter 5, to compute the overall performance. Part of the results are shown in Tables (6.3) to (6.6). In Table (6.3) a summary of typical computed flow details along streamlines are given at one operating condition. The overall non-dimensional performance results are given in Table (6.4) and the corresponding estimates of the distribution of losses are given in Table (6.5). As an example the performance expressed in absolute terms is given in Table (6.6) for a rotational speed of 800 rev/min.

The computed losses and the internal head-flow rate characteristic are now discussed in turn.

6.5.1 Losses in the linear section

When this work was started, it was thought that the dominant source of loss in the pumping passage would be associated with the high incidence loss arising out of the total lack of guidance of the flow approaching the blades from the channel. However, now that detailed calculations have been carried out, the results seem to support this only at high pressure gradients, see Table (6.5) and Fig. (6.15). In these the same computed distribution of losses is given as percentages of the various sources of loss referred to the toal energy input to the fluid. At low pressure gradients losses in the channel seem to be the major losses in the linear section.

Losses at entry to blades

As has been shown in the previous section, at high pressure gradients reversals of the flow occur in parts of the channel. This causes higher relative tangential velocity at entry to blades than is the case at low pressure gradients, see Fig. (6.16). This figure shows computed relative tangential velocity at entry to blades plotted against pressure rise for various streamlines. It can be seen that

at high pressure rises, the flow appears to approach the blades with a negative relative velocity throughout the working range. This is to be expected because the flow in leaving the impeller and re-entering it suffers from

a) the slip effect

b) the frictional losses in the channel and

c) the exchange of its tangential velocity for a pressure rise.

It can be seen from the same figure that along outer streamlines at high pressure rises the flow approaches the blades with a negative relative tangential velocity greater in magnitude than that of the blade tip. On the other extreme, at zero pressure gradient condition only slip and friction effects act on the flow and these can be seen from the figure to have resulted in W_θ/U_2 of about -0.4.

Losses in channel

Even though the intensity of the circulatory motion is greater at high pressure gradients than at low ones, the total velocity in the channel is greater at lower pressure gradients than at higher ones. This is because the magnitude of the meridional velocity is small compared with the tangential velocity, see Table (6.3). This explains the trend in Fig. (6.15) of losses in the channel increasing as the pressure rise drops.

Losses in blade passages

Referring to Fig. (6.15), these appear to be significant losses and seem to constitute almost a constant proportion of the energy input to the fluid. Being proportional to the square of the relative velocity, which is essentially the meridional velocity in a radially bladed machine, their magnitude is greater at higher pressure gradients than at lower ones. However, the impeller power decreases too at the latter conditions.

6.5.2 Other losses

These include the port, carry-over and leakage losses, see Table (6.5) and Fig. (6.15).

As expected, the port losses are shown to be considerable at low pressure gradients since they have been assumed to depend on through-flow rate.

The carry-over losses have been estimated assuming zero efficiency of recovery of the energy of the fluid trapped in the blade pockets and carried through the stripper to the inlet port region. Thus it is natural that estimates of these losses increase with the increase of the energy imparted to the fluid in the linear section, the pocket volume and the fluid density being the same.

The leakage losses seem to be generally of small magnitude except at high pressure gradients where they can be considered as significant.

6.5.3. Internal head-flow rate characteristic

The computed overall performance characteristics are shown in Table (6.4) These are obtained using default values of slip factor and friction level. The internal head-flow rate characteristic is shown plotted in Fig. (6.17) together with the experimental equivalent obtained from ref. (7). It can be seen that the predicted curve (1) is too steep to be described as an adequate representation of the experimental results The flow rate has been increasingly over-estimated as the tangential pressure gradient increased. Even at zero head across the pump (equivalent to about $\psi_{\ell} = 0.2$ across the linear section) at which the prediction is nearest to the experimental value, the flow rate has been slightly over estimated.

The following elements used in the calculations have been questioned:

1) the magnitude of the friction factors
2) the length of the effective pumping passage
3) the applicability of the conventional model used to estimate the effect of slip.

The results of the investigation of these factors are now discussed in turn.

6.6 Effect of Increased Friction Levels

The effect of friction has been accounted for using the concept of hydraulic diameter, as described in Chapter 2. The values of the friction coefficients, used to estimate the friction losses in the blade passages and in the channel, and the value of the average eddy viscosity have all been determined in terms of values of the hydraulic diameter. Since the effect of streamtube curvature could not be simply described and accounted for when determining the values of the hydraulic diameter, it was felt that the latter could have been over-estimated and the resulting friction factors were thus under-estimated.

To investigate the effect of increased friction, the default values of the hydraulic diameters were reduced arbitrarily by factors of 2, 4 and 6 (beyond that, friction losses became too large for any positive head to be maintained across the linear section). For example a reduction of the hydraulic diameter default value by a factor of 4 resulted in an increase of the friction coefficient for the channel flow from about 0.007 to 0.012 and that for the impeller flow from about 0.0098 to 0.013. Using these increased friction factors, the previous calculation were repeated and the most important effects were found to be:

a) the intensity of themeridional circulatory motion increased as the friction effect was increased. The flow made more flow cycles to sustain a pressure gradient when the friction levels increased.

b) all the losses in the linear section increased with the increase in friction as expected. The consequence of this is that the tangential velocity in the channel decreased with increased frictions. However, the magnitude of the reduction in the tangential velocity was found to be almost the same at all pressure gradients. Thus the corresponding predicted head-flow rate characteristics, curve 2 in Fig. (6.17), has been found to be simply a curve almost parallel to that resulting from the use of the default value of the friction factors, see Fig. (6.17): the characteristic can be seen to be as steep as before and with a further snag of an under-estimated zero-head flow rate.

It seems that whatever enhanced friction factors are used, they cause closely similar effects at all pressure gradients.

Thus it appears that the influence of friction is not responsible for the too steep nature of the predicted Head-Flow rate characteristics. Therefore the default values of the friction factors have been used in the rest of this work.

6.7 Variable Length of Pumping Passage

It has been mentioned in section (3.4) that experimental results published by various investigators indicate that the length of the effective pumping passage varies with the tangential gradient of pressure. Some results suggest that it decreases with the increase of the pressure rise, see ref. (7). However, results due to Senoo (1) seem to suggest that it increases with the increase in the pressure rise.

The length of the effective passage is obviously not involved in the computation of the pump flow rate as mentioned in chapter 3. However, it is directly used to compute the total flow rate through the impeller (to be distinguished from the pump flow rate) and consequently its choice determines the value of the computed head across the pumping passage, other parameters being fixed.

Since the head-flow rate characteristic predicted using a constant length of the pumping passage has been found to be too steep, it is obvious that the use of an effective passage length decreasing with the rise in pressure should pull the default characteristic towards the experimental results. The use of an effective passage length increasing with the pressure rise certainly results in an even more steep characteristic. In order to test the influence of reducing the effective passage, the following linear relation has been used:

$$\theta_p = \theta'_p - 0.25(\psi - 0.2) \qquad (6.2)$$

where:

θ_p = effective pumping passage angle

θ'_p = effective passage angle at the lowest pressure rise used in the computations (i.e. $\psi = 0.2$)

The corresponding predicted characteristics are summarised in Tables (6.7) and (6.8). The internal Head-Flow rate characteristic in this case is shown as curve 3 in Fig. (6.17). The effect of using the arbitrarily selected relationship of equation (6.2) tilted the predicted curve considerably towards the experimental results as can be seen from comparing curve 3 with curve 1 for which θ_p was taken constant.

This means that the way in which the length of the pumping passage varies with the tangential gradient of pressure must be known before a reliable prediction of the overall performance can be made.

6.8 Effect of Slip

The methods in the literature for the assessment of the effect of slip, see refs. (34 and (35), have been developed for cases where there is essentially no tangential energy gradient. Yet it has been shown in ref. (35) that the slip factor is one of the vital items of design information because of its direct effect on the energy transfer. Since this is the case when $\partial H/\partial\theta \simeq 0$, then it can be expected that the slip effect is even more vital in regenerative machines whose very purpose is to develop tangential pressure gradients.

6.8.1 Increased slip level

For the configruations investigated in this work the conventional slip model used gives a value of 0.96 for the slip facotr, the latter being defined by equation (4.7). In order to investigate the effect of increasing the slip effect, an arbitrary value of 0.8 was used and the corresponding results obtained indicate some major differences regarding various aspects of the flow in comparison with those obtained earlier at a slip factor of 0.96. These differences are now discussed.

a) Internal flow details

The procedure of establishing the optimum relationship between the pressure gradient in the linear section and the streamfunction parameters has produced the results which are summarised in Figs. (6.18) to (6.20). Referring to Fig. (6.18), it can be seen that the curve $\psi = 1.0$ lies below the matching condition line of $A_1/A_5 = 1.0$

at all tested values of the radius of the centre of the meridional circulation. One interpretation of this result is that the representation of the flow by the streamfunction at such a high pressure gradient may be inadequate and therefore the condition that $A_1/A_5 = A_1/A_9 = 1.0$ is not satisfied. Alternatively, this result can be interpreted as showing that such high pressure cannot be sustained if the slip effect is as high as represented by the value used.

The relationships between the pressure gradient and the streamfunction parameters are summarised in Fig. (6.20). Comparsing these with those in Fig. (6.9), it can be seen that the increase of the slip effect has resulted in the following:

1) The centre of the meridional circulation has been moved inwards. i.e. corresponding to any particular pressure rise the radius R'_m has been greatly reduced.

2) The shape of the profile of the meridional velocity has become more nearly linear than before. This can be seen from the increased values of the index a at all pressure gradients.

3) The intensity of the meridional circulation has been reduced, though not significantly, as can be seen from a comparison of the curves $\psi = \psi\ (A')$ in the two figures.

b) Overall performance

The relationships shown in Fig. (6.20) have been used to compute the overall performance characteristics. The corresponding results are shown in Tables (6.9) and (6.10). From Table (6.9) the internal head-flow rate characteristic has been plotted in Fig. (6.17) as curve 4. Comparing this characteristic with curve 1 it can be seen that the decrease of the value of the slip factor from 0.96 to 0.8 has resulted in two major effects:

1) The computed flow rate has been considerably lowered at all the operating points considered.

2) The reduction effected in the magnitude of the calculated flow rate has been such that the resulting characteristic is less steep than curve 1.

Although curve 4 is still too steep to be described as an adequate representation of the experimental results, the consequence of the above two effects is that the value of the slip factor is of vital importance in these calculations and its choice greatly determines the outcome of the prediction. For example, referring to curves 1 and 4 of Fig. (6.17), it can be seen that at a pressure rise of 1.2, the decrease of the slip factor from 0.96 to 0.8 has resulted in more than 50% reduction in the computed flow rate.

However, it can be seen in Fig. (6.17) that although decreasing the value of the slip factor has reduced, and thus somewhat corrected, the otherwise greatly over-estimated flow rate at high pressure gradients, it has resulted in increasingly under-estimated flow rate as the reference zero-pressure rise is approached. This means that a more accurate prediction can be expected if the slip factor is appropriately chosen to decrease with the increase of the tangential gradient of pressure. In section (6.8.3) it will be shown that the slip effect should increase with the tangential gradient of pressure.

6.8.2 Increased slip and variable pumping passage

Tables (6.11) to (6.12) show the overall performance parameters computed using a slip factor of 0.8 while the length of the effective pumping passage has been varied according to equation (6.2). The internal head-flow rate characteristic is shown as curve 5 in Fig. (6.17). On the average, this curve appears to be the closest approximation of the experimental results in that figure. However, the more important implication of this result is that while at high pressure rises the flow rate has still been over-estimated, at low pressure rises it has been increasingly under-estimated as the zero-pressure rise is approached. The latter effect seems to be a consequence of using a too low value of the slip factor at these low pressure rise conditions as mentioned earlier.

From these results it can be expected that the use of a variable slip factor of 0.96 at $\psi = 0.2$ and 0.8 at $\psi = 1.0$ should result in a characteristic which coincides with curve 1 at $\psi = 0.2$ and with curve 5 at $\psi = 0.5$. Compared with the experimental result, such a characteristic would reasonably represent the experimental trend throughout the operating range.

It will be of considerable significance to the approach developed in this work to show that the slip effect increases with the tangential gradient of pressure.

6.8.3 Variable slip factor

One of the bases upon which some conventional models of slip factor have been formulated is the expression for the axial vorticity in the blade passage. This has been derived for a general case in Appendix (A) and the result of interest here is that given by equation (A.52), i.e.:

$$\xi_{Z2} = -2\omega \left(1 + 2 \frac{\omega r_2}{W_{r2}} \frac{\psi}{\theta_p}\right) \tag{6.3}$$

where:

ξ_{Z2} = axial vorticity or relative eddy of fluid at exit from impeller.

$\frac{\omega r_2}{W_{r2}}$ = ratio of impeller speed to the relative radial velocity of fluid at exit from impeller.

$\frac{\psi}{\theta_p}$ = non-dimensional tangential pressure gradient.

The bracketed term of equation (6.3) is simply equal to unity when there is no tangential pressure gradient. However, its value is certainly greater than unity for regenerative machines. To examine the order or magnitude of this term, results computed using the default value of the conventional slip factor of equation (4.8) (slip factor = 0.96) have been used. Referring to Fig. (6.21), the bracketed term of equation (6.3) is shown plotted against the pressure rise across the linear section. Since at a particular operating point the value of r_2/W_{r2} depends on the exit location of the particular streamline, the bracketed term has been evaluated and plotted for three streamlines, at the exit of each of which W_r is greater than zero, i.e. the flow has a radial component. From these results it can be seen that the slip effect is significantly increased by the presence of a tangential pressure gradient. This means that in regenerative machines the slip factor should be viewed as a function of the tangential pressure gradient, i.e.

$$\sigma = f(\psi) \tag{6.4}$$

However, the appropriate form of the relationship may not be as simple as that of equation (6.3) because the latter is not complete: a term has been dropped from equation (A.50) of Appendix A to obtain it. It must also be mentioned that equation (A.50) itself has been obtained based on the assumptions that the flow is frictionless, steady and isentripic. This implies that a proper formulation of the relationship of equation (6.4) may require comprehensive measurements of the tangential velocity at impeller exit.

6.9 Summary

Samples of the computed results of the flow details and overall performance have been presented and discussed. The calculated details of the internal flow show that the intensity of the meridional circulation increases with the increase of the pressure rise across the pumping passage. The position of its centre and the shape of its profile are also shown to vary with the tangential gradient of pressure. The computed distributions of the tangential velocity show that in agreement with published experimental observations, reversals of flow occur in parts of the channel at high pressure gradients.

The internal head-flow rate characteristic predicted using default values of friction factors, a conventional slip factor and a constant length of the active pumping section has been found to be too steep compared to the experimental results: although the zero-head flow rate has been well predicted, the flow rate has been increasingly over-estimated as the pressure gradient increased. Investigations into this have led to the identification of the slip factor and the length of the pumping passage as the two items responsible for the slope of the characteristic.

Configuration No.	C mm	X_c mm	L_c mm	$\frac{C}{X_c}$	$\frac{C}{L_c}$	A_c cm^2	$\frac{A_c}{A_i}$
0 	4.6	7.8	26	0.59	0.17	2.3	1.8
1 	22.2	43.2	100	0.52	0.22	47.6	3.0
2 	9.3	43.2	94	0.22	0.1	39.4	2.5
3 	28.7	35.8	106	0.8	0.27	44.0	2.8
4 	15.7	26.9	94	0.59	0.17	28.3	1.8
5 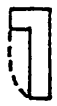	22.2	14.3	100	1.2	0.22	38.8	2.5
6 	9.3	19.3	87	0.48	0.11	18.7	1.2

Configuration (O): R_o = 69 mm
R_i = 47 mm
X_b = 6 mm

Configurations (1) - (6):

R_o = 240 mm
R_i = 162 mm
X_b = 20 mm

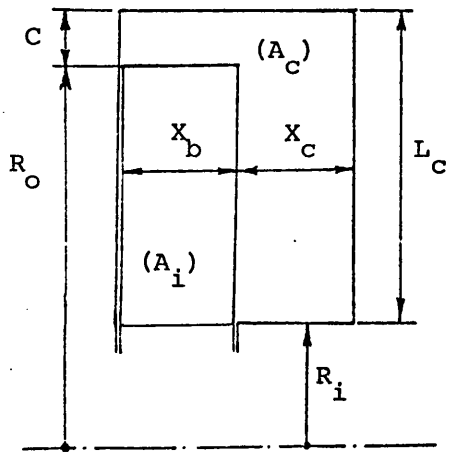

Table (6.1): Main dimensions of configurations tested by Wilson et al (7)

THEORETICAL PREDICTION OF PERFORMANCE PARAMETERS

OF REGENERATIVE PUMPS

A SAMPLE OF RESULTS OBTAINED USING ALGEBRAIC STREAMFUNCTION RELATIONSHIP

PUMP PARTICULARS :-

MANUFACTURER NAME OF PUMP	;	STA-RITE TH-7 PUMP
MODEL AND CLASS	;	WILSON MODEL CONF(1)
CHANNEL OUTER RADIUS	=0.262005	(M)
CHANNEL INNER RADIUS	=0.162050	(M)
IMPELLER OUTER RADIUS	=0.239780	(M)
IMPELLER INNER RADIUS	=0.162050	(M)
AVERAGE BLADE WIDTH	=0.020193	(M)
AVERAGE SIDE CHANNEL WIDTH	=0.043180	(M)
AVERAGE BLADE THICKNESS	=0.002314	(M)
AVERAGE DISK-CASING CLEARANCE	=0.001000	(M)
NUMBER OF IMPELLER BLADES	= 44	
EFFECTIVE WORKING SECTION OF PUMP	= 305	DEG
AVERAGE RADIAL DEVIATION OF BLADE	= 0	DEG
AVERAGE BLADE ANGLE	= 0	DEG

DIMENSIONS OF CHANNEL-IMPELLER MERIDIONAL X-SECTION:
RATIO OF MERIDIONAL SECTION WIDTH TO HEIGHT=0.634
RATIO OF PERIPHERAL-CHANNEL DEPTH TO IMP.HT=0.286
RATIO OF SIDE-CHANNEL WIDTH TO IMP.WIDTH =2.138

Table (6.2): Summary of design information used in computations

```
(A) SOLUTION OF FLOWS ALONG STREAMLINES FOR THE
    PREDICTION OF THE PERFORMANCE PARAMETERS

LAYOUT OF STREAMLINES :-
     STREAMFUNCTION: PSI=A*(1.0-RR**REX)**RN*(1.0-ZZ**ZEX)**ZN
       6 STREAMLINES ARE CHOSEN FOR ANALYSIS
     STREAMLINES ARE NUMBERED FROM THE WALL INWARDS
     THEIR STREAMFUNCTION VALUES ,PSI=CONST., ARE GIVEN
     THE MAIN COORDINATES (RR,ZZ) OF THEIR PROJECTION
     ONTO A MERIDIONAL PLANE ARE GIVEN IN BRACKETS AND
     REFERED TO AXESE RR: THROUGH CENTRE OF CIRCULATION
                      ZZ: ALONG BOTTOM OF THE CHANNEL

MEAN FRICTION FACTORS:-
     FRICTION FACTOR FOR CHANNEL MERIDIONAL FLOW=0.0060
     FRICTION FACTOR FOR CHANNEL TANGENTIAL FLOW=0.0075
     FRICTION FACTOR FOR IMPELLER FLOW          =0.0098


OPERATION CONDITIONS AT TEST POINT ( 1) :-

     NON-D HEAD ACROSS LINEAR SECTION   =    0.90
     NON-D HEAD GRADIENT IN L. SECTION  =    0.22 (1/RAD)
     ABSOLUTE HEAD ACROSS LINEAR SECTION=    0.09 (M)
     TANGENTIAL HEAD GRADIENT IN L.S.   =    0.02 (M/RAD)
     IMPELLER ANGULAR SPEED             =  104.72 (RAD/S)
     BLADE SPEED AT OUTER RADIUS (U2)   =   25.11 (M/S)

STREAMFUNCTION INDICES :-
     RN     = 1.000
     ZN     = 1.000
     REX    = 1.760
     ZEX    = 1.760
     RNN    = 0.660


     STREAMLINES CHOSEN AT EQUAL INCREMENTS OF RADIUS
     NON-D RADIAL STEP = 0.16667

DISTRIBUTION OF CIRCULATORY FLOW :-
     NON-DIMENSIONAL CIRCULATORY VOLUME FLOW RATE
     THROUGH STREAMTUBES PER UNIT ANGLE:

     STREAMTUBE NO     INNER-RADIUS     QQ-CIR
                1         0.833         0.274
                2         0.667         0.236
                3         0.500         0.195
                4         0.333         0.151
                5         0.167         0.102
                6         0.000         0.043
```

Table (6.3): Typical summary of flow details along particular streamlines (continued)

STREAMLINE NO (1) :-

ITS NON-D STREAMFUNCTION VALUE =0.1420
(0.972, 0.000)(0.660, 0.396)(0.055, 0.000)(0.660,-0.185)

(I) PARAMETERS OBTAINED FOLLOWING THE STREAMLINE THROUGH ONE FLOW-CYCLE VIS. STREAMFUNCTION COEFFICIENT (AM) :-

AM	THEATA	SUMTR	ENACT	ENNET	HLOSTS	HLOSTI	HLOSTC	SUMTHP	SUMTHS	SUMTHI	EATAHI	VT.EX.CH.
0.105E-01	0.704E 00	0.704E 00	0.398E 03	0.398E 03	0.273E 03	0.153E 03	0.470E 02	0.130E 00	0.278E 00	0.295E 00	0.457E 00	-0.583E 01

(II) KEY NON-DIMENSIONAL VELOCITIES :

	VRR	VZZ	VTT	VHH	VTOTAL
AT OUTLET FROM IMPELLER :	1.37	0.08	0.96	1.37	1.67
AT OUTER INTERSECTION WITH THE R-AXIS:	0.00	0.90	0.72	0.90	1.15
AT INTERSECTION WITH (RC) IN CHANNEL :	-0.81	0.00	0.37	0.81	0.89
AT INLET TO IMPELLER :	0.00	-0.72	-0.23	0.72	0.76
AT INTERSECTION WITH (RC) IN IMPELLER:	1.76	0.00	0.95	1.76	2.00

STREAMLINE NO (2) :-

ITS NON-D STREAMFUNCTION VALUE =0.3973
(0.915, 0.000)(0.660, 0.324)(0.165, 0.000)(0.660,-0.152)

(I) PARAMETERS OBTAINED FOLLOWING THE STREAMLINE THROUGH ONE FLOW-CYCLE VIS. STREAMFUNCTION COEFFICIENT (AM) :-

AM	THEATA	SUMTR	ENACT	ENNET	HLOSTS	HLOSTI	HLOSTC	SUMTHP	SUMTHS	SUMTHI	EATAHI	VT.EX.CH.
0.105E-01	0.728E 00	0.728E 00	0.412E 03	0.412E 03	0.145E 03	0.107E 03	0.512E 02	0.914E-01	0.382E 00	0.254E 00	0.576E 00	0.164E 01

(II) KEY NON-DIMENSIONAL VELOCITIES :

	VRR	VZZ	VTT	VHH	VTOTAL
AT OUTLET FROM IMPELLER :	1.13	0.22	0.96	1.15	1.49
AT OUTER INTERSECTION WITH THE R-AXIS:	0.00	0.79	0.79	0.79	1.12
AT INTERSECTION WITH (RC) IN CHANNEL :	-0.69	0.00	0.52	0.69	0.87
AT INLET TO IMPELLER :	0.00	-0.58	0.07	0.58	0.58
AT INTERSECTION WITH (RC) IN IMPELLER:	1.50	0.00	0.95	1.50	1.78

STREAMLINE NO (3) :-

ITS NON-D STREAMFUNCTION VALUE =0.6127
(0.858, 0.000)(0.660, 0.252)(0.275, 0.000)(0.660,-0.118)

(I) PARAMETERS OBTAINED FOLLOWING THE STREAMLINE THROUGH ONE FLOW-CYCLE VIS. STREAMFUNCTION COEFFICIENT (AM) :-

AM	THEATA	SUMTR	ENACT	ENNET	HLOSTS	HLOSTI	HLOSTC	SUMTHP	SUMTHS	SUMTHI	EATAHI	VT.EX.CH.
0.106E-01	0.702E 00	0.702E 00	0.398E 03	0.398E 03	0.993E 02	0.714E 02	0.542E 02	0.654E-01	0.399E 00	0.238E 00	0.639E 00	0.575E 01

(II) KEY NON-DIMENSIONAL VELOCITIES :

	VRR	VZZ	VTT	VHH	VTOTAL
AT OUTLET FROM IMPELLER :	0.86	0.34	0.96	0.92	1.33
AT OUTER INTERSECTION WITH THE R-AXIS:	0.00	0.68	0.84	0.68	1.08
AT INTERSECTION WITH (RC) IN CHANNEL :	-0.58	0.00	0.62	0.58	0.85
AT INLET TO IMPELLER :	0.00	-0.46	0.23	0.46	0.51
AT INTERSECTION WITH (RC) IN IMPELLER:	1.25	0.00	0.95	1.25	1.57

Table (6.3)

Table (6.3) - continued

STREAMLINE NO (4) :-

ITS NON-D STREAMFUNCTION VALUE =0.7858
(0.802, 0.000)(0.660, 0.130)(0.385, 0.000)(0.660,-0.084)

(I) PARAMETERS OBTAINED FOLLOWING THE STREAMLINE THROUGH ONE FLOW-CYCLE VIS. STREAMFUNCTION COEFFICIENT (AM) :-

AM	THETA	SUMTH	ENACT	ENMET	HLOSTS	HLOSTI	HLOSTC	SUMTHP	SUMTHS	SUMTHI	EATAHI	VT.EX.CH.
0.105E-01	0.679E 00	0.679E 00	0.385E 03	0.385E 03	0.809E 02	0.435E 02	0.563E 02	0.350E-01	0.402E 00	0.242E 00	0.681E 00	0.828E 01

(II) KEY NON-DIMENSIONAL VELOCITIES :

	VRR	VZZ	VTT	VMM	VTOTAL
AT OUTLET FROM IMPELLER :	0.47	0.43	0.96	0.64	1.15
AT OUTER INTERSECTION WITH THE R-AXIS:	0.00	0.53	0.90	0.53	1.05
AT INTERSECTION WITH (RC) IN CHANNEL :	-0.44	0.00	0.69	0.44	0.82
AT INLET TO IMPELLER :	0.00	-0.33	0.33	0.33	0.47
AT INTERSECTION WITH (RC) IN IMPELLER:	0.95	0.00	0.95	0.95	1.35

STREAMLINE NO (5) :-

ITS NON-D STREAMFUNCTION VALUE =0.9128
(0.745, 0.000)(0.660, 0.108)(0.405, 0.000)(0.660,-0.051)

(I) PARAMETERS OBTAINED FOLLOWING THE STREAMLINE THROUGH ONE FLOW-CYCLE VIS. STREAMFUNCTION COEFFICIENT (AM) :-

AM	THETA	SUMTH	ENACT	ENMET	HLOSTS	HLOSTI	HLOSTC	SUMTHP	SUMTHS	SUMTHI	EATAHI	VT.EX.CH.
0.106E-01	0.611E 00	0.611E 00	0.346E 03	0.346E 03	0.660E 02	0.229E 02	0.503E 02	0.000E 00	0.371E 00	0.239E 00	0.713E 00	0.107E 02

(II) KEY NON-DIMENSIONAL VELOCITIES :

	VRR	VZZ	VTT	VMM	VTOTAL
AT OUTLET FROM IMPELLER :	0.00	0.37	0.94	0.37	1.01
AT OUTER INTERSECTION WITH THE R-AXIS:	0.00	0.37	0.94	0.37	1.01
AT INTERSECTION WITH (RC) IN CHANNEL :	-0.30	0.00	0.75	0.30	0.81
AT INLET TO IMPELLER :	0.00	-0.22	0.42	0.22	0.48
AT INTERSECTION WITH (RC) IN IMPELLER:	0.66	0.00	0.95	0.66	1.16

STREAMLINE NO (6) :-

ITS NON-D STREAMFUNCTION VALUE =0.9874
(0.688, 0.000)(0.660, 0.036)(0.605, 0.000)(0.660,-0.017)

(I) PARAMETERS OBTAINED FOLLOWING THE STREAMLINE THROUGH ONE FLOW-CYCLE VIS. STREAMFUNCTION COEFFICIENT (AM) :-

AM	THETA	SUMTH	ENACT	ENMET	HLOSTS	HLOSTI	HLOSTC	SUMTHP	SUMTHS	SUMTHI	EATAHI	VT.EX.CH.
0.100E-01	0.495E 00	0.497E 00	0.282E 03	0.280E 03	0.661E 02	0.607E 01	0.409E 02	0.000E 00	0.302E 00	0.195E 00	0.712E 00	0.118E 02

(II) KEY NON-DIMENSIONAL VELOCITIES :

	VRR	VZZ	VTT	VMM	VTOTAL
AT OUTLET FROM IMPELLER :	0.00	0.16	0.92	0.16	0.93
AT OUTER INTERSECTION WITH THE R-AXIS:	0.00	0.16	0.92	0.16	0.93
AT INTERSECTION WITH (RC) IN CHANNEL :	-0.12	0.00	0.76	0.12	0.77
AT INLET TO IMPELLER :	0.00	-0.08	0.47	0.08	0.48
AT INTERSECTION WITH (RC) IN IMPELLER:	0.27	0.00	0.95	0.27	0.99

Table (6.3)

Table (6.3)

(B) PREDICTED NON-DIMENSIONAL PERFORMANCE PARAMETERS :-

FACTORS USED FOR NON-DIMENSIONALIZING ARE:-

DISCHARGE: OMEGA*DIA**3
POWER : ROH*OMEGA**3*DIA**5
HEAD : OMEGA**2*DIA**2/GEE

TEST POINT NO	INPUT HEAD HEAD ACROSS LINEAR SECTION ψ	$\partial\psi/\partial\theta$	PREDICTED NON-DIMENSIONAL PERFORMANCE PARAMETERS								
			HEAD ACROSS PUMP	FLOW RATE THRO L.S.	PUMP VOL. FLOW RATE	IMP. EFFY	VOL. EFFY	HYDRAULIC POWER	HYD. EFFY	SHAFT POWER	O/A EFFY
1	1.20	0.22	1.128	0.722E-02	0.427E-02	0.57	0.83	0.481E-02	0.318	0.154E-01	0.312
2	1.00	0.19	0.907	0.772E-02	0.483E-02	0.59	0.86	0.438E-02	0.334	0.134E-01	0.328
3	0.80	0.15	0.684	0.823E-02	0.541E-02	0.60	0.88	0.370E-02	0.338	0.112E-01	0.331
4	0.60	0.11	0.459	0.871E-02	0.597E-02	0.59	0.90	0.274E-02	0.309	0.905E-02	0.303
5	0.40	0.07	0.232	0.917E-02	0.653E-02	0.54	0.92	0.151E-02	0.221	0.697E-02	0.217
6	0.20	0.04	0.000	0.963E-02	0.711E-02	0.41	0.94	0.212E-05	0.000	0.485E-02	0.000

Table (6.4): Predicted overall performance results
(reference friction levels, slip factor = 0.96, effective pumping passage constant)

Table (6.4).

(C) ESTIMATION OF POWER LOSSES

TEST POINT NO	SHAFT POWER INPUT	% LOST IN MECH LOSSES*	POWER INPUT TO FLUID	% LOST IN SHOCKS	% LOST IN BLADE PASSAGES	% LOST IN CHANNEL	% LOST IN LEAKAGE	% LOST IN CARRY OVER	% LOST IN PORTS
1	0.154E-01	2.02	0.151E-01	22.08	13.25	7.47	6.71	16.67	2.03
2	0.134E-01	2.02	0.131E-01	18.37	13.52	9.28	5.97	16.03	3.40
3	0.112E-01	2.02	0.110E-01	14.05	13.73	12.12	5.21	15.36	5.73
4	0.905E-02	2.03	0.887E-02	10.40	13.89	16.83	4.28	14.22	9.50
5	0.697E-02	2.03	0.683E-02	7.27	14.00	25.03	3.16	12.32	16.09
6	0.485E-02	2.05	0.475E-02	4.53	13.99	40.70	1.76	8.89	30.01

* MECHANICAL LOSSES INCLUDE DISC FRICTION LOSSES
(2.0% OF SHAFT POWER ASSUMED LOST IN BEARINGS AND PACKINGS)

Table (6.5): Typical distribution of losses resulting from calculations
(reference friction levels, slip factor = 0.96, effective pumping length constant)

(D) PERFORMANCE PREDICTION AT SELECTED SPEEDS :-

FLUID MASS DENSITY = 0.100E 04 (KG/M**3)
FLUID KINEMATIC VISCOSITY = 0.100E-05 (M**2/S)

(1) AT IMPELLER ROTATIONAL SPEED = 800 (RPM)

TEST POINT NO	INPUT HEAD ACROSS LINEAR SECTION		PREDICTED ABSOLUTE PERFORMANCE PARAMETERS								
	H	∂H/∂θ	HEAD ACROSS PUMP	FLOW RATE THRO L.S.	PUMP VOL. FLOW RATE	IMP. EFFY	VOL. EFFY	HYDRAULIC POWER	HYD. EFFY	SHAFT POWER	O/A EFFY
1	197.62	37.00	185.756	0.667E-01	0.394E-01	0.57	0.83	0.718E 05	0.318	0.230E 06	0.312
2	164.65	30.83	149.452	0.713E-01	0.446E-01	0.59	0.86	0.654E 05	0.334	0.200E 06	0.328
3	131.76	24.67	112.667	0.760E-01	0.500E-01	0.60	0.88	0.552E 05	0.338	0.167E 06	0.331
4	98.78	18.50	75.551	0.805E-01	0.552E-01	0.59	0.90	0.409E 05	0.309	0.135E 06	0.303
5	65.88	12.34	38.144	0.847E-01	0.603E-01	0.54	0.92	0.225E 05	0.221	0.104E 06	0.217
6	33.02	6.18	0.049	0.890E-01	0.657E-01	0.41	0.94	0.317E 02	0.000	0.723E 05	0.000

Table (6.6): Absolute performance characteristics at 800 rev/min
(reference friction levels, slip factor = 0.96, effective passage constant)

(B) PREDICTED NON-DIMENSIONAL PERFORMANCE PARAMETERS :-

FACTORS USED FOR NON-DIMENSIONALIZING ARE:-

DISCHARGE: OMEGA*DIA**3
POWER : ROH*OMEGA**3*DIA**5
HEAD : OMEGA**2*DIA**2/GEE

TEST POINT NO	INPUT HEAD HEAD ACROSS LINEAR SECTION		PREDICTED NON-DIMENSIONAL PERFORMANCE PARAMETERS								
	ψ	$\partial\psi/\partial\theta$	HEAD ACROSS PUMP	FLOW RATE THRO L.S.	PUMP VOL. FLOW RATE	IMP. EFFY	VOL. EFFY	HYDRAULIC POWER	HYD. EFFY	SHAFT POWER	O/A EFFY
1	0.90	0.17	0.825	0.722E-02	0.436E-02	0.57	0.85	0.360E-02	0.317	0.116E-01	0.311
2	0.80	0.15	0.705	0.772E-02	0.490E-02	0.59	0.87	0.345E-02	0.329	0.107E-01	0.323
3	0.68	0.13	0.562	0.823E-02	0.546E-02	0.60	0.89	0.307E-02	0.330	0.950E-02	0.323
4	0.54	0.10	0.397	0.871E-02	0.600E-02	0.59	0.91	0.238E-02	0.299	0.815E-02	0.293
5	0.38	0.07	0.211	0.917E-02	0.654E-02	0.54	0.93	0.138E-02	0.213	0.662E-02	0.208
6	0.20	0.04	0.000	0.963E-02	0.711E-02	0.41	0.94	0.212E-05	0.000	0.485E-02	0.000

Table (6.7): Predicted overall performance results
(slip factor = 0.96, effective pumping length varying)

(C) ESTIMATION OF POWER LOSSES

TEST POINT NO	SHAFT POWER INPUT	% LOST IN MECH LOSSES*	POWER INPUT TO FLUID	% LOST IN SHOCKS	% LOST IN BLADE PASSAGES	% LOST IN CHANNEL	% LOST IN LEAKAGE	% LOST IN CARRY OVER	% LOST IN PORTS
1	0.116E-01	2.02	0.114E-01	22.08	13.25	7.47	5.94	16.67	2.90
2	0.107E-01	2.02	0.105E-01	18.37	13.52	9.28	5.43	16.03	4.44
3	0.950E-02	2.02	0.931E-02	14.05	13.73	12.12	4.87	15.36	6.92
4	0.815E-02	2.03	0.798E-02	10.40	13.89	16.83	4.10	14.22	10.69
5	0.662E-02	2.04	0.649E-02	7.27	14.00	25.03	3.09	12.32	17.03
6	0.485E-02	2.05	0.475E-02	4.53	13.99	40.78	1.76	8.89	30.01

* MECHANICAL LOSSES INCLUDE DISC FRICTION LOSSES
(2.0% OF SHAFT POWER ASSUMED LOST IN BEARINGS AND PACKINGS)

Table (6.8): Distribution of losses resulting from computations
(slip factor = 0.96, effective pumping length varying)

(B) PREDICTED NON-DIMENSIONAL PERFORMANCE PARAMETERS :-

FACTORS USED FOR NON-DIMENSIONALIZING ARE:-

DISCHARGE; OMEGA*DIA**3
POWER ; ROH*OMEGA**3*DIA**5
HEAD ; OMEGA**2*DIA**2/GEE

TEST POINT NO.	INPUT HEAD ACROSS LINEAR SECTION		PREDICTED NON-DIMENSIONAL PERFORMANCE PARAMETERS								
	ψ	$\partial\psi/\partial\theta$	HEAD ACROSS PUMP	FLOW RATE THRO L.S.	PUMP VOL. FLOW RATE	IMP. EFFY	VOL. EFFY	HYDRAULIC POWER	HYD. EFFY	SHAFT POWER	O/A EFFY
1	1.20	0.22	1.183	0.501E-02	0.206E-02	0.41	0.71	0.243E-02	0.167	0.149E-01	0.164
2	1.00	0.19	0.961	0.601E-02	0.312E-02	0.48	0.80	0.300E-02	0.240	0.127E-01	0.236
3	0.80	0.15	0.738	0.676E-02	0.395E-02	0.53	0.85	0.291E-02	0.284	0.105E-01	0.278
4	0.60	0.11	0.515	0.738E-02	0.465E-02	0.54	0.88	0.239E-02	0.293	0.833E-02	0.287
5	0.40	0.07	0.288	0.797E-02	0.532E-02	0.52	0.91	0.153E-02	0.252	0.622E-02	0.246

Table (6.9): Predicted overall performance results
(slip factor = 0.8, effective pumping length constant)

(C) ESTIMATION OF POWER LOSSES

TEST POINT NO	SHAFT POWER INPUT	% LOST IN MECH LOSSES*	POWER INPUT TO FLUID	% LOST IN SHOCKS	% LOST IN BLADE PASSAGES	% LOST IN CHANNEL	% LOST IN LEAKAGE	% LOST IN CARRY OVER	% LOST IN PORTS
1	0.149E-01	2.02	0.146E-01	40.40	13.91	4.50	6.96	17.30	0.24
2	0.127E-01	2.02	0.125E-01	30.75	16.04	5.11	6.26	16.83	0.97
3	0.105E-01	2.02	0.103E-01	23.03	17.50	6.77	5.55	16.39	2.37
4	0.833E-02	2.03	0.816E-02	17.61	18.52	9.59	4.66	15.47	4.86
5	0.622E-02	2.04	0.610E-02	12.41	19.74	15.57	3.54	13.80	9.79

* MECHANICAL LOSSES INCLUDE DISC FRICTION LOSSES
(2.0% OF SHAFT POWER ASSUMED LOST IN BEARINGS AND PACKINGS)

Table (6.10): Distribution of losses using slip facotr = 0.8
(effective pumping length constant)

(B) PREDICTED NON-DIMENSIONAL PERFORMANCE PARAMETERS :-

FACTORS USED FOR NON-DIMENSIONALIZING ARE:-

DISCHARGE: OMEGA*DIA**3
POWER : ROH*OMEGA**3*DIA**5
HEAD : OMEGA**2*DIA**2/GEE

TEST POINT NO	INPUT HEAD ACROSS LINEAR SECTION		PREDICTED NON-DIMENSIONAL PERFORMANCE PARAMETERS								
	ψ	$\partial\psi/\partial\theta$	HEAD ACROSS PUMP	FLOW RATE THRO L.S.	PUMP VOL. FLOW RATE	IMP. EFFY	VOL. EFFY	HYDRAULIC POWER	HYD. EFFY	SHAFT POWER	O/A EFFY
1	0.90	0.17	0.881	0.501E-02	0.216E-02	0.41	0.74	0.190E-02	0.174	0.112E-01	0.170
2	0.80	0.15	0.759	0.601E-02	0.319E-02	0.48	0.82	0.243E-02	0.243	0.102E-01	0.238
3	0.68	0.13	0.617	0.676E-02	0.399E-02	0.53	0.86	0.246E-02	0.282	0.890E-02	0.277
4	0.54	0.10	0.454	0.738E-02	0.467E-02	0.54	0.89	0.212E-02	0.289	0.750E-02	0.283
5	0.38	0.07	0.268	0.797E-02	0.533E-02	0.52	0.91	0.143E-02	0.246	0.591E-02	0.241

Table (6.11): Overall performance results predicted using slip factor = 0.8
(effective pumping length varying)

(C) ESTIMATION OF POWER LOSSES

TEST POINT NO	SHAFT POWER INPUT	% LOST IN MECH LOSSES*	POWER INPUT TO FLUID	% LOST IN SHOCKS	% LOST IN BLADE PASSAGES	% LOST IN CHANNEL	% LOST IN LEAKAGE	% LOST IN CARRY OVER	% LOST IN PORTS
1	0.112E-01	2.02	0.109E-01	40.40	13.91	4.50	6.16	17.30	0.36
2	0.102E-01	2.02	0.999E-02	30.75	16.04	5.11	5.70	16.83	1.29
3	0.890E-02	2.03	0.872E-02	23.03	17.50	6.77	5.19	16.39	2.89
4	0.750E-02	2.03	0.734E-02	17.61	18.52	9.59	4.46	15.47	5.49
5	0.591E-02	2.04	0.579E-02	12.41	19.74	15.57	3.47	13.80	10.37

* MECHANICAL LOSSES INCLUDE DISC FRICTION LOSSES
(2.0% OF SHAFT POWER ASSUMED LOST IN BEARINGS AND PACKINGS)

Table (6.12): Distribution of losses resulting grom calculations
(slip facotr = 0.8, effective pumping length varying)

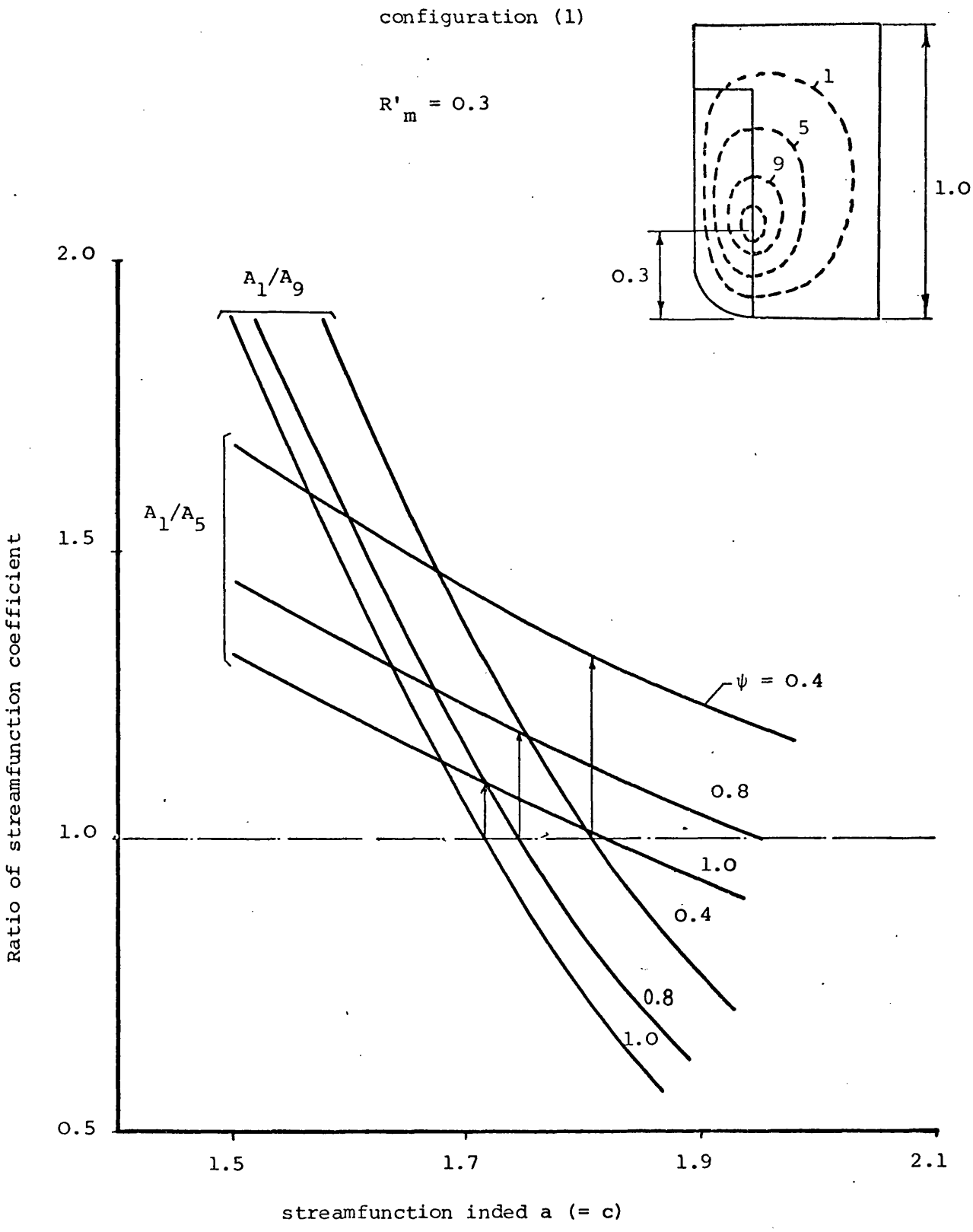

Fig. (6.1): Variation of streamfunction coefficient across flow with index a for various pressure rises

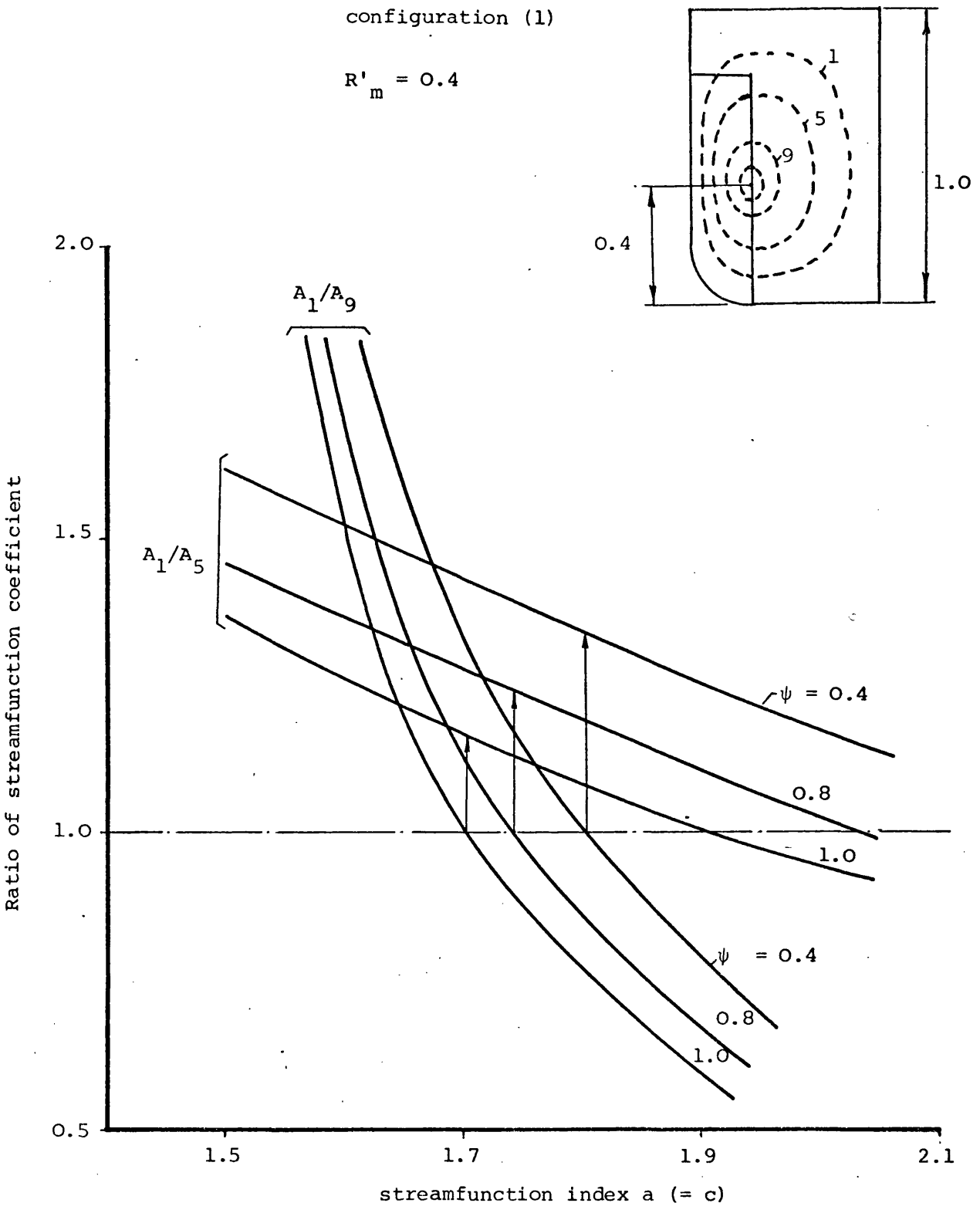

Fig. (6.2): Variation of streamfunction coefficient across flow with index a for various pressure rises

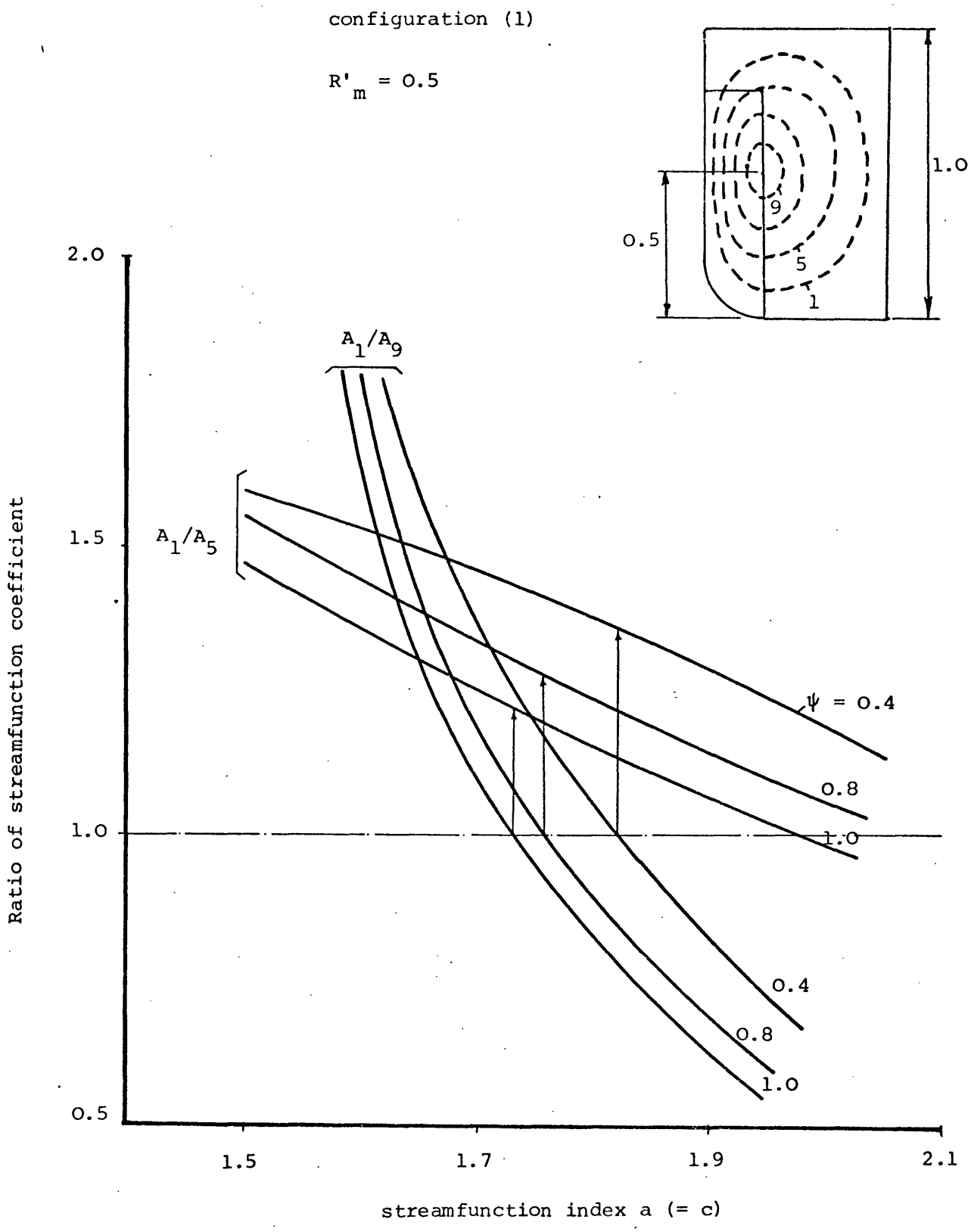

Fig. (6.3): Variation of streamfunction coefficient across flow with index a for various pressure rises

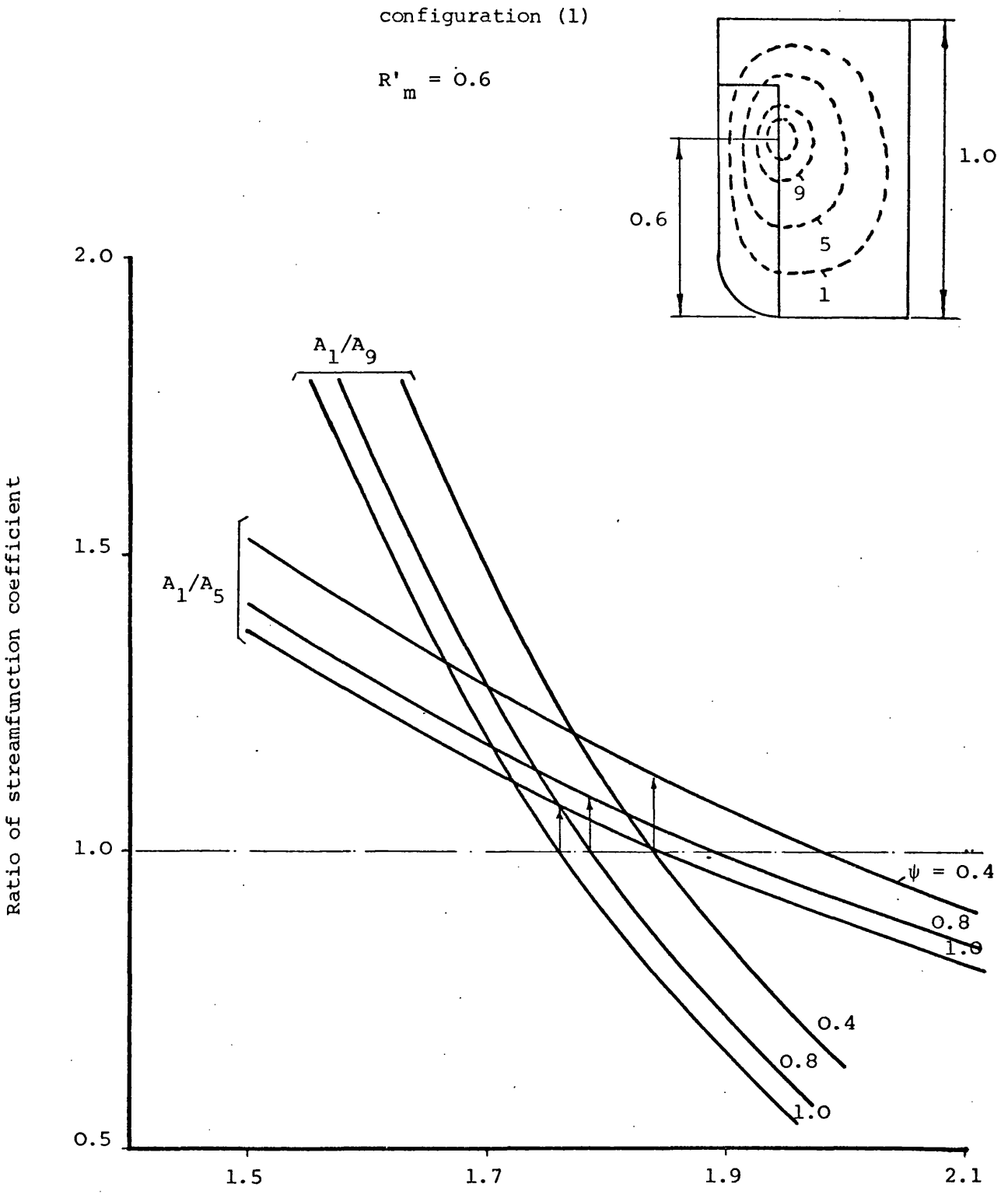

Fig. (6.4): Variation of streamfunction coefficient across flow with index a for various pressure rises

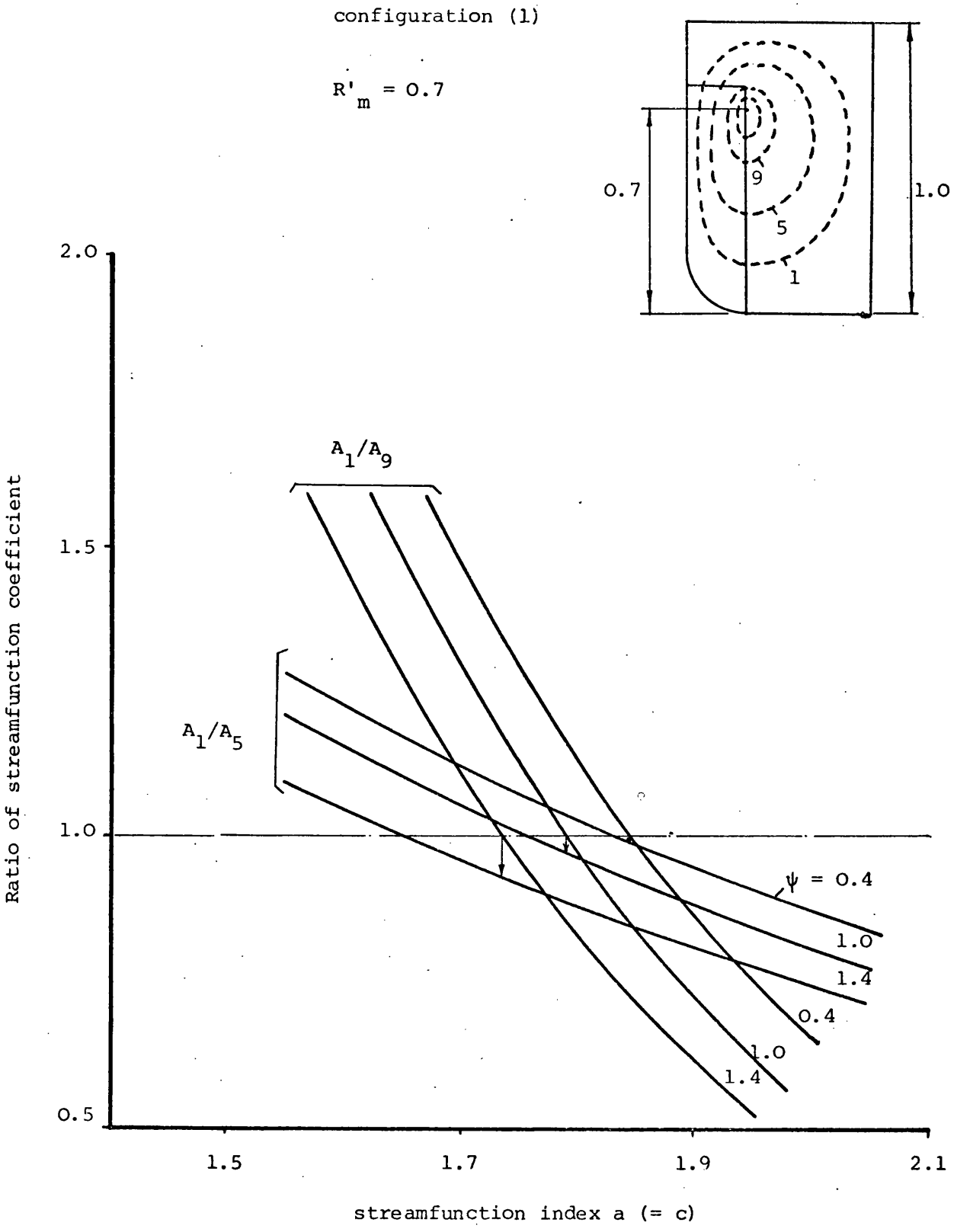

Fig. (6.5): Variation of streamfunction coefficient across flow with index a for various pressure rises

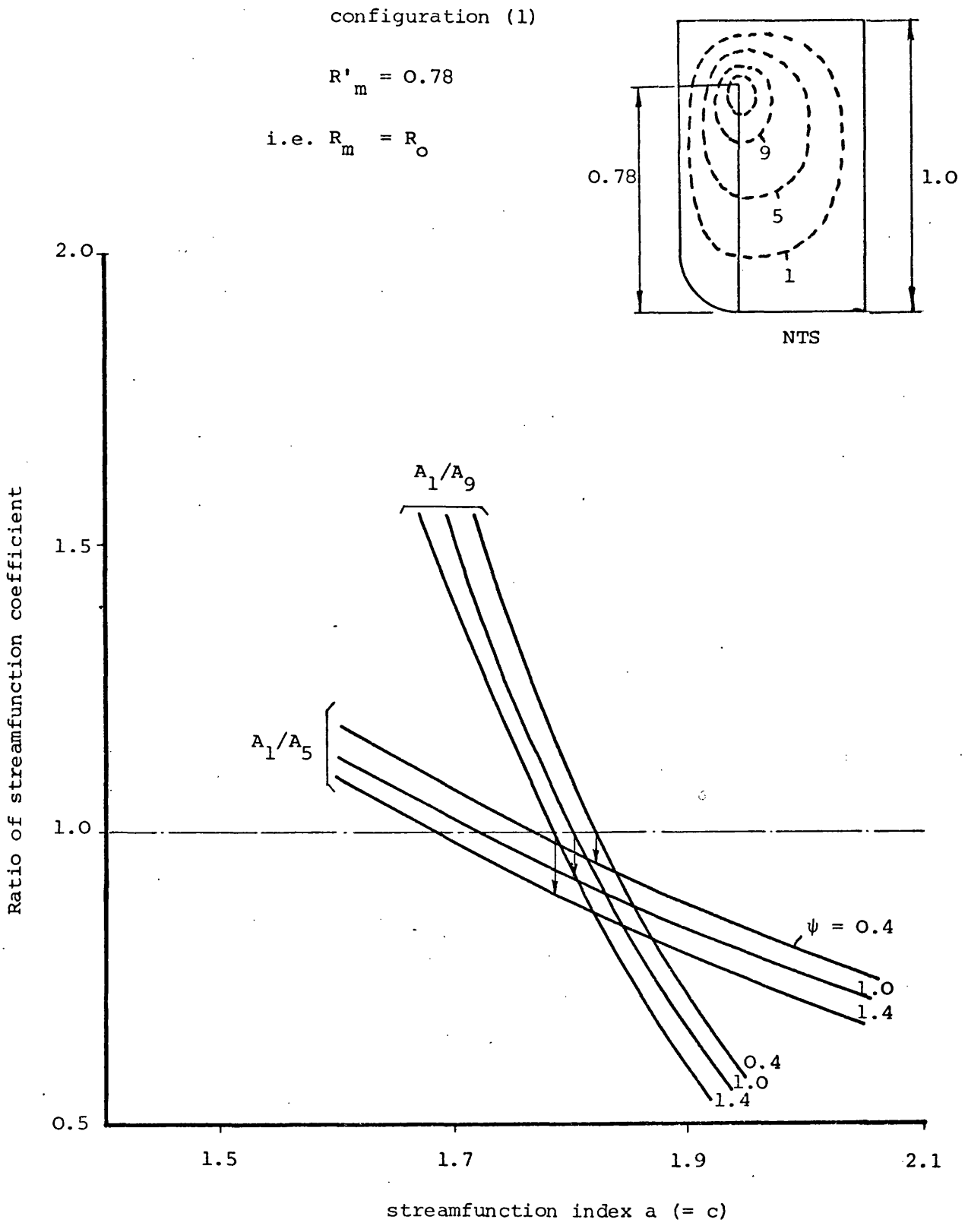

Fig. (6.6): Variation of streamfunction coefficient across flow with index a for various values of pressure rise.

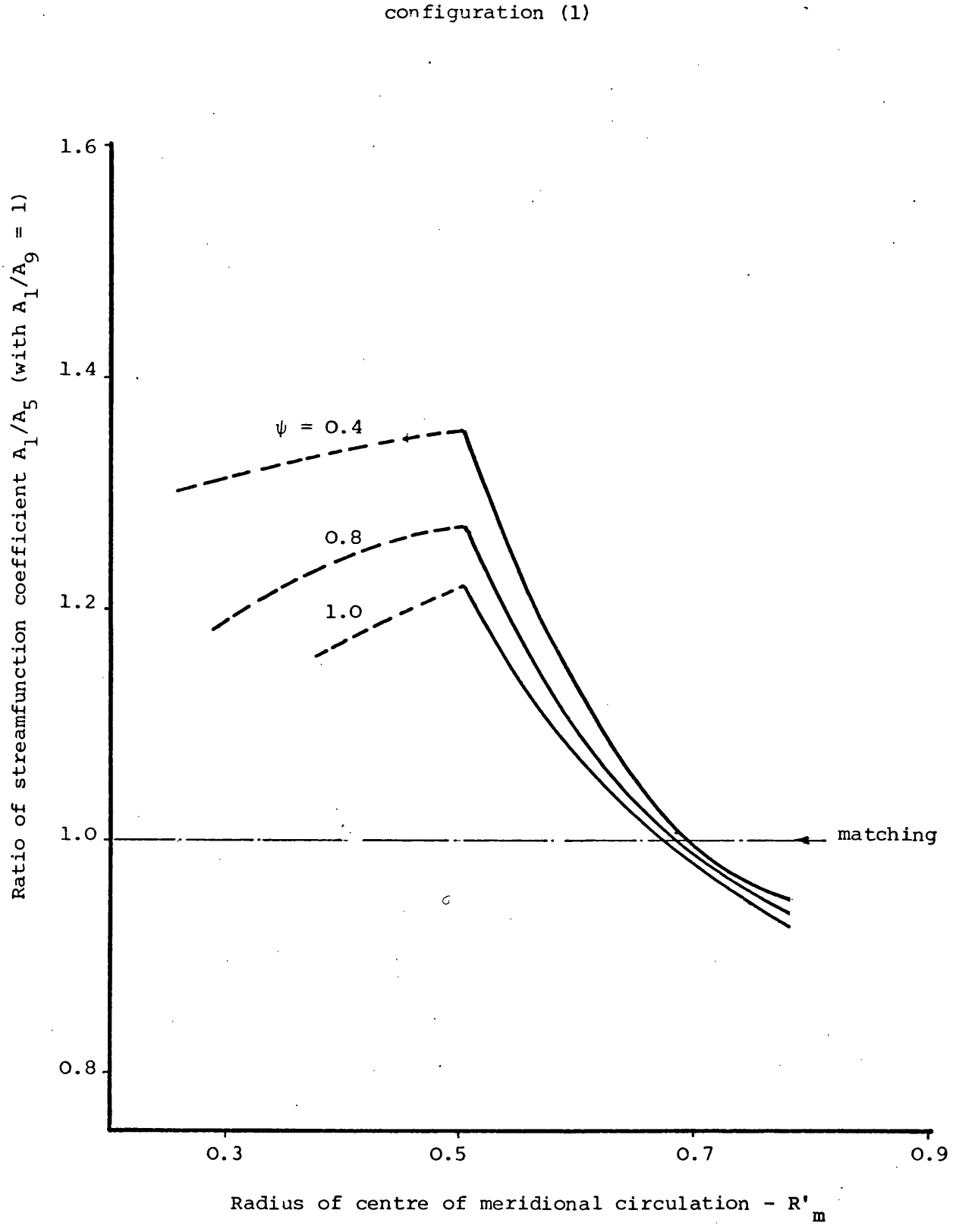

Fig. (6.7): Determination of optimum radius of meridional circulation centre - R'_m

configuration (1)

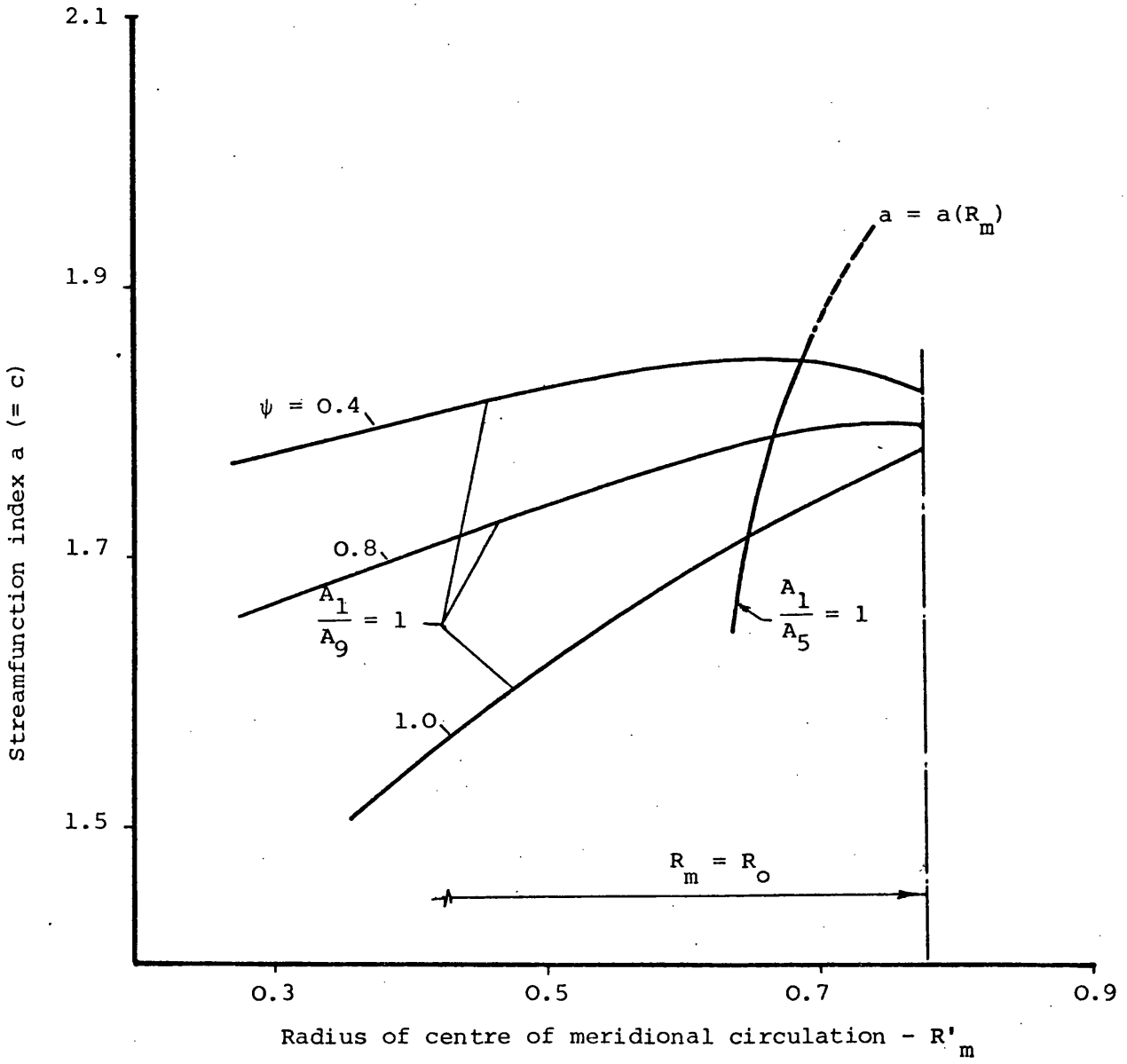

Fig. (6.8): Optimisation of streamfunction index a

configuration (1)

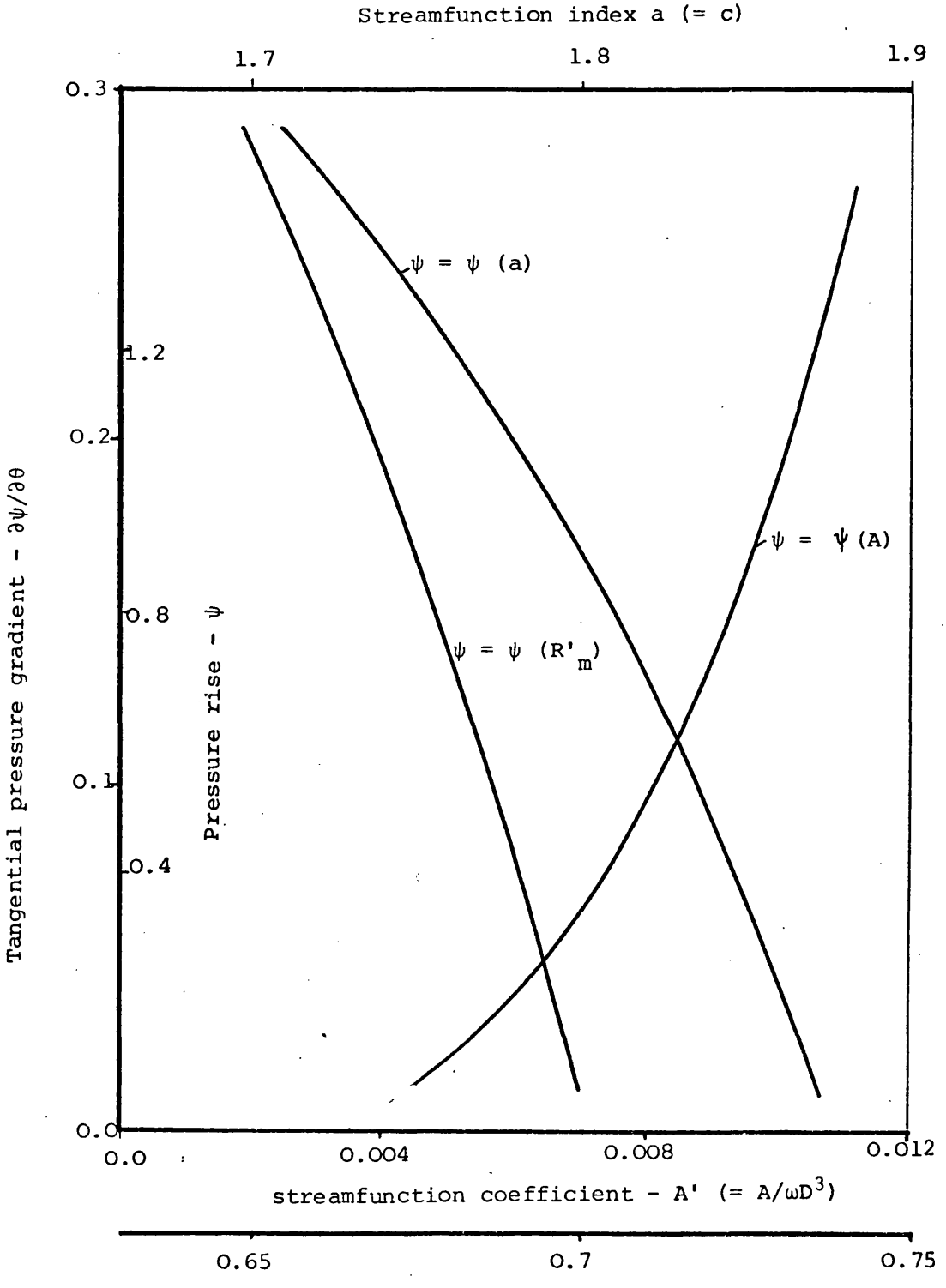

Fig. (6.9): Variation of streamfunction parameters with pressure gradient. (Slip factor = 0.96 Reference Friction levels)

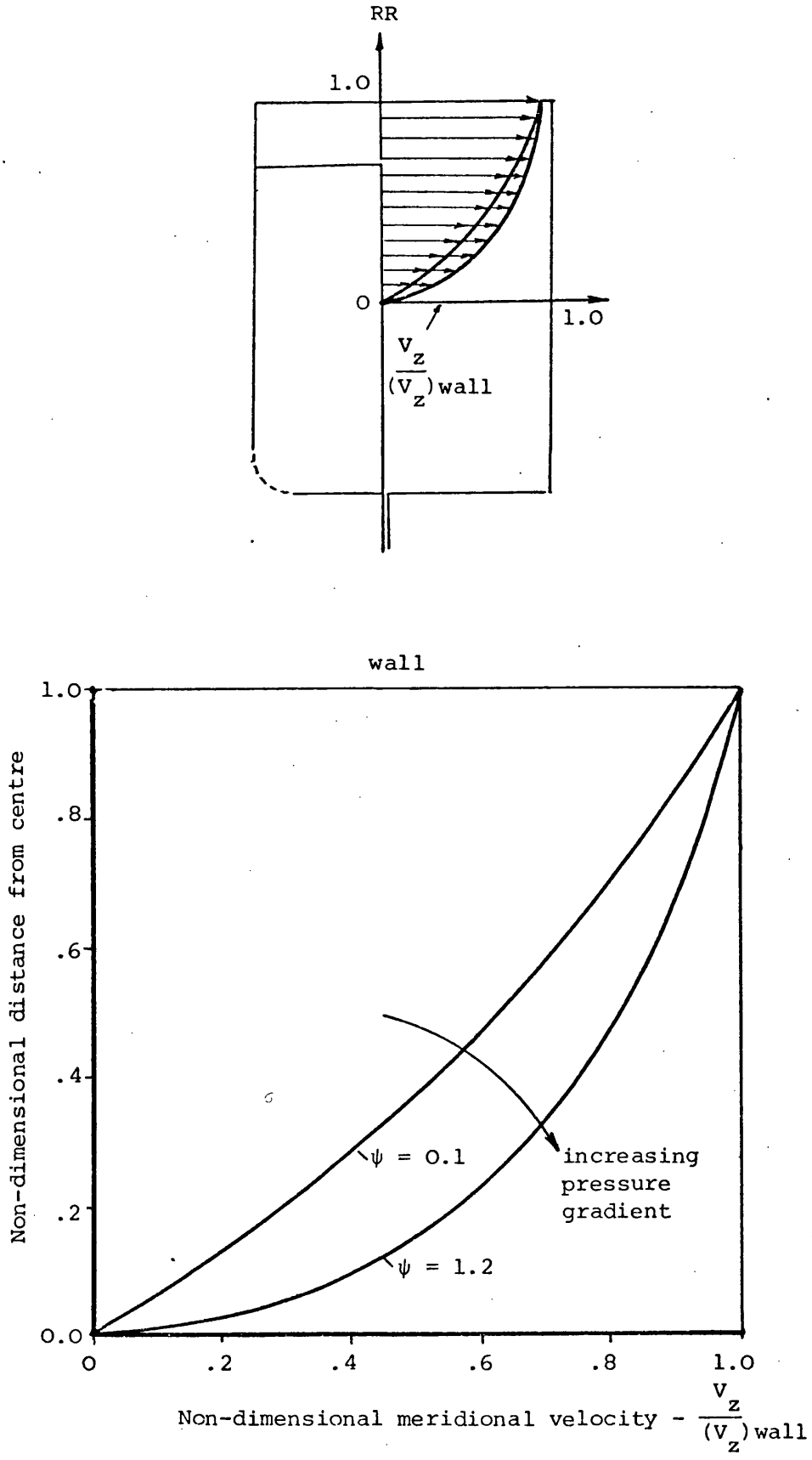

Fig. (6.10): Change of meridional velocity profile shape with tangential pressure rise ψ

configuration (1)

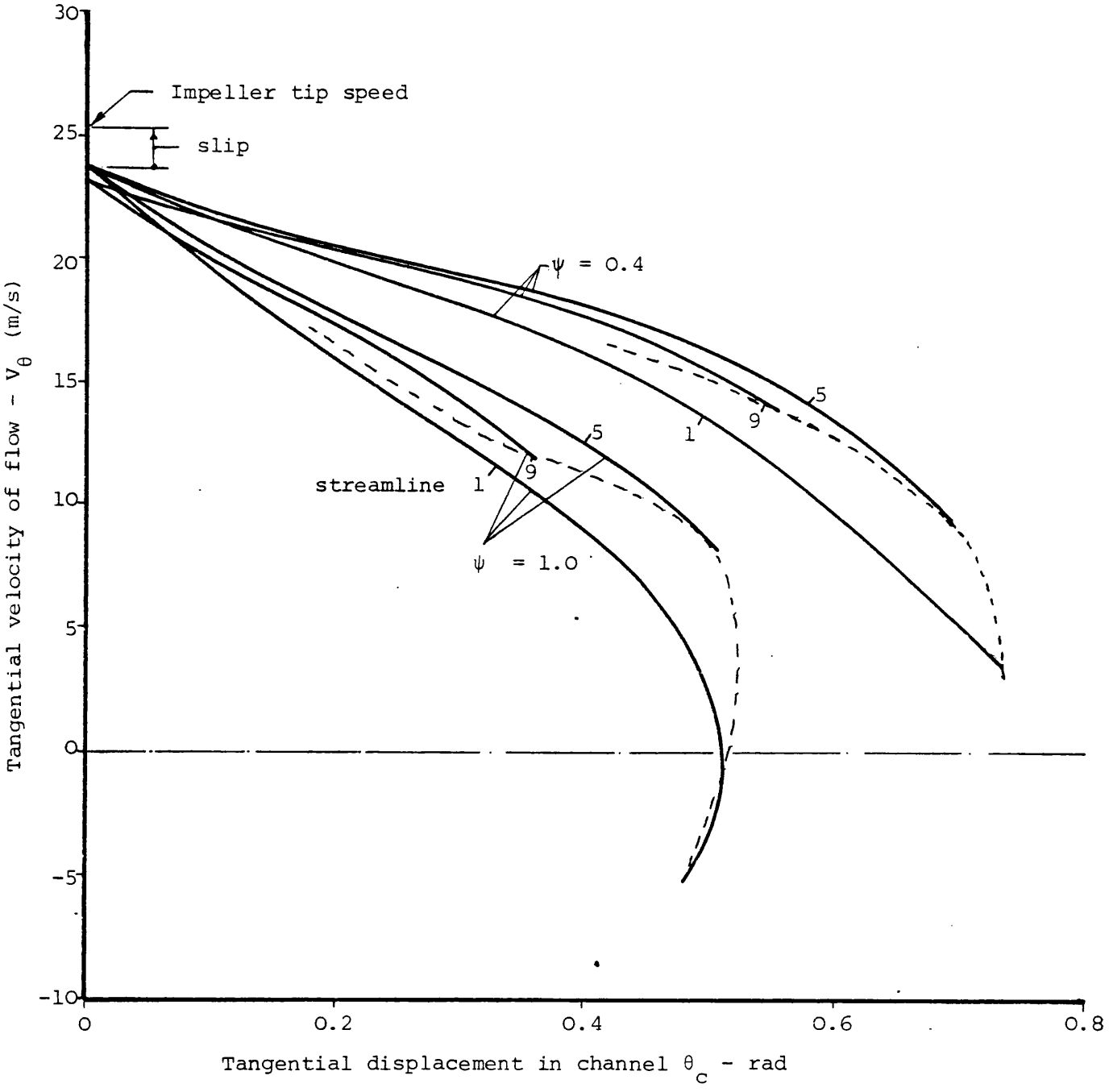

Fig. (6.11): Variations of tangential velocity along streamlines in channel with angular displacement at two pressure rises

configuration (1)

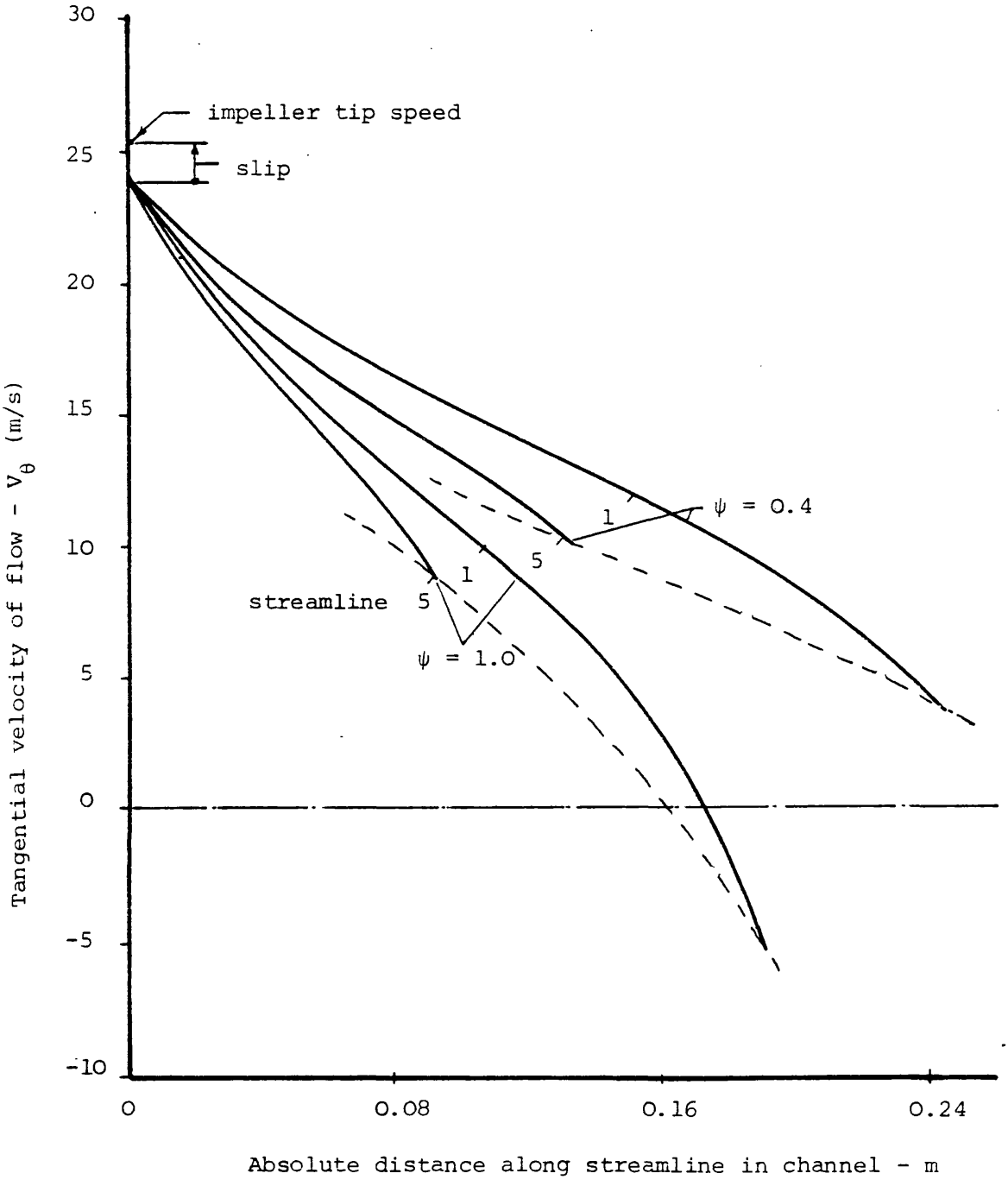

Fig. (6.12): Variation of tangential velocity along distance travelled in channel

configuration (1)

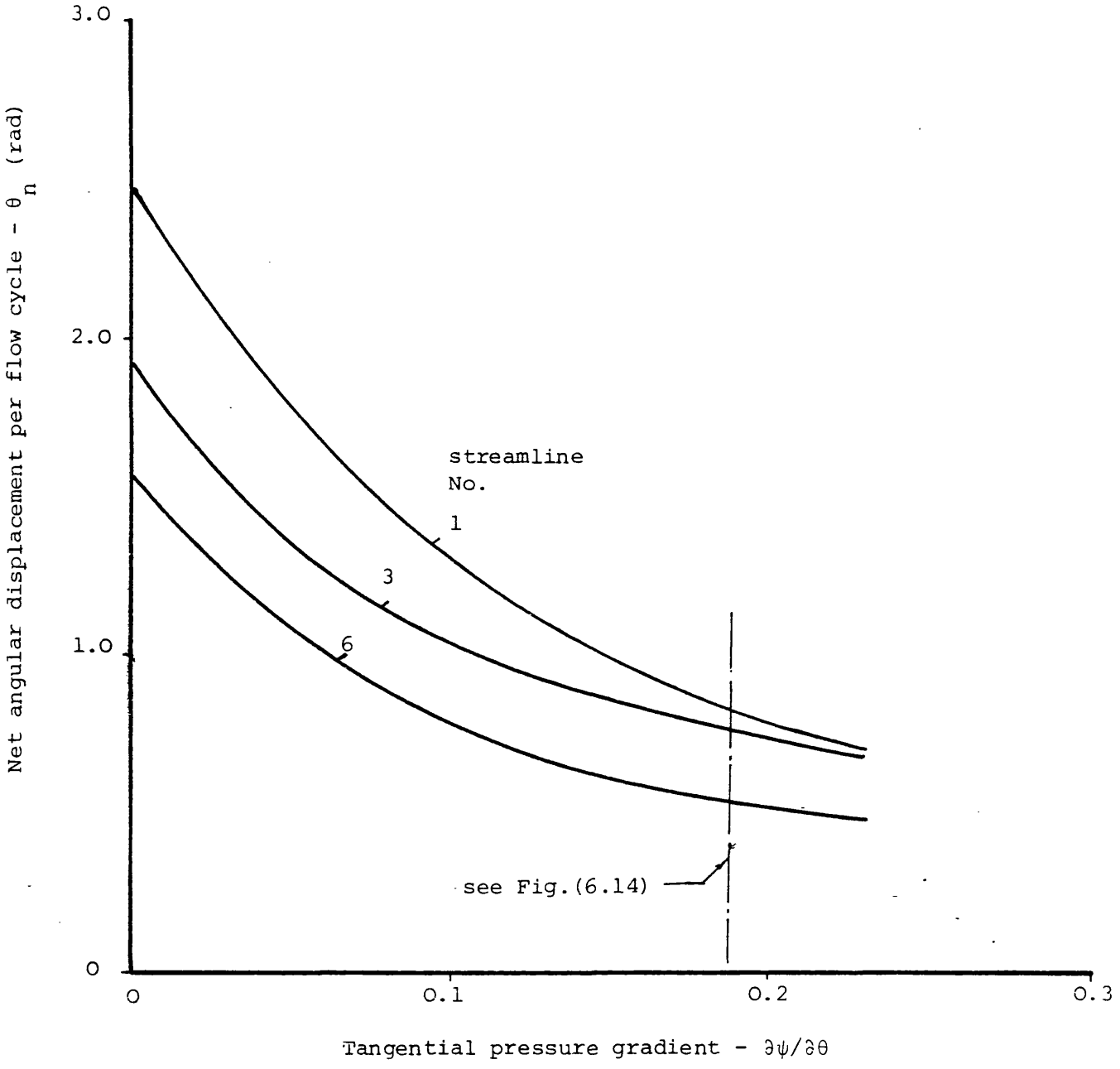

Fig. (6.13): Tangential displacement against pressure gradient along various streamlines

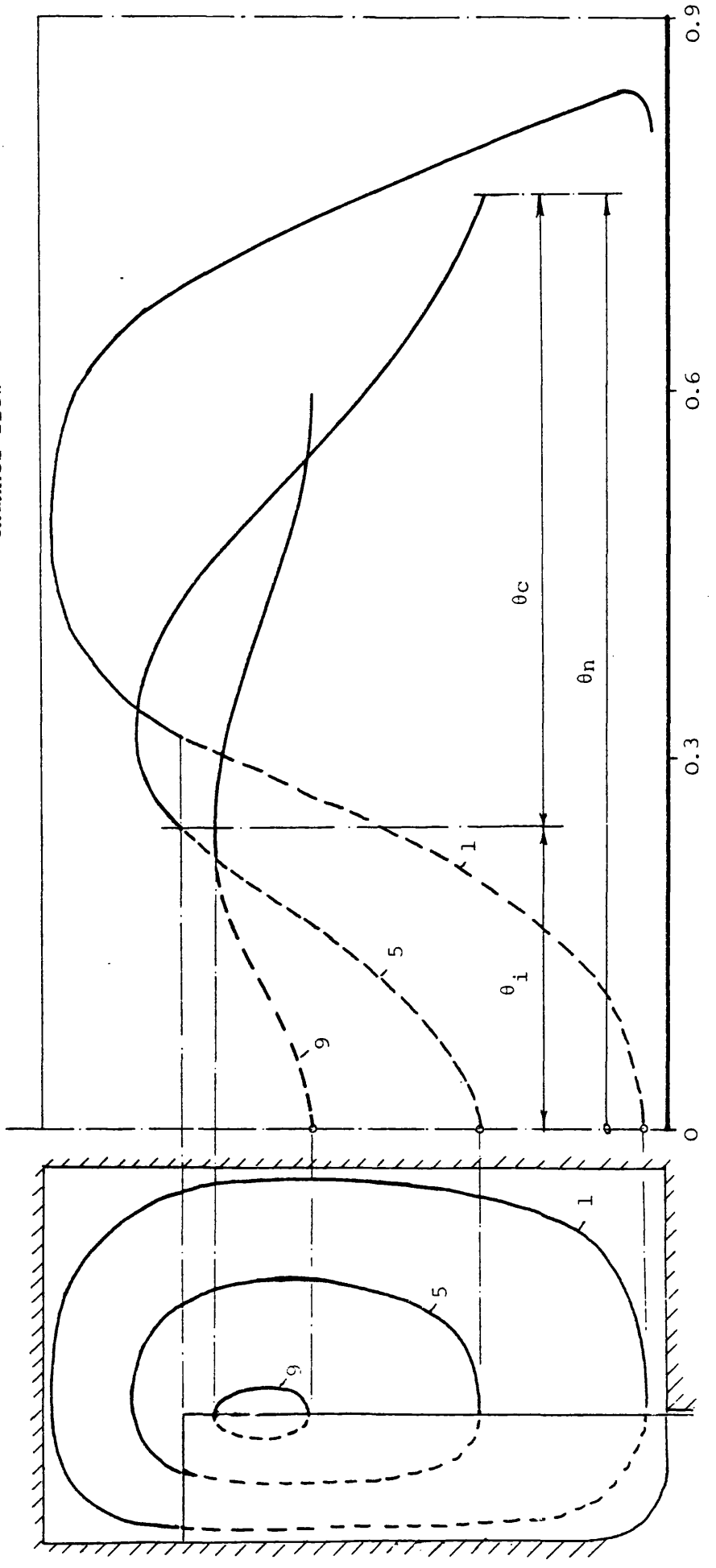

Fig. (6.14): Developed trajectories of 3 streamlines starting at the same meridional section

configuration (1)

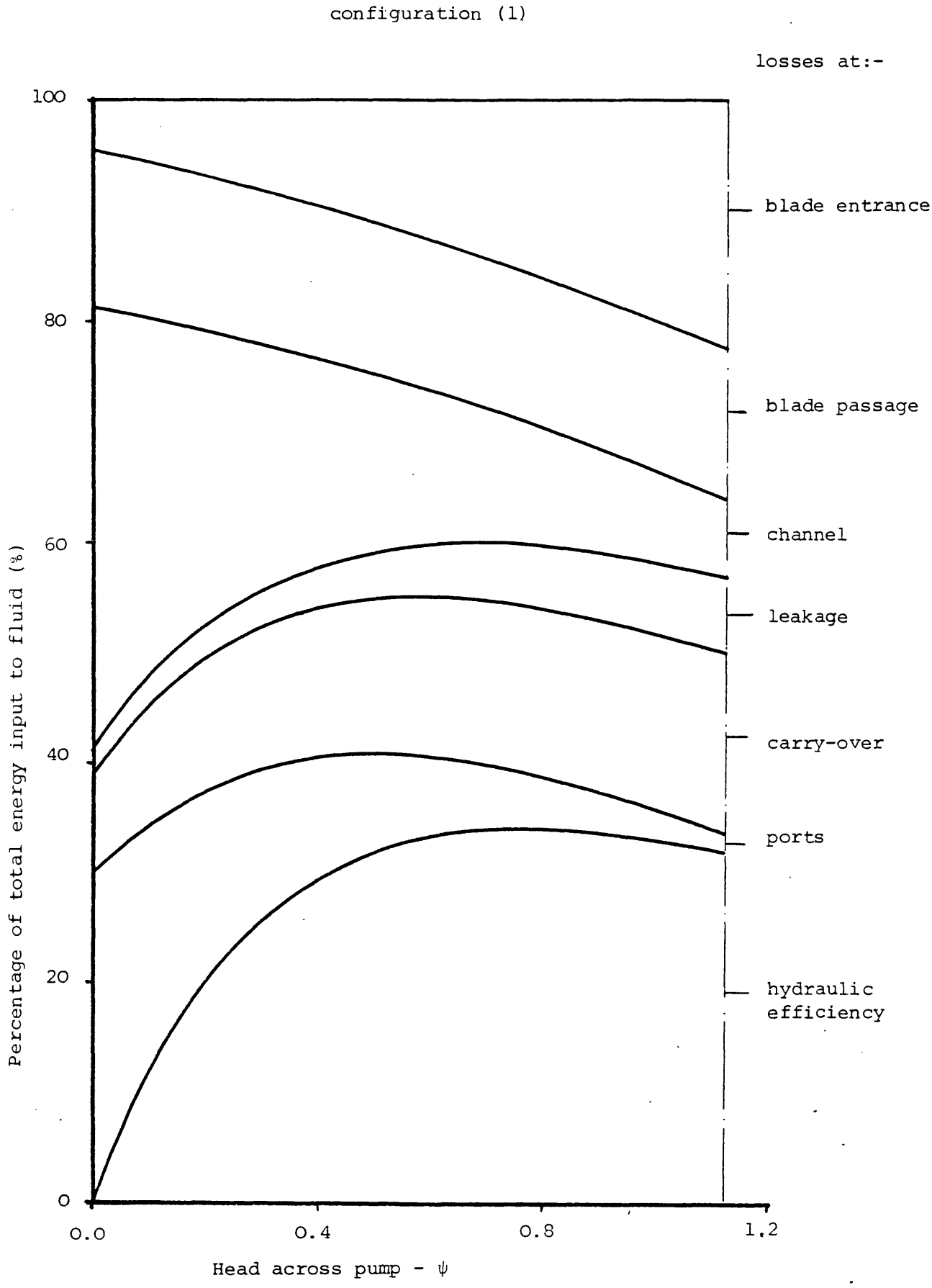

Fig. (6.15): Computed distribution of losses
(reference friction levels, slip factor = 0.96,
length of effective passage constant)

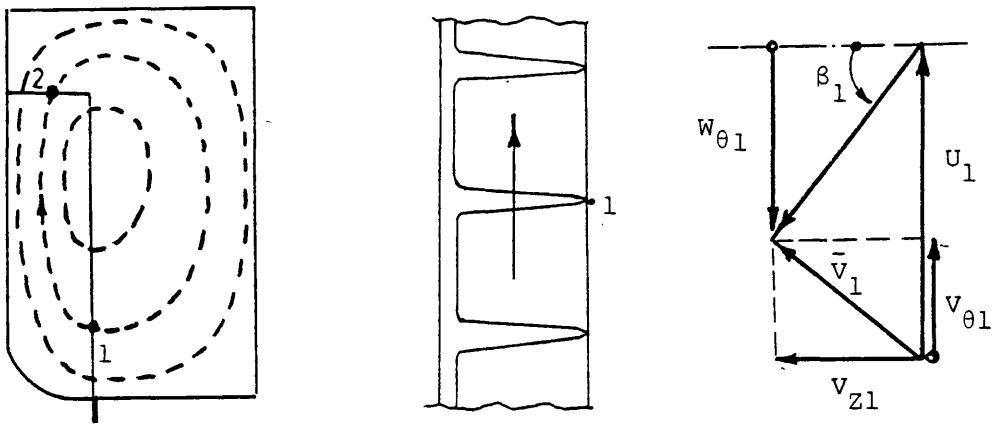

NTS

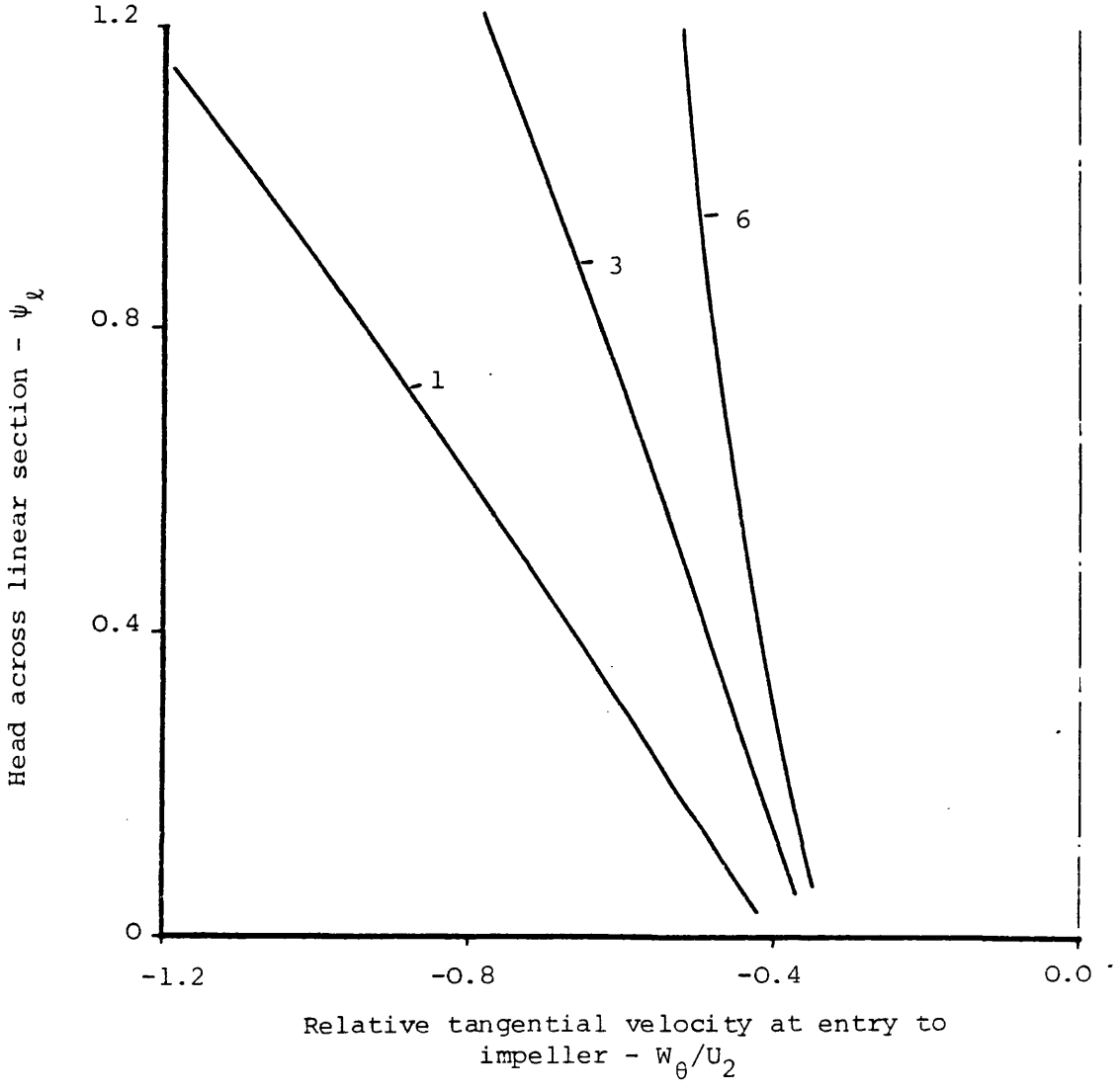

Fig. (6.16): Variation of relative tangential velocity at entry to blades with pressure rise along 3 streamlines

configuration (1)

——— experimental

——— computed

PPLC ≡ pumping passage length is constant
PPLV ≡ " " " is variable

1: default friction levels, slip factor = 0.96, PPLC
2: increased friction levels, slip factor = 0.96, PPLC
3: default friction levels, slip factor = 0.96, PPLC
4: default friction levels, slip factor = 0.8, PPLC
5: default friction levels, slip factor = 0.8, PPLV

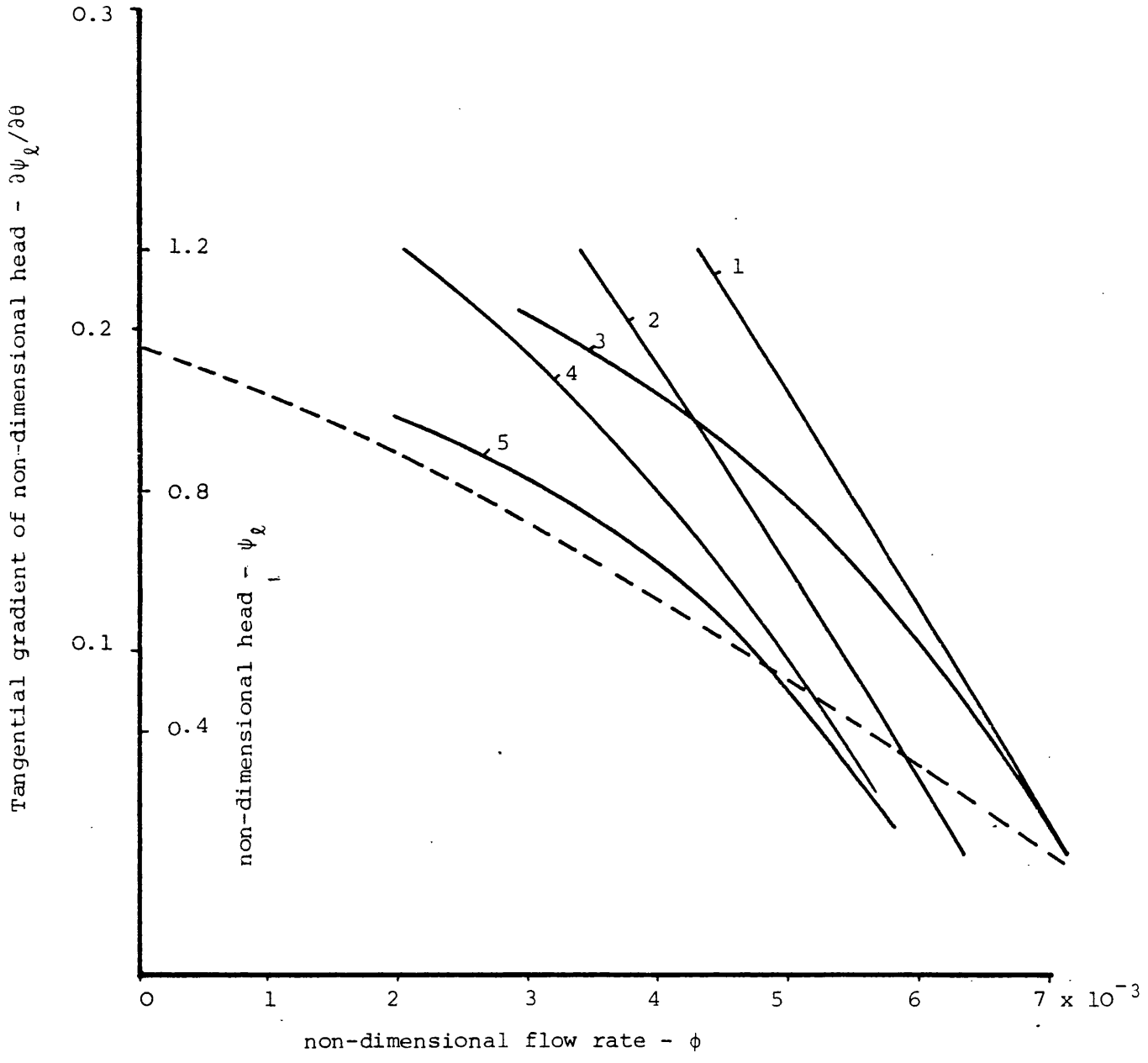

Fig. (6.17): Comparison of computed internal head-flow rate characteristic with experimental results

configuration (1)

slip factor = 0.8

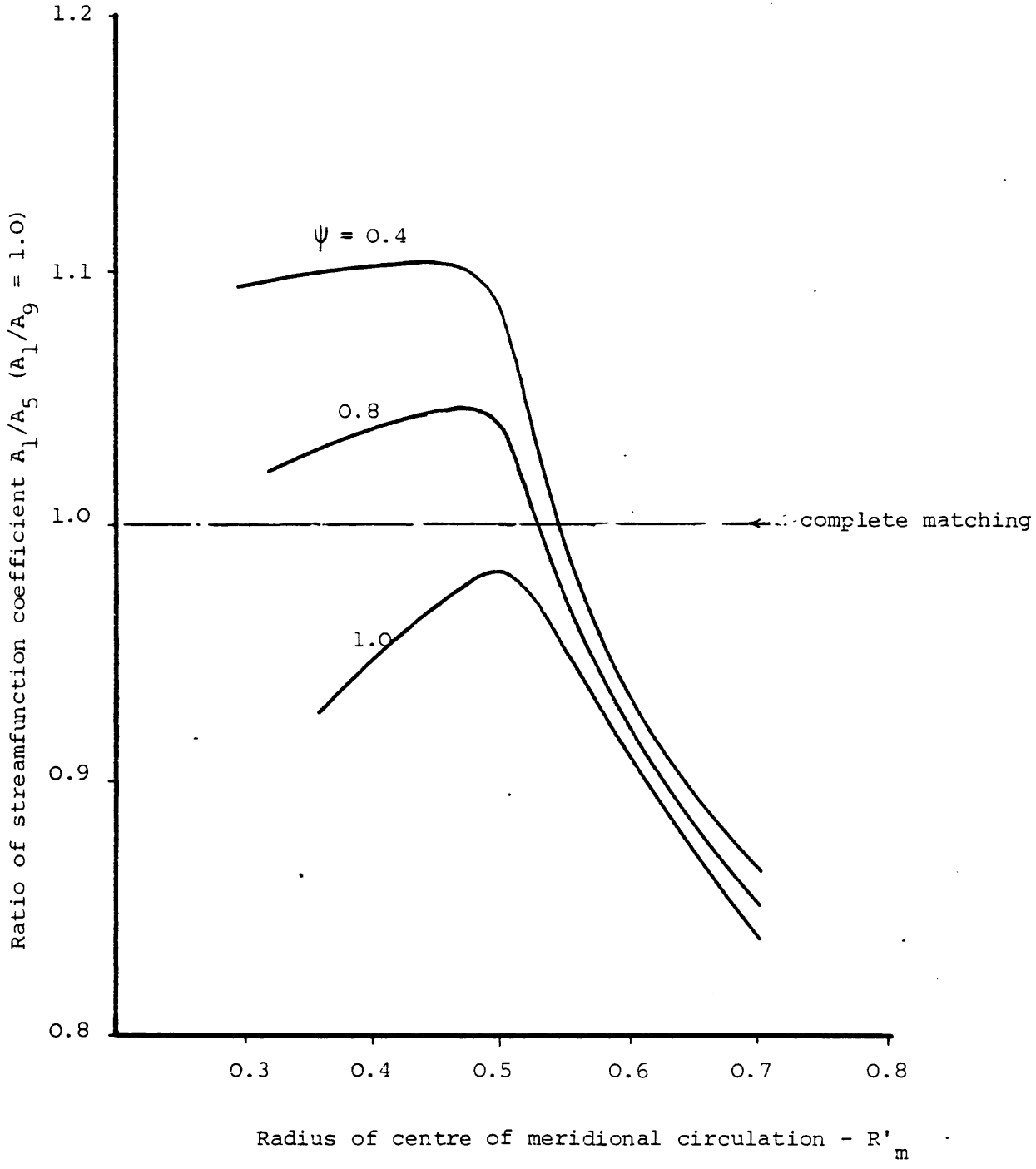

Fig. (6.18): Determination of optimum radius of centre of meridional circulation

configuration (1)

slip factor = 0.8

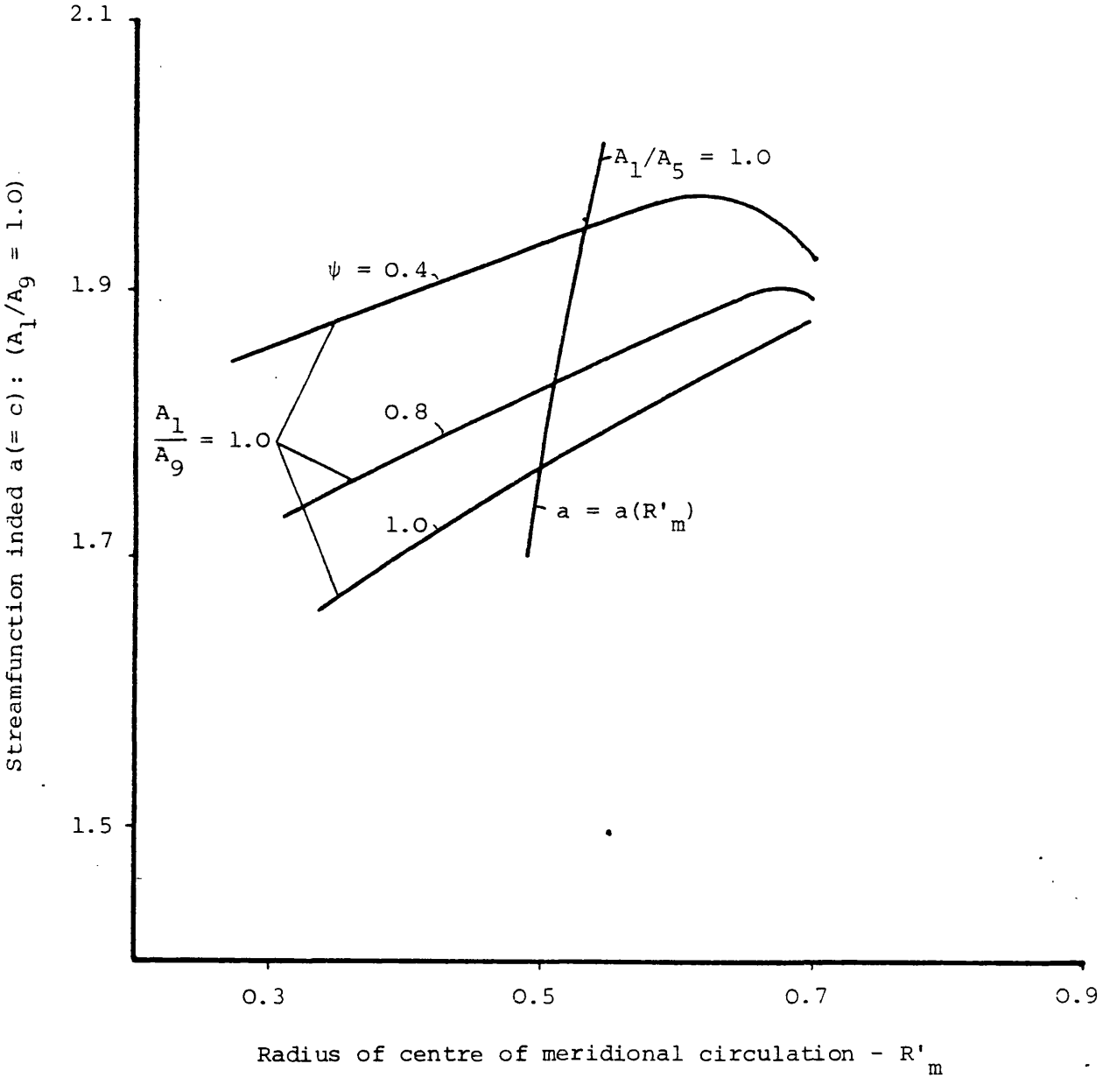

Fig. (6.19): Optimisation of streamfunction index a

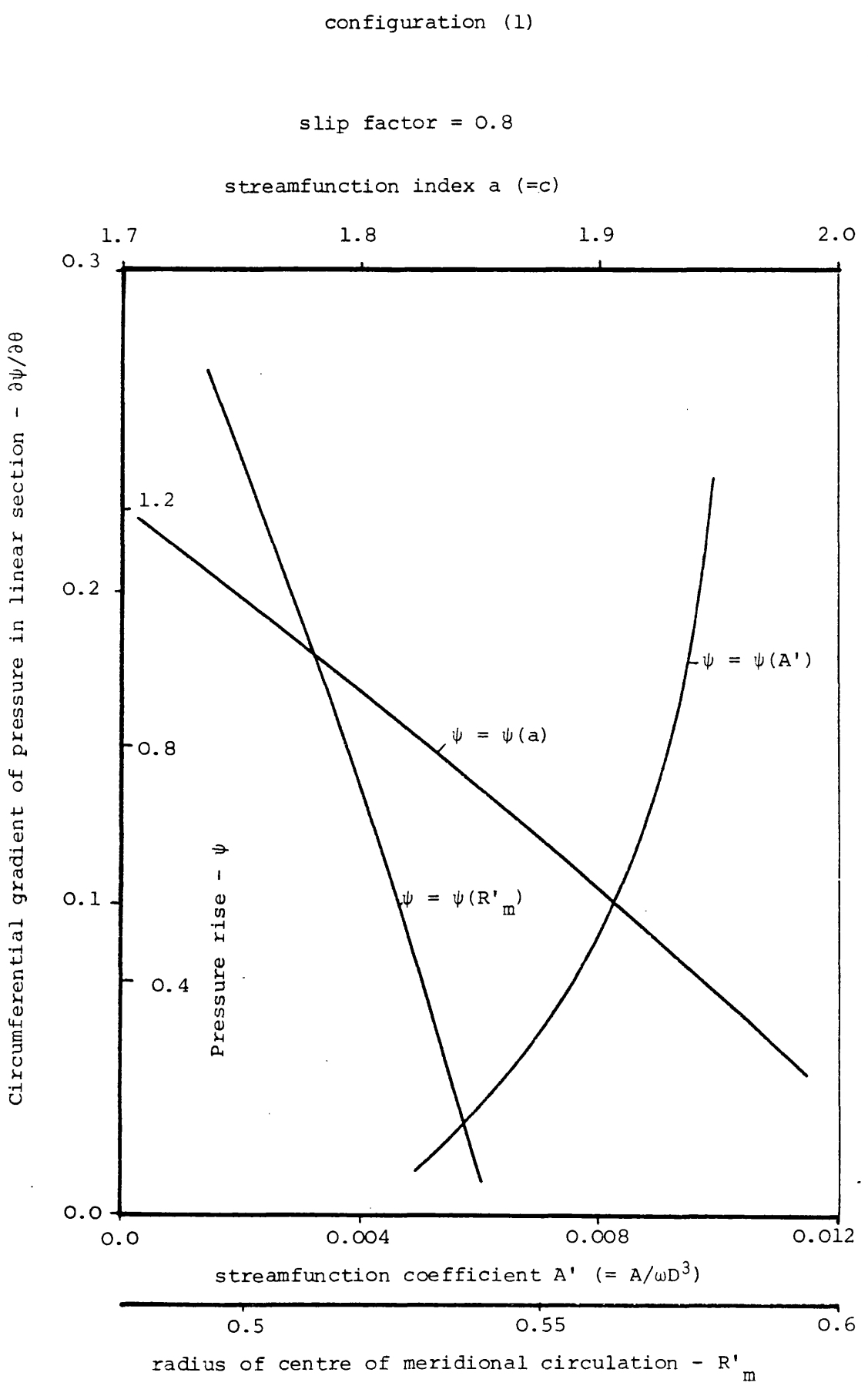

Fig. (6.20): Variation of streamfunction parameters with pressure gradient (slip factor = 0.8, default friction levels)

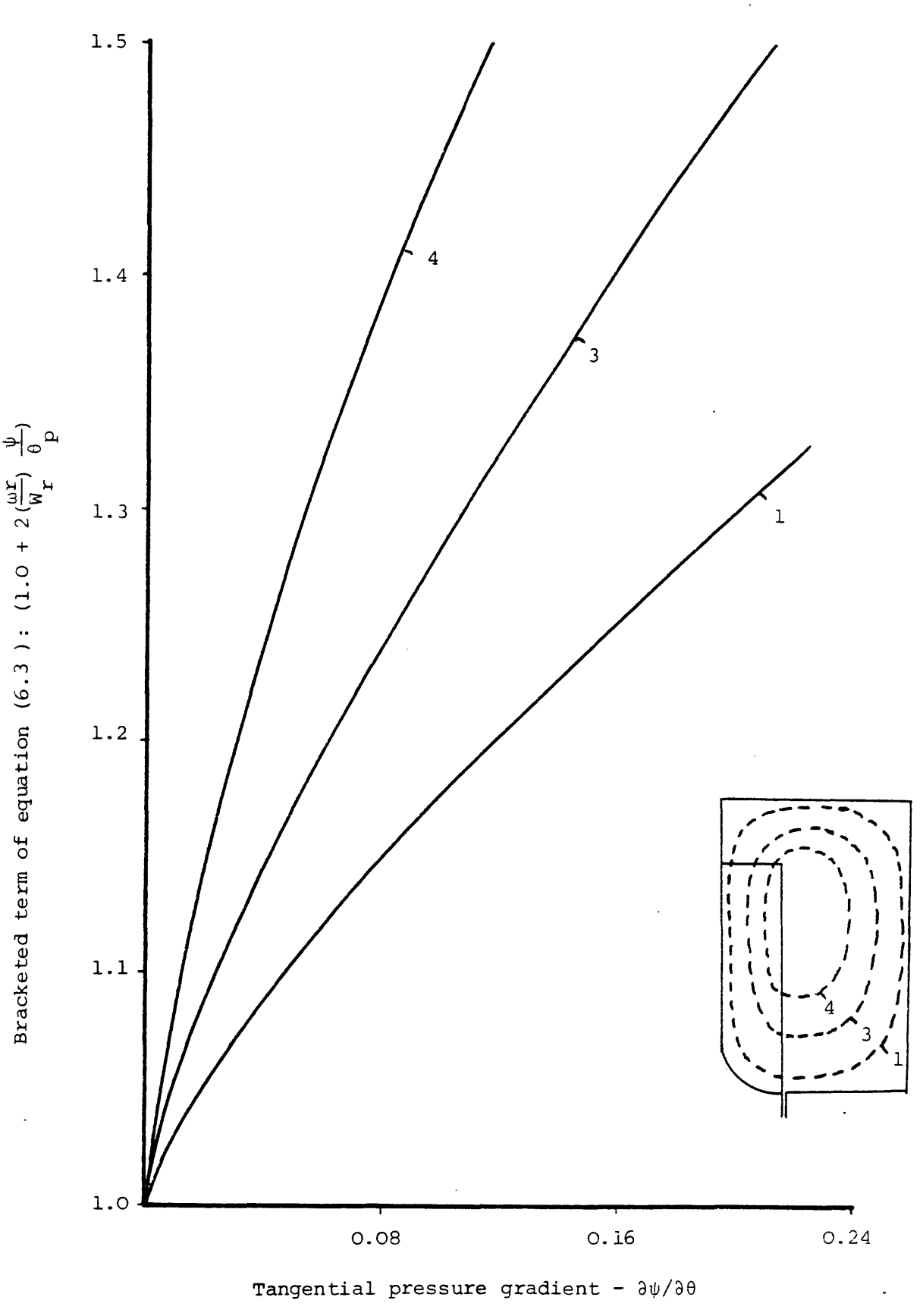

Fig. (6.21): Computed values of a factor in the axial vorticity equation at exit of various streamlines.

7. CONCLUSIONS AND RECOMMENDATIONS FOR FURTHER WORK

7.1 Conclusions

The aim of this project was to develop a theoretical method of analysis of the flow in regenerative pumps. Previous theoretical approaches have been directed at the prediction of the overall performance characteristics and have required empirical constants to be determined from experiments. The better of such analyses have concluded that there is a quadratic relationship between Head and Flow rate, and three parameters are of course the minimum required to fully determine such a relationship.

Many methods of calculating the details of the flow in axial and centrifugal machinery have now been published and have allowed considerable performance improvements to be made by virtue of the better understanding which they have afforded. However, a detailed solution of the flow in regenerative machines comparable to these has not been published yet. The present work has attempted to provide a more firmly based flow model for the regenerative machines. This required effort in

a) the development of the theory and

b) its implementation on a digital computer.

The major conclusions to be drawn from each of these principal areas of effort are now presented in turn.

7.1.1 Theoretical analysis

The published previous work was reviewed and detailed analysis did not seem to have been attempted so that the present approach has not borrowed heavily from previous reported experience.

The view was formed that these machines operate as genuine rotodynamic devices, applying forces to the fluid by virtue of pressure differences developed over the blade surface rather than by applying tangential friction forces through the medium of an enhanced hydraulic roughness effect. In modelling the flow, it was recognised that the flow near the inlet and outlet ports could not be described so simply, and the internal regime had therefore to be subdivided into linear and port

sections. The modelling effort in this work has mainly been concerned with the linear section.

A. Linear Section

The detailed flow analyses applied to the axial and centrifugal machines invariably assume that both the pressure and velocity fields are axi-symmetric, the inevitable flow fluctuations between blades being averaged out for this purpose. However, since the very purpose of the regenerative device is to develop a circumferential pressure gradient, such sweeping assumptions were clearly inappropriate. Instead, it has been assumed that the velocity field is axi-symmetric while the pressure field can be represented by a linear gradient of pressure with circumferential angle.

(i) Head across regenerative impeller

The assumption of an axi-symmetric pressure field is so universal that even the most fundamental works of reference (e.g. Vavra (22)) employ it without question. This meant that the basic flow equations had to be rederived for the present approach.

The publish analyses of the flow in regenerative machines have assumed the well known Euler equation of elementary fluid mechanics to apply to the case where there is a circumferential pressure gradient. Equations have been developed here which show this to be incorrect and that the usual form of the equation has to be supplemented by an extra term accounting for the tangential pressure gradient.

The most general statement which can be made about the flow in the impeller is that along streamlines the relative total enthalpy remains constant irrespective of the presence of a tangential energy gradient, see equation (A.20). This leads to an equation for the head rise along a streamline in one passage through the impeller blading given by, see equation (A.27):

$$H_2 - H_1 = \omega(r_2 V_{\theta 2} - r_1 V_{\theta 1}) + \int_1^2 \frac{\partial H}{\partial \theta} \, d\theta$$

where H is the total energy of the fluid and 1 and 2 refer to conditions at inlet and outlet of impeller respectively. With the introduction of the assumptions that

a) the velocity field is axi-symmetric

b) the density is constant and

c) the pressure gradient in the tangential direction is constant

the change of fluid energy across the impeller is then given by, see equation (A.38):

$$\Delta(\rho)_{12} = \omega(r_2 V_{\theta 2} - r_1 V_{\theta 1}) + \frac{1}{\rho}\frac{\partial p}{\partial \theta}\Delta\theta$$

where $\Delta\theta$ is the angular displacement along the streamline between impeller inlet and exit.

This appears to be an important new result for this class of machines.

It means that the head rise cannot be computed without a knowledge of the flow angular displacements in the impeller. This is an important conclusion regarding theoretical calculations of the flow in regenerative machines.

(ii) Compatability conditions in regenerative machines

The meridional flow has been modelled using a streamfunction given by an empirical expression incorporating implicitly the appropriate boundary conditions at the impeller and channel walls and identifying the centre of circulation. The method developed can accommodate any such suitable expression, and in the present work attention has been particularly directed at a polynomial type of formulation.

The principal condition to be fulfilled between the ends of a streamline during the completion of one flow cycle is that the net total pressure rise exactly matches the product of the circumferential displacement and pressure gradient. This condition applies to any and all of the streamlines and, in principle, by applying it to an appropriate number of streamlines, can be used as a governing requirement to determine as many features of the empirical streamfunction as necessary. This can be seen as an extension of the work by Sivalingam (47) in which such a condition (although without circumferential pressure gradient) was applied to a single streamline in order to determine the angular velocity of the meridional vortex of

the flow in fluid couplings and torque convertors.

In the present work compatability along three streamlines has been assumed to adquately meet the satisfaction of the above condition for the whole flow. However, as has been pointed out, the method is apparently capable of indefinite extension and, in principle, appears to allow the representation of the flow to any required degree of accuracy (within the framwork of the other assumptions made).

This is felt to be new and useful extension to the methods available for treating this type of flow problem in fluid machinery.

(iii) Flow in channel

A major requirement for the solution of the meridional flow is a method of treating the unguided channel flow, taking into account the influence of the circumferential pressure gradient. This requirement is not a major feature in the analyses of other types of rotodynamic machines in which that part of the flow path outside the impeller is either largely guided by stationary blading or is of a simpler character because of the absence of the tangential pressure gradient.

Since the meridional velocity and its gradients are obtainable in terms of the streamfunction, the employment of the latter has facilitated the inclusion of the friction forces due to momentum exhange in the equation of motion in terms of an eddy viscosity. The latter and the empirical friction factors used in the energy equation to estimate the frictional losses have been obtained using the established concept of hydraulic diameter. Thus, it is concluded that a degree of consistency seemed to have been maintained in writing the equations of the flow. However, it has proved to be extremely difficult to set up a thoroughly convincing model for the friction effects and until this can be done, there seems to be little hope that inclusion of friction can be made without recourse to empirical factors.

B. Port Region

No attempt has been made in the present work to investigate the flow in the port regions in detail. The port losses have been estimated using an empirical factor based on the flow rate only: the port

geometry has not been accounted for. Obviously, such a relationship could not be used to predict the performance of the ports of other designs with any great confidence. A more convincing correlation of the port losses is required.

7.1.2 Results

(i) The meridional flow distrubtion

The calculated results of the flow show that the intensity of the meridional circulation increases non-linearly with the increase of the tangential gradient of pressure. The position of the centre of the circulatory motion and the shape of its profile have also been found to vary with the pressure gradient. These are basic findings which are revealed by the present method. However, in the absence of published measurements of the meridional flow, judgement cannot be passed about their general validity at present.

The determination of the appropriate relationship between the meridional flow parameters and the tangential gradient of pressure is basic for the present approach. It has been the part of the work requiring the largest amount of effort mainly because part of it was done extenral to the programs. A more comprehensive optimisation algorithm in the program should enable the entire job to be carried out on the computer.

(ii) Distribution of tangential velocity in channel

The computed results show that reversals of flow occur in parts of the channel at high overall pressure rises. This characteristic of the internal flow was observed experimentally by Lazo and Hopkins (5). It explains the large magnitude of the blade entrance losses computed by the present method at low flow rates. According to these results, the blade entrance losses are the dominant losses in the pumping passage at high pressure gradients. At a particular pressure gradient, these are shown to vary with the radial co-ordinate of the location at which a streamline enters the blades. It is concluded therefore that it should be possible to reduce these losses if the blade inlet angles are designed in accordance with the distribution of the velocity along the inlet edge of the blade. In this respect it seems that a proper design should consider the use of blade inlet angles varying with

radius. It may also be that a proper route for the future development of this class of machine is the inclusion of stator blading in the channel. With these changes it is probable that efficiency improvements could be obtained.

The present method would be of value in the design of the impeller blading since it would automatically allow for the corresponding change in the flow parameters which would be implicit in a reduction of the impeller entry loss.

(iii) Overall performance

The results have demonstrated that the prediction of the overall performance depends crucially on the assessment of three factors: a) the friction factors, b) the relationship between the length of the effective pumping passage and the tangential gradient of pressure, and c) the slip factor. Effects of varying these have been investigated. However, b) and c) have not been determined and therefore it has not been possible to satisfactorily predict the overall performance. Conclusions to be drawn from the investigations are as follows.

a) friction levels

It is found that the slope of the computed head-flow rate characteristic is hardly altered by the choice of the magnitude of the friction factors. However, the computed flow rate of course depends on their choice.

The problem of including the effect of friction in detailed fluid flow calculations is, of course, universal in character but is of greater than usual significance in the present case because of the long unguided portion in the flow path. No great merit is claimed for the present approach and additional work is required on this feature of the analysis. However, the zero-head flow rate has been well predicted using the default values of the friction factors. It would therefore seem to be appropriate to use these values until improved methods are available.

b) length of pumping passage

The present results have shown that the length of the effective pumping passage used in the calculations has a great effect on the

predicted overall results.

The experimental results reported in the literature certainly show that the length of the pumping passage varies with the tangential gradient of pressure and/or the flow rate but no consistent trend has been identified. Obviously the way in which the length of the pumping passage varies with the tangential gradient of pressure should be known before a prediction of the overall performance characteristics can be made.

c) slip factor

New equations derived in this work have shown that the intensity of the axial component of vorticity increases with the tangential gradient of pressure.

Furthermore, the computed performance characteristics obtained at different values of slip factor have shown that the use of a degree of slip which increases with the tangential gradient of pressure results in a more accurate prediction. It is required therefore to deduce an appropriate formulation of the slip factor paralleling the expressions already deduced by Stodola and Stanitz for radial flow machinery.

7.2 Recommendations for Further Work

7.2.1 Experimental work

The program results have allowed the identification of the following experimental objectives in the linear section:

a) Careful measurement of the tangential velocity at the impeller exit could provide a much needed experimental assessment of the effect of slip in regenerative machines.

b) Measurements of the flow velocity and direction at impeller inlet are required for comparision with predicted results and consequently could be used to quantify the effect of friction in the channel.

c) Measurement of the pressure in the pumping passage is required for the verification or otherwise of the constancy of its gradient

with the angular co-ordinate. The assumption that it is constant has been a basic element in this work. Such measurements could also be used to quantify the dependence of the length of the effective pumping passage on the pressure gradient.

Regarding the non-linear section, the flow in the port regions has up to now defied any theoretical modelling. It seems therefore that an experimental programme centred mainly on port design should be carried out so that a firmly based correlation of the port performance could be established.

7.2.2 Theoretical work

Theoretical investigation of the effect of slip in regenerative machines is required. The flow between the blades of a regenerative machine differs from the case of radial blades considered by Stanitz (37) and others mainly because

(i) there is a circumferential pressure gradient,

(ii) the flow is axial at inlet and is not necessarily radial at exit (certainly not for all streamlines) and

(iii) the rotor is unshrouded.

Similarly, the validity of using an incidence loss model originally developed for machines with no circumferential pressure gradient should also be investigated.

7.2.3 Generalising the cross-section

The method has been developed for dealing explicitly with pumps in which the meridional cross sections of the impeller-channel configuration are rectangular in shape. The method might with advantage be extended to deal with other types of cross-section. In this respect the inherent generality of the streamfunction approach could be exploited. This could be done for example by use of unequal values of the indices a and c which were taken the same in this work, or the use of other streamlines than $\psi = 0$ for the wall boundary. Alternatively, an altogether different class of streamfunction expression could be used.

7.2.4 Refinement of computer programs

Part of the work of optimisation was done externally to the programs. It must be seen as essential to incorporate such work in new form of the programs which should then be designed in such a way as to give final results. In a new layout of the programs, use could be made of the potentiality of using compatibility conditions at any desired number of streamlines. It should be possible to accomplish such a task without much effort now that the unknown areas of the problem, such as methods for achieving the convergence of iterative methods which prevented this from being done when the programs were originally generated, have been sufficiently clarified.

7.2.5 Use of method in other machines

The present method may in principle be applied to analyse the flow in regenerative blowers since the basic flow equations derived in Appendix A are not limited to incompressible flows. Regarding these machines, however, it has been reported recently by Croker (55) that the tangential gradient of pressure was found to vary in the pumping passage. This should be borne in mind when applying the method to such machines.

8. REFERENCES

(1) Y. Senoo.
'Theoretical Research on Friction Pump',
Reports of the Research Institute for Fluid Engineering, Japan, Vol. No. 1, 1978.
'Researches on Peripheral Pump' and 'Influences of the Suction Nozzle on the Characteristics of a Peripheral Pump and an Effective Method of their Removal'.
Reports of Research Institute for Applied Mechanics, Kyushu University, Japan, Vol. 3, No. 11, 1954.

(2) W. E. Wilson.
'Analysis of Turbine Pumps',
Product Engineering, Vol. 18, October, 1947, pp. 163-166.

(3) A. Miyadzu.
'Theory of the Westco-type Rotary Pump'.
Trans. Soc. Mech. Engrs., Japan, Vol. 5, No. 18, February 1939, pp. 109-115.

(4) H. W. Iversen.
'Performance of the Periphery Pump'.
Trans. ASME, Vol. 77, January 1955, pp. 19-22.

(5) L. Lazo and T. Hopkins.
'Theoretical and Experimental Analysis of Regenerative Turbine Pumps'.
Senior Thesis, Massachusetts Institute of Technology, Cambridge, Mass., January 1953.

(6) G. F. Lutz.
'Experimental Investigation of the Pressure Distribution in a Regenerative Turbine PUmp, the Sta-Rite TH-7'.
Senior Thesis, Massachusetts Institute of Technology, Cambridge, Mass., May 1953.

(7) W. A. Wilson, M. A. Santalo and J. A. Oelrich.
'Theory of Fluid-Dynamic Mechanism of Regenerative Pumps'.
Trans. ASME, Vol. 77, No. 8, November 1955, pp. 1303-11.

(8) C. Pfleiderer.
'Die Kreiselpumpen fur Flussigkeiten und Gase'.
1949 Translation, Third Edition, British Hydromechanics Research Association, Publication No. T448, February 1953.

(9) Jerome Bartels.
Discussion, Ref. (4).

(10) A. M. Wright.
Discussion, Ref. (4).

(11) Y. Senoo.
'Comparison of Regenerative Pump Theories supported by New Performance Data'.
ASME, Trans., Vol. 77, No. 8, November 1955, p. 1312.

(12) G. F. Wislicenus.
Discussion, Ref. (7).

(13) E. Crewdson and E. A. Jackson.
'Water-Ring Self-Priming Pumps'.
Inst. Mech. Engrs. - Proc. Vol. 170, No. 13, 1956, pp. 407-17.

(14) F. S. Weinig.
'Analysis of Traction Pumps'.
ASME No. 55-SA-35, Meeting June, 1955 (19 p).

(15) S. Hasinger.
'Study of Peripheral Pump'.
US Air Force, Wright Air Department Centre, WADC Tech. Report 57-333, May 1957 (64 p).

(16) W. A. Wilson, M. A. Santalo and J. A. Oelrich.
'Relationship of Regenerative Pump Performance to Casing Geometry'.
ASME n 54-A-60, Meeting November 1954 (15 p).

(17) M. Shimosaka and S. Yamazaki.
'Research on Characteristic of Regenerative Pump - 1'.
'Influence of Flow-channel and Impeller'.
Japan Soc. Mech. Engrs. - BUL Vol. 3 No. 10, May 1960, pp. 185-99.

(18) M. J. Kocwin.
'Liquid-ring Pumps for Handling Gases and Vapours'.
Sulzer Tech. Rev. Vol. 55, No. 2, 1973, pp. 63-71.

(19) A. Brown and K. J. Wilcox.
'Rotary Pumps'.
Eng. Mater Des. Vol. 18, No. 10, November 1974, pp. 23-25.

(20) H. E. Wilson.
Discussion, Ref. (4).

(21) H. Schlichting.
'Boundary-layer Theory'.
McGraw-Hill Book, 6th Edition.

(22) M. H. Vavra.
'Aero-Thermodynamics and Flow in Turbomachines'.
John Wiley & Sons, Inc., 1960.

(23) S. Lazarkiewicz and A. Troskolanski.
'Impeller Pumps'.
Wydawnictwa Naukowo-Techniczne.
Warszawa 1965.

(24) H. Sixsmith.
'Carry-over Loss in the Stripper Seal of a Regenerative Compressor'.
Dept. of Engineering Science, University of Oxford, Parks Road,
Oxford OX1 3PJ.

(25) F. J. Wallace.
'Theoretical Assessment of the Performance Characteristics of Inward Radial Flow Turbines'.
Proc. Inst. Mech. Engrs. 1958, 172, pp. 931-952.

(26) S. M. Futral and C. A. Wasserbauer.
"Off-design Performance Prediction with Experimental Verification for a Radial-inflow Turbine'.
NASA TN D-2621.

(27) C. Rodgers.
'Efficiency and Performance Characteristics of Radial Turbines'.
SAE Trans. 1969.

(28) E. A. Bridle and R. A. Boulter.
'A Simple Theory for the Prediction of Losses in the Rotors of Inward Radial Flow Turbines'.
Proc. Inst. Mech. Engrs. 1967-68, 182 (Pt 3H), 393-405.

(29) T. Sawad and A. Nishi.
'Investigations of Radial Inflow Turbine, 2nd Report, a Method of Performance Estimation for Variable Geometry Radial Inflow Turbine'.
Bull J.S.M.E. 1970, 13, No. 62.

(30) A. Whitfield and F. J. Wallace.
'Study of Incidence Loss Models in Radial and Mixed-flow Turbomachinery'.
Inst. Mech. Engrs., Conference Publication 3, 1973.

(31) W. Spannhake.
'Centrifugal Pumps, Turbines and Propellors'.
1934 (MIT Cambridge, Mass).

(32) C. F. Colebrook.
'Turbulent Flow in Pipes with Particular Reference to the Transition Region Between the Smooth and Rough Pipe Laws'.
J. Inst. Civil Engrs. 1939.

(33) A. J. Stepanoff.
'Centrifugal and Axial Flow Pumps'.
(2nd Edition), Wiley, New York, 1957.

(34) G. F. Wislicenus.
'Fluid Mechanics of Turbomachinery'.
(2nd Edition), Dover, New York, 1965.

(35) D. G. Shepherd.
'Principles of Turbomachinery'.
Macmillan, New York, 1956.

(36) B. S. Massey.
'Mechanics of Fluids'.
(2nd Edition), Van Nostrand Reinhold, London 1970.

(37) J. D. Stanitz.
'Some Theoretical Aerodynamic Investigations of Impellers in Radial and Mixed Flow Centrifugal Compressors'.
Trans. ASME 74, 4, 1952.

(38) G. T. Csanady.
'Head Correction Factors for Radial Impellers'.
Engineering, London, 190, 1960.

(39) F. J. Wiesner.
'A Review of Slip Factor for Centrifugal Impellers'.
ASME paper 66-WA-FE-18, 1966.

(40) R. W. Detra.
'The Secondary Flow in Curved Pipes'.
Mitt. Inst. Aerodyn. ETH Zurich, No. 20, 1953.

(41) H. G. Cuming.
'The Secondary Flow in Curved Pipes'.
ARC RM 2880, 1955.

(42) H. Ito.
'Friction Factors for Turbulent Flow in Curved Pipes'.
J. Basic Eng. 81D, 123-34, 1959.

(43) H. Ito.
'Pressure Losses in Smooth Pipe Bends'.
J. Basic Eng. 82D, 131-43, 1960.

(44) T. B. Ferguson.
'The Centrifugal Compressor Stage'.
Butterworth, London (1963).

(45) O. Reynolds.
'On the Dynamic Theory of Incompressible Viscous Fluids and the Determination of the Criterion'.
Phil. Trans. Roy. Soc. T 186, A 123, or Sci. Papers I, 355.

(46) J. W. Daily and R. Nece.
'Chamber Dimension Effects on Induced Flow and Frictional Resistance of Enclosed Rotating Discs'.
J. Basic Eng. Trans ASME, 1960, 82, 217.

(47) R. Sivalingam.
"Flow Modelling and Computer-Aided Design of Fluid Couplings and Torque Converters'.
PhD Thesis, Bath University 1977.

(48) M. Shimosaka.
'Researches on the Characteristics of Regenerative Pump'.
2nd Report 'Theoretical Research on Performance'.
Bulletin of J.S.M.E., Vol. 3, No. 10, 1960, 191-9.

(49) J. Bartels.
'Initial Analysis of Operation of the Regenerative Pump'.
Graduate Thesis, New York University, 1947.

(50) S. Yamazaki and Y. Tomita.
'Researches on the Performance of the Regenerative Pump with Non-radial Vanes', 1st Report 'Performance and Inner Flow'.
J.S.M.E., Vol. 14, No. 77, 1971, 1178-1186.

(51) S. Yamazaki.
'Research on the Performance of the Regenerative Pump with Non-radial Vanes. 3rd Report ' An Analysis of the Pump Performance'.
Bulletin of J.S.M.E., Vol. 17, No. 106, April 1974.

(52) J. D. Burton.
'A Theoretical and Experimental Analysis of the Flow in Regenerative Pumps and Turbines'.
Ph.D. Thesis, Southampton University, 1966.

(53) R. J. Vrana.
'Regenerative Blower Replaces High Capacity Compressor'.
Design News 29(6), p. 137, 1974.

(54) G. Grabow.
'Influence of the Number of Vanes and Vane on the Suction Behaviour of Regenerative Pumps'.
1975 Budapest Fluid Machinery Conference.

(55) M. D. Croker.
'Pressure, Flow and Noise Performance of Toroidal Blowers'.
Report No. ME/77/9, May 1977.

APPENDIX A

FLOW EQUATIONS FOR REGENERATIVE MACHINES

A.1 General Equilibrium Conditions

The equation of motion of flows in a rotor with an infinite number of blades rotating at a constant angular velocity is, see ref. (22):

$$\frac{\partial \bar{W}}{\partial t} + \bar{\nabla} H_R = \bar{W} \times (\bar{\nabla} \times \bar{W} + 2\bar{\omega}) + T\bar{\nabla}s + \bar{f} + \bar{F}_b \qquad (A.1)$$

where H_R is the relative total enthalpy which is defined by the following expression:

$$H_R = h + \frac{W^2}{2} - \frac{\omega^2 r^2}{2} + gz \qquad (A.2)$$

Equation (A.1) is valid for all flow fields where the fluid properties can be expressed by uniform continuous point functions. It holds at any time at any location where the fluid has the following parameters:

$\bar{W}$ = the fluid velocity relative to the rotor at the location.
r = the radial co-ordinate of the location from the axis of the rotor.
z = the vertical distance of the location from a reference surface.
T = the temperature of the fluid.
s = its specific entropy.
h = its specific enthalpy.
$\bar{f}$ = the frictional force per unit mass of the fluid.
$\bar{F}_b$ = the force exerted by the blade on the flow per unit mass.
$\bar{\omega}$ = the angular velocity of the rotor.
g = acceleration due to gravity.
t = time

For steady isentropic flows in a rotor equation (A.1) reduces to the form:

$$\bar{\nabla} H_R = \bar{W} \times (\bar{\nabla} \times \bar{W} + 2\bar{\omega}) + \bar{F}_b \qquad (A.3)$$

Expressions for the three terms of this equation are obtained as follows using the orthogonal system of co-ordinates ($\hat{i}_\theta$, $\hat{i}_m$, $\hat{i}_n$) which has been defined in Fig. (2.4) of the main text.

The blade force $\bar{F}_b$:

Since in writing equation (A.3) the assumption has been made that the flow is isentropic, the blade force $\bar{F}_b$ must be perpendicular to the blade surface everywhere, i.e. $\bar{F}_b$ must be parallel to the normal vector $d\bar{S}$ of the blade surface which can be expressed in terms of the blade geometry defined in Chapter (4) in the following way; see Vavra (22):

$$d\bar{S} = dm\ dn\ (\hat{i}_\theta - \hat{i}_m \tan(\beta) + \hat{i}_n \tan(\beta) \tan(\delta)) \qquad (A.4)$$

The blade force can be written in the form:

$$\bar{F}_b = F_u \left(\hat{i}_\theta + \frac{F_m}{F_u} \hat{i}_m + \frac{F_n}{F_u} \hat{i}_n\right) \qquad (A.5)$$

At any location on the blade surface there is:

$$\bar{F}_b \times d\bar{S} = 0 \qquad (A.6)$$

Substituting equations (A.4) and (A.5) into equation (A.6), the following are obtained:

$$\frac{F_m}{F_u} = -\tan(\beta) \quad \text{and} \quad \frac{F_n}{F_u} = \tan(\beta) \tan(\delta)$$

Substituting these into equation (A.5), the blade force can be expressed in terms of F_u, β and δ as follows:

$$F_b = F_u \left(\hat{i}_\theta - \tan(\beta)\ \hat{i}_m + \tan(\beta) \tan(\delta)\ \hat{i}_n\right) \qquad (A.7)$$

The gradient $\bar{\nabla}H_R$:

$$\bar{\nabla}H_R = \frac{1}{r} \frac{\partial H_R}{\partial \theta} \hat{i}_\theta + \frac{\partial H_R}{\partial m} \hat{i}_m + \frac{\partial H_R}{\partial n} \hat{i}_n \qquad (A.8)$$

Expansion of $\bar{W} \times (\bar{\nabla} \times \bar{W} + 2\bar{\omega})$:

A detailed expansion of this expression is given in ref. (22). Here the final result is given:

$$\bar{W} \times (\bar{\nabla} \times \bar{W} + 2\bar{\omega}) = \frac{W_m}{r}\left[\frac{\partial W_n}{\partial \theta} - \frac{\partial}{\partial m}(rW_\theta + r^2)\right]\hat{i}_\theta$$

$$+ \frac{W_\theta}{r}\left[\frac{\partial}{\partial m}(rW_\theta + \omega r^2) - \frac{\partial W_m}{\partial \theta}\right]\hat{i}_m$$

$$+ \frac{W_\theta}{r}\left[\frac{\partial}{\partial n}(rW_\theta + \omega r^2) - \frac{\partial W_n}{\partial \theta} - W_m \frac{\partial W_n}{\partial m} + W_m \frac{\partial W_m}{\partial n} + W_m{}^2 k_m\right]\hat{i}_n \qquad (A.9)$$

where k_m is the curvature of the streamline at a point.

Substituting equations (A.7), (A.8) and (A.9) into equation (A.3), the following terms are obtained:

The i_θ term:

Collecting the i_θ - terms, the following equation is obtained:

$$F_u + \frac{W_m}{r}\left[\frac{\partial W_m}{\partial \theta} - \frac{\partial}{\partial m}(rW_\theta + \omega r^2)\right] - \frac{1}{r}\frac{\partial H_R}{\partial \theta} = 0 \qquad (A.10)$$

From this equation the specific torque of the tangential component of the blade force can be obtained at any location. For an axi-symmetric velocity field the torque is given by:

$$rF_u = W_m \frac{\partial}{\partial m}(rW_\theta + \omega r^2) + \frac{\partial H_R}{\partial \theta} \qquad (A.11)$$

From which it can be seen that the specific torque of a blade of a regenerative pump must be greater than that of other rotodynamic machines because in the former there is a sustantial tangential energy gradient while in the latter $\partial H/\partial \theta = 0$.

The i_m term:

The i_m - component of equation (A.3) when expanded is:

$$\frac{W_\theta}{r}\frac{\partial}{\partial m}(rW_\theta + \omega r^2) - \frac{\partial W_m}{\partial \theta} - F_u \tan(\beta) - \frac{\partial H_R}{\partial m} = 0 \qquad (A.12)$$

Substituting for F_u from equation (A.11) and using the axi-symmetric assumption, the following equation is obtained:

$$\frac{W_\theta}{r}\ \frac{\partial}{\partial m}\ (W_\theta + \omega r^2) - \frac{W_m}{r}\ \tan(\beta)\ \frac{\partial}{\partial m}\ (rW_\theta + \omega r^2) - \frac{\tan(\beta)}{r}\ \frac{\partial H_R}{\partial \theta} - \frac{\partial H_R}{\partial m} = 0 \qquad (A.1$$

since at any location in the impeller the relative tangential velocity is given by, see Chapter (4):

$$W_\theta = W_m \tan(\beta) \qquad (A.14)$$

the first two terms of equation (A.13) cancel out and it reduces to the following form:

$$\frac{\partial H_R}{\partial m} = -\frac{\tan(\beta)}{r}\ \frac{\partial H_R}{\partial \theta} \qquad (A.15)$$

From this equation it can be seen that if the blade angle (β) is different from zero, the relative total enthalpy H_R changes along the co-ordinate m in a meridional plane in regenerative pumps. This is in contrast with the cases in other rotodynamic machines where $\partial H/\partial\theta = 0$ and where from equation (A.15) above H_R is constant along the co-ordinate m irrespective of the blade shape.

However, it must be pointed out that these m-co-ordinates are the generatrices of the stream surface: they are not streamlines. Along streamlines the relative total enthalpy remains constant irrespective of the presence of the tangential energy gradient as will be shown in the following:

At any location in the impeller the tangent of the blade angle is given by, see Fig. (4.4):

$$\tan(\beta) = \frac{r d\theta}{dm} \qquad (A.16)$$

Equation (A.15) can then be put in the form:

$$\frac{\partial H_R}{\partial m}\ dm + \frac{\partial H_R}{\partial \theta}\ d\theta = 0 \qquad (A.17)$$

The total change of the relative rotal enthalpy is given by its total derivative dH_R where:

$$dH_R = \frac{\partial H_R}{\partial \theta}\ d\theta + \frac{\partial H_R}{\partial m}\ dm + \frac{\partial H_R}{\partial n}\ dn \qquad (A.18)$$

Since along a streamline the co-ordinate n does not change, i.e. $dn = 0$, then the total change of the relative total enthalpy along a streamline is:

$$dH_R = \frac{\partial H_R}{\partial \theta} d\theta + \frac{\partial H_R}{\partial m} dm \qquad (A.19)$$

Comparing equation (A.19) with equation (A.17), it can be seen that along a streamline:

$$dH_R = 0 \qquad (A.20)$$

Hence, the relative total enthalpy does not change along a streamline in a regenerative impeller as is the case in any other rotodynamic rotor. This is a necessary consequence of the general energy equation for steady adiabatic relative flows with or without friction, see ref. (22).

A.2 Change of Energy Across the Impeller

The total energy of a fluid particle is given by:

$$H = h + \frac{V^2}{2} + gz \qquad (A.21)$$

where:

H = absolute total enthalpy

V = absolute total velocity which is given by:

$$\bar{V} = \bar{W} + \bar{\omega} \times \bar{r}$$

where:

$\bar{\omega} \times \bar{r} = \omega r \, \hat{i}_\theta$

Then $V^2 = (W_\theta + \omega r)^2 + W_r^2 + W_z^2$

$= W^2 + 2\omega r V_\theta - \omega^2 r^2$

Therefore $H = h + \frac{W^2}{2} - \frac{\omega^2 r^2}{2} + gz + \omega r V_\theta \qquad (A.22)$

Comparing equation (A.22) with equation (A.15), there is:

$$H = H_R + \omega r V_\theta \qquad (A.23)$$

Substituting for H_R from this equation into equation (A.15), there is:

$$\frac{\partial H}{\partial m} = \frac{\partial (\omega r V_\theta)}{\partial m} - \frac{\tan(\beta)}{r} \frac{\partial H}{\partial \theta} \tag{A.24}$$

The total change of the total energy of the fluid particle along a streamline (dn = 0) is:

$$dH = \frac{\partial H}{\partial m} dm + \frac{\partial H}{\partial \theta} d\theta \tag{A.25}$$

This equation can be integrated from point (1) at the inlet to the impeller to point (2) at the exit from it to give the total change of the total energy of a fluid particle which follows a streamline between the two locations. Thus:

$$H_2 - H_1 = \int_1^2 \frac{\partial H}{\partial m} dm + \int_1^2 \frac{\partial H}{\partial \theta} d\theta \tag{A.26}$$

Substituting for $\frac{\partial H}{\partial m}$ from equation (A.24) and using equation (A.16), there is:

$$H_2 - H_1 = \int_1^2 \left[\frac{\partial}{\partial m} (\omega r V_\theta) - \frac{d\theta}{dm} \frac{\partial H}{\partial \theta} \right] dm + \int_1^2 \frac{\partial H}{\partial \theta} d\theta$$

i.e.

$$H_2 - H_1 = \omega(r_2 V_{\theta 2} - r_1 V_{\theta 1}) + \int_1^2 \frac{\partial H}{\partial \theta} d\theta \tag{A.27}$$

If the tangential energy gradient is assumed constant along the streamline, then:

$$H_2 - H_1 = \omega(r_2 V_{\theta 2} - r_1 V_{\theta 1}) + \frac{\partial H}{\partial \theta} (\theta_2 - \theta_1) \tag{A.28}$$

$(H_2 - H_1)$ is the total energy change that a fluid particle experiences each time it passes through the impeller.

The first term on the RHS of equation (A.28) is the familiar Euler head. The second term is the energy added to the particle because of its angular displacement in a field in which there is a tangential energy gradient. $(\theta_2 - \theta_1)$ is the angular displacement between point (1), at the inlet to the blades, and point (2) at the exit from them.

Exactly the same expression for the total energy change, equation (A.28), can be obtained for any steady adiabatic flow with or without friction by applying the unrestricted law of moment of momentum.

A.3 Incompressible Flow

For steady isentropic flow the equation of motion in a rotor of infinite number of blades is, see ref. (22), given by:

$$\bar{\nabla}\left(\frac{p_{SR}}{\rho}\right) = \bar{W} \times (\bar{\nabla} \times \bar{W} + 2\bar{\omega}) + \bar{F}_b \tag{A.29}$$

where p_{SR}, the relative total pressure, is defined by the equation:

$$\frac{p_{SR}}{\rho} = \frac{p}{\rho} + \frac{W^2}{2} - \frac{\omega^2 r^2}{2} + gz \tag{A.30}$$

p = static pressure of the fluid.

The procedure used to derive equation (A.28) can be repeated here to obtain the following expression:

$$\frac{1}{\rho}(p_{S2} - p_{S1}) = \omega(r_2 V_{\theta 2} - r_1 V_{\theta 1}) + \frac{\partial}{\partial \theta}\left(\frac{p_S}{\rho}\right)(\theta_2 - \theta_1) \tag{A.31}$$

where p_S is the total or stagnation pressure defined by the following equation:

$$p_S = p + \rho\frac{V^2}{2} + \rho gz \tag{A.32}$$

Equation (A.31) gives the total change of fluid energy across the impeller because the flow is assumed isentropic and the difference in the total pressure is equal to the change in the total energy. The same equation can also be obtained in the following way:

From thermodynamics:

$$\frac{\bar{\nabla}p}{\rho} = \bar{\nabla}h - T\bar{\nabla}s \tag{A.33a}$$

Then for isentropic flows there is:

$$\frac{\bar{\nabla}p}{\rho} = \bar{\nabla}h \tag{A.33b}$$

Since ρ = constant, there is from this equation:

$$\bar{\nabla}\left(\frac{p}{\rho}\right) = \bar{\nabla}h \tag{A.33c}$$

With equation (A.33b) and comparing equation (A.30) with equation (A.2), there is for isentropic incompressible flows:

$$\bar{\nabla}\left(\frac{p_{SR}}{\rho}\right) = \bar{\nabla}H_R \tag{A.34}$$

Similarly:

$$\bar{\nabla}\left(\frac{p_S}{\rho}\right) = \bar{\nabla}H \tag{A.35}$$

Then all relations derived earlier for a steady isentropic flow can be reduced to fit incompressible steady isentropic flows by replacing H_R by $\frac{p_{SR}}{\rho}$ and H by $\frac{p_S}{\rho}$. Then equation (A.31) can be directly obtained from equation (A.28).

Since the velocity field is assumed to be axi-symmetric, the following is obtained from equation (A.32), ignoring the variation in z:

$$\frac{\partial}{\partial\theta}\left(\frac{p_S}{\rho}\right) = \frac{\partial}{\partial\theta}\left(\frac{p}{\rho}\right) \tag{A.36}$$

Then equation (A.31) can be written as:

$$\frac{1}{\rho}\left(p_{S2} - p_{S1}\right) = \omega(r_2V_{\theta 2} - r_1V_{\theta 1}) + \frac{\partial}{\partial\theta}\left(\frac{p}{\rho}\right)(\theta_2 - \theta_1) \tag{A.37}$$

This equation is obtained assuming isentropic flows. In such flows the increase in the stagnation pressure is equal to the increase in the total energy of the fluid. However, in actual flows where there is friction, this equality does not hold. Hence in more general form the difference of the stagnation pressure in the equation should be replaced by the difference in the total energy of the fluid and the former can then be obtained by deducting frictional losses from the expression, i.e.

$$\Delta e_{12} = \omega(r_2V_{\theta 2} - r_1V_{\theta 1}) + \frac{\partial}{\partial\theta}\left(\frac{p}{\rho}\right)(\theta_2 - \theta_1) \tag{A.38}$$

where Δe_{12} is the specific increase in the total energy of the fluid

between points 1 and 2. The increase in the useful energy of the fluid ($= p_{S2} - p_{S1}$) is then obtained by deducing the losses encountered between the two locations.

It must be mentioned that although $(H_2 - H_1)$ of equation (A.28) and Δe_{12} of equation (A.38) represent the difference in the total energy of the fluid, they are not equal. This is because, in the former equation the gradient of the total energy $\partial H/\partial\theta$ is used to compute $(H_2 - H_1)$, while in the latter equation the useful energy gradient $\frac{\partial}{\partial\theta}\left(\frac{p}{\rho}\right)$ is used. The two gradients are not equal when friction is considered, see equation (A.33a). Losses which are to be deduced from the two terms are therefore not the same: they must be such that:

$$(H_2 - H_1) - L_1 - L_2 = \Delta e_{12} - L_2 \qquad (A.39)$$

where:

L_1 = losses to be deducted from $\frac{\partial H}{\partial\theta}(\theta_2 - \theta_1)$ to make it equal to $\frac{\partial}{\partial\theta}\left(\frac{p}{\rho}\right)(\theta_2 - \theta_1)$. They are the losses which occur in the tangential direction and hence they are zero in rotodynamic machines which have no tangential energy gradients.

L_2 = losses to be deducted from Euler head. They are the losses which are encountered because of the energy gradients in directions other than the θ-direction. They occur, therefore, in all rotodynamic machines.

Note that L_1 does not necessarily have to be evaluated since it suffices to know, or to assume, the tangential gradient of the useful energy $\frac{1}{\rho}\frac{\partial p}{\partial\theta}$ to use equation (A.38).

A.4 Effect of Slip

The following is not an attempt to formulate a slip factor for regenerative machines: rather, it is intended to investigate the hitherto unconsidered importance of tangential pressure gradient.

(a) Conventional models

The best of the known theoretical methods of assessing the slip effect, e.g. those of Stodola and Busemann, see ref. (34) and (35), disregard the effect of friction. Along with this they assume the flow to be steady and isentropic. With such assumptions the equation of motion for relative flows in passages of finite dimensions rotating at constant angular velocity is, from equation (A.1):

$$\bar{\nabla}H_R = \bar{W}x(\bar{\nabla}x\bar{W} + 2\bar{\omega}) \tag{A.40}$$

i.e $$\bar{\nabla}H_R = Wx(\bar{\xi} + 2\bar{\omega}) \tag{A.41}$$

where $\bar{\xi}$ is the relative vorticity of the flow.

The above equation may be expanded in the form:

$$\frac{\partial H_R}{\partial r}\hat{i}_r + \frac{1}{r}\frac{\partial H_R}{\partial \theta}\hat{i}_\theta + \frac{\partial H_R}{\partial z}\hat{i}_z = (W_\theta \xi_z - W_z \xi_\theta + 2W_\theta\omega)\hat{i}_r$$

$$- (W_r \xi_z - W_z \xi_r + 2W_r\omega)\hat{i}_\theta$$

$$+ (W_r \xi_\theta - W_\theta \xi_r)\hat{i}_z \tag{A.42}$$

since $\omega = \omega \hat{i}_z$.

The conventional expression for the axial vorticity in rotodynamic machines is obtained by making two further assumptions:

1) The total energy of the absolute flow before entry to the rotor is constant everywhere. One of the requirements of this is that the flow is axi-symmetric and in particular $\partial H/\partial\theta = 0$. Thus, if suffix 1 refers to the inlet to the rotor everywhere, there is:

$$H_1 = \text{constant} \tag{A.43}$$

2) The absolute velocity before entry to the rotor has peripheral velocity components which vary inversely with the radius, i.e. a free vortex flow, or:

$$r_1 V_{\theta 1} = \text{constant} \tag{A.44}$$

With equations (A.43) and (A.44), equation (A.23) yields the following:

$$H_{R1} = \text{constant} \tag{A.45}$$

Hence, using the general equation (A.20), the total relative enthalpy H_R must be an absolute constant equal to H_{R1} everywhere in the relative flow field. Then it follows from eqution (A.41) that:

$$\bar{\xi} = -2\bar{\omega} = \text{constant} \tag{A.46}$$

This establishes the condition that the vorticity of the relative flows specified above is constant and that the elementary rotation of the fluid particles is equal and opposite to the rotation of the rotor, since the vorticity of a fluid particle is twice its angular velocity, see Vavra (22).

For these special flows, the i_θ - component of equation (A.42) gives:

$$\xi_z = -2\omega + \frac{W_z}{W_r} \xi_r \tag{A.47}$$

Now if the further assumption is made that the flow is wholly radial at rotor exit, this equation reduces to:

$$\xi_z = -2\omega \tag{A.48}$$

i.e. the relative angular velocity of the flow in the axial direction is equal and opposite to the angular velocity of the rotor. This is the condition used by Stodala to obtain the following well known and accepted expression for the slip factor:

$$\sigma = 1.0 - \frac{U_2}{V_{\theta 2}} \frac{\pi \sin \beta_2}{Z} \tag{A.49}$$

where Z is the number of blades.

(b) Effect of tangential energy gradient

Assumptions (1) and (2) above cannot be made for regenerative machines. Therefore the i_o - component of equation (A.42) gives:

$$\xi_z = - \left(2\omega + \frac{1}{r}\frac{1}{W_r}\frac{\partial H_R}{\partial \theta}\right) + \frac{W_z}{W_r}\xi_r \qquad (A.50)$$

If, in common with conventional approaches, the flow is assumed to be wholly radial at rotor exit, this equation gives:

$$\xi_z = - \left(2\omega + \frac{1}{r}\frac{1}{W_r}\frac{\partial H_R}{\partial \theta}\right) \qquad (A.51)$$

In comparison with equation (A.48), this equation shows that in regenerative machines, since W_r and $\partial H_R/\partial\theta$ are both positive, the intensity of the axial vorticity is enhanced by the presence of the tangential energy gradient. The relative rotation of the fluid particles is therefore of greater magnitude than the rotation of the impeller.

The above equation can be put in the form:

$$\xi_z = - 2\omega \left(1.0 + 2 \left(\frac{\omega r_2}{W_{r2}}\right) \frac{\psi}{\theta_p}\right) \qquad (A.52)$$

where:

$\frac{\omega r_2}{W_{r2}}$ = ratio of impeller speed to the relative radial velocity of fluid.

$\frac{\psi}{\theta_p}$ = non-dimensional tangential pressure gradient.

The magnitude of the bracketed term of equation (A.52) is investigated in Chapter 6 using the velocities obtained from the computer model.

In general, however, equation (A.50), rather than equation (A.51), should be used to determine the axial vorticity of the relative flow. For example, the assumption that the meridional circulation in regenerative machines has its centre in the axial outlet plane of the impeller automatically means that $W_r = 0$ everywhere in this plane.

Obviously equation (A.51) cannot describe the vorticity in this plane because, unlike equation (A.50), it assumes that the flow is wholly radial.

APPENDIX B

FLOW EQUATIONS IN TERMS OF STREAMFUNCTION

B.1 Flow Inside the Impeller

Following the axi-symmetric approach, it was shown in section (4.3.1) that the problem of solving the flow inside the impeller reduced to finding the meridional velocity components. The streamfunction $\psi = \psi(r, z)$ has been defined in Chapter 4 such that these components are given by:

$$V_r = \frac{1}{B}\frac{1}{r}\frac{\partial \psi}{\partial z} \tag{B.1}$$

and $$V_z = -\frac{1}{B}\frac{1}{r}\frac{\partial \psi}{\partial r}$$

where B is the blockage factor defined by equation (4.4) as:

$$B = 1.0 - \frac{Zt}{2\pi r}\frac{1}{\cos\beta}\sqrt{1.0 + \sin^2(\beta)\ \tan^2(\delta)} \tag{B.3}$$

In general, the blade thickness t, the relative flow angle β and the angle δ are all functions of r and z.

Employing a streamfunction relationship, equation (4.1) and (4.5) may be used to determine the two angles at any location. The blade thickness t, however, is required to be specified as a function of r and z so that equation (B.3) may be evaluated at any point inside the impeller. Two cases may be considered:

1) Constant blade thickness

It may be assumed that the blade thickness is constant over the blade surface.

In this case the meridional velocities V_r and V_z will necessarily have discontinuities at the blade edges if the blade thickness is finite. This may represent the actual situation at the blade edges of impellers where the sudden change in flow area causes discontinuities and eddies.

However, it is usual practice to assume continuous meridional

velocities and hence to ignore the effect of flow area change in a first approximation, see section (2.4). Accordingly, it has been assumed throughout this work that the meridional velocity just outside the impeller is the same as that just inside it. To maintain consistency, therefore, it has to be assumed that the blade thickness at the edges is zero. This situation cannot be described when a constant finite blade thickness is assumed.

Consistency can be maintained by considering the blade to be of variable thickness.

2) Variable blade thickness

The objective is to account for the blade thickness in such a way that the thickness at the edges may be set equal to zero.

This may be achieved by considering that along the edges the blade has the same thickness t_e which may be zero. The thickness at any other point on the blade is assumed to vary linearly with both r and z. Using the symbols of Fig. (4.7), the thickness at any point is given by:

$$t = t_e + ZZ(t_r - t_e) - \frac{r - R_i}{R_o - R_i} ZZ(t_r - t_e) \qquad (B.4)$$

where:

t = blade thickness at any location

t_e = blade thickness at the edges

t_r = maximum thickness at the root of blade.

Other symbols are as shown in Fig. (4.7).

The blockage factor may then be evaluated from equation (B.3) and the meridional velocity components determined from equations (B.1) and (B.2) at any point inside the impeller.

B.2 Flow in the Channel

In the channel there are no blades. Therefore equations (B.1) and (B.2) may be put without the blockage factor:

$$V_r = \frac{1}{r}\frac{\partial \psi}{\partial z} \tag{B.5}$$

$$V_z = -\frac{1}{r}\frac{\partial \psi}{\partial r} \tag{B.6}$$

The solution of the flow in the channel involves the solution of the equation of motion: (see equations (2.10) and (2.13))

$$(\bar{V}.\bar{\nabla})\bar{V} = -\bar{\nabla}\left(\frac{p}{\rho}\right) + (\nu + \varepsilon)\bar{\nabla}^2\bar{V} \tag{B.7}$$

which was discussed in detail in chapter 2.

The two meridional components of this equation were obtained as:

$$V_r\frac{\partial V_r}{\partial r} + V_z\frac{\partial V_r}{\partial z} - \frac{V_\theta^2}{r} = -\frac{1}{\rho}\frac{\partial p}{\partial r} + (\nu + \varepsilon)\left[\frac{\partial^2 V_r}{\partial r^2} + \frac{1}{r}\frac{\partial V_r}{\partial r} + \frac{\partial^2 V_r}{\partial z^2} - \frac{V_r}{r^2}\right] \tag{B.8}$$

$$V_r\frac{\partial V_z}{\partial r} + V_z\frac{\partial V_z}{\partial z} = -\frac{1}{\rho}\frac{\partial p}{\partial z} + (\nu + \varepsilon)\left[\frac{\partial^2 V_z}{\partial r^2} + \frac{1}{r}\frac{\partial V_z}{\partial r} + \frac{\partial^2 V_z}{\partial z^2}\right] \tag{B.9}$$

The θ-component of the equation of motion:

$$\frac{1}{\rho}\frac{\partial p}{\partial \theta} = \text{constant} \tag{B.10}$$

does not require substitution in terms of the streamfunction.

All the differentials of V_r and V_z which appear in equations (B.8) and (B.9) are to be expressed in terms of the streamfunction.

From equations (B.5) and (B.6) there is:

$$\frac{\partial V_r}{\partial r} = \frac{1}{r}\frac{\partial}{\partial r}\frac{\partial \psi}{\partial z} - \frac{1}{r^2}\frac{\partial \psi}{z} \tag{B.11}$$

$$\frac{\partial V_r}{\partial z} = \frac{1}{r}\frac{\partial^2 \psi}{\partial z^2} \tag{B.12}$$

$$\frac{\partial V_z}{\partial r} = \frac{1}{r^2}\frac{\partial \psi}{\partial r} - \frac{1}{r}\frac{\partial^2 \psi}{\partial r^2} \tag{B.13}$$

$$\frac{\partial V_z}{\partial z} = -\frac{1}{r}\frac{\partial}{\partial z}\frac{\partial \psi}{\partial r} \tag{B.14}$$

$$\frac{\partial^2 V_r}{\partial r^2} = \frac{1}{r}\frac{\partial^2}{\partial r^2}\frac{\partial \psi}{\partial z} - \frac{2}{r^2}\frac{\partial}{\partial r}\frac{\partial \psi}{\partial z} + \frac{2}{r^3}\frac{\partial \psi}{\partial z} \tag{B.15}$$

$$\frac{\partial^2 V_r}{\partial z^2} = \frac{1}{r}\frac{\partial^3 \psi}{\partial z^3} \tag{B.16}$$

$$\frac{\partial^2 V_z}{\partial r^2} = \frac{2}{r^2}\frac{\partial^2 \psi}{\partial r^2} - \frac{2}{r^3}\frac{\partial \psi}{\partial r} - \frac{1}{r}\frac{\partial^3 \psi}{\partial r^3} \tag{B.17}$$

$$\frac{\partial^2 V_z}{\partial z^2} = -\frac{1}{r}\frac{\partial^2}{\partial z^2}\frac{\partial \psi}{\partial r} \tag{B.18}$$

The above derivatives are easily evaluated at any point in the channel once the streamfunction equation is chosen. The appropriate differentials of the latter are derived, in general notation, in the following section.

B.3 Differentials of Streamfunction

The equation of the streamfunction chosen in chapter 4 is given by:

$$\psi = A(1.0 - RR^a)^b\ (1.0 - ZZ^c)^d \tag{B.19}$$

where, referring to Fig. (4.7a):

$$\text{In sectors I and IV : } RR = \frac{r - R_m}{R_o - R_m} = \frac{r - R_m}{Y} \tag{B.20}$$

$$\text{In sectors II and III : } RR = \frac{R_m - r}{R_m - R_i} = \frac{R_m - r}{Y} \tag{B.21}$$

(the non-dimensionalising length Y has different values in the two equations).

$$\text{In sectors I and II (z is +ve) : } ZZ = \frac{z}{Z_c} = \frac{z}{X} \tag{B.22}$$

$$\text{In sectors III and IV (z is -ve) : } ZZ = \frac{z}{-X_b} = \frac{z}{-X} \tag{B.23}$$

(the non-dimensionalising length X stands for the width of the channel and the width of the impeller respectively in the above two equations).

Equation (4.19) can be put in the following form which is more suitable for expressing the differentials:

$$\psi = AR^b Z^d \tag{B.24}$$

where:

$$R = 1.0 - RR^a \tag{B.25}$$

$$Z = 1.0 - ZZ^c \tag{B.26}$$

Differentiating the last two equations, there is:

$$\frac{\partial R}{\partial r} = \pm a\, RR^{a-1} \frac{1}{Y} \tag{B.27}$$

$$\frac{\partial^2 R}{\partial r^2} = - a(a - 1)\, RR^{a-2} \frac{1}{Y^2} \tag{B.28}$$

$$\frac{\partial^3 R}{\partial r^3} = \pm a(a - 1)(a - 2)\, RR^{a-3} \frac{1}{Y^3} \tag{B.29}$$

$$\frac{\partial Z}{\partial z} = \pm c\, ZZ^{c-1} \frac{1}{X} \tag{B.30}$$

$$\frac{\partial^2 Z}{\partial z^2} = - c(c - 1)\, ZZ^{c-2} \frac{1}{X^2} \tag{B.31}$$

$$\frac{\partial^3 Z}{\partial z^3} = \pm c(c - 1)(c - 2)\, ZZ^{c-3} \frac{1}{X^3} \tag{B.32}$$

These expressions may then be introduced in the following differentials of ψ obtained from differentiating equation (B.24):

Differentials with respect to r:-

$$\frac{\partial \psi}{\partial r} = A\, Z^d\, b\, R^{b-1} \frac{\partial R}{\partial r} \tag{B.33}$$

$$\frac{\partial^2\psi}{\partial r^2} = A\ Z^d\ \ b(b-1)\ R^{b-2}\ \left(\frac{\partial R}{\partial r}\right)^2 + bR^{b-1}\ \frac{\partial^2 R}{\partial r^2} \qquad (B.34)$$

$$\frac{\partial^3\psi}{\partial r^3} = A\ Z^d\ \ b(b-1)(b-2)\ R^{b-3}\ \left(\frac{\partial R}{\partial r}\right)^3 + b(b-1)\ R^{b-2}\ 2\ \frac{\partial R}{\partial r}\ \frac{\partial^2 R}{\partial r^2} +$$

$$+ b(b-1)\ R^{b-2}\ \frac{\partial R}{\partial r}\ \frac{\partial^2 R}{\partial r^2} + bR^{b-1}\ \frac{\partial^3 R}{\partial r^3} \qquad (B.35)$$

Differentials with respect to z:-

$$\frac{\partial\psi}{\partial z} = A\ R^b\ d\ Z^{d-1}\ \frac{\partial Z}{\partial z} \qquad (B.36)$$

$$\frac{\partial^2\psi}{\partial z^2} = A\ R^b\ \ d(d-1)\ Z^{d-2}\ \left(\frac{\partial Z}{\partial z}\right)\ + d\ Z^{d-1}\ \frac{\partial^2 Z}{\partial z^2} \qquad (B.37)$$

$$\frac{\partial^3\psi}{\partial z^3} = A\ R^b\ \ d(d-1)(d-2)\ Z^{d-3}\ \left(\frac{\partial Z}{\partial z}\right)^3 + d(d-1)\ Z^{d-2}\ \frac{\partial^2 Z}{\partial z^2} +$$

$$+ d(d-1)\ Z^{d-2}\ \frac{\partial Z}{\partial z}\ \frac{\partial^2 Z}{\partial z^2} + d\ Z^{d-1}\ \frac{\partial^3 Z}{\partial z^3} \qquad (B.38)$$

Further differentials:

$$\frac{\partial}{\partial r}\ \frac{\partial\psi}{\partial z} = \frac{\partial}{\partial z}\ \frac{\partial\psi}{\partial r} = A\ d\ Z^{d-1}\ \frac{\partial Z}{\partial z}\ b\ R^{b-1}\ \frac{\partial R}{\partial r} \qquad (B.39)$$

$$\frac{\partial^2}{\partial r^2}\ \frac{\partial\psi}{\partial z} = \frac{\partial}{\partial z}\ \frac{\partial^2\psi}{\partial r^2} = A\ d\ Z^{d-1}\ \frac{\partial Z}{\partial z}\ \ b(b-1)\ R^{b-2}\ \left(\frac{\partial R}{\partial r}\right)^2 + b\ R^{b-1}\ \frac{\partial^2 R}{\partial r^2} \qquad (B.40)$$

$$\frac{\partial^2}{\partial z^2}\ \frac{\partial\psi}{\partial r^2} = \frac{\partial}{\partial r}\ \frac{\partial^2\psi}{\partial z^2} = A\ b\ R^{b-1}\ \frac{\partial R}{\partial r}\ \ d(d-1)\ Z^{d-1}\ \left(\frac{\partial Z}{\partial z}\right)^2 + d\ Z^{d-1}\ \frac{\partial^2 Z}{\partial z^2} \qquad (B.41$$

When the streamfunction relationship (B.19) is declared, the differentials given by equations (B.33) to (B.41) are readily computed. These are then introduced into equations (B.11) to (B.18). Then substitution can be made into the equation of motion, equations (B.8) and (B.9), for the meridional velocity components and their derivatives.

APPENDIX C

COMPUTE PROGRAMS LISTINGS

```
C   MAIN PROGRAM NAME       : REGEF1
C   LIBRARY CLASSIFICATION :
C   TITLE    : DETERMINATION OF STREAMFUNCTION RELATIONSHIP
C   PROGRAM  : FORTRAN IV       ICL 4-50       OCTOBER,1978
C              NO SPECIAL HARDWARE REQUIREMENTS
C   AUTHOR   : A. IBRAHIM
C   PURPOSE  : FOR A GIVEN HOMOLOGOUS SERIES OF REGENERATIVE PUMPS
C              THIS PROGRAM DETERMINES THE SIX PARAMETERS OF THE
C              STREAMFUNCTION RELATIONSHIP:
C              PSI=A*(1.0-RR**REX)**RN*(1.0-ZZ**ZEX)**ZN
C              SUCH THAT THE FUNCTION APPROXIMATES THE MERIDIONAL
C              VELOCITY FIELD AT SPECIFIED CIRCUMFERENTIAL PRESSURE
C              GRADIENTS
C   METHOD   : REFERENCE:- 'THEORETICAL ANALYSIS OF REGENERATIVE PUMPS'
C              A. IBRAHIM, PH.D. THESIS (BATH),1979
C   VARIABLES :-
C       TYPES : SYMBOLS USED ARE ACCORDING TO STANDARD FORTRAN IV
C       UNITS : QUANTITIES ARE MEASURED IN S.I. UNITS
C   SUBROUTINES USED: MOTION,FIRST,SECOND,STREAM,POINT2 & MATCH
C   INPUT AND OUTPUT: SEE GLOSSARY AND REFERENCE ABOVE
C
C
      PROGRAM REGEF1
C
      DIMENSION NAME(20),MODEL(20),PSIH(20),RAD(20),DRAD(20)
      DIMENSION REXA(10),ZEXA(10),RNA(10),ZNA(10),RMFA(10),ARRAY(10)
      COMMON /SRZ1/ VR,VZ,RR1,ZZ1,REX,ZEX,RN,ZN,XO,W,D,R
      COMMON /SRZ2/ RR2,ZZ2,DSC,DSSC,DSS2,PSII,RRLIM,ZZLIM
      COMMON /FIR1/ RR,ZZ,NBI,BETAO,RDIV,PI,PSTAT1,DPDR,DPDZT,OMEGA,VT1
      COMMON /FIR2/ VT2ACT,VM1,VC,VC1,VC2,VELH1,HEAD1,DPDRT1,DPDZT1
      COMMON /FIR3/ VEL,VR1,VZ1
      COMMON /MOT1/ A,MS,NS,ROI,RII,TROOT,TEDGE,EPSOL,FNIU
      COMMON /MOT2/ CHANN,IMPEL
      COMMON /SEC1/ R1,Z1,R2,Z2,F1,DPDZT2,DPDZT3,VTA,VTB,DHCM,DHCT,TOLEN
      COMMON /SEC2/ VT2,HEAD2,PSTAT2,VELH2,FRICM,FRICT,L
      COMMON /SEC3/ NDTH1,NDTH2,KPROP,KONV,CURVM,CURVT,DT,DTH,TIME,TOT
C
C   (A) INPUT INFORMATION
C   (I)-PUMP AND FLUID PARTICULARS:-
      READ(5,1)NAME
      READ(5,1)MODEL
      READ(5,3)ROI,RII,ROC,RIC,WB,WC,C
      READ(5,2)NBI,LBETA,LRDIV
      READ(5,3)EPSOL,ROUGH,SECT,BROOT,BEDGE
      READ(5,3)PASS,CHANN,SHOCK,CURVET,CURVEM,CURVEI
      READ(5,3)RGH,FNIU
```

```
C   (II)-EXPERIMENTAL PARAMETERS OF STREAMFUNCTION RELATION
      READ(5,2)MBREX,NREX,JUMREX
      READ(5,2)MBZEX,NZEX,JUMZEX
      READ(5,2)MBRN,NRN,JUMRN
      READ(5,2)MBZN,NZN,JUMZN
      READ(5,2)MBRM,NRM,JUMRM
      READ(5,3)(REXA(I),I=1,NREX)
      READ(5,3)(ZEXA(I),I=1,NZEX)
      READ(5,3)(RNA(I),I=1,NRN)
      READ(5,3)(ZNA(I),I=1,NZN)
      READ(5,3)(RMFA(I),I=1,NRM)
C   (III)-OPERATING CONDITIONS:-
      READ(5,2)MBEGP,NEP,JUMPP
      READ(5,3)(PSIN(I),I=1,NEP)
      READ(5,3)RPN
C   (IV)-MISCELANEOUS INFORMATION:-
      READ(5,3)DSCELL,DSVERT
      READ(5,3)AMMN,AULIM1,ALLIM1
      READ(5,2)MBEGS,NSTL,JUMPS,LASTS
      READ(5,2)KKONV,IALAST
      READ(5,3)(ARRAY(I),I=1,NSTL)
      READ(5,2)MDELRR,KRMA
      READ(5,2)NDTH1,NDTH2
      READ(5,2)NFLAG1,NFLAG2
      READ(5,2)KPROP,KONV,NBASIC
      READ(5,2)NOTS,NOTRM,NOTREX,NOTRN,NOTP
      READ(5,3)TOLEN,TOTVT,TOLTH,TOLDS
C   ALL PARAMETERS READ-IN ARE WRITEN OUT FOR A CHECK ;-
      WRITE(6,1)NAME
      WRITE(6,1)MODEL
      WRITE(6,6)RUI,RII,ROC,RIC,WB,WC,C
      WRITE(6,4)NBI,LBETA,LRDIV
      WRITE(6,6)EPSOL,ROUGH,SECT,BROOT,BEDGE
      WRITE(6,5)PASS,CHANN,SHOCK,CURVET,CURVEM,CURVEI
      WRITE(6,5)RGH,FNIU
      WRITE(6,4)MBREX,NREX,JUMREX
      WRITE(6,4)MBZEX,NZEX,JUMZEX
      WRITE(6,4)MBRN,NRN,JUMRN
      WRITE(6,4)MBZN,NZN,JUMZN
      WRITE(6,4)MBRM,NRM,JUMRM
      WRITE(6,5)(REXA(I),I=1,NREX)
      WRITE(6,5)(ZEXA(I),I=1,NZEX)
      WRITE(6,5)(RNA(I),I=1,NRN)
      WRITE(6,5)(ZNA(I),I=1,NZN)
      WRITE(6,5)(RMFA(I),I=1,NRM)
      WRITE(6,4)MBEGP,NEP,JUMPP
      WRITE(6,5)(PSIN(I),I=1,NEP)
      WRITE(6,5)RPN
      WRITE(6,5)DSCELL,DSVERT
      WRITE(6,5)AMMN,AULIM1,ALLIM1
      WRITE(6,4)MBEGS,NSTL,JUMPS,LASTS
      WRITE(6,4)KKONV,IALAST
      WRITE(6,5)(ARRAY(I),I=1,NSTL)
      WRITE(6,4)MDELRR,KRMA
      WRITE(6,4)NDTH1,NDTH2
      WRITE(6,4)NFLAG1,NFLAG2
      WRITE(6,4)KPROP,KONV,NBASIC
      WRITE(6,4)NOTS,NOTRM,NOTREX,NOTRN,NOTP
      WRITE(6,6)TOLEN,TOTVT,TOLTH,TOLDS
    1 FORMAT(20A4)
```

```
    2   FORMAT(10I0)
    3   FORMAT(10F0.0)
    4   FORMAT(20I5)
    5   FORMAT(12F10.2)
    6   FORMAT(12F10.5)
C   (B)  PREPARATORY COMPUTATIONS
C   (I)-GEOMETRY AND DIMENSIONS:-
C
        PI=3.14159265
        GEE=9.8
        BETA0=FLOAT(LBETA)/180.0*PI
        RDIV=FLOAT(LRDIV)/180.0*PI
        FNEW=FNIU
        IF(CHANN.EQ.0.0) FNIU=0.0
        ANG = SECT*2.0*PI
        NDEG=ANG*180.0/PI
        DIA= 2.0*ROI
        DB = ROI-RII
        DC = ROC-RIC
        IF((C+DB).GE.DC) GO TO 30
        DEADC= RII-RIC
        EDB= DB
        EDC= DB+C
        RI = RII
        GO TO 40
   30   DEADI= RIC-RII
        EDB= DC-C
        EDC= DC
        RI = RIC
   40   RO= ROC
        D = RO-RI
        DS=(WB+WC+D)/DSCELL
        DSS=DS/D
   60   IF(NDI.EQ.0) GO TO 61
        TROOT= 2.0*RI*PI/NBI/BROOT
        TEDGE= BEDGE*TROOT
        GO TO 62
   61   CONTINUE
        TROOT=0.0
        TEDGE=0.0
   62   CONTINUE
        BTHICK=(TROOT+TEDGE)/2.0
        RHA=SQRT((RO**2+RI**2)/2.0)
        RHB=2./3.*(RO**3-RI**3)/(RO**2-RI**2)
        RHAA=(RHA-RI)/D
        RHBB=(RHB-RI)/D
        RHA0=RHA/RO
        RHB0=RHB/RO
C   (II)-FRICTION FACTORS
        WETTH=D+ANG*(RO+RI)/2.0
        AREAH=ANG*(RO**2-RI**2)/4.0
        IF(C.EQ.0.0) GO TO 33
        WETTT=WB+C+2.0*WC+D
        AREAT=C*WB+D*WC
        GO TO 34
   33   CONTINUE
        WETTT=2.0*WC+D
        AREAT=WC*D
   34   CONTINUE
        WETTI1=(ROI-RII)/4.0+WB/2.0
```

```
      WETTI2=2.0*PI*(ROI+RII)/2.0/NBI-BTHICK
      WETTI=2.0*WETTI1+WETTI2
      AREAI=WETTI1*WETTI2
      IF(CHANN.EQ.0.0) GO TO 25
      DHCM=AREAM/WETTM/CHANN
      DHCT=AREAT/WETTT/CHANN
   25 IF(PASS.EQ.0.0) GO TO 26
      DHIM=AREAI/WETTI/PASS
   26 CONTINUE
      FRICM=1.0/(4.0*ALOG10(DHCM*2.0/ROUGH)+3.48)**2
      FRICT=1.0/(4.0*ALOG10(DHCT*2.0/ROUGH)+3.48)**2
      FRICI=1.0/(4.0*ALOG10(DHIM*2.0/ROUGH)+3.48)**2
      EPSOLM=EPSOL*2.0*DHCM*SQRT(FRICM/2.0)
      EPSOLT=EPSOL*2.0*DHCT*SQRT(FRICT/2.0)
      EPSOL=(EPSOLM+EPSOLT)/2.0
      WRITE(6,35)EPSOLM,EPSOLT,EPSOL
      WRITE(6,36)DHCM,DHCT,DHIM
      WRITE(6,37)FRICM,FRICT,FRICI
   35 FORMAT(/2X,'EDDY VISCOSITY FACTORS (E=FACTOR*V):-',5E12.5)
   36 FORMAT(/2X,'HYDRAULIC DIAMETERS:-',5E12.5)
C  (III)-OUTPUT HEADINGS:-
      WRITE(6,4000)
      WRITE(6,4005)
      WRITE(6,4405)
      WRITE(6,4406)
      WRITE(6,4407)
      WRITE(6,4006)
      WRITE(6,4007)
      WRITE(6,4014)
      WRITE(6,4015)NAME
      WRITE(6,4115)MODEL
      WRITE(6,4016)ROC
      WRITE(6,4017)RIC
      WRITE(6,4018)ROI
      WRITE(6,4019)RII
      WRITE(6,4020)WB
      WRITE(6,4021)WC
      WRITE(6,4022)BTHICK
      WRITE(6,4023)NBI
      WRITE(6,4024)NDEG
      WRITE(6,4025)LRDIV
      WRITE(6,4026)LBETA
      WRITE(6,38)
      WRITE(6,4067)ROH
      WRITE(6,4068)PNEW
      RATIO6=(WC+WB)/D
      RATIO7=C/(ROI-RII)
      RATIO8=WC/WB
      WRITE(6,4080)
      WRITE(6,4480)
      WRITE(6,4081)
      WRITE(6,5551)RATIO6
      WRITE(6,5552)RATIO7
      WRITE(6,5553)RATIO8
      WRITE(6,4083)NSTL
      WRITE(6,4084)
      WRITE(6,4401)
      WRITE(6,4402)
      WRITE(6,4403)
      WRITE(6,4096)
```

```
      WRITE(6,4498)
C   (IV)-STREAMTUBE MERIDIONAL WIDTH:-
      IF(NDELRR.EQ.1) GO TO 67
      DELPSI=1.0/FLOAT(NSTL)
      PSIFF=DELPSI/2.0
      WRITE(6,4085)
      WRITE(6,4086)DELPSI
      GO TO 68
   67 CONTINUE
      DELRR=1.0/FLOAT(NSTL)
      RRFF=1.0-DELRR/2.0
      WRITE(6,4087)
      WRITE(6,4088)DELRR
      RAD(1)=RRFF-DELRR/2.0
      DRAD(1)=1.0-RAD(1)
   68 CONTINUE
      IF(KRMA.EQ.0) GO TO 168
C  OTHERWISE ONLY ONE VALUE OF RM WILL BE CONSIDERED
      RM=RMB
      GO TO 169
  168 CONTINUE
      DO 8500 JRM=MBRM,NRM,JUMRM
C   (C)   MAJOR LOOPS
C   (I)-LOOP-ONE: FOR CHANGING THE RADIUS OF THE
C                 CENTRE OF MERIDIONAL CIRCULATION
      RM=RI+RMRA(JRM)*D
  169 CONTINUE
      IF(RM.GT.ROI) KRMA=1
      IF(RM.GT.ROI) RM=ROI
      RMM=(RM-RI)/D
      RMO=RM/RO
      DUPP=RO-RM
      DLOW=RM-RI
      RRR=(ROI-RM)/DUPP
C   (II)-LOOP-TWO: FOR VARYING THE CIRCUMFERENTIAL
C                  PRESSURE GRADIENT (DP/DTHETA)
      DO 8000 JP=MBEGP,NEP,JUMPP
      KPOINT=0
      OMEGA= 2.0*PI*RPM/60.0
      DELP= ROH*PSIH(JP)*OMEGA**2*DIA**2
      AA1=DELP/(GEE*ROH)
      AA2=AA1/ANG
      VTROI= ROI*OMEGA
      F1 = DELP/(ROH*ANG)
      DPDTH= DELP/ANG
      AMU=PSIH(JP)/AMMH
      ALIM = VTROI*(WB*C+WC*D)
      WRITE(6,4070) JP
      WRITE(6,4071)PSIH(JP)
      WRITE(6,4072)AA1
      WRITE(6,4073)AA2
      WRITE(6,4074)OMEGA
      WRITE(6,4474)VTROI
C   (III)-LOOP-THREE: FOR VARYING THE INDICES RM AND ZM
      DO 7000 JRM=MBRM,NRM,JUMRM
      RM=RMA(JRM)
      ZM=ZMA(JRM)
C   (IV)-LOOP-FOUR: FOR VARYING THE INDICES REX AND ZEX
      DO 5000 JREX=MBREX,NREX,JUMREX
      REX=REXA(JREX)
```

```
      ZEX=ZEXA(JREX)
      KPOINT=KPOINT+1
      WRITE(6,4008)KPOINT
      WRITE(6,4009)RN
      WRITE(6,4010)ZN
      WRITE(6,4011)REX
      WRITE(6,4012)ZEX
      WRITE(6,4013)RMM
C  DETERMINING THE INNER RADII OF ALL STREAMTUBES
      IF(MDELRR.EQ.1) GO TO 440
      RAD(1)=(1.0-DELPSI**(1./RN))**(1./REX)
      DRAD(1)=1.0-RAD(1)
      PSII=DELPSI
      DO 200 I=2,NSTL
      PSII=PSII+DELPSI
      RAD(I)=(1.0-PSII**(1./RN))**(1./REX)
      DRAD(I)=RAD(I-1)-RAD(I)
  200 CONTINUE
      GO TO 450
  440 CONTINUE
      DO 445 I=2,NSTL
      RAD(I)=RAD(I-1)-DELRR
      DRAD(I)=DELRR
  445 CONTINUE
  450 CONTINUE
C   INITIALIZING A VALUE FOR THE COEFFICIENT (A)
      A= AMM*OMEGA*DIA**3
      DELA= A/2.0
C   (V)-LOOP-FIVE: FOR CONSIDERING DIFFERENT STREAMLINES
      DO 1800 JS=MBEGS,NSTL,JUMPS
      IF(KKONV.EQ.1)A=ARRAY(JS)*OMEGA*DIA**3
      IF(JS.GT.LASTS) GO TO 1800
      AULIM=AULIM1
      ALLIM=ALLIM1
      KONV=0
      IF(KKONV.EQ.1)KONV=1
      IF(MDELRR.EQ.1) GO TO 455
      PSII= PSIFF+(JS-1)*DELPSI
      RRS = (1.0-PSII**(1.0/RN))**(1.0/REX)
      GO TO 460
  455 CONTINUE
      RRS= RRFF-(JS-1)*DELRR
      PSII= (1.0-RRS**REX)**RN
  460 CONTINUE
      RR1= RRS
      ZZ1= 0.0
      RRMID= 0.0
      ZZMID= (1.0-PSII**(1.0/ZN))**(1.0/ZEX)
      RRE = RRS
      ZZE = ZZ1
C   SELECTING A STEP-LENGTH
      VERTIC= RRS*(DUPP+DLOW)
      DRAV=DRAD(JS)*(DUPP+DLOW)/2.0
      RONE=RM-RRE*DUPP
      R3=RM+RRS*DUPP
      IF(VERTIC.GE.DS*DSVERT) GO TO 470
      DS1=VERTIC/DSVERT
      DSS1= DS1/D
      GO TO 480
  470 DS1 = DS
```

```
      DSS1= DSS
  480 CONTINUE
      DS2 = DS1
      DSS2=DSS1
      RITE1=RNN+RRS*DUPP/D
      RITE2=RNN-RRS*DLOW/D
      ZITE1=ZZNID*WC/D
      ZITE2=-ZZNID*WB/D
      IF(KPROP.EQ.1) WRITE(6,4089)
      WRITE(6,4095)JS
      IF(NBASIC.EQ.0) GO TO 458
      WRITE(6,4096)PSII
      WRITE(6,4090)RITE1,ZZ1,RNN,ZITE1,RITE2,ZZE,RNN,ZITE2
      IF(KKONV.EQ.0) WRITE(6,484)
  458 CONTINUE
      IF(KKONV.EQ.0)WRITE(6,485)
      KOOL= 0
C KOOL : IS THE NUMBER OF TIMES A VALUE OF (A) IS TESTED
C   (VI)-LOOP-SIX: FOR SEARCHING FOR A COVERGING VALUE OF (A)
      DO 1700 IA=1,IALAST
  486 CONTINUE
      IF(KPROP.EQ.1.AND.KONV.EQ.1) WRITE(6,180)
C   INITIALIZING QUANTITIES AT BEGINING OF FLOW-CYCLE
      RLOSTI=0.0
      IMPEL= 0
      PSTAT1= 0.0
      SUMTHP=0.0
      SUMTH = 0.0
      TIME = 0.0
      TIMEP= 0.0
      TOT= 0.0
C   (1) SOLUTION OF FLOW ALONG THE SELECTED STREAMLINE IN
C   THE CHANNEL:-
      XO = DUPP
      NS= -1
      IF(C.EQ.0.0.OR.RRS.LE.RRR) GO TO 701
C   (1-1) IN PERIPHERAL CHANNEL:-
      IPERI= 1
      W = WB
      NS= 1
      TIMEP= 0.0
      SUMTHP= 0.0
      RRLIM= RRS
      ZZLIM= 0.0
      RR= RRR
      ZZ = (1.0-(PSII/(1.0-RR**REX)**RN)**(1.0/ZN))**(1.0/ZEX)
      R = RNN+RR*XO
      VT1=0.0*R*OMEGA
      R1= R
      Z1= -ZZ*W
      CALL MOTION
      CALL FIRST
      VTA=VT1
      VTB=0.95*VT1
      VRR1=VR/VTROI
      VZZ1=VZ/VTROI
      VTT1=VT2ACT/VTROI
      VNN1=VN1/VTROI
      VTOT1=SQRT(VRR1**2+VZZ1**2+VTT1**2)
      RFIRST= RR
```

```
      ZFIRST= ZZ
      NEXITI= HEAD1
      DO 600 I=2,100
      L= I
      CALL POINT2
      R = RH+RR2*XO
      R2= R
      Z2= -ZZ2*W
      RR = RR2
      IF(NFLAG2.EQ.0) GO TO 501
      NFLAG1=3
      CALL MOTION
      DPDZT3=DPDZT
  501 CONTINUE
      ZZ = ZZ2
      CALL MOTION
      CALL SECOND
      TOT= TOT+DTH
      SUMTHP= SUMTHP+DTH
      TIMEP= TIMEP+DT
      IF(ZZ2.EQ. 0.0) GO TO 700
  600 CONTINUE
C  (1-2) IN THE SIDE CHANNEL:-
  700 CONTINUE
      VRR2=VR/VTROI
      VZZ2=VZ/VTROI
      VTT2=VT2/VTROI
      VHH2=VH1/VTROI
      VTOT2=SQRT(VRR2**2+VZZ2**2+VTT2**2)
  701 CONTINUE
      ISIDE=1
      IPERI= 0
      W = WC
      NS= -1
      TIMES= 0.0
      SUMTHS= 0.0
      RRLIM= 0.0
      ZZLIM= ZZNID
      IF(RR1.GT.RRR) GO TO 800
      L= 1
      RR= RR1
      ZZ= ZZ1
      R = RH+RR*XO
      VT1=0.9*R*OMEGA
      R1= R
      Z1= ZZ1*W
      CALL MOTION
      CALL FIRST
      VTA=VT1
      VTB=0.95*VT1
      VRR1=VR/VTROI
      VZZ1=VZ/VTROI
      VTT1=VT2ACT/VTROI
      VHH1=VH1/VTROI
      VTOT1=SQRT(VRR1**2+VZZ1**2+VTT1**2)
      VRR2=VRR1
      VZZ2=VZZ1
      VTT2=VTT1
      VHH2=VHH1
      VTOT2=VTOT1
```

```
      VTOT4=SQRT(VMM4**2+VTT4**2)
      VTONE=VT2
      RTWO=RM+RFIRST*DUPP
      SINTHB=ABS(VR)/VM1
      COSTHB=ABS(VZ)/VM1
      BETA1=BETAO*COSTHB+RDIV*SINTHB
      VTONEI=VM1*SIN(BETA1)/COS(BETA1)+OMEGA*R
      HLOSTS=SHOCK*(VTONEI-VTONE)**2/2.0
      IMPEL=1
      ISIDE= 0
      W = WB
      MS= 1
      TIMEI=0.0
      SUMTHI=0.0
      VT1=VTONEI
      VELM1=(VM1**2+VT1**2)/2.0
      DPDRT1= DPDR+VT1**2/R
      RRLIM= 0.0
      ZZLIM= ZZMID
      DO 1300 I=1,100
      L=L+1
      CALL STREAM
      R= RM-RR2*XO
      R2= R
      Z2= -ZZ2*W
      RR = RR2
      IF(MFLAG2.EQ.0) GO TO 1201
      MFLAG1=3
      CALL MOTION
      DPDZT3=DPDZT
1201  CONTINUE
      ZZ = ZZ2
      CALL MOTION
      CALL SECOND
      VTOT=SQRT(VELM1+VELM2)
      TOT= TOT+DTH
      TIMEI= TIMEI+DT
      HLOSTI=HLOSTI+DSC/DHIM*(VELM1+VELM2)/2.0*FRICI
      IF(ZZ2.EQ.ZZMID)GO TO 1400
1300  CONTINUE
1400  CONTINUE
      VRR5=VR/VTROI
      VZZ5=VZ/VTROI
      VTT5=VT2/VTROI
      VMM5=VM1/VTROI
      VTOT5=SQRT(VMM5**2+VTT5**2)
      AVVEL=SQRT(VZ**2+VR**2)
      XO = DUPP
      MS= -1
      RRLIM= RFIRST
      ZZLIM= ZFIRST
      DO 1500 I=1,100
      L=L+1
      CALL POINT2
      R = RM+RR2*XO
      R2= R
      Z2= -ZZ2*W
      RR = RR2
      IF(MFLAG2.EQ.0)GO TO 1401
      MFLAG1=3
```

```
      RFIRST= RR
      ZFIRST= ZZ
      HEXITI= HEAD1
  800 DO 900 I=1,100
      L = L+1
      CALL STREAM
      R = RM+RR2*XO
      R2= R
      Z2= ZZ2*W
      RR = RR2
      IF(NFLAG2.EQ.0) GO TO 801
      NFLAG1=3
      CALL MOTION
      DPDZT3=DPDZT
  801 CONTINUE
      ZZ = ZZ2
      CALL MOTION
      CALL SECOND
      TOT= TOT+DTH
      SUMTHS= SUMTHS+DTH
      TIMES= TIMES+DT
      IF(ZZ2.EQ.ZZMID) GO TO 1000
  900 CONTINUE
 1000 CONTINUE
      VRR3=VR/VTROI
      VZZ3=VZ/VTROI
      VTT3=VT2/VTROI
      VHH3=VH1/VTROI
      VTOT3=SQRT(VRR3**2+VZZ3**2+VTT3**2)
      XO= DLOW
      NS= 1
      RRLIM= RRS
      ZZLIM= 0.0
      DO 1100 I=1,100
      L=L+1
      CALL POINT2
      R= RM-RR2*XO
      R2= R
      Z2= ZZ2*W
      RR = RR2
      IF(NFLAG2.EQ.0) GO TO 1001
      NFLAG1=3
      CALL MOTION
      DPDZT3=DPDZT
 1001 CONTINUE
      ZZ = ZZ2
      CALL MOTION
      CALL SECOND
      TOT= TOT+DTH
      SUMTHS= SUMTHS+DTH
      TIMES= TIMES+DT
      IF(ZZ2.EQ.0.0) GO TO 1200
 1100 CONTINUE
 1200 CONTINUE
      HLOSTC=HEXITI-HEAD2
      IF(CHANN.EQ.0.0)HLOSTC=0.0
      VRR4=VR/VTROI
      VZZ4=VZ/VTROI
      VTT4=VT2/VTROI
      VHH4=VH1/VTROI
```

```
      CALL MOTION
      DPDZT3=DPDZT
 1401 CONTINUE
      ZZ = ZZ2
      CALL MOTION
      CALL SECOND
      VTOT=SQRT(VELH1+VELH2)
      TOT= TOT+DTH
      TIMEI= TIMEI+DT
      HLOSTI=HLOSTI+DSC/DHIM*(VELH1+VELH2)/2.0*FRICI
      IF(RR2.EQ.RFIRST) GO TO 1600
 1500 CONTINUE
 1600 CONTINUE
      TIME= TIMEP+TIMES+TIMEI
      SUMTHI= OMEGA*TIMEI
      SUMTH = SUMTHP+SUMTHS+SUMTHI
C  ENACT ;IS THE DIFFERENCE OF SPECIFIC ENERGY OF THE
C         FLUID AT TWO POINTS WHICH HAVE THE SAME R AND
C         Z COORDINATES BUT 'SUMTH' RADIAN APART. IT
C         IS COMPUTED USING THE ASSUMED CIRCUMFERENTIAL
C         ENERGY GRADIENT AND THE CALCULATED 'SUMTH'
C  EINPUT;SPECIFIC ENERGY IN-PUT BY THE IMPELLER TO THE
C         FLUID PER FLOW CYCLE
C  ENNET ;NET RISE OF SPECIFIC ENERGY PER FLOW CYCLE
C  EATAHI;HYDRAULIC EFFICIENCY OF IMPELLER IN THE FLOW
C         CYCLE BEING CONSIDERED (TAKING INTO ACCOUNT
C         LOSSES IN BLADE PASSAGE,IN CHANNEL AND IN
C         ENTERY REGION TO THE BLADES: WITHOUT CONSIDERING
C         LOSSES IN PORTS AND THE STRIPPER)
C  THEATA;ANGLE GIVEN BE THE CAL. NET ENERGY DIVIDED BY
C         THE ASSUMED TANGENTIAL ENERGY GRADIENT
      ENACT=SUMTH*F1
      EINPUT=OMEGA*(RTWO*VT2ACT-RONE*VTONE)+SUMTHI*F1
      HLOSS=HLOSTI+HLOSTS
      IF(HLOSTC.GT.0.0)HLOSS=HLOSS+HLOSTC
      ENNET=EINPUT-HLOSS
      EATAHI=ENNET/EINPUT
      THEATA=ENNET/F1
      AM=A/(OMEGA*DIA**3)
      IF(NBASIC.EQ.0) GO TO 1639
      IF(KKONV.EQ.1) WRITE(6,484)
      IF(KKONV.EQ.1)WRITE(6,485)
      WRITE(6,1650)AM,THEATA,SUMTH,ENACT,ENNET,HLOSTS,HLOSTI,
     2HLOSTC,SUMTHP,SUMTHS,SUMTHI,EATAHI,VTONE
      GO TO 1649
 1639 CONTINUE
      IF(ABS(1.0-ENNET/ENACT).LT.TOLEN.OR.IA.EQ.IALAST)WRITE(6,1650)AM
     2,THEATA,SUMTH,ENACT,ENNET,HLOSTS,HLOSTI,HLOSTC,SUMTHP,SUMTHS,
     3SUMTHI,EATAHI,VTONE
 1649 CONTINUE
      IF(KKONV.EQ.1) GO TO 1800
      IF(ABS(1.0-ENNET/ENACT).LT.TOLEN.OR.IA.EQ.IALAST)GO TO 1770
C  CORRECTION OF THE VALUE OF THE COEFFICIENT (A)
      A2LOG= ALOG10(A)
      AA2=A
      ENACT2= ENACT
      ENNET2= ENNET
      IF(ENACT.GT.0.0) GO TO 1655
      ALLIM= A
      A=2.5*A
```

```
      DELA=A/2.0
      IF(A.LT.AULIM) GO TO 1700
      GO TO 1667
 1655 IF(ENNET.GT.0.0) GO TO 1656
      AULIM= A
      A=A/3.0
      DELA=A/2.0
      IF(A.GT.ALLIM) GO TO 1700
      GO TO 1667
 1656 CONTINUE
      KOOL= KOOL+1
      IF(KOOL.LT.2) GO TO 1660
      BB1=(ENACT2-ENACT1)/(A2LOG-A1LOG)
      CC1=ENACT1-BB1*A1LOG
      BB2=(ENNET2-ENNET1)/(A2LOG-A1LOG)
      CC2=ENNET1-BB2*A1LOG
      AMLOG=(CC1-CC2)/(BB2-BB1)
      ANEW=10.0**AMLOG
      DELA=ANEW-A
      IF(ENACT.LT.ENNET.AND.DELA.LT.0.0) GO TO 1662
      IF(ENACT.GT.ENNET.AND.DELA.GT.0.0) GO TO 1661
      IF(ANEW.GT.AULIM) GO TO 1662
      IF(ANEW.LT.ALLIM) GO TO 1661
      IF(DELA.GT.0.0) ALLIM=A
      IF(DELA.LT.0.0) AULIM=A
      IF(DELA.EQ.0.0) DELA=0.2*A
 1660 A1LOG=A2LOG
      ENACT1=ENACT2
      ENNET1= ENNET2
      IF(KOOL.NE.1) GO TO 1666
 1661 DELA=-0.25*A
      IF(KOOL.NE.1)AULIM=A
      IF(0.75*A.LE.ALLIM) DELA=(ALLIM-A)/2.0
      IF(KOOL.NE.1) GO TO 1666
      IF(ENACT.LT.ENNET) GO TO 1662
      AULIM=A
      GO TO 1666
 1662 DELA=0.5*A
      ALLIM=A
      IF(1.5*A.GE.AULIM) DELA=(AULIM-A)/2.0
 1666 CONTINUE
      A=A+DELA
      DELA=ABS(DELA)
      IF(A.GT.ALLIM.AND.A.LT.AULIM) GO TO 1700
 1667 CONTINUE
      A=(AULIM+ALLIM)/2.0
      IF(A.EQ.AA2) A=1.1*A
      DELA=A/2.0
 1700 CONTINUE
 1770 CONTINUE
C  OUT OF LOOP-SIX: WRITE PARAMETERS AT END OF CYCLE
      KONV=KONV+1
      IF(KPROP.EQ.1.AND.KONV.EQ.1)GO TO 486
      IF(NBASIC.EQ.0) GO TO 1777
      WRITE(6,1771)
      WRITE(6,1772)VRR1,VZZ1,VTT1,VMM1,VTOT1
      WRITE(6,1773)VRR2,VZZ2,VTT2,VMM2,VTOT2
      WRITE(6,1774)VRR3,VZZ3,VTT3,VMM3,VTOT3
      WRITE(6,1775)VRR4,VZZ4,VTT4,VMM4,VTOT4
      WRITE(6,1776)VRR5,VZZ5,VTT5,VMM5,VTOT5
```

```
1777 CONTINUE
     IF(NOTS.EQ.1)GO TO 1808
     DELA= A/2.0
1800 CONTINUE
1808 CONTINUE
     IF(NOTREX.EQ.1) GO TO 5050
5000 CONTINUE
5050 CONTINUE
     IF(NOTRN.EQ.1) GO TO 7070
7000 CONTINUE
7070 IF(NOTP.EQ.1) GO TO 9000
8000 CONTINUE
     IF(NOTRN.EQ.1.OR.KRMA.EQ.1) GO TO 8550
8500 CONTINUE
8550 CONTINUE
9000 WRITE(6,9001)
9001 FORMAT(/2X,27HMY GOODNESS : JOP COMPLETED)
  37 FORMAT(/2X,'FRICTION FACTORS:-',5E12.5)
4000 FORMAT(1H1,///18X,'THEORETICAL ANALYSIS OF FLOWS')
4005 FORMAT(/21X,'IN REGENERATIVE PUMPS')
4405 FORMAT(/5X,'(1) SOLUTION OF FLOW ALONG STREAMLINES TO DETERMINE')
4406 FORMAT(9X,'A STREAMFUNCTION RELATIONSHIP TO REPRESENT THE')
4407 FORMAT(9X,'MERIDIONAL VELOCITY')
4006 FORMAT(/10X,'A SAMPLE OF RESULTS OBTAINED USING ALGEBRAIC')
4007 FORMAT(10X,'STREAMFUNCTION RELATIONSHIP'//)
4008 FORMAT(/5X,'STREAMFUNCTION INDICES FOR RUN (',I2,') :-')
4009 FORMAT(/10X,'RN      = ',F5.3)
4010 FORMAT(10X,'ZN      = ',F5.3)
4011 FORMAT(10X,'REX     = ',F5.3)
4012 FORMAT(10X,'ZEX     = ',F5.3)
4013 FORMAT(10X,'RMM     = ',F5.3)
4014 FORMAT(/5X,'(A) PUMP PARTICULARS :-')
4015 FORMAT(/10X,'MANUFACTURER NAME OF PUMP : ',20A4)
4115 FORMAT (10X,'MODEL AND CLASS          : ',20A4)
4016 FORMAT(/10X,'CHANNEL OUTER RADIUS                =',F8.6,2X,'(M)')
4017 FORMAT(/10X,'CHANNEL INNER RADIUS                =',F8.6,2X,'(M)')
4018 FORMAT(/10X,'IMPELLER OUTER RADIUS               =',F8.6,2X,'(M)')
4019 FORMAT(/10X,'IMPELLER INNER RADIUS               =',F8.6,2X,'(M)')
4020 FORMAT(/10X,'AVERAGE BLADE WIDTH                 =',F8.6,2X,'(M)')
4021 FORMAT(/10X,'AVERAGE SIDE CHANNEL WIDTH          =',F8.6,2X,'(M)')
4022 FORMAT(/10X,'AVERAGE BLADE THICKNESS             =',F8.6,2X,'(M)')
4023 FORMAT(/10X,'NUMBER OF IMPELLER BLADES           =',I3)
4024 FORMAT(/10X,'EFFECTIVE WORKING SECTION OF PUMP   =',I4,1X,'DEG')
4025 FORMAT(/10X,'AVERAGE RADIAL DEVIATION OF BLADE   =',I3,2X,'DEG')
4026 FORMAT(/10X,'AVERAGE BLADE ANGLE                 =',I3,2X,'DEG')
  38 FORMAT(/5X,'(B) FLUID PROPERTIES:-')
4067 FORMAT(10X,'FLUID MASS DENSITY          =',E10.3,' (KG/M**3)')
4068 FORMAT(10X,'FLUID KINEMATIC VISCOSITY =',E10.3,' (M**2/S)')
4070 FORMAT(1H1,///5X,'OPERATION CONDITIONS AT TEST POINT (',I2,') :-')
4071 FORMAT(/10X,'NON-D HEAD ACROSS LINEAR SECTION   =',F8.2)
4072 FORMAT(10X,'ABSOLUTE HEAD ACROSS LINEAR SECTION=',F8.2,' (M)')
4073 FORMAT(10X,'TANGENTIAL HEAD GRADIENT IN L.S.    =',F8.2,' (M/RAD)')
4074 FORMAT(10X,'IMPELLER ANGULAR SPEED              =',F8.2,' (RAD/S)')
4474 FORMAT(10X,'BLADE SPEED AT OUTER RADIUS (U2)    =',F8.2,' (M/S)')
4080 FORMAT(/5X,'(C) LAYOUT OF STREAMLINES :-')
4480 FORMAT(10X,'STREAMFUNCTION: PSI=A*(1.0-RR**REX)**RN*(1.0-ZZ**ZEX)*
    2*ZH')
4081 FORMAT(10X,'DIMENSIONS OF CHANNEL-IMPELLER MERIDIONAL X-SECTION:')
5551 FORMAT(10X,'RATIO OF MERIDIONAL SECTION WIDTH TO HEIGHT=',F5.3)
5552 FORMAT(10X,'RATIO OF PERIPHERAL-CHANNEL DEPTH TO IMP.HT=',F5.3)
```

```
5553 FORMAT(10X,'RATIO OF SIDE-CHANNEL WIDTH TO IMP.WIDTH   =',F5.3)
4083 FORMAT(10X,I3,' STREAMLINES ARE CHOSEN FOR ANALYSIS')
4084 FORMAT(10X,'STREAMLINES ARE NUMBERED FROM THE WALL INWARDS')
4401 FORMAT(10X,'THEIR STREAMFUNCTION VALUES ,PSI=CONST., ARE GIVEN')
4402 FORMAT(10X,'THE MAIN COORDINATES (RR,ZZ) OF THEIR PROJECTION')
4403 FORMAT(10X,'ONTO A MERIDIONAL PLANE ARE GIVEN IN BRACKETS AND')
4085 FORMAT(10X,'STREAMLINES CHOSEN AT EQUAL INCREMENTS OF ST.F.')
4086 FORMAT(10X,'INCREMENT OF STREAMFUNCTION =',F8.5)
4087 FORMAT(10X,'STREAMLINES CHOSEN AT EQUAL INCREMENTS OF RADIUS')
4088 FORMAT(10X,'NON-D RADIAL STEP =',F8.5)
4089 FORMAT(1H1)
4095 FORMAT(///5X,'STREAMLINE NO (',I2,') :-')
4096 FORMAT(/10X,'ITS NON-D STREAMFUNCTION VALUE     =',F6.4)
4097 FORMAT(10X,'REFERED TO AXESE RR: THROUGH CENTRE OF CIRCULATION')
4498 FORMAT(10X,'                     ZZ: ALONG BOTTOM OF THE CHANNEL')
4099 FORMAT(10X,4('(',F6.3,',',F6.3,')'))
 180 FORMAT(/6X,'RR',7X,'ZZ',6X,'VR',7X,'VZ',7X,'VT',6X,'VTEST',3X,'ANG
    2HOM',3X,'VELH',4X,'PSTAT',3X,'HEAD',6X,'DSC',7X,'DT',8X,'DTH',6X,'
    3SUMTH',4X,'KK')
 484 FORMAT(/5X,'(I) PARAMETERS OBTAINED FOLLOWING THE STREAMLINE THROU
    2GH ONE FLOW-CYCLE VIS. STREAMFUNCTION COEFFICIENT (AM) :-')
 485 FORMAT(/5X,2HAM,6X,6HTHEATA,4X,5HSUMTH,5X,5HENACT,5X,5HENNET,
    25X,6HHLOSTS,4X,6HHLOSTI,4X,6HHLOSTC,4X,6HSUMTHP,4X,6HSUMTHS,
    34X,6HSUMTHI,4X,6HEATAHI,3X,9HVT.EX.CH.)
1650 FORMAT(13E10.3)
1771 FORMAT(/5X,'(II) KEY NON-DIMENSIONAL VELOCITIES       :',4X,'VRR'
    2,7X,'VZZ',7X,'VTT',7X,'VMM',6X,'VTOTAL')
1772 FORMAT(10X,'AT OUTLET FROM IMPELLER                  :',3X,5(F5.2,5X))
1773 FORMAT(10X,'AT OUTER INTERSECTION WITH THE R-AXIS:',3X,5(F5.2,5X))
1774 FORMAT(10X,'AT INTERSECTION WITH (RC) IN CHANNEL :',3X,5(F5.2,5X))
1775 FORMAT(10X,'AT INLET TO IMPELLER                 :',3X,5(F5.2,5X))
1776 FORMAT(10X,'AT INTERSECTION WITH (RC) IN IMPELLER:',3X,5(F5.2,5X))
     STOP
     END
```

```
C   MAIN PROGRAM NAME       : CHARA1
C   LIBRARY CLASSIFICATION :
C   TITLE    : PREDICTION OF PERFORMANCE CHARACTERISTICS
C              OF REGENERATIVE PUMPS
C   PROGRAM  : FORTRAN IV       ICL 4-50       OCTOBER,1978
C              NO SPECIAL HARDWARE REQUIREMENTS
C   AUTHOR   : A. IBRAHIM
C   PURPOSE  : TO PREDICT THE PERFORMANCE CHARACTERISTICS
C              OF A GIVEN REGENERATIVE PUMP USING SPECIFIED
C              STREAMFUNCTION RELATIONSHIPS
C   METHOD   : REFERENCE:- 'THEORETICAL ANALYSIS OF REGENERATIVE PUMPS'
C              A. IBRAHIM, PH.D. THESIS (BATH),1979
C   VARIABLES :-
C       TYPES : SYMBOLS USED ARE ACCORDING TO STANDARD FORTRAN IV
C       UNITS : QUANTITIES ARE MEASURED IN S.I. UNITS
C   INPUT AND OUTPUT: SEE GLOSSARY AND REFERENCE ABOVE
C   SUBROUTINES USED: MOTION,FIRST,SECOND,STREAM,POINT2 & SUBCON
      PROGRAM CHARA1
      DIMENSION NAME(20),MODEL(20),RPMM(10),PSIH(10)
      DIMENSION PSIHC(10),PSIHP(10),PHPP(10),PIMPP(10),PSHAFF(10)
      DIMENSION EFFHP(10),EFFVO(10),EPORT(10),EFFO(10),DISQQ(10)
      DIMENSION CENT(10),CENT1(10),CENT2(10),CENT3(10),CENT4(10)
      DIMENSION CENT5(10),CENT6(10),RAD(30),DRAD(30),DQ(30),QTANL(10)
      DIMENSION REXA(10),ZEXA(10),RNA(10),ZNA(10),RMFA(10),ANGA(10)
      DIMENSION AMAX(10),AMIN(10)
      COMMON /SRZ1/ VR,VZ,RR1,ZZ1,REX,ZEX,RN,ZN,XO,W,D,R
      COMMON /SRZ2/ RR2,ZZ2,DSC,DSSC,DSS2,PSII,RRLIM,ZZLIM
      COMMON /FIR1/ RR,ZZ,NBI,BETAO,RDIV,PI,PSTAT1,DPDR,DPDZT,OMEGA,VT1
      COMMON /FIR2/ VT2ACT,VM1,VC,VC1,VC2,VELH1,HEAD1,DPDRT1,DPDZT1
      COMMON /FIR3/ VEL,VR1,VZ1
      COMMON /MOT1/ A,HS,NS,ROI,RII,TROOT,TEDGE,EPSOL,FNIU
      COMMON /MOT2/ CHANN,IMPEL
      COMMON /SEC1/ R1,Z1,R2,Z2,F1,DPDZT2,DPDZT3,VTA,VTB,DHCH,DHCT,TOLEN
      COMMON /SEC2/ VT2,HEAD2,PSTAT2,VELH2,FRICH,FRICT,L
      COMMON /SEC3/ HDTH1,HDTH2,KPROP,KONV,CURVH,CURVT,DT,DTH,TIME,TOT
      COMMON /CON1/ P1,P2,P3,S1,S2,S3,XX,KOOL
C   (A) INPUT INFORMATION
C   (I)-PUMP AND FLUID PARTICULARS:-
      READ(5,1)NAME
      READ(5,1)MODEL
      READ(5,3)ROI,RII,ROC,RIC,WD,WC,C
      READ(5,2)NBI,LBETA,LRDIV
      READ(5,3)EPSOL,ROUGH,SECT,DROOT,BEDGE
      READ(5,3)PASS,CHANN,SHOCK,CURVET,CURVEH,CURVEI
      READ(5,3)RON,FNIU
      READ(5,3)SIDE,FRACT,EFFH,EFFST,ORIFIC,CLEAR
```

```
C   (II)-OPERATING CONDITIONS AND CORRESPONDING FUNCTIONS
      READ(5,2)NBEGP,NEP,JUMPP
      READ(5,3)(PSIH(I),I=1,NEP)
      READ(5,2)NSPEED
      READ(5,3)(RPMM(I),I=1,NEP)
      READ(5,3)(REXA(I),I=1,NEP)
      READ(5,3)(ZEXA(I),I=1,NEP)
      READ(5,3)(RNA(I),I=1,NEP)
      READ(5,3)(ZNA(I),I=1,NEP)
      READ(5,3)(RNFA(I),I=1,NEP)
      READ(5,3)(ANGA(I),I=1,NEP)
      READ(5,3)(AMAX(I),I=1,NEP)
      READ(5,3)(AMIN(I),I=1,NEP)
C   (III)-MISCELANEOUS INFORMATION
      READ(5,3)DSCELL,DSVERT
      READ(5,3)AMNN,AULIM1,ALLIM1
      READ(5,2)NBEGS,NSTL,JUMPS,LASTS
      READ(5,2)KKONV,IALAST
      READ(5,2)NDELRR,KRMA
      READ(5,2)NDTH1,NDTH2
      READ(5,2)NFLAG1,NFLAG2
      READ(5,2)KPROP,KONV,NBASIC
      READ(5,2)NOTS,NOTRN,NOTREX,NOTRN,NOTP
      READ(5,3)TOLEN,TOTVT,TOLTH,TOLDS
C   (B) ECHO WRITE-OUT OF INPUT DATA
C   (I)-PUMP AND FLUID PARTICULARS:-
      WRITE(6,1)NAME
      WRITE(6,1)MODEL
      WRITE(6,6)ROI,RII,ROC,RIC,WB,WC,C
      WRITE(6,4)NBI,LBETA,LRDIV
      WRITE(6,6)EPSOL,ROUGH,SECT,BROOT,BEDGE
      WRITE(6,5)PASS,CHANN,SHOCK,CURVET,CURVEM,CURVEI
      WRITE(6,5)ROH,FNIU
      WRITE(6,5)SIDE,FRACT,EFFM,EFFST,ORIFIC,CLEAR
C   (II)-OPERATION CONDITIONS AND CORRESPONDING FUNCTIONS
      WRITE(6,4)NBEGP,NEP,JUMPP
      WRITE(6,5)(PSIH(I),I=1,NEP)
      WRITE(6,4)NSPEED
      WRITE(6,5)(RPMM(I),I=1,NEP)
      WRITE(6,5)(REXA(I),I=1,NEP)
      WRITE(6,5)(ZEXA(I),I=1,NEP)
      WRITE(6,5)(RNA(I),I=1,NEP)
      WRITE(6,5)(ZNA(I),I=1,NEP)
      WRITE(6,5)(RNFA(I),I=1,NEP)
      WRITE(6,5)(ANGA(I),I=1,NEP)
      WRITE(6,5)(AMAX(I),I=1,NEP)
      WRITE(6,5)(AMIN(I),I=1,NEP)
C   (III)-MISCELANEOUS INFORMATION
      WRITE(6,5)DSCELL,DSVERT
      WRITE(6,5)AMNN,AULIM1,ALLIM1
      WRITE(6,4)NBEGS,NSTL,JUMPS,LASTS
      WRITE(6,4)KKONV,IALAST
      WRITE(6,4)NDELRR,KRMA
      WRITE(6,4)NDTH1,NDTH2
      WRITE(6,4)NFLAG1,NFLAG2
      WRITE(6,4)KPROP,KONV,NBASIC
      WRITE(6,4)NOTS,NOTRN,NOTREX,NOTRN,NOTP
      WRITE(6,6)TOLEN,TOTVT,TOLTH,TOLDS
    1 FORMAT(20A4)
    2 FORMAT(10I0)
```

```
    3   FORMAT(10F0.0)
    4   FORMAT(20I5)
    5   FORMAT(12F10.2)
    6   FORMAT(12F10.5)
C   (C) PREPARATORY COMPUTATIONS
C   (I)-GEOMETRY AND DIMENSIONS
        WRITE(6,4321)
        WRITE(6,4322)
        WRITE(6,4323)
        WRITE(6,4324)
C       CALL ICL9HEMASK(64,IFLOW)
        PI=3.14159265
        GEE=9.8
        DETA0=FLOAT(LDETA0)/180.0*PI
        RDIV=FLOAT(LRDIV)/180.0*PI
        REFF=3.0*10**5
        FNEW=FNIU
        IF(CHANN.EQ.0.0)FNIU=0.0
        ANG1 = SECT*2.0*PI
        NDEG=ANG1*180.0/PI
        BARRI=(2.0*PI-ANG1)/(2.0*PI)*FLOAT(NBI)
        DIA= 2.0*ROI
        DB = ROI-RII
        DC = ROC-RIC
        IF((C+DB).GE.DC) GO TO 30
        DEADC= RII-RIC
        EDB= DB
        EDC= DB+C
        RI = RII
        GO TO 40
   30   DEADI= RIC-RII
        EDB= DC-C
        EDC= DC
        RI = RIC
   40   RO= ROC
        D = RO-RI
        DS=(WB+WC+D)/DSCELL
        DSS=DS/D
   60   IF(NBI.EQ.0.0) GO TO 61
        TROOT= 2.0*RI*PI/NBI/BROOT
        TEDGE=BEDGE*TROOT
        GO TO 62
   61   CONTINUE
        TROOT=0.0
        TEDGE=0.0
   62   CONTINUE
        BTHICK=(TROOT+TEDGE)/2.0
        VBLADE=BTHICK*WB*(ROI-RII)*NBI
        VANNU=PI*WB*(ROI**2-RII**2)
C  (II)-FRICTION FACTORS
        WETTH=D+ANG1*(RO+RI)/2.0
        AREAN=ANG1*(RO**2-RI**2)/4.0
        IF(C.EQ.0.0) GO TO 33
        WETTT=WB+C+2.0*WC+D
        AREAT=C*WB+D*WC
        GO TO 34
   33   CONTINUE
        WETTT=2.0*WC+D
        AREAT=WC*D
   34   CONTINUE
```

```
      WETTI1=(ROI-RII)/4.0+WB/2.0
      WETTI2=2.0*PI*(ROI+RII)/2.0/NBI-BTHICK
      WETTI=2.0*WETTI1+WETTI2
      AREAI=WETTI1*WETTI2
      IF(CHANN.EQ.0.0) GO TO 25
      DHCM=AREAM/WETTM/CHANN
      DHCT=AREAT/WETTT/CHANN
   25 IF(PASS.EQ.0.0) GO TO 26
      DHIM=AREAI/WETTI/PASS
   26 CONTINUE
      FRICM=1.0/(4.0*ALOG10(DHCM*2.0/ROUGH)+3.48)**2
      FRICT=1.0/(4.0*ALOG10(DHCT*2.0/ROUGH)+3.48)**2
      FRICI=1.0/(4.0*ALOG10(DHIM*2.0/ROUGH)+3.48)**2
      EPSOLM=EPSOL*2.0*DHCM*SQRT(FRICM/2.0)
      EPSOLT=EPSOL*2.0*DHCT*SQRT(FRICT/2.0)
      EPSOL=(EPSOLM+EPSOLT)/2.0
      RATIO6=(WC+WB)/D
      RATIO7=C/(ROI-RII)
      RATIO8=WC/WB
      WRITE(6,4080)
      WRITE(6,4480)
      WRITE(6,4081)
      WRITE(6,5551)RATIO6
      WRITE(6,5552)RATIO7
      WRITE(6,5553)RATIO8
      WRITE(6,4083)NSTL
      WRITE(6,4084)
      WRITE(6,4501)
      WRITE(6,4502)
      WRITE(6,4403)
      WRITE(6,4098)
      WRITE(6,4498)
      WRITE(6,35)
      WRITE(6,36)FRICM
      WRITE(6,37)FRICT
      WRITE(6,38)FRICI
C   (D) LOOP-ONE: FOR CONSIDERING DIFFERENT OPERATING CONDITIONS
      DO 2800 JP=NBEGP,LASTP,LEAVEP
      ANG=ANGA(JP)*ANG1
      OMEGA= 2.0*PI*RPM/60.0
      DELP= ROH*PSIH(JP)*OMEGA**2*DIA**2
      VTROI= ROI*OMEGA
      F1 = DELP/(ROH*ANG)
      DPDTH= DELP/ANG
      QLIH = VTROI*(WB*C+WC*D)
      BB1=DELP/(GEE*ROH)
      BB2=BB1/ANG
      IF(KBASIC.EQ.1)WRITE(6,4071)
      WRITE(6,4070)JP
      WRITE(6,4371)PSIH(JP)
      WRITE(6,4072)BB1
      WRITE(6,4073)BB2
      WRITE(6,4074)OMEGA
      WRITE(6,4474)VTROI
C   (I)-SET UP STREAMFUNCTION CORRESPONDING TO THE
C       SELECTED OPERATION CONDITION (DP/DTHEATA)
      REX=REXA(JP)
      ZEX=ZEXA(JP)
      RH=RHA(JP)
      ZH=ZHA(JP)
```

```
      RMM=RMFA(JP)
      RM=RI+RMM*D
      WRITE(6,4008)
      WRITE(6,4009)RN
      WRITE(6,4010)ZN
      WRITE(6,4011)REX
      WRITE(6,4012)ZEX
      WRITE(6,4013)RMM
      DUPP= RO-RM
      DLOW= RM-RI
      ERR= (ROI-RM)/DUPP
      IF(NDELRR.EQ.1) GO TO 440
      DELPSI=1.0/FLOAT(NSTL)
      PSIFF=DELPSI/2.0
      WRITE(6,4085)
      WRITE(6,4086)DELPSI
      DQ(1)=DELPSI
      RAD(1)=(1.0-DELPSI**(1./RN))**(1./REX)
      DRAD(1)=1.0-RAD(1)
      PSII=DELPSI
      DO 200 I=2,NSTL
      DQ(I)=DELPSI
      PSII=PSII+DELPSI
      RAD(I)=(1.0-PSII**(1./RN))**(1./REX)
      DRAD(I)=RAD(I-1)-RAD(I)
  200 CONTINUE
      GO TO 450
  440 CONTINUE
      DELRR=1.0/FLOAT(NSTL)
      RRFF=1.0-DELRR/2.0
      WRITE(6,4087)
      WRITE(6,4088)DELRR
      RAD(1)=RRFF-DELRR/2.0
      DRAD(1)=1.0-RAD(1)
      DQ(1)=(1.0-RAD(1)**REX)**RN
      BEFOR=DQ(1)
      DO 445 I=2,NSTL
      RAD(I)=RAD(I-1)-DELRR
      DRAD(I)=DELRR
      DQ(I)=(1.0-RAD(I)**REX)**RN-BEFOR
      BEFOR=BEFOR+DQ(I)
  445 CONTINUE
  450 CONTINUE
      WRITE(6,220)
      WRITE(6,221)
      WRITE(6,222)
      WRITE(6,223)
      SUMDQC=0.0
      DO 250 I=1,NSTL
      WRITE(6,224)I,RAD(I),DQ(I)
      SUMDQC=SUMDQC+DQ(I)
  250 CONTINUE
      PNET=0.0
      PINT=0.0
      QTANC=0.0
      CENT2(JP)=0.0
      CENT3(JP)=0.0
      CENT4(JP)=0.0
C   (E) LOOP-TWO: FOR CONSIDERING DIFFERENT STREAMLINES
      DO 1300 JS=NBEGS,NSTL,JUMPS
```

```
      AULIM1=PSIH(JP)/AMMIN*OMEGA*DIA**3
      ALLIM1=PSIH(JP)/AMMAX*OMEGA*DIA**3
      A=(AULIM1+ALLIM1)/2.0
      DELA=(AULIM1-ALLIM1)/4.0
      LALA=0
      IF(NDELRR.EQ.1) GO TO 455
      PSII= PSIFF+(JS-1)*DELPSI
      RRS = (1.0-PSII**(1.0/RN))**(1.0/REX)
      GO TO 460
  455 CONTINUE
      RRS= RRFF-(JS-1)*DELRR
      PSII= (1.0-RRS**REX)**RN
  460 CONTINUE
      RR1= RRS
      ZZ1= 0.0
      RRMID= 0.0
      ZZMID= (1.0-PSII**(1.0/ZN))**(1.0/ZEX)
      RRE = RRS
      ZZE = ZZ1
      VERTIC= RRS*(DUPP+DLOW)
      DRAV=DRAD(JS)*(DUPP+DLOW)/2.0
      RONE=RM-RRE*DUPP
      R3=RM+RRS*DUPP
      IF(VERTIC.GE.DS*DSVERT) GO TO 470
      DS1=VERTIC/DSVERT
      DSS1= DS1/D
      GO TO 480
  470 DS1 = DS
      DSS1= DSS
  480 CONTINUE
      DS2 = DS1
      DSS2= DSS1
      RITE1=RMM+RRS*DUPP/D
      RITE3=RMM-RRS*DLOW/D
      ZITE1=0.0
      ZITE2=ZZMID*WC/D
      ZITE4=-ZZMID*WB/D
      IF(KPROP.EQ.1.AND.KONV.EQ.1) WRITE(6,180)
C   (F) LOOP-THREE; FOR SEARCHING FOR A CONVERGING VALUE
C       FOR THE COEFFICIENT 'A'
      DO 1700 IA=1,10
      KOOL=IA
      HLOSTI=0.0
      INDEL= 0
      PSTAT1= 0.0
      SUMTHP=0.0
      SUMTH = 0.0
      TIME = 0.0
      TIMEP= 0.0
      TOT= 0.0
      XO = DUPP
C   (I)-SOLUTION OF FLOW CYCLE IN THE CHANNEL
      NS= -1
  490 IF(C.EQ.0.0.OR.RRS.LE.RRR) GO TO 701
      IPERI= 1
      W = WB
      CD=CDP
      CW=CWP
      NS= 1
      TIMEP= 0.0
```

```
      SUMTHP= 0.0
      RRLIM= RRS
      ZZLIM= 0.0
      RR= RRR
      ZZ = (1.0-(PSII/(1.0-RR**REX)**RN)**(1.0/ZN))**(1.0/ZEX)
      R = RM+RR*XO
      VT1=0.9*R*OMEGA
      R1= R
      Z1= -ZZ*W
      IF(NFLAG2.EQ.1)NFLAG1=1
      CALL MOTION
      CALL FIRST
      VTA=VT1
      VTB=0.95*VT1
      VRR1=VR/VTROI
      VZZ1=VZ/VTROI
      VTT1=VT2ACT/VTROI
      VHH1=VH1/VTROI
      VTOT1=SQRT(VHH1**2+VTT1**2)
      RFIRST= RR
      ZFIRST= ZZ
      HEXITI=HEAD1
      DO 600 IIP=2,300
      L=IIP
      CALL POINT2
      R = RM+RR2*XO
      R2= R
      Z2= -ZZ2*W
      RR = RR2
      IF(NFLAG2.EQ.0) GO TO 501
      NFLAG1=3
      CALL MOTION
      DPDZT3=DPDZT
  501 CONTINUE
      ZZ = ZZ2
      IF(NFLAG2.EQ.1)NFLAG1=2
      CALL MOTION
      CALL SECOND
      TOT= TOT+DTH
      SUMTHP= SUMTHP+DTH
      TIMEP= TIMEP+DT
      IF(ZZ2.EQ.ZZLIM.OR.RR2.EQ.RRLIM) GO TO 700
  600 CONTINUE
  700 CONTINUE
      VRR2=VR/VTROI
      VZZ2=VZ/VTROI
      VTT2=VT2/VTROI
      VHH2=VH1/VTROI
      VTOT2=SQRT(VHH2**2+VTT2**2)
  701 CONTINUE
      ISIDE=1
      IPERI= 0
      W = WC
      NS= -1
      TIMES= 0.0
      SUMTHS= 0.0
      RRLIM= 0.0
      ZZLIM= ZZMID
      IF(RR1.GT.RRR) GO TO 800
      L= 1
```

```
      RR= RR1
      ZZ= ZZ1
      R = RM+RR*XO
      VT1=0.9*R*OMEGA
      R1= R
      Z1= ZZ1*W
      IF(NFLAG2.EQ.1)NFLAG1=1
      CALL MOTION
      CALL FIRST
      VTA=VT1
      VTB=0.95*VT1
      VRR1=VR/VTROI
      VZZ1=VZ/VTROI
      VTT1=VT2ACT/VTROI
      VHH1=VH1/VTROI
      VTOT1=SQRT(VHH1**2+VTT1**2)
      VRR2=VRR1
      VZZ2=VZZ1
      VTT2=VTT1
      VHH2=VHH1
      VTOT2=VTOT1
      RFIRST= RR
      ZFIRST= ZZ
      NEXITI=NEAD1
  300 DO 900 IIU=1,300
      L = L+1
      CALL STREAM
      R = RM+RR2*XO
      R2= R
      Z2= ZZ2*W
      RR = RR2
      IF(NFLAG2.EQ.0) GO TO 801
      NFLAG1=3
      CALL MOTION
      DPDZT3=DPDZT
  801 CONTINUE
      ZZ = ZZ2
      IF(NFLAG2.EQ.1)NFLAG1=2
      CALL MOTION
      CALL SECOND
      TOT= TOT+DTH
      SUMTHS= SUMTHS+DTH
      TIMES= TIMES+DT
      IF(ZZ2.EQ.ZZLIM.OR.RR2.EQ.RRLIM) GO TO 1000
  900 CONTINUE
 1000 CONTINUE
      VRR3=VR/VTROI
      VZZ3=VZ/VTROI
      VTT3=VT2/VTROI
      VHH3=VH1/VTROI
      VTOT3=SQRT(VHH3**2+VTT3**2)
      XO= DLOW
      NS= 1
      RRLIM= RRS
      ZZLIM= 0.0
      DO 1100 IIL=1,300
      L=L+1
      CALL POINT2
      R= RM-RR2*XO
      R2= R
```

```
      Z2= ZZ2*W
      RR = RR2
      IF(NFLAG2.EQ.0) GO TO 1001
      NFLAG1=3
      CALL MOTION
      DPDZT3=DPDZT
 1001 CONTINUE
      ZZ = ZZ2
      IF(NFLAG2.EQ.1)NFLAG1=2
      CALL MOTION
      CALL SECOND
      TOT= TOT+DTH
      SUMTHS= SUMTHS+DTH
      TIMES= TIMES+DT
      IF(ZZ2.EQ.ZZLIM.OR.RR2.EQ.RRLIM) GO TO 1200
 1100 CONTINUE
 1200 CONTINUE
      HLOSTC=HEXIT-HEAD2
      IF(CHANN.EQ.0.0)HLOSTC=0.0
      VRR4=VR/VTROI
      VZZ4=VZ/VTROI
      VTT4=VT2/VTROI
      VMM4=VM1/VTROI
      VTOT4=SQRT(VMM4**2+VTT4**2)
      RTWO=RH+RFIRST*DUPP
      VTONE=VT2
C   (II)-SOLUTION OF FLOW IN THE IMPELLER
      SINTHB=ABS(VR)/VM1
      COSTHB=ABS(VZ)/VM1
      BETA1=BETAO*COSTHB+RDIV*SINTHB
      VTONEI=VM1*SIN(BETA1)/COS(BETA1)+OMEGA*R
      HLOSTS=SHOCK*(VTONEI-VTONE)**2/2.0
      IMPEL=1
      ISIDE= 0
      W = WB
      MS= 1
      TIMEI=0.0
      SUMTHI=0.0
      VT1=VTONEI
      VELM1=(VM1**2+VT1**2)
      DPDRT1= DPDR+VT1**2/R
      RRLIM= 0.0
      ZZLIM= ZZMID
      DO 1300 III=1,300
      L=L+1
      CALL STREAM
      R= RH-RR2*XO
      R2= R
      Z2= -ZZ2*W
      RR = RR2
      IF(NFLAG2.EQ.0) GO TO 1201
      NFLAG1=3
      CALL MOTION
      DPDZT3=DPDZT
 1201 CONTINUE
      ZZ = ZZ2
      CALL MOTION
      CALL SECOND
      VTOT=SQRT(VELM1+VELM2)
      TOT= TOT+DTH
```

```
      TIMEI= TIMEI+DT
      HLOSTI=HLOSTI+DSC/DHIM*(VELH1+VELH2)/2.0*FRICI
      IF(ZZ2.EQ.ZZMID)GO TO 1400
 1300 CONTINUE
 1400 CONTINUE
      VRR5=VR/VTROI
      VZZ5=VZ/VTROI
      VTT5=VT2/VTROI
      VMM5=VM1/VTROI
      VTOT5=SQRT(VMM5**2+VTT5**2)
      AVVEL=SQRT(VZ**2+VR**2)
      PATH=(RRS*DLOW+RFIRST*DUPP)*(PI/4.0+0.5)
      XO = DUPP
      NS= -1
      RRLIN= RFIRST
      ZZLIN= ZFIRST
      DO 1500 III=1,300
      L=L+1
      CALL POINT2
      R = RM+RR2*XO
      R2= R
      Z2= -ZZ2*W
      RR = RR2
      IF(NFLAG2.EQ.0) GO TO 1401
      NFLAG1=3
      CALL MOTION
      DPDZT3=DPDZT
 1401 CONTINUE
      ZZ = ZZ2
      CALL MOTION
      CALL SECOND
      VTOT=SQRT(VELH1+VELH2)
      TOT= TOT+DTH
      TIMEI= TIMEI+DT
      HLOSTI=HLOSTI+DSC/DHIM*(VELH1+VELH2)/2.0*FRICI
      IF(RR2.EQ.RFIRST) GO TO 1600
 1500 CONTINUE
 1600 CONTINUE
      TIME= TIMEP+TIMES+TIMEI
      SUMTHI= OMEGA*TIMEI
      SUMTH = SUMTHP+SUMTHS+SUMTHI
C   (III)-FLOW-CYCLE COMPLETED: TEST FOR MATCHING
C   ENACT :IS THE DIFFERENCE OF SPECIFIC ENERGY OF THE
C          FLUID AT TWO POINTS WHICH HAVE THE SAME R AND
C          Z COORDINATES BUT 'SUMTH' RADIAN APART. IT
C          IS COMPUTED USING THE ASSUMED CIRCUMFERENTIAL
C          ENERGY GRADIENT AND THE CALCULATED 'SUMTH'
C   EINPUT:SPECIFIC ENERGY IN-PUT BY THE IMPELLER TO THE
C          FLUID PER FLOW CYCLE
C   ENNET :NET RISE OF SPECIFIC ENERGY PER FLOW CYCLE
C   EATAHI:HYDRAULIC EFFICIENCY OF IMPELLER IN THE FLOW
C          CYCLE BEING CONSIDERED (TAKING INTO ACCOUNT
C          LOSSES IN BLADE PASSAGE,IN CHANNEL AND IN
C          ENTERY REGION TO THE BLADES: WITHOUT CONSIDERING
C          LOSSES IN PORTS AND THE STRIPPER).
C   THEATA:ANGLE GIVEN BE THE CAL. NET ENERGY DIVIDED BY
C          THE ASSUMED TANGENTIAL ENERGY GRADIENT
      ENACT=SUMTH*F1
      EINPUT=OMEGA*(RTWO*VT2ACT-RONE*VTONE)+SUMTHI*F1
      HLOSS=HLOSTI+HLOSTC+HLOSTS
```

```
      IF(HLOSTC.GT.0.0)HLOSS=HLOSS-HLOSTC
      ENNET=EINPUT-HLOSS
      EATANI=ENNET/EINPUT
      THEATA=ENNET/P1
      AM=A/(OMEGA*DIA**3)
      IF(ABS(ENNET/ENACT-1.0).LT.TOLEN) GO TO 1770
C   (IV)-CORRECT THE ESTIMATE OF THE COEFFICIENT 'A'
      IF(LALA.NE.0) GO TO 1692
      S3=ENACT-ENNET
      P3=A
      IF(IA.GT.1) GO TO 1691
      IF(ENACT.GT.ENNET) DELA=-DELA
      XX=A+DELA
 1691 CALL SUBCON
      A=P3
      IF(A.GT.ALLIM1.AND.A.LT.AULIM1) GO TO 1700
      LALA=LALA+1
      A=XX
      GO TO 1700
 1692 DELA=ABS(DELA)/2.0
      IF(ENACT.GT.ENNET) GO TO 1693
      A=A+DELA
      GO TO 1700
 1693 A=A-DELA
 1700 CONTINUE
 1770 CONTINUE
C   (V)-WRITE-OUT FLOW-CYCLE PARAMETERS
      IF(KBASIC.EQ.0) GO TO 1651
      WRITE(6,4095)JS
      WRITE(6,4096)PSII
      WRITE(6,4099)RITE1,ZITE1,RMM,ZITE3,ZITE1,RMM,ZITE4
      WRITE(6,484)
      WRITE(6,485)
      WRITE(6,1650)AM,THEATA,SUMTH,ENACT,ENNET,HLOSTS,HLOSTI,
     2HLOSTC,SUMTHP,SUMTHS,SUMTHI,EATANI,VTONE
      WRITE(6,1771)
      WRITE(6,1772)VRR1,VZZ1,VTT1,VMM1,VTOT1
      WRITE(6,1773)VRR2,VZZ2,VTT2,VMM2,VTOT2
      WRITE(6,1774)VRR3,VZZ3,VTT3,VMM3,VTOT3
      WRITE(6,1775)VRR4,VZZ4,VTT4,VMM4,VTOT4
      WRITE(6,1776)VRR5,VZZ5,VTT5,VMM5,VTOT5
 1651 CONTINUE
      DELM=ROH*A*DQ(JS)*ANG
      PINT=PINT+DELM*EINPUT
      PNET=PNET+DELM*ENNET
      CENT2(JP)=CENT2(JP)+DELM*HLOSTS
      CENT3(JP)=CENT3(JP)+DELM*HLOSTI
      CENT4(JP)=CENT4(JP)+DELM*HLOSTC
      QTANC=QTANC+A*DQ(JS)*(SUMTHP+SUMTHS)
 1000 CONTINUE
C   (VI)-ALL STREAMTUBES HAVE BEEN CONSIDERED; COMPUTE
C         PERFORMANCE PARAMETERS AT THIS PINT
      QDIMEN=OMEGA*DIA**3
      PDIMEN=ROH*OMEGA**3*DIA**5
      HDIMEN=OMEGA**2*DIA**2/GEE
      PNET=SIDE*PNET/PDIMEN
      PINT=SIDE*PINT/PDIMEN
      QTANC=SIDE*QTANC/QDIMEN
      QCIRC=SIDE*A*ANG/QDIMEN
      QTRAPP=FRACT*SIDE*OMEGA/(2.0*PI)*(VANNU-VBLADE)/QDIMEN
```

```
      QTANL(JP)=QTANC+QTRAPP
      PSIHC(JP)=PNET/QTANL(JP)
      RETURN=QTRAPP*PSIHC(JP)*EFFST
      PINTF=PINT-RETURN
      CENT2(JP)=SIDE*CENT2(JP)/PDIMEN/PINTF*100.0
      CENT3(JP)=SIDE*CENT3(JP)/PDIMEN/PINTF*100.0
      CENT4(JP)=SIDE*CENT4(JP)/PDIMEN/PINTF*100.0
      PIMPP(JP)=PINTF
C  ESTIMATE LEAKAGE THROUGH STRIPPER-IMPELLER CLEARANCE
      Q1=ORIFIC*(RO-RI+WB)*CLEAR*SQRT(2.0/BARRI*PSIHC(JP))*OMEGA*DIA
      Q2=CLEAR*OMEGA*(RO**2-RI**2)/4.0
      Q3=CLEAR*OMEGA*WB*ROI/2.0
      QLEAK=SIDE*(Q1+Q2+Q3)/QDIMEN
      DISQQ(JP)=QTANC-QLEAK
      EFFVO(JP)=DISQQ(JP)/QTANC
      PLEAK1=QTRAPP*PSIHC(JP)*(1.0-EFFST)
      CENT(JP)=PLEAK1/PIMPP(JP)*100.0
      PLEAK2=QLEAK*PSIHC(JP)
      CENT5(JP)=PLEAK2/PIMPP(JP)*100.0
      HPORTT=PORT*DISQQ(JP)**2
      PSIHP(JP)=PSIHC(JP)-HPORTT
      IF(PSIHP(JP).LT.0.0) GO TO 2805
      KNEP=JP
      PHPP(JP)=PSIHP(JP)*DISQQ(JP)
      EFFHP(JP)=PHPP(JP)/PIMPP(JP)
      CENT6(JP)=HPORTT*DISQQ(JP)/PINTF*100.0
      RENII=OMEGA*RII**2/FNEW
      IF(RENII.GT.REFF) GO TO 2201
      COEFI=3.7*(CLEAR/RII)**0.1/SQRT(RENII)
      GO TO 2202
 2201 COEFI=0.0102*(CLEAR/RII)**0.1/RENII**0.2
 2202 DISKP1=COEFI*ROH*OMEGA**3*RII**5/4.0
      DISKP2=DISKP1
      IF(SIDE.GT.1.0) GO TO 2206
      RENOI=OMEGA*ROI**2/FNEW
      IF(RENOI.GT.REFF) GO TO 2204
      COEFO=3.7*(CLEAR/ROI)**0.1/SQRT(RENOI)
      GO TO 2205
 2204 COEFO=0.0102*(CLEAR/ROI)**0.1/RENOI**0.2
 2205 DISKP2=COEFO*ROH*OMEGA**3*ROI**5/4.0
 2206 CONTINUE
      DISKP=(DISKP1+DISKP2)/PDIMEN
      PSHAFF(JP)=(PINTF+DISKP)/EFFM
      EFFO(JP)=PHPP(JP)/PSHAFF(JP)
      CENT1(JP)=(PSHAFF(JP)-PIMPP(JP))/PSHAFF(JP)*100.0
      IF(NOTP.EQ.1) GO TO 2805
 2800 CONTINUE
 2805 CONTINUE
C   (VII)-ALL OPERATING CONDITIONS HAVE BEEN CONSIDERED;
C        WRITE OUT PERFORMANCE CHARACTERISTICS
      WRITE(6,4000)
      WRITE(6,4005)
      WRITE(6,4006)
      WRITE(6,4007)
      WRITE(6,4014)
      WRITE(6,4015) NAME
      WRITE(6,4315)MODEL
      WRITE(6,4016) ROC
      WRITE(6,4017) RIC
      WRITE(6,4018) ROI
```

```
      WRITE(6,4019) RII
      WRITE(6,4020) WB
      WRITE(6,4021) WC
      WRITE(6,4022) BTHICK
      WRITE(6,4401) CLEAR
      WRITE(6,4023) NBI
      WRITE(6,4024) NDEG
      WRITE(6,4025)LRDIV
      WRITE(6,4026)LBETA
      WRITE(6,4030)
      WRITE(6,4031)
      WRITE(6,4032)
      WRITE(6,4033)
      WRITE(6,4034)
      WRITE(6,4040)
      WRITE(6,4041)
      WRITE(6,4042)
      WRITE(6,4044)
      DO 4045 I=1,KNEP
      WRITE(6,4043)I,PSIHC(I),PSIHP(I),QTANL(I),DISQQ(I),
     2EFFVQ(I),PHPP(I),EFFHP(I),PSHAFF(I),EFFQ(I)
4045  CONTINUE
      WRITE(6,4109)
      WRITE(6,4105)
      WRITE(6,4106)
      WRITE(6,4107)
      DO 4111 I=1,KNEP
      WRITE(6,4108)I,PSHAFF(I),CENT1(I),PIMPP(I),CENT2(I),CENT3(I),
     2CENT4(I),CENT5(I),CENT(I),CENT6(I)
4111  CONTINUE
      BEARGS=(1.0-EFFM)*100.0
      WRITE(6,4112)
      WRITE(6,4113) BEARGS
      WRITE(6,4060)
      WRITE(6,4067) ROH
      WRITE(6,4068) FNEW
      DO 5080 I5=1,NSPEED
      LROTOR=RPMM(I5)
      WRITE(6,4061)I5,LROTOR
      WRITE(6,4062)
      WRITE(6,4041)
      WRITE(6,4042)
      WRITE(6,4044)
      OMEGA=2.0*PI*RPMM(I5)/60.0
      QDIMEN=OMEGA*DIA**3
      PDIMEN=ROH*OMEGA**3*DIA**5
      HDIMEN=OMEGA**2*DIA**2/GEE
      DO 5070 I=1,KNEP
      HEADL=PSIH(I)*HDIMEN
      HEADC=PSIHC(I)*HDIMEN
      HEADP=PSIHP(I)*HDIMEN
      DISQ=DISQQ(I)*QDIMEN
      QTL=QTANL(I)*QDIMEN
      PHP=PHPP(I)*PDIMEN
      PSHAF=PSHAFF(I)*PDIMEN
      WRITE(6,4043)I,HEADC,HEADP,QTL,DISQ,EFFVQ(I),PHP,
     2EFFHP(I),PSHAF,EFFQ(I)
5070  CONTINUE
      WRITE(6,4071)
4071  FORMAT(1H1)
```

```
5080 CONTINUE
     WRITE(6,9001)
9001 FORMAT(/2X,27HMY GOODNESS : JOP COMPLETED)
4321 FORMAT(1H1,///18X,'THEORETICAL ANALYSIS OF FLOWS')
4322 FORMAT(/21X,'IN REGENERATIVE PUMPS')
4323 FORMAT(//5X,'(2) SOLUTION OF FLOWS ALONG STREAMLINES FOR THE')
4324 FORMAT(9X,'PREDICTION OF THE PERFORMANCE PARAMETERS')
4070 FORMAT(///5X,'OPERATION CONDITIONS AT TEST POINT (',I2,') :-')
4371 FORMAT(/10X,'NON-D HEAD ACROSS LINEAR SECTION    =',F8.2)
4072 FORMAT(10X,'ABSOLUTE HEAD ACROSS LINEAR SECTION=',F8.2,' (M)')
4073 FORMAT(10X,'TANGENTIAL HEAD GRADIENT IN L.S.    =',F8.2,' (M/RAD)')
4074 FORMAT(10X,'IMPELLER ANGULAR SPEED              =',F8.2,' (RAD/S)')
4474 FORMAT(10X,'BLADE SPEED AT OUTER RADIUS (U2)    =',F8.2,' (M/S)')
4080 FORMAT(/5X,'LAYOUT OF STREAMLINES :-')
4480 FORMAT(10X,'STREAMFUNCTION: PSI=A*(1.0-RR**REX)**RN*(1.0-ZZ**ZEX)*
    2*ZN')
4081 FORMAT(10X,'DIMENSIONS OF CHANNEL-IMPELLER MERIDIONAL X-SECTION:')
5551 FORMAT(10X,'RATIO OF MERIDIONAL SECTION WIDTH TO HEIGHT=',F5.3)
5552 FORMAT(10X,'RATIO OF PERIPHERAL-CHANNEL DEPTH TO IMP.HT=',F5.3)
5553 FORMAT(10X,'RATIO OF SIDE-CHANNEL WIDTH TO IMP.WIDTH   =',F5.3)
4083 FORMAT(10X,I3,' STREAMLINES ARE CHOSEN FOR ANALYSIS')
4084 FORMAT(10X,'STREAMLINES ARE NUMBERED FROM THE WALL INWARDS')
4085 FORMAT(10X,'SREAMLINES CHOSEN AT EQUAL INCREMENTS OF ST.FUNCTION')
4086 FORMAT(10X,'INCREMENT OF STREAMFUNCTION =',F8.5)
4087 FORMAT(10X,'STREAMLINES CHOSEN AT EQUAL INCREMENTS OF RADIUS')
4088 FORMAT(10X,'NON-D RADIAL STEP =',F8.5)
4501 FORMAT(10X,'THEIR STREAMFUNCTION VALUES ,PSI=CONST., ARE GIVEN')
4502 FORMAT(10X,'THE MAIN COORDINATES (RR,ZZ) OF THEIR PROJECTION')
4403 FORMAT(10X,'ONTO A MERIDIONAL PLANE ARE GIVEN IN BRACKETS AND')
4095 FORMAT(///5X,'STREAMLINE NO (',I2,') :-')
4096 FORMAT(/10X,'ITS NON-D STREAMFUNCTION VALUE     =',F6.4)
4098 FORMAT(10X,'REFERED TO AXESE RR: THROUGH CENTRE OF CIRCULATION')
4498 FORMAT(10X,'                     ZZ: ALONG BOTTOM OF THE CHANNEL')
4099 FORMAT(10X,4('(',F6.3,',',F6.3,')'))
 484 FORMAT(/5X,'(I) PARAMETERS OBTAINED FOLLOWING THE STREAMLINE THROU
    2GH ONE FLOW-CYCLE VIS. STREAMFUNCTION COEFFICIENT (AM) :-')
 180 FORMAT(6X,2HRR,8X,2HZZ,8X,2HVR,8X,2HVZ,8X,2HVT,7X,4HVELH,5X,5HPSTA
    2T,6X,4HHEAD,7X,3HDSC,7X,2HDT,8X,3HDTH,6X,5HSUMTH)
  35  FORMAT(/5X,'MEAN FRICTION FACTORS:-')
  36  FORMAT(10X,'FRICTION FACTOR FOR CHANNEL MERIDIONAL FLOW=',F6.4)
  37  FORMAT(10X,'FRICTION FACTOR FOR CHANNEL TANGENTIAL FLOW=',F6.4)
  38  FORMAT(10X,'FRICTION FACTOR FOR IMPELLER FLOW          =',F6.4)
 220 FORMAT(/5X,'DISTRIBUTION OF CIRCULATORY FLOW :-')
 221 FORMAT(10X,'NON-DIMENSIONAL CIRCULATORY VOLUME FLOW RATE')
 222 FORMAT(10X,'THROUGH STREAMTUBES PER UNIT ANGLE;')
 223 FORMAT(/10X,'STREAMTUBE NO    INNER-RADIUS    QQ-CIR')
 224 FORMAT(21X,I2,7X,F5.3,7X,F6.3)
 485 FORMAT(/5X,2HAN,6X,6HTHEATA,4X,5HSUMTH,5X,5HENACT,5X,5HENNET,
    25X,6HHLOSTS,4X,6HHLOSTI,4X,6HHLOSTC,4X,6HSUMTHP,4X,6HSUMTHS,
    34X,6HSUMTHI,4X,6HEATAHI,3X,2HVT.EX.CH.)
1771 FORMAT(/5X,'(II) KEY NON-DIMENSIONAL VELOCITIES       :',4X,'VRR'
    2,7X,'VZZ',7X,'VTT',7X,'VHH',6X,'VTOTAL')
1772 FORMAT(10X,'AT OUTLET FROM IMPELLER                  :',3X,5(F5.2,5X))
1773 FORMAT(10X,'AT OUTER INTERSECTION WITH THE R-AXIS:',3X,5(F5.2,5X))
1774 FORMAT(10X,'AT INTERSECTION WITH (RC) IN CHANNEL :',3X,5(F5.2,5X))
1775 FORMAT(10X,'AT INLET TO IMPELLER                 :',3X,5(F5.2,5X))
1776 FORMAT(10X,'AT INTERSECTION WITH (RC) IN IMPELLER:',3X,5(F5.2,5X))
1050 FORMAT(13E10.3)
4000 FORMAT(1H1,///9X,'THEORETICAL PREDICTION OF PERFORMANCE PARAMETERS
    2')
```

```
4005 FORMAT(/21X,'OF REGENERATIVE PUMPS')
4006 FORMAT(//11X,'A SAMPLE OF RESULTS OBTAINED USING ALGEBRAIC')
4007 FORMAT(18X,'STREAMFUNCTION RELATIONSHIP'//)
4008 FORMAT (/5X,'STREAMFUNCTION INDICES :-')
4009 FORMAT(/10X,'RN      = ',F5.3)
4010 FORMAT(10X,'ZN      = ',F5.3)
4011 FORMAT(10X,'REX     = ',F5.3)
4012 FORMAT(10X,'ZEX     = ',F5.3)
4013 FORMAT(10X,'RMM     = ',F5.3//)
4014 FORMAT (/5X,'(A) PUMP PARTICULARS :-')
4015 FORMAT(/10X,'MANUFACTURER NAME OF PUMP : ',20A4)
4315 FORMAT(/10X,'MODEL AND CLASS           : ',20A4)
4016 FORMAT(/10X,'CHANNEL OUTER RADIUS                =',F8.6,2X,'(M)')
4017 FORMAT(/10X,'CHANNEL INNER RADIUS                =',F8.6,2X,'(M)')
4018 FORMAT(/10X,'IMPELLER OUTER RADIUS               =',F8.6,2X,'(M)')
4019 FORMAT(/10X,'IMPELLER INNER RADIUS               =',F8.6,2X,'(M)')
4020 FORMAT(/10X,'AVERAGE BLADE WIDTH                 =',F8.6,2X,'(M)')
4021 FORMAT(/10X,'AVERAGE SIDE CHANNEL WIDTH          =',F8.6,2X,'(M)')
4022 FORMAT(/10X,'AVERAGE BLADE THICKNESS             =',F8.6,2X,'(M)')
4401 FORMAT(/10X,'AVERAGE DISK-CASING CLEARANCE       =',F8.6,2X,'(M)')
4023 FORMAT(/10X,'NUMBER OF IMPELLER BLADES           =',I3)
4024 FORMAT(/10X,'EFFECTIVE WORKING SECTION OF PUMP   =',I4,1X,'DEG')
4025 FORMAT(/10X,'AVERAGE RADIAL DEVIATION OF BLADE   =',I3,2X,'DEG')
4026 FORMAT(/10X,'AVERAGE BLADE ANGLE                 =',I3,2X,'DEG')
4030 FORMAT(1H1,///20X,'(B) PREDICTED NON-DIMENSIONAL PERFORMANCE PARAM
    2ETERS :-'/)
4031 FORMAT(/25X,'FACTORS USED FOR NON-DIMENSIONALIZING ARE:-')
4032 FORMAT(/26X,'DISCHARGE: OMEGA*DIA**3  ')
4033 FORMAT(26X,'POWER     : ROH*OMEGA**3*DIA**5')
4034 FORMAT(26X,'HEAD      : OMEGA**2*DIA**2/GEE')
4040 FORMAT(//3X,'TEST',3X,'INPUT MEAN',12X,'PREDICTED   NON-DIMENSIONA
    2L  PERFORMANCE   PARAMETERS')
4041 FORMAT(3X,'POINT',2X,'HEAD ACROSS')
4042 FORMAT(3X,' NO    LINEAR SECTION  HEAD ACR- FLOW RATE  PUMP VOL.
    2  VOL.   HYDRAULIC   HYD.   SHAFT      O/A ')
4044 FORMAT(3X,'                                OSS PUMP  THRO L.S.  FLOW RATE
    2  EFFY      POWER      EFFY   POWER      EFFY ')
4060 FORMAT(1H1,//20X,'(D) PERFORMANCE PREDICTION AT SELECTED SPEEDS :-
    2'//)
4061 FORMAT(//24X,'(',I1,') AT IMPELLER ROTATIONAL SPEED =',I5,' (RPM)'
    2)
4062 FORMAT(//3X,'TEST       INPUT',13X,'PREDICTED   ABSOLUTE   PERFORMA
    2NCE   PARAMETERS')
4067 FORMAT(24X,'FLUID MASS DENSITY          =',E10.3,' (KG/M**3)')
4068 FORMAT(24X,'FLUID KINEMATIC VISCOSITY =',E10.3,' (M**2/S)')
4043 FORMAT(/4X,I2,4X,F7.3,9X,F7.3,2X,E10.3,1X,E10.3,2X,F5.3,2X,E10.3,
    22X,F5.3,1X,E10.3,2X,F5.3)
4105 FORMAT(//3X,5HTEST ,4X,5HSHAFT,4X,7H% LOST ,3X,8HPOWER   ,3X,6H% L
    20ST,3X,8H% LOST  ,3X,7H% LOST ,3X,8H% LOST  ,2X,2(6H% LOST,4X))
4106 FORMAT(3X,5HPOINT,4X,5HPOWER,4X,7HIN MECH,3X,8HINPUT   ,3X,6HIN
    2 ,3X,8HIN BLADE,3X,7HIN     ,3X,7HIN     ,3X,8HIN CARRY,2X,2HIN)
4107 FORMAT(3X,5H NO  ,4X,5HINPUT,4X,7HLOSSES*,3X,8HTO FLUID,3X,6HSHOCK
    26,3X,8HPASSAGES,3X,7HCHANNEL,3X,7HLEAKAGE,3X,4HOVER,6X,5HPORTS)
4108 FORMAT(/4X,I2,3X,E10.3,2X,F5.2,3X,E10.3,3(3X,F5.2,2X),2(3X,F5.2,3X
    2),F5.2)
4109 FORMAT(1H1,//20X,'(C) ESTIMATION OF POWER LOSSES')
4112 FORMAT(//10X,'* MECHANICAL LOSSES INCLUDE DISC FRICTION LOSSES')
4113 FORMAT(12X,'(',F3.1,'% OF SHAFT POWER ASSUMED LOST IN BEARINGS AND
    2 PACKINGS)')
     STOP
     END
```

```
C  SUBPROGRAM NAME          : MOTION
C  PURPOSE : TO DETERMINE THE MERIDIONAT VELOCITY COMPONENTS
C            VR & VZ AND THE PARTIAL DERIVATIVES OF THE PRESSURE
C            DP/DR & DP/DZ
C  METHOD  : REFERENCE:- 'THEORETICAL ANALYSIS OF REGENERATIVE PUMPS'
C            A. IBRAHIM, PH.D. THESIS (BATH),1979
C  INPUT INFORMATION : ALL PARAMETERS IN COMMON BLOCKS: /MOT1/ & /MOT2/
C                      & REX,ZEX,RN,ZN,XO,W,R,NBI,BETAO,RDIV
C  OUTPUT INFORMATION: VR,VZ,DPDR,DPDZT

      SUBROUTINE MOTION
      COMMON /SRZ1/ VR,VZ,RR1,ZZ1,REX,ZEX,RN,ZN,XO,W,D,R
      COMMON /FIR1/ RR,ZZ,NBI,BETAO,RDIV,PI,PSTAT1,DPDR,DPDZT,OMEGA,VT1
      COMMON /MOT1/ A,MS,NS,ROI,RII,TROOT,TEDGE,EPSOL,FNIU
      COMMON /MOT2/ CHANN,IMPEL
      IF(IMPEL.EQ.0) GO TO 1
      T=TEDGE+ZZ*(TROOT-TEDGE)-(R-RII)/(ROI-RII)*ZZ*(TROOT-TEDGE)
      SINB=ABS(VR)/SQRT(VR**2+VZ**2)
      COSB=ABS(VZ)/SQRT(VR**2+VZ**2)
      FANG=BETAO*COSB+RDIV*SINB
      IF(FANG.EQ.0.0)GO TO 101
      TAND=SINB/COSB-SIN(RDIV)/COS(RDIV)/SIN(FANG)*COS(FANG)/COSB
      GO TO 102
  101 CONTINUE
      TAND=1.0
  102 CONTINUE
      D=FLOAT(NBI)*T/(2.0*PI*R*COS(FANG))
      D=1.0-D*SQRT(1.0+SIN(FANG)**2*TAND**2)
      GO TO 2
    1 D=1.0
    2 CONTINUE
      IF(ZZ.NE.0.0) GO TO 3
      DTZ=0.0
      GO TO 5
    3 IF(ZEX.NE.1.0) GO TO 4
      DTZ=MS/W
      GO TO 5
    4 DTZ=MS*ZEX*ZZ**(ZEX-1.0)/W
    5 IF (RR.NE.0.0) GO TO 6
      DTR=0.0
      GO TO 8
    6 IF(REX.NE.1.0) GO TO 7
      DTR=MS/XO
      GO TO 8
    7 DTR=MS*REX*RR**(REX-1.0)/XO
    8 CONTINUE
```

```
      TZ = 1.0-ZZ**ZEX
      TR = 1.0-RR**REX
      PSIR=A*TZ**ZN*RN*TR**(RN-1.0)*DTR
      PSIZ=A*TR**RN*ZN*TZ**(ZN-1.0)*DTZ
      VR=PSIZ/R/B
      VZ=-PSIR/R/B
      IF(IMPEL.EQ.1)RETURN
      IF(ZZ.NE.0.0) GO TO 9
      DTZZ=0.0
      DTZZZ=0.0
      GO TO 30
    9 CONTINUE
      IF(ZEX.NE.1.0) GO TO 10
      DTZZ= 0.0
      DTZZZ=0.0
      GO TO 30
   10 DTZ=NS*ZEX*ZZ**(ZEX-1.0)/W
      IF(ZEX.NE.2.0) GO TO 20
      DTZZ= -2.0/W**2
      DTZZZ=0.0
      GO TO 30
   20 DTZZ=-ZEX*(ZEX-1.0)*ZZ**(ZEX-2.0)/W**2
      IF(ZEX.NE.3.0) GO TO 25
      DTZZZ=NS*6.0/W**3
      GO TO 30
   25 DTZZZ=NS*ZEX*(ZEX-1.0)*(ZEX-2.0)*ZZ**(ZEX-3.0)/W**3
   30 IF(RR.NE.0.0) GO TO 35
      DTRR=0.0
      DTRRR=0.0
      GO TO 60
   35 CONTINUE
      IF(REX.NE.1.0) GO TO 40
      DTRR= 0.0
      DTRRR=0.0
      GO TO 60
   40 DTR=NS*REX*RR**(REX-1.0)/X0
      IF(REX.NE.2.0) GO TO 45
      DTRR= -2.0/X0**2
      DTRRR=0.0
      GO TO 60
   45 DTRR=-REX*(REX-1.0)*RR**(REX-2.0)/X0**2
      IF(REX.NE.3.0) GO TO 50
      DTRRR=NS*6.0/X0**3
      GO TO 60
   50 DTRRR=NS*REX*(REX-1.0)*(REX-2.0)*RR**(REX-3.0)/X0**3

   60 CONTINUE
      PSIRR= A*TZ**ZN*((RN-1.0)*TR**(RN-2.0)*DTR**2+TR**(RN-1.)*DTRR)*RN
      PSIZZ= A*TR**RN*ZN*((ZN-1.0)*TZ**(ZN-2.)*DTZ**2+TZ**(ZN-1.)*DTZZ)
      PSIRZ= A*RN*TR**(RN-1.0)*DTR*ZN*TZ**(ZN-1.0)*DTZ
      PSIZR = PSIRZ
      DVRDR=PSIZR/R-PSIZ/R**2
      DVRDZ=PSIZZ/R
      DVZDR=PSIR/R**2-PSIRR/R
      DVZDZ=-PSIRZ/R
      DPDR=-(VR*DVRDR+VZ*DVRDZ)
      DPDZT=-(VR*DVZDR+VZ*DVZDZ)
      EPNIU=PNIU+EPSOL*SQRT(VR**2+VZ**2+VT1**2)
      IF(CHANN.EQ.0.0.OR.EPNIU.LE.0.0) RETURN
      PSIRRZ=PSIRR/TZ*ZN*DTZ
```

```
      PSIZZR=PSIZZ/TR*RN*DTR
      PSIZRR=PSIRRZ
      PSIRZR=PSIRRZ
      PSIRZZ=PSIZZR
      PSIZRZ=PSIZZR
      PSIRRR=A*TZ**ZN*RN*((RN-1.)*((RN-2.)*TR**(RN-3.)*DTR**3+
     2TR**(RN-2.)*2.*DTR*DTRR)+(RN-1.)*TR**(RN-2.)*DTR*DTRR+TR**
     2(RN-1.)*DTRRR)
      PSIZZZ=A*TR**RN*ZN*((ZN-1.)*((ZN-2.)*TZ**(ZN-3.)*DTZ**3+
     2TZ**(ZN-2.)*2.*DTZ*DTZZ)+(ZN-1.)*TZ**(ZN-2.)*DTZ*DTZZ+TZ**
     2(ZN-1.)*DTZZZ)
      DVRDRR=PSIZRR/R-2.*PSIZR/R**2+2.*PSIZ/R**3
      DVRDZZ=PSIZZZ/R
      DVZDRR=2.*PSIRR/R**2-2.*PSIR/R**3-PSIRRR/R
      DVZDZZ=-PSIRZZ/R
      DPDR=DPDR+EFNIU*(DVRDRR+DVRDR/R+DVRDZZ-VR/R**2)
      DPDZT=DPDZT+EFNIU*(DVZDRR+DVZDR/R+DVZDZZ)
      RETURN
      END
```

```
C
C   SUBPROGRAM NAME          : FIRST
C   PURPOSE : TO DETERMINE THE TANGENTIAL VELOCITY AT EXIT
C             OF IMPELLER & SET UP FLOW CODITIONS AT THAT POINT
C   METHOD  : REFERENCE:- 'THEORETICAL ANALYSIS OF REGENERATIVE PUMPS'
C             A. IBRAHIM, PH.D. THESIS (BATH),1979
C   INPUT INFORMATION : RR,ZZ,VR,VZ,R,NBI,BETAO,RDIV,OMEGA
C   OUTPUT INFORMATION: VT1,VELH1,HEAD1,DPDRT1,DPDZT1

      SUBROUTINE FIRST
      COMMON /FIR3/ VEL,VR1,VZ1
      COMMON /SRZ1/ VR,VZ,RR1,ZZ1,REX,ZEX,RN,ZN,XO,W,D,R
      COMMON /FIR1/ RR,ZZ,NBI,BETAO,RDIV,PI,PSTAT1,DPDR,DPDZT,OMEGA,VT1
      COMMON /FIR2/ VT2ACT,VM1,VC,VC1,VC2,VELH1,HEAD1,DPDRT1,DPDZT1
      VM1=SQRT(VZ**2+VR**2)
      BETA2=BETAO*ABS(VZ)/VM1+RDIV*ABS(VR)/VM1
      VT2ID=VM1*SIN(BETA2)/COS(BETA2)+R*OMEGA
      FAI2=VM1/(R*OMEGA)
      IF(NBI.EQ.0) GO TO 10
      SLIPF=1.0-0.63*PI/NBI/(1.0-FAI2*SIN(BETA2)/COS(BETA2))
      GO TO 20
   10 SLIPF=1.0
   20 CONTINUE
      VT2ACT=SLIPF*VT2ID
      VT1=VT2ACT
      VEL=VT1
      VC=0.0
      VC1=0.0
      VC2=0.0
      RR1= RR
      ZZ1= ZZ
      VR1= VR
      VZ1= VZ
      VELH1=(VM1**2+VT1**2)/2.0
      HEAD1= PSTAT1+VELH1
      DPDRT1= DPDR+VT1**2/R
      DPDZT1= DPDZT
      RETURN
      END
```

```
C   SUBPROGRAM NAME          ; SECOND
C   LIBRARY CLASSIFICATION ;
C   PURPOSE : TO SOLVE SIMULTANEOUSLY THE EQUATION OF MOTOIN
C             AND THE ENERGY EQUATION ITERATIVELY TO DETERMINE
C             THE TANGENTIAL VELOCIT AND HENCE COMPUTE THE
C             VELOCITY & PRESSURE HEADS
C   METHOD  : REFERENCE:- 'THEORETICAL ANALYSIS OF REGENERATIVE PUMPS'
C             A. IBRAHIM, PH.D. THESIS (BATH),1979
C   INPUT INFORMATION : ALL PARAMETERS IN  COMMON BLOCKS: /FIR1/,
C                       /FIR2/,/FIR3/,MOT2/,/SEC1/,/SEC3/
C                       AND: VR,VZ,FRICM,FRICT,L
C   OUTPUT INFORMATION: VT2,HEAD2,PSTAT2,VELH2

      SUBROUTINE SECOND
      COMMON /SRZ1/ VR,VZ,RR1,ZZ1,REX,ZEX,RN,ZN,XO,W,D,R
      COMMON /SRZ2/ RR2,ZZ2,DSC,DSSC,DSS2,PSII,RRLIM,ZZLIM
      COMMON /FIR1/ RR,ZZ,NBI,BETAO,RDIV,PI,PSTAT1,DPDR,DPDZT,OMEGA,VT1
      COMMON /FIR2/ VT2ACT,VM1,VC,VC1,VC2,VELH1,HEAD1,DPDRT1,DPDZT1
      COMMON /FIR3/ VEL,VR1,VZ1
      COMMON /MOT2/ CHANN,IMPEL
      COMMON /SEC1/ R1,Z1,R2,Z2,F1,DPDZT2,DPDZT3,VTA,VTB,DHCM,DHCT,TOLEN
      COMMON /SEC2/ VT2,HEAD2,PSTAT2,VELH2,FRICM,FRICT,L
      COMMON /SEC3/ NDTH1,NDTH2,KPROP,KONV,CURVM,CURVT,DT,DTH,TIME,TOT

      VR2= VR
      VZ2= VZ
      VM22=VR2**2+VZ**2
      VM2=SQRT(VM22)
      DR= R2-R1
      DZ= Z2-Z1
      VMAV=(VM1+VM2)/2.0
      IF(VR1.EQ.0.0 .OR.VR2.EQ.0.0) GO TO 20
      IF((ABS(VZ1)+ABS(VZ2))-(ABS(VR1)+ABS(VR2))) 10,10,20
   10 DT=(1.0/VR1+1.0/VR2)/2.0*DR
      GO TO 30
   20 IF(VZ1.EQ.0.0.OR.VZ2.EQ.0.0) GO TO 25
      DT=(1.0/VZ1+1.0/VZ2)/2.0*DZ
      GO TO 30
   25 DSC=SQRT(DR**2+DZ**2)
      DT=DSC/VMAV
   30 CONTINUE
      IF(IMPEL.NE.1) GO TO 60
      BETA=BETAO*ABS(VZ)/VM2+RDIV*ABS(VR)/VM2
      VT2=VM2*SIN(BETA)/COS(BETA)+OMEGA*R
      DTH=0.5*(VT1/R1+VT2/R)*DT
      VELH2=(VM22+VT2**2)/2.0
```

```
      HEAD2=HEAD1+OMEGA*(R2*VT2-R1*VT1)+F1*DTH
      GO TO 79
   60 CONTINUE
      PRESS2=PSTAT1+(DPDRT1+DPDR)*DR/2.0+(DPDZT1+DPDZT)*DZ/2.0+VM22/2.0
      IF(NFLAG2.EQ.0) GO TO 61
      PRESS3=PSTAT1+DPDRT1*DR+(DPDZT3+DPDZT)*DZ/2.0+VM22/2.0
   61 CONTINUE
      IF(L.LT.3)DSC1=DSC
      VT2=VTB-DSC/DSC1*(VTA-VTB)
      VT22=VT2
      IF(VT2.LT.VT1.AND.VT2.NE.0.0) GO TO 50
      NSIGN=-1
      GO TO 55
   50 NSIGN=VT2/ABS(VT2)
   55 CONTINUE
      HEAD2A=HEAD1
      IF(CHANN.EQ.0.0) GO TO 59
      HLOSTM=DSC/DHCM*VMAV**2/2.0*FRICM
      HEAD2A=HEAD1-HLOSTM
   59 CONTINUE
      DO 70 LL=1,5
      IF(CHANN.EQ.0.0) GO TO 56
      VTAV=ABS(VT1+VT2)/2.0
      HLOSTT=VTAV*DT/DHCT*VTAV**2/2.0*FRICT
      HEAD2A=HEAD2A-HLOSTT
   56 KK=LL
      VTB=VT2
      IF(NDTH1.NE.1) GO TO 62
      DTH=0.5*(VT1/R1+VTB/R2)*DT
      GO TO 64
   62 IF(NDTH2.NE.1.OR.VT1.EQ.0.0.OR.VTB.EQ.0.0) GO TO 63
      DTH=2.0*(R1/VT1+R2/VTB)*DT
      GO TO 64
   63 DTH=DT*(.25*(VT1/R1+VTB/R2)+VT1*VTB/(VTB*R1+VT1*R2))
   64 CONTINUE
      IF(NFLAG2.EQ.0) GO TO 65
      HEAD2B=PRESS3+VT2**2*(0.5+DR/R)+F1*DTH
      VT2=NSIGN*SQRT(ABS((HEAD2A-PRESS3-F1*DTH)/(0.5+DR/R)))
      GO TO 66
   65 CONTINUE
      HEAD2B=PRESS2+VT2**2*(0.5+0.5*DR/R)+F1*DTH
      VT2=NSIGN*SQRT(ABS((HEAD2A-PRESS2-F1*DTH)/(0.5+0.5*DR/R)))
   66 CONTINUE
      IF(ABS(HEAD2B/HEAD2A-1.0).LT.TOLEN) GO TO 75
      IF(VT2.EQ.0.0) GO TO 75
      IF(ABS(VTB/VT2-1.0).LT.TOLEN) GO TO 75
   70 CONTINUE
   75 CONTINUE
      VELH2=(VM22+VT2**2)/2.0
      HEAD2=HEAD2A
   79 CONTINUE
      PSTAT2=HEAD2-VELH2
      ANGMOM=VT1*R1
      IF(KPROP.EQ.1.AND.KONV.EQ.1)WRITE(6,80)RR1,ZZ1,VR1,VZ1,
     2VT1,VEL,ANGMOM,VELH1,PSTAT1,HEAD1,VC,VC1,VC2,TOT,KK
   80 FORMAT(7(2X,F7.3),3(2X,F6.2),2X,4(E9.2,1X),I3)
      VEL=VT22
      DSC1=DSC
      VTA=VT1
      VTB=VT2
```

```
      VC=VC+DSC
      VC1=VC1+DT
      VC2=DTH
      R1=R2
      Z1=Z2
      RR1=RR2
      ZZ1=ZZ2
      VR1=VR2
      VZ1=VZ2
      VT1=VT2
      VH1=VH2
      VELH1=VELH2
      PSTAT1=PSTAT2
      HEAD1=HEAD2
      IF(IMPEL.EQ.1) RETURN
      DPDRT1=DPDR+VT2**2/R
      DPDZT1=DPDZT
      RETURN
      END



C   SUBPROGRAM NAME          : STREAM
C   LIBRARY CLASSIFICATION :
C   TITLE    : STEPPING ALONG A STREAMLINE-1
C   PURPOSE : TO MOVE A STEP OF A SPECIFIED MERIDIONAL LENGTH
C             ALONG A SPECIFIED STREAMLINE WHEN COORDINATE R DECREASES
C   METHOD  : REFERENCE:- 'THEORETICAL ANALYSIS OF REGENERATIVE PUMPS'
C             A. IBRAHIM, PH.D. THESIS (BATH),1979
C   INPUT INFORMATION : VR,VZ,REX,ZEX,RN,ZN,XO,W,DSS2,PSII
C                       RR1,ZZ1RRLIM,ZZLIM
C   OUTPUT INFORMATION: RR2,ZZ2,DSC
      SUBROUTINE STREAM
      COMMON /SRZ1/ VR,VZ,RR1,ZZ1,REX,ZEX,RN,ZN,XO,W,D,R
      COMMON /SRZ2/ RR2,ZZ2,DSC,DSSC,DSS2,PSII,RRLIM,ZZLIM
      DELTA=DSS2
      IF(ABS(VR).GT.ABS(VZ)) GO TO 60
      ZZ2= ZZ1+DELTA
      IF(ZZ2.GT.ZZLIM) ZZ2=ZZLIM
      DO 50 J=1,10
      DZZ= ABS(ZZ2-ZZ1)
      ZZP2= ZZ2
      IF(ZZ2.LT.ZZLIM) GO TO 15
      ZZ2= ZZLIM
      ZZP2= ZZLIM
      RR2= RRLIM
      DZZ= ABS(ZZ2-ZZ1)
      GO TO 25
   15 CONTINUE
      RR2= (1.0-(PSII/(1.0-ZZ2**ZEX)**ZN)**(1.0/RN))**(1.0/REX)
   25 DRR= ABS(RR2-RR1)
      DSC= SQRT((DRR*XO)**2+(DZZ*W)**2)
      DSSC= DSC/D
      IF(DSSC.LT.DSS2) GO TO 55
      ZZ2= ZZ2-DELTA
      DELTA=DELTA/2.0
      ZZ2=ZZ2+DELTA
```

```
   50   CONTINUE
   55   ZZ2= ZZP2
        IF(ZZ2.GT.ZZLIM) ZZ2=ZZLIM
        IF(ZZ2.EQ.ZZLIM) RR2= RRLIM
        RETURN
   60   CONTINUE
        RR2= RR1-DELTA
        IF(RR2.LT.RRLIM) RR2=RRLIM
        DO 90 I=1,10
        DRR= ABS(RR2-RR1)
        RRP2= RR2
        IF(RR2.GT.RRLIM) GO TO 62
        RR2= RRLIM
        RRP2= RRLIM
        ZZ2= ZZLIM
        DRR= ABS(RR2-RR1)
        GO TO 66
   62   CONTINUE
        ZZ2= (1.0-(PSII/(1.0-RR2**REX)**RN)**(1.0/ZN))**(1.0/ZEX)
   66   DZZ= ABS(ZZ2-ZZ1)
        DSC= SQRT((DRR*XO)**2+(DZZ*W)**2)
        DSSC= DSC/D
        IF(DSSC.LT.DSS2) GO TO 100
        RR2= RR2-DELTA
        DELTA=DELTA/2.0
        RR2=RR2+DELTA
   90   CONTINUE
  100   RR2= RRP2
        IF(RR2.LT.RRLIM) RR2= RRLIM
        IF(RR2.EQ.RRLIM) ZZ2= ZZLIM
        RETURN
        END
```

```
C   SUBPROGRAM NAME          : POINT2
C   LIBRARY CLASSIFICATION :
C   TITLE    : STEPPING ALONG A STREAMLINE-2
C   PURPOSE  : TO MOVE A STEP OF A SPECIFIED MERIDIONAL LENGTH
C              ALONG A SPECIFIED STREAMLINE WHEN COORDINATE R INCREASES
C   METHOD   : REFERENCE:- 'THEORETICAL ANALYSIS OF REGENERATIVE PUMPS'
C              A. IBRAHIM, PH.D. THESIS (BATH),1979.
C   INPUT INFORMATION : VR,VZ,REX,ZEX,RN,ZN,XO,W,DSS2,PSII
C                       RR1,ZZ1RRLIM,ZZLIM
C   OUTPUT INFORMATION: RR2,ZZ2,DSC

        SUBROUTINE POINT2
        COMMON /SRZ1/ VR,VZ,RR1,ZZ1,REX,ZEX,RN,ZN,XO,W,D,R
        COMMON /SRZ2/ RR2,ZZ2,DSC,DSSC,DSS2,PSII,RRLIM,ZZLIM
        IF(ABS(VR).GT.ABS(VZ)) GO TO 60
        DELTA= DSS2
        ZZ2= ZZ1-DELTA
        IF(ZZ2.LT.ZZLIM) ZZ2=ZZLIM
        DO 50 J=1,10
        DZZ= ABS(ZZ2-ZZ1)
```

```
      ZZP2= ZZ2
      IF(ZZ2.GT.ZZLIM) GO TO 15
      ZZ2= ZZLIM
      ZZP2= ZZLIM
      RR2= RRLIM
      DZZ= ABS(ZZ2-ZZ1)
      GO TO 25
   15 CONTINUE
      RR2= (1.0-(PSII/(1.0-ZZ2**ZEX)**ZN)**(1.0/RN))**(1.0/REX)
   25 DRR= ABS(RR2-RR1)
      DSC= SQRT((DRR*XO)**2+(DZZ*W)**2)
      DSSC= DSC/D
      IF(DSSC.LT.DSS2) GO TO 55
      ZZ2= ZZ2-DELTA
      DELTA=DELTA/2.0
      ZZ2=ZZ2+DELTA
   50 CONTINUE
   55 ZZ2= ZZP2
      IF(ZZ2.LT.ZZLIM) ZZ2=ZZLIM
      IF(ZZ2.EQ.ZZLIM) RR2= RRLIM
      RETURN
   60 DELTA= DSS2
      RR2= RR1+DELTA
      IF(RR2.GT.RRLIM) RR2=RRLIM
      DO 90 I=1,10
      DRR= ABS(RR2-RR1)
      RRP2= RR2
      IF(RR2.LT.RRLIM) GO TO 62
      RR2= RRLIM
      RRP2= RRLIM
      ZZ2= ZZLIM
      DRR= ABS(RR2-RR1)
      GO TO 66
   62 CONTINUE
      ZZ2= (1.0-(PSII/(1.0-RR2**REX)**RN)**(1.0/ZN))**(1.0/ZEX)
   66 DZZ= ABS(ZZ2-ZZ1)
      DSC= SQRT((DRR*XO)**2+(DZZ*W)**2)
      DSSC= DSC/D
      IF(DSSC.LT.DSS2) GO TO 100
      RR2= RR2-DELTA
       DELTA=DELTA/2.0
      RR2=RR2+DELTA
   90 CONTINUE
  100 RR2= RRP2
      IF(RR2.GT.RRLIM) RR2= RRLIM
      IF(RR2.EQ.RRLIM) ZZ2= ZZLIM
      RETURN
      END
```